INAUGURAL-DISSERTATION

zur
Erlangung der Doktorwürde
der Naturwissenschaftlich-Mathematischen Gesamtfakultät
der
Ruprecht-Karls-Universität
Heidelberg

vorgelegt von

Diplom-Biologin Michaela Viktorija Bilic

aus Heidelberg

Tag der mündlichen Prüfung:

DFer Protein-Tyrosine Kinase – Its involvement in the Amyloid Precursor Protein (APP)-induced blistered wing phenotype and its functional characterization in *Drosophila melanogaster*

Gutacher: Prof. Dr. Renato Paro
Prof. Dr. Dr. h. c. Konrad Beyreuther

Mome tati

Danksagung

Mein besonderer Dank gilt Prof. Dr. Renato Paro für die Bereitstellung des Projektes in seiner Gruppe und die Betreuung dieser Arbeit, die doch „etwas“ vom guten alten Chromatin- und Alzheimerfeld abweicht. Bei Prof. Dr. Dr. Konrad Beyreuther bedanke ich mich für die Übernahme des Zweitgutachtens, und entschuldige mich schon mal im Voraus für die auf ihn zukommende Fliegengenetik.

Herzlichen Dank an Gunter Merdes für seine Betreuung sowie ständige Diskussions- und Hilfsbereitschaft; der es seltsamerweise schaffte, Kritik, Lob, Trost und Ansporn in einen Satz zu packen, und trotz zahlreicher Tiefschläge meine Freunde und Enthusiasmus für die Wissenschaft aufrecht erhielt. Ebenso gilt mein Dank Alex Löwer, der immer freundschaftlich mit offenem Ohr, Kritik, Ratschlägen und Diskussion zur Seite stand (Euch beiden nochmals Danke für das Gegenlesen dieser Lektüre!); und Melanie Müller, insbesondere für ihre Hilfe bei der Injektion von Zigtausenden von Embryonen und für so manches andere.

Und natürlich den lieben Paros, die nie einen Laboralltag aufkommen ließen und viel zur Freude an der Wissenschaft beigetragen haben. Dank euch allen für den Spaß, die Diskussionen, Motivation, Unternehmungen und für die außergewöhnliche relaxte und familiäre Atmosphäre, auch wenn der ein oder andere Ehekrach mit Stefan sich nicht vermeiden lies... :-)
Da wären: Gunter (for being more than a supervisor), Alexos (mein liebster Alzheimerkollege und Administrator), Melanus (Spaßfaktor: 10), Sabine (Bienchen – müssen wieder mal ausschwärmen...), Stefanos („Rotator“, Ex-Champion im Gummischießen,... sorry, der Platz reicht nicht für mehr), Narali (“Süßer”), Ana (Stefan’s yin with southern temperament), Heidi (Labormama), Tariq (best Pakistanian barbeque ever), Leonie (English food is good), Gero (oppla, franz. Croissants), Brittus (Frau Dr. Koch trinkt 10 auf den Malediven), Christian (auch Sauer’s sind ok ☺), Sylv (pers. PR Beraterin), Andrea (Wiesel), Ian (mein Inbegriff von Zen), Sybille (die wahre Koordinatorin) und Renato (neuer Champion –siehe Stefan- und Baseler Fastnachts Marathonläufer).
Und wie könnte ich unsere ehemaligen Paros vergessen? Marciboy (alias “König Dickbauch”, “die wilde Hilde”, „Lance“, ich könnte seitenweise weiter schreiben...), mali Ma“th“eo, Chraze (Poppy), Cedricos; die fleißigen Händchen Christina, Cheng und Septimia; Frau Schwartz, David, Nathalie, Inhua, Gerrard, Mikel Spitzel, Cora, das Lämmchen Bodo und die zahlreichen Hiwis, die es mir leider (?) vergönnt ließen, meine kleinen, lieben Biesterchen (alias Drosophilen) selbst zu bekochen... Axel (die Feuerwehr)... sowie Tweety (wie heißt sie eigentlich wirklich?), Pjodre (die Geduld in Person), Simone und Essensdetektor Grübelchen nimmersatt, die, obwohl sie “Beyreuthers” sind (sorry Herr Beyreuther :-)), doch noch resozialisiert/ re“paro“isiert werden konnten.
Ich werde euch alle vermissen.

An dieser Stelle möchte ich auch meinen “Leidensgenossen” Kevin Hill (für die nicht mutierten Clone) und Mikel Murrey und Catherine Davidson (für die Mutante) danken, die, ebenso wie ich, von *zwirbelmütze* gelernt haben, dass nicht alle Dinge so sind wie sie scheinen...

Hvala hvala hvala….. mojoj mami i mome tati, nek te dragi bog cuva, i mome Brüderchen Mikel, sa vas podrsak, razum i vasu ljubavi. I hvala tebi, veliki ☺

I Zusammenfassung

Das “Amyloid Precursor Protein” APP ist das Vorläuferprotein des Aβ-Peptides, welches als Bestandteil der amyloiden Plaques im Gehirn von Alzheimer Patienten auftritt. Obwohl die Entstehung von Aβ durch die proteolytische Spaltung von APP sehr gut untersucht ist, ist die physiologische Funktion von APP weitgehend unbekannt. Die APP zugesprochenen biologischen Aktivitäten umfassen auch eine Funktion in der Zelladhäsion und in intrazellulären Signalwegen. In früheren Studien wurde die Fruchtfliege *Drosophila melanogaster* als Modellsystem genutzt. Dabei konnte gezeigt werden, dass die Expression von APP während der Flügelentwicklung zu einer Blasenbildung („blistered wing“ Phänotyp) im Flügel führt, einem Zelladhäsionsdefekt, der auf eine Funktion von APP in der Zelladhäsion hinweist. Basierend auf diesem Phänotype wurde ein genetischer Screen durchgeführt und zahlreiche Suppressoren des APP induzierten Phänotyps isoliert.

In der vorliegenden Arbeit wurden diese genetischen Interaktoren identifiziert. Die neun stärksten Suppressoren kodieren für Proteine involviert in Zell-Zelladhäsions-Prozessen, Calcium-Signalwegen, Organisation des Zytoskeletts und transkriptionelle Regulation. Eines der Proteine, die DFer Protein-Tyrosin Kinase, deren Funktion in *Drosophila* unbekannt ist, wurde weitergehend untersucht. Mithilfe eines transgenen Ansatzes konnte die genetische Interaktion zwischen APP und *dfer* verifiziert werden. Zellkultur- sowie *in vivo*-Experimente in *Drosophila* zeigten jedoch, dass die Interaktion zwischen den beiden Proteinen indirekt ist, ausgelöst durch generelle Interferenzen mit Zelladhäsion. Dementsprechend hatte die Expression von *dfer* weder einen Effekt auf den Metabolismus, die Prozessierung, die Phosphorylierung, noch auf die Sekretion von APP.

Die DFer Kinase stellt das einzige *Drosophila* Homolog zur Fes und Fer Kinase von Säugetieren dar, die mit der Regulation von Zelladhäsion und zytoskelettalem Umbau vermittelt durch adhäre Verbindungen und fokalen Adhäsionen in Verbindung gebracht werden. Im Rahmen dieser Arbeit konnte gezeigt werden, dass die DFer Kinase in ihrer funktionellen Regulation ihren vertebraten Homologen ähnelt und Tyrosin-Phosphorylierungsaktivität *in vivo* aufweist. Die *dfer* Expression im Fliegenembryo war besonders stark in Geweben, die morphologische Entwicklungsvorgänge durchlaufen, bei denen Zelladhäsionsprozesse eine wichtige Rolle spielen, insbesondere im Zentralen Nervensystem, an den Muskelbefestigungen, und den Zellen der Führungskante („leading edge“) während des dorsalen Rückenschlusses des Embryos. Im Gegensatz zu den vertebraten Homologen konnte für *dfer* gezeigt werden, dass mind. drei unterschiedliche Transkripte auftreten, deren Expression teilweise zeitlich und räumlich beschränkt ist.

Durchgeführte Überexpressionstudien in *Drosophila* legen eine Rolle von DFer in der Modulation von Zelladhäsionsprozessen nahe. Das Entstehen von „blistered wing“ Phänotypen weist auf einen Verlust von Funktionen der Integrine hin. Das Fehlen von Flügelgewebe („wing margin notching“) kann als eine Beeinflussung des Notch- und Wingless-Signalweges interpretiert werden, wahrscheinlich bedingt durch einen Verlust von Zell-Zelladhäsionen. Dies wird unterstützt durch die Identifizierung von weiteren genetischen Faktoren, die diese Phänotypen beeinflussen. Da die Überexpression der vertebraten Homologe gleiche Phänotypen hervorrief, kann von einer funktionellen Konservierung zwischen den Proteinen ausgegangen werden.

Des weiteren wurden *dfer* mutante Fliegen hergestellt, die lebensfähig und fruchtbar sind und damit bestätigen, dass *dfer* für die Entwicklung von *Drosophila* nicht essentiell ist. Überraschenderweise konnten nur sehr kleine Deletionen generiert werden, die weiterhin ein funktionelles DFer Protein produzieren, oder sehr große Deletionen. Mutanten mit großen Deletionen erwiesen sich als letal. Es konnte gezeigt werden, dass neben *dfer* drei weitere Gene entfernt wurden. Experimente mit genomischen Konstrukten belegten, dass eines dieser Gene, CG33188, ein für die Entwicklung essentieller neuronaler Transkriptionsfaktor ist. Obwohl die DFer Kinase nicht essentiell ist, weisen ca. 10% der Embryonen Defekte während des embryonalen dorsalen Rückenschlusses auf, ein Prozess, der Integrin- und Cadherin-vermittelte Zelladhäsion benötigt. Die Aufklärung der exakten Funktion von DFer während dieser Prozesse wird in der Zukunft wichtige Rückschlüsse auch auf die Funktion von APP in der Zelladhäsion offenbaren.

II Summary

The Amyloid Precursor Protein APP is the source of the Aβ peptide found in neuritic plaques of Alzheimer's Disease patients. Although the Aβ generation from APP is well investigated, the actual physiological functions of APP remain still unclear. Nevertheless, multiple biological activities have been suggested, among these functions in cell adhesion and intracellular signaling. Using *Drosophila melanogaster* as a model system, it has been shown that overexpression of human APP during *Drosophila* wing development leads to cell adhesion defects visible as wing blisters, pinpointing to an involvement of APP in cell adhesion. Based on this APP-induced blistered wing phenotype, a genetic dominant modifier screen was performed and numerous suppressors isolated.

In this study, the genetic modifiers of the APP-induced blistered wing phenotype were identified. The nine strongest suppressors encode for proteins involved in cell adhesion, calcium signaling, organization of the cytoskeleton and transcriptional regulation. One of the proteins, the DFer protein-tyrosine kinase with uncharacterized function in *Drosophila*, was further investigated. Using a transgenic approach, the genetic interaction between APP and DFer could be verified. However, the interaction between these proteins was revealed to be of an indirect nature caused through general interference with cell adhesion. This was evident from cell culture and *in vivo* experiments in the *Drosophila* organism, where *dfer* expression had no effect on APP metabolism, processing, phosphorylation and secretion.

DFer kinase is the only *Drosophila* homolog of mammalian Fes and Fer kinases, which are implicated in the regulation of cell adhesion and cytoskeletal rearrangement mediated by adherens junctions and focal adhesions. Here, it could be shown that DFer kinase displays a functional regulation similar to its vertebrate homologs and showed tyrosine phosphorylation *in vivo*. In the fly embryo, *dfer* was ubiquitously expressed with particularly high levels in the developing CNS, at muscle attachment sites and in the leading edge cells during the morphological process of dorsal closure, interestingly, all sites of cell migration where adhesion takes place. In contrast to its vertebrate homologs, *dfer* produced at least three different transcripts, which seem to be in part spatially and temporally restricted.

The results obtained from overexpression studies of *dfer* in *Drosophila* imply an accessory role in modulating cell adhesion processes. While ubiquitous expression resulted in lethality, more selective expression gives phenotypes such as wing blistering, characteristic for loss of integrin function. Another striking phenotype, wing margin notching, suggests an interference with the Notch and Wingless signaling pathways, probably by interfering with cell adhesion processes. Moreover, genetic modifiers of the overexpression phenotype were identified, encoding proteins with functions in cell adhesion. Overexpression of the mammalian *fes* and *fer* in *Drosophila* caused similar defects, supporting a functional conversation between these proteins.

Dfer mutant flies were generated that are viable and fertile, demonstrating that *dfer* is not essential for developmental or physiological functions in *Drosophila*. Surprisingly, only very small deletions, resulting in functional DFer protein expression, or very large deletions were recovered. Mutants with large deletions displayed lethality, and it could be shown that three *dfer* neighboring genes were additionally deleted. With genomic rescue constructs containing these three genes, it could be revealed that one of them, CG33188, is an essential neuronal transcription factor. Although DFer kinase was shown to be not critical for *Drosophila* development, 10% of the *Dfer* mutant embryos displayed defects during dorsal closure, a process requiring integrin- and cadherin-mediated cell adhesion. The elucidation of DFer function during these processes in the future may shed also light on aspects of APP function in cell adhesion.

Table of Contents

ZUSAMMENFASSUNG

SUMMARY

1 INTRODUCTION 2

1.1 *Drosophila* as a model system for human diseases 2

1.2 Alzheimer's Disease and the APP protein family 3

1.3 Processing of the APP protein family 4

1.4 Functions of APP family members 5

1.5 The *Drosophila* homolog APPL 6

1.6 Transgenic approach to study human APP in *Drosophila* 7

1.7 Wing development 9

1.8 Genetic screen for modifiers of the APP-induced blistered wing phenotype 11

1.9 Aim of this study 13

2 RESULTS 15

2.1 Identification of suppressors of the APP-induced blistered wing phenotype 15

2.2 The suppressor *zwirbelmütze* encodes for DFer 17

2.3 Functional overexpression analyses of *dfer* in *Drosophila* 21

2.4 Generation and overexpression analyses of *dfer* isoforms and *dfer* mutants 27

2.5 Generation and overexpression analyses of the mammalian homologs of DFer kinase 29

2.6 Analyses of the developmental and spatial expression of *dfer* 31

2.7 Generation of DFer antibodies and DFer protein expression analysis 34

2.8 The relationship between APP and DFer interaction 37

2.9 Localization of the DFer protein 40

2.10 Functional analyses of DFer in larval wing imaginal discs 42

2.11 Genetic interaction partners of *dfer* 49

2.12 Generation and identification of *dfer* mutant alleles 52

2.13 Functional analysis of the $dfer^{\Delta 252}$ mutant 55

2.14 Functional analysis of the $dfer^{del1}$ mutant and the mutants $dfer^{w39.2}$, $dfer^{49Sb}$ and $dfer^{41.1}$ 59

2.15 Analysis of *dfer* RNAi *in vivo* 66

2.16 Genomic rescue constructs for *dfer* and the genes CG8129, CG18473 and CG33188 69

3 DISCUSSION 77

3.1 Suppressors of the APP-induced blistered wing phenotype 77

3.2 The DFer kinase and APP do not interact directly 81

3.3 DFer kinase is similar to vertebrate Fes and Fer kinase in structure and function, but differs in expression 82

3.4 *Dfer* overexpression phenotypes – closing in on the biological function of DFer 86

3.5 *Dfer* is a non-essential *Drosophila* gene 94

3.6 Conclusion and outlook 97

4 MATERIAL 99

4.1 Molecular Weight Markers 99

4.2 Enzymes 99

4.3 Antibodies 100

4.4 Oligonucleotides 101

4.5 Plasmids, cosmids and BACs 103

4.6 Bacterial cell lines 104

4.7 Cell culture lines 105

4.8 Fly lines 105

5 METHODS 108

5.1 Molecular methods 108

5.1.1 Phenol-chloroform extraction of DNA 108
5.1.2 Ethanol precipitation of DNA 108
5.1.3 Analysis of DNA fragments by agarose gel electrophoresis 108
5.1.4 Pulsed field gel electrophoresis (PFGE) 109
5.1.5 PCR purification / gel extraction 109
5.1.6 Extraction of DNA from LMP agarose gels 110
5.1.7 Extraction of DNA by electroelution 110
5.1.8 Restriction digestion of DNA 110
5.1.9 Phosphatase treatment of DNA 110
5.1.10 Nuclease treatment of DNA 111
5.1.11 Hybridisation of oligonucleotides 111
5.1.12 Ligation of DNA fragments 111
5.1.13 TOPO TA cloning 111
5.1.14 Ligation of genomic DNA into cosmids 112
5.1.15 Phage packaging of cosmid DNA 112
5.1.16 Preparation of bacterial agar plates 112
5.1.17 Freezing of bacteria 113
5.1.18 Production of electro-competent *E. coli* cells 113
5.1.19 Transformation of *E. coli* using electroporation 114
5.1.20 Transformation of chemo-competent cells 114
5.1.21 Plasmid isolation 114
5.1.22 Isolation of BACs and cosmids 115
5.1.23 Preparation of cosmid DNA from mini lysates 115
5.1.24 Preparation of cosmid DNA by boiling lysis 116
5.1.25 DNA purification by CsCl-ethidium bromide gradient equilibrium centrifugation 116
5.1.26 Sequencing of plasmids and cosmids 117
5.1.27 PCR (Polymerase chain reaction) 117
5.1.28 Colony PCR 118
5.1.29 Isolation of genomic DNA (Quick Fly Genomic DNA Prep) 118
5.1.30 Plasmid rescue 118
5.1.31 Single Fly PCR 120
5.1.32 Southern Blot 120

5.1.33 Isolation of total RNA from fly heads 122
5.1.34 Reverse Transcription 122
5.1.35 Northern Blot 123

5.2 Biochemical protein methods 124

5.2.1 Discontinuous SDS-polyacrylamide gel electrophoresis (SDS-PAGE) 124
5.2.2 Bis-Tris-HCl polyacrylamide gel electrophoresis 124
5.2.3 Coomassie staining of proteins 125
5.2.4 Western blotting (wet blot) 125
5.2.5 Coupled in vitro transcription and translation 126
5.2.6 Autoradiography of gels with radioactive samples 127
5.2.7 Recombinant expression and purification of GST fusion proteins 127
5.2.8 Immunization of rabbits 128
5.2.9 Antigen-coupling to sepharose 129
5.2.10 Purification of polyclonal antibodies by antigen-antibody affinity chromatography 129
5.2.11 Immunoprecipitation of *in vitro* translated protein 130
5.2.12 Co- / Immunoprecipitation of cell lysates 130

5.3 *Drosophila* handling and genetic methods 131

5.3.1 *Drosophila* handling 131
5.3.2 P-element mediated germ line transformation 131
5.3.3 Injection of cosmids for P-element mediated germ line transformation 132
5.3.4 Establishment of transgenic *Drosophila* lines and mapping of the integration site 132
5.3.5 Collection of embryos 132
5.3.6 Determination of embryonic lethality 133

5.4 *Drosophila* dissections and histological methods 133

5.4.1 Preparation of fly head extract for western blot analysis 133
5.4.2 Alkaline Phophatase treatment of fly head extract 133
5.4.3 Preparation of wing imaginal discs for western blot analysis 133
5.4.4 Cuticle preparation 133
5.4.5 Pharate adult preparation 134
5.4.6 In situ hybridization of embryos 134
5.4.7 Immunostaining of whole embryos 136
5.4.8 Dissection and immunostaining of imaginal discs and salivary glands 137
5.4.9 Phalloidin staining 138
5.4.10 DAPI staining 138
5.4.11 Histochemical detection of ß-galactosidase activity in imaginal discs 138

5.5 Cell culture methods 139

5.5.1 Cultivation of COS-7 cells 139
5.5.2 Cultivation of Schneider 2 (S2) cells 139
5.5.3 Freezing of cells for long term storage 139
5.5.4 Thawing of frozen cells 139
5.5.5 Transfection of COS-7 cells with Lipofectamine Plus 140
5.5.6 Transient transfection of Schneider cells with Effectene 140
5.5.7 Cell lysis 140

6 CLONING STRATEGIES 141

7 LITERATURE 149

8 APPENDIX 162

8.1 Abbreviations 162

8.2 Vector maps 166

8.3 Publications 181

Introduction

1 Introduction

1.1 *Drosophila* as a model system for human diseases

The fruit fly *Drosophila melanogaster* is one of the best-studied multicellular organisms and widely used as an animal model system to elucidate fundamental processes and pathways underlying development and diseases. Despite the difference in morphology between flies and mammals, numerous gene products required for basic processes of development and differentiation have been highly conserved in structure and function during evolution. In fact, approximately 75% of human genes known to be associated with human disease have a *Drosophila* ortholog (Reiter et al. 2001). The powerful genetic tools *Drosophila* offers with thousands of available mutants and sophisticated molecular techniques, together with the availability of the complete genome sequence, make the fruit fly a formidable model system to investigate the normal physiological function of genes implicated in human diseases. Presently, *Drosophila* already serves as a transgenic model system for Cancer and metastasis; diseases induced by serpins; Fragile X Syndrome; Ataxia; and several neurodegenerative diseases including Huntington, Tauopathies, Parkinson and Alzheimer's Disease (reviewed in Tapon 2003; Muqit and Feany 2002; Carrell and Corral 2004; Bonini and Fortini 2003).

A broad variety of genetic and molecular tools exist in *Drosophila* to influence gene expression. The inducible dual GAL4/UAS system (Fig. 1.1) e.g., allows controlled ectopic expression of transgenes and of targeted genomic transcription units in a spatially and developmentally regulated manner (reviewed in Duffy 2002; Brand and Perrimon 1993). In principle, the gene of interest is cloned into a P-element vector carrying an upstream activating sequences (UAS) element required for binding of the yeast transcriptional activator GAL4 and is subsequently integrated into the *Drosophila* genome by P-element mediated germ line transformation (Rubin et al. 1982; Spradling et al. 1982). Transgene expression is induced by crossing these fly lines to defined GAL4 driver lines expressing GAL4 under a variety of endogenous, tissue-specific enhancers, thus allowing expression in all tissues and during almost any time point in development. Similarly, endogenous genes can be misexpressed if a modified transposable Enhancer-Promoter-element (EP-element) carrying a tandem array of five UAS sites required for GAL4 binding in front of a minimal promoter at the end of the P-element, is inserted upstream of a genomic transcription unit, inducing the overexpression of the adjacent gene (Fig. 1.1) (Rorth 1996; Rorth et al. 1998). This EP-element vector is widely used for large-scale mutagenesis screens as, dependent on the orientation and the insertion site of the inserted EP-element, endogenous genes can be either overexpressed or knocked out (reviewed in Duffy 2002; Roman 2004).

In addition, vectors have been generated for the induction of RNA-interference (RNAi) *in vivo* under the control of GAL4 to knock down genes in a temporally and spatially controlled manner (Lee and Carthew 2003).

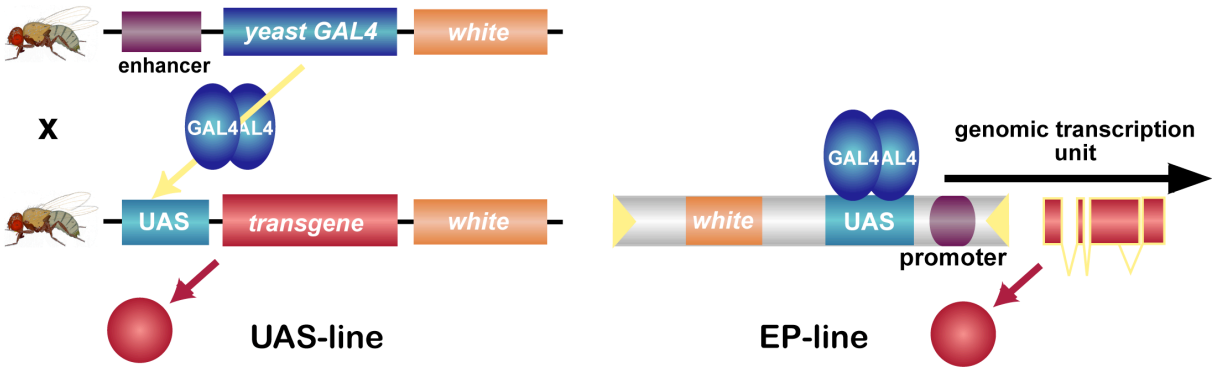

Fig. 1.1 The GAL4/UAS system in *Drosophila*. Flies carrying a transgene under the control of GAL4 upstream activating sequences (UAS) are crossed with flies expressing GAL4 under a tissue-specific promotor or enhancer. In the resulting offspring, the binding of the GAL4 transcriptional activator to the UAS induces the expression of the transgene or a transcription unit in close vicinity to an EP-element. *white*, mini-*white* marker gene.

Accordingly, the dual system allows a very detailed analysis of the impact of transgene overexpression on development and disease progression. Because of the large number of known phenotypes, which result from the inactivation or overexpression of genes, in many cases a corresponding function or a particular involvement in specific physiological pathways can be attributed to the human genes. Importantly, the resulting phenotype can often be used to perform large-scale genetic screen, which are not possible in mammalian models, for identifying factors required for the induction of the phenotype. The basics for such screens is the fact, that dominant phenotypes usually can be dominantly enhanced or suppressed by factors involved in the same regulatory cascade.

1.2 Alzheimer's Disease and the APP protein family

Alzheimer's disease (AD) is the most common neurodegenerative disorder affecting cognitive functions of the brain. Important pathological features of AD are the formation of neurofibrillary tangles and amyloid plaques in the brain (reviewed in Selkoe 2002). The predominant constituents of plaques are beta-amyloid peptides (Aβ), derived by the proteolytic processing from the amyloid precursor protein (APP). APP is the founding member of the APP protein family with known homologs in *C. elegans* (APL-1), *D. melanogaster* (APPL) and mouse. In mice as well as in humans, a single *app* and two *app-like* genes (*aplp1*, *aplp2*) have been identified (reviewed in Coulson et al. 2000). The APP

family members encode type I transmembrane proteins with high sequence conservation between each other and between different species. The pathogenic Aβ domain of APP, however, is not conserved.

1.3 Processing of the APP protein family

APP is cleaved *in vivo* by several proteases at α-, β-, γ-, and/or ε-sites (Fig. 1.2). In the amyloidogenic pathway, the Aβ peptide is produced through the sequential processing of APP by two proteases termed β- and γ-secretase (reviewed in Annaert & De Strooper 2002). The first cleavage occurs in the extracellular domain (EC) near the transmembrane region of APP by the β-secretase and allows secretion of sAPPβ. The remaining C-terminal fragment serves as a substrate for the γ-secretase, which mediates proteolysis within the transmembrane region at the γ- and/or ε-site, releasing the cytoplasmic domain (A^{ID}) and the Aβ peptide. The production of Aβ is counteracted by an alternative non-amyloidogenic pathway, where α-secretase cleaves within the Aβ sequence, leading to the subsequent release of the sAPPα and A^{ID} together with the smaller p3 peptide. The β-secretase is a transmembrane aspartyl protease termed BACE and members of the ADAM (a disintegrin and metallo-protease) family have been implicated to mediate cleavage of APP at the α-site (reviewed in Annaert & De Strooper 2002). γ-secretase activity is carried out by a core complex consisting of at least four proteins: Presenilin, Nicastrin, Aph-1 and Pen-2 (reviewed in Aguzzi & Haass 2003). Presenilin contains two aspartate residues, which are considered to form the active centre of the protease, whereas Nicastrin, Aph-1 and Pen-2 stabilize the complex.

APLP1, APLP2, and other type-I transmembrane proteins follow a similar juxta- and intramembranous processing which has been termed regulated intramembrane proteolysis (reviewed in De Strooper 2003; Selkoe and Kopan 2003; Brown et al. 2000). The most prominent example is the Notch receptor, being part of an evolutionarily conserved signaling pathway that is involved in many developmental processes (Artavanis-Tsakonas et al. 1999). Although the γ-complex cleaving these molecules comprises the same core components being present in almost all cell types, there are differences between APP and Notch processing in distinct cell types that are regulated on the level of γ-secretase cleavage (Loewer et al. 2004).

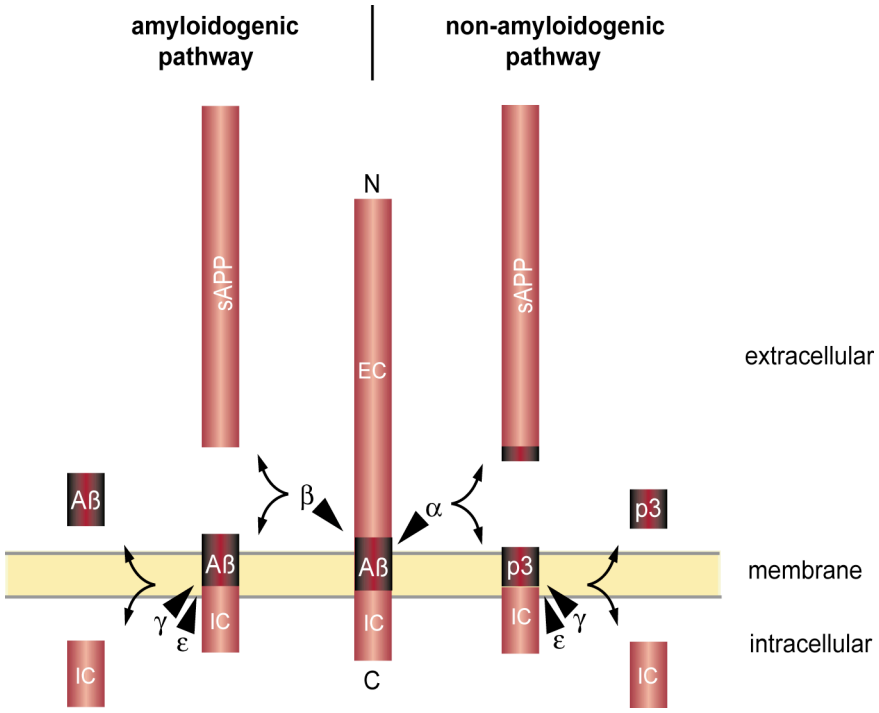

Fig. 1.2: Proteolytic processing of APP. Indicated are the cleavage sites for the proteases. APP is initially cleaved either at the α- or β-site releasing the large ectodomain (sAPPα/β). The membrane-retained C-terminal fragment is further processed by the γ-secretase complex at the γ- and/or ε-cleavage sites, generating Aβ in the amyloidogenic pathway or p3 in the non-amyloidogenic pathway, and releasing the intracellular domain of APP (ID). EC, extracellular domain.

1.4 Functions of APP family members

Despite extensive investigation, the physiological function of APP family proteins has not been clearly defined yet. Numerous functions have been attributed to APP, including growth factor properties, involvement in cell adhesion and a receptor-like function with signal transduction (reviewed in Annaert et al. 2002). Additionally, it has been implicated in various processes regulating neuronal activity, such as neurite outgrowth, neuronal cell adhesion, cell migration and neural progenitor cell proliferation (reviewed in Turner et al. 2003). However, the mechanism of how APP participates in these processes still remains unclear.

In mouse genetic knockout studies, inactivation of the *app* gene does not result in lethality, but rather in changes in locomotion and in memory impairment (Muller et al. 1994; Muller et al. 1996). These functional studies have been complicated by a partial redundancy among the three APP family proteins. Whereas double-knockouts of *app-aplp1* are viable, *app-aplp2* and *aplp1-aplp2* double-knockouts are lethal with no obvious phenotypes, suggesting an essential function of APLP2 during development (Heber et al. 2000; von Koch et al. 1997). A new triple mutant model, however, provides evidence for a crucial role of the APP family members in neuronal adhesion and the survival of neuronal cells, with mice

displaying a phenotype resembling human type II lissencephaly with cortical dysplasias and a partial loss of cortical Cajal Retzius cells (Herms et al. 2004). Intriguingly, a recent study revealing the x-ray structure of an APP domain favors the idea that APP dimerizes in an antiparallel orientation (Wang and Ha 2004). Moreover, homo- and hetero-trans-dimerization of APP family proteins was observed in cell culture assays, strengthening an involvement of APP family members in cell adhesion (P. Soba, unpublished data).

Biochemical and genetic analyses have led to the identification of both extracellular and multiple intracellular binding partners, consistent with putative roles of APP/APLPs in adhesion and in mediating signal transduction processes (reviewed in De Strooper and Annaert. 2000; Koo 2002). Besides interaction with extracellular matrix molecules such as laminin, heparin and collagen, APP also binds to a putative extracellular ligand, namely F-spondin (Ho and Sudhof 2004). Furthermore, APP was shown to colocalize with β-1-integrin on the surface of axons and at sides of adhesion (Storey et al. 1996; Yamazaki et al. 1997; Sabo et al. 2001). With regards to the cytoplasmic APP domain, the highly conserved NPTY motif, which confers clathrin-mediated endocytosis, was shown to bind several intracellular adaptor proteins, including X11, mDab1, Numb and Fe65 family proteins. Binding of some of these intracellular adaptor proteins can affect APP processing, trafficking, and transcriptional modulation (reviewed in Turner et al. 2003). In the case of the adaptor protein Fe65, it gets activated upon binding to the A^{ID} and, together with the Histone-Acetyl-Transferase Tip60, it is able to activate the transcription of reporter genes (Cao and Sudhof 2001; Baek et al. 2002). The mechanism how this transcriptional activation is mediated, however, is still mysterious. It was proposed that upon Fe65 binding, A^{ID} and Fe65 translocate into the nucleus and form a transcriptionally active complex together with Tip60, but there is emerging evidence that nuclear translocation of the A^{ID} may actually be dispensable (Cao and Sudhof 2004). Recently, APP itself, together with BACE, Tip60, Kai1, and GSK3β were identified as transcriptional targets, corroborating a function of APP in nuclear signaling (von Rotz et al. 2004).

1.5 The *Drosophila* homolog APPL

The expression of the *Drosophila* amyloid precursor protein-like protein APPL is limited to neurons and some glial cell of the central nervous system (Martin-Morris et al. 1990). Mutations in *appl* have been correlated to a neurodegenerative phenotype, resulting in behavioral deficits in fast phototaxis and impaired axonal transport (Luo et al. 1992). Interestingly, overexpression of APPL or human APP can partially rescue the behavioral phenotype, suggesting that APP functions are conserved from invertebrates to mammals. Although in *Drosophila* the *appl* gene seems not to be required for viability and fertility, loss-

and gain-of-function studies have revealed a role for APPL in synaptogenesis at the neuromuscular junction and in axonal transport (Gunawardena and Goldstein 2001; Torroja et al. 1999a, Torroja et al. 1999b). While APPL overexpression causes a strong increase in synaptic bouton numbers and changes in the synaptic structure, APPL null mutants exhibit decreased bouton numbers. An additionally observed axonal transport deficit in larvae is possibly correlated to impaired kinesin-mediated axonal transport.

The protein processing events seem to be conserved in *Drosophila*, as APPL follows a similar processing with detectable α- and γ-secretase activity *in vivo* (Torroja et al. 1996; Fossgreen et al. 1998). However, no BACE homolog has been identified in flies. Nevertheless, overexpression of human APP together with the BACE, which leads to a release of an Aβ-like fragment, or direct expression of the Aβ-peptide induces neurotoxicity and neurodegeneration (Greeve et al. 2004; Iijima et al. 2004).

1.6 Transgenic approach to study human APP in *Drosophila*

Previously, *Drosophila melanogaster* was established as a transgenic model system to gain new insights into the function of APP during development of an organism (Fossgreen et al. 1998). For this purpose, transgenic fly lines expressing wildtype and various mutant forms of the neuron-specific human APP 695 isoform were generated. One phenotype observed upon overexpression of APP, and also of its family members, were transformations of cell fates during the development of the peripheral nervous system. A genetic dissection of the phenotype showed that APP proteins interfere with the Notch signaling cascade upstream of Notch, supporting an involvement of APP family members in neuronal development (Merdes et al. 2004).

Additionally, transgenic flies expressing full-length forms of APP in the wing imaginal discs display a blistered wing phenotype, suggesting that the expression of human APP interferes with intracellular adhesion (Fossgreen et al. 1998; Yagi et al. 2000). This effect was initially shown to depend on both the intra- and extracellular domain of APP, since deletion constructs lacking either the C-terminal or N-terminal domain of APP induced no phenotype (Fig. 1.3).

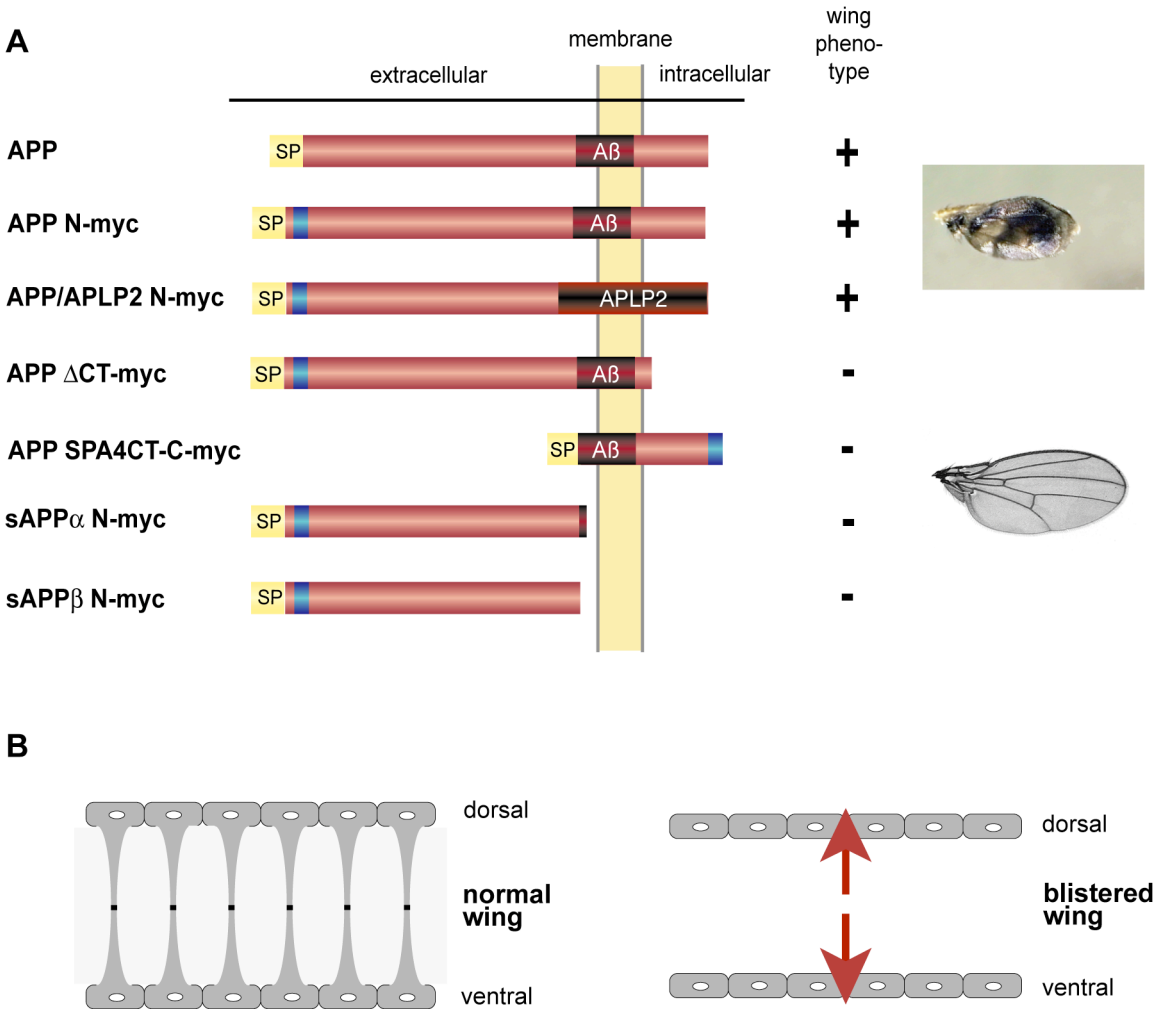

Fig. 1.3: Different APP protein forms expressed in the *Drosophila* wing induce a blistered wing phenotype. (A) Schematic representation of the human APP derivatives used for generation of transgenic fly lines. Flies expressing full-length or membrane-retained N-terminal constructs under the wing-specific driver line *ap*-GAL4 develop abnormal wings characterized by blisters. (B) The adult wing consists of single dorsal and ventral epithelial cell layers, which are held together by integrin-mediated cell adhesion. Wing blistering occurs as a consequence of a loss in cell adhesion or integrin-mediated signaling events between the two cell monolayers. SP, signal peptide; CT, cytoplasmic tail; myc, myc-tag.

The phenotype resulting from ectopic APP expression pinpoints to a receptor-like function of APP in the regulation of cell adhesion, and that APP interacts with evolutionarily conserved protein partners involved in the adhesion of the two epithelia during wing development. Similar wing phenotypes are caused by a disruption of the integrin-mediated cell-cell adhesion or interference with integrin signaling between the dorsal and ventral epithelial cell monolayers forming the adult wing structure (reviewed in Brown et al. 2000). Integrin-mediated cell adhesion also plays an important role for neuronal networks and memory, e.g. *Drosophila integrin* mutants display disrupted short-term memory and a loss of

synaptic plasticity (Beumer et al. 2002; Beumer et al. 1999). Since APP has been found to colocalize with β1-integrin subunits in neurons (Storey et al. 1996; Yamazaki et al. 1997), these findings might implicate a functional interaction of APP with integrins.

1.7 Wing development

The *Drosophila* wing is a well-characterized tissue and thus provides an ideal environment to study the effects of human APP overexpression. In order to analyse the processes underlying the phenotypic observation, it is crucial to understand the development of the wing structure. In *Drosophila*, the progenitor cells of the adult structures are organized in imaginal discs, clusters of undifferentiated cells, which are set aside in the embryo, and proliferate and differentiate during larval and pupal development (Cohen 1993). During development, the *Drosophila* wing imaginal disc is transformed from a simple epithelial sheet into a complex adult wing structure, giving rise to the wing blade, as well as to body wall cuticles of the dorsal (notum) and ventral thorax (pleura), and to the wing hinge, which attaches the wing blade to the body wall (Fig. 1.4). In the imaginal disc, the wing blade primordium is often referred to as the wing pouch, as it is separated from the rest of the disc by a fold in the epithelium.

The growth and patterning of the disc is governed by several key pathways that regulate genetic cascades essential for subdividing the disc in non-intermingling cellular compartments. Boundaries form along both the anteroposterior (A/P) and dorsoventral (D/V) axes of the wing and serve as organizing centers, patterning the disc epithelium and directing outgrowth of the wing tissue (reviewed in Tabata and Takei 2004; Irvine and Rauskolb 2001; Irvine and Vogt 1997).

Two transcription factors, *engrailed* (*en*) and *apterous* (*ap*), serve as selector genes of the posterior and dorsal compartment, respectively, and control signaling events that participate in many aspects of wing development. *en* is expressed in the posterior half of the wing disc (Kornberg et al. 1985). *en* cells produce the secreted molecule Hedgehog (Hh) and Hh signaling to adjacent anterior cells induces *decapentaplegic* (*dpp*) expression in A/P border cells. Dpp acts as a morphogen, determining cell fates along the A/P axis and directing wing outgrowth (reviewed in Tabata and Takei 2004; Vervoort 2000; Podos and Ferguson 1999).

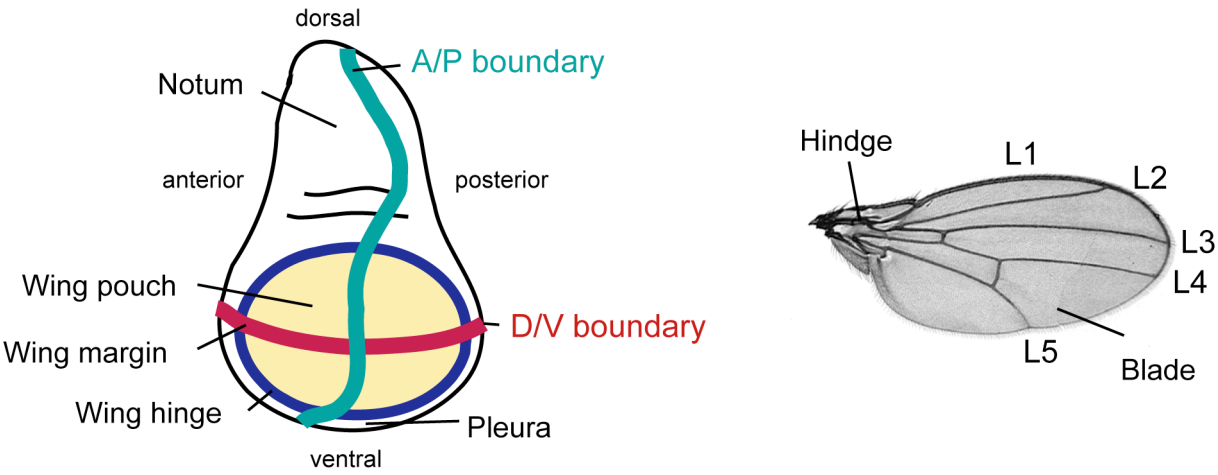

Fig. 1.4 Wing development in *Drosophila*. (A) Schematic organization of a third instar imaginal wing disc. The presumptive wing pouch is shaded in *yellow* and gives rise to the wing blade. Parts that form the wing hinge are shown in *blue*. The D/V boundary coincides with the developing wing margin (labelled *red*). The Notum and the Pleura form the dorsal and ventral thoracic cuticle, respectively. The A/P boundary is denoted in a *green* line. (B) The adult wing. The hinge attaches the wing blade to the thorax. Positions of the wing veins L1-L5 are indicated. A/P, anteroposterior; D/V, dorsoventral.

In much the same way, *ap* acts as the selector gene for the dorsal compartment. *ap* expression in the dorsal wing disc begins during the second larval instar, and it establishes the D/V boundary along the wing margin, separating the future dorsal and ventral wing surfaces (reviewed in Irvine and Rauskolb 2001; Cohen et al. 1992; Diaz-Benjumea and Cohen 1993; Williams et al. 1993; Blair et al. 1994). This depends on the localized activation of the Notch signaling pathway in cells adjacent to the D/V boundary. *ap* controls Notch activation through regulation of the Notch ligands Serrate and Delta, and through Fringe, which controls the sensitivity of Notch for its ligands (reviewed in Irvine 1999). Notch signaling induces *wingless* (*wg*) expression at the D/V boundary, forming a morphogen gradient exerting long-range influences on gene expression in surrounding wing cells (reviewed in Tabata and Takei 2004; Irvine and Rauskolb 2001; Zecca et al. 1996; Neumann and Cohen 1997). Notch also induces expression of the homeobox protein *cut* (*ct*) and the selector gene *vestigial* (*vg*) along the D/V boundary. Vg interacts with the product of the gene *scalloped* (*sd*), forming a transcriptional activation complex, which is known to regulate the expression of downstream genes involved in wing development (Halder and Carroll 2001; Halder et al. 1998; Kim et al. 1996; Klein and Martinez-Arias 1998). Ectopic *vg* expression is sufficient to convert cells in other discs to wing like fates (Kim et al. 1996).

Wg, in addition to promoting wing blade development, is also required for wing-margin specific *ct* expression, which itself promotes expression of *wg* and inhibits expression of Serrate and Delta (Micchelli et al. 1997; Neumann and Cohen 1996).

1.8 Genetic screen for modifiers of the APP-induced blistered wing phenotype

In order to identify factors required for the effect of APP on cell adhesion, a large-scale genetic gain-of-function screen was performed to isolate modifiers of the APP-induced blistered wing phenotype (Fig. 1.5; G. Merdes, unpublished data). This cell adhesion defect can be enhanced or suppressed by mutations in genes involved in cell-cell adhesion and/or genes interacting with APP. The screen took advantage of the fact that mutagenesis with a modified transposable EP-element can result in a loss-of-function or a gain-of-function of the target gene, depending on the orientation and the insertion site of the inserted EP-element (Fig. 1.5 B) (reviewed in Duffy 2002; Roman 2004; Rorth 1996; Rorth et al. 1998). Following insertion of this element into the genome, a neighboring gene can be ectopically misexpressed in response to a GAL4-pulse if the orientation of the EP-element corresponds with the orientation of the genomic transcription unit. In this way, gain-of-function phenotypes can be induced. Genes can also be knocked-out if the orientation of the EP-element is not identical with its neighboring gene or if the EP-element inserts within a transcriptional unit, inducing loss-of-function phenotypes.

For the genetic screen, an EP-element was mobilized and flies with potential new EP-element insertion sites were crossed with flies constitutively overexpressing human APP in the wing under the control of the *ap*-GAL4 driver (Fig. 1.5 C). Of the 1.2 million offspring from these crosses, 125.000 had the required genotype and were examined for changes in the wing phenotype. Several strong suppressors and enhancers could be isolated along with a high number (300) of very weak suppressors. The relevance of weak suppressors was verified by crossing EP-lines, which affect the same gene but have been isolated independently several times, to APP overexpressing flies under more restrictive conditions (G. Merdes, unpublished data).

The outline of the screen was focused on isolating suppressors, as, for enhancers, overexpression of any factor involved in imaginal disc development strongly interferes with the normal development of the wing disc independently of APP.

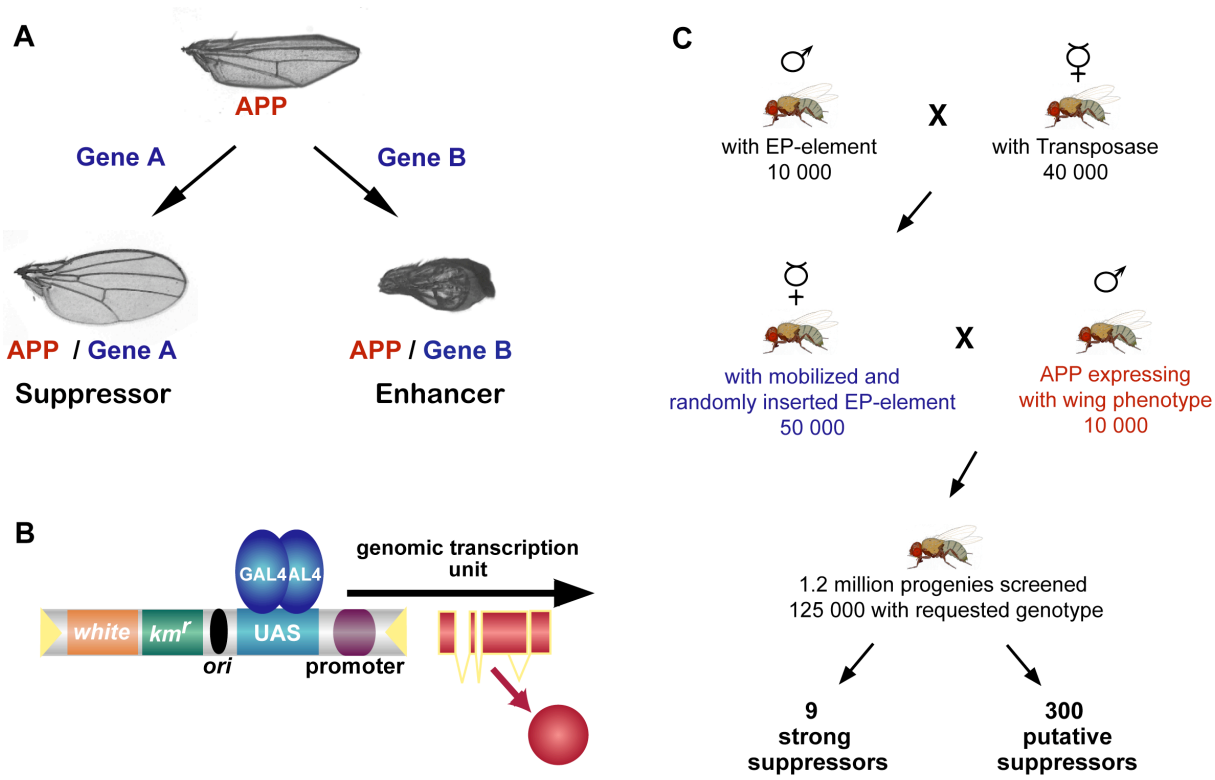

Fig. 1.5 Genetic screen for enhancers and suppressors of the APP-induced wing phenotype in *Drosophila*. (A) The blistered wing phenotype caused by ectopic APP expression can be enhanced or suppressed by mutations in genes interacting with APP. (B) EP-element. A minimal promotor at the end of the EP-element facilitates the overexpression of the adjacent transcription unit upon binding of the yeast transcriptional activator GAL4 to a tandem array of UAS sites. (C) Outline of the genetic screen. Gain-of-function genetics were utilized to identify suppressors of the APP-induced blistered wing phenotype. Flies with one copy of an EP-element are crossed with flies carrying a transposase source. In the F1 generation the EP-element is mobilized by the transposase in the germ line, which results in progeny with new EP-element insertion sites in the genome. Crossing of these flies with flies expressing GAL4 in the wing results in the binding of the GAL4 transactivator to the UAS at one end of the EP-element. In the cases where the EP-element inserted close to a transcription unit, ectopic misexpression of the endogenous gene occurs, and the consequences of this forced expression can be studied in the next generation. Genes of interest can then be cloned by isolation and sequencing of the genomic DNA flanking the EP-element. *white*, mini-*white* marker gene; *km*^{r}, Kanamycin resistance; *ori*, origin of replication.

One of the strongest suppressors isolated in the screen is an EP-element insertion on the third chromosome of the *Drosophila* genome. Because of the striking wing phenotype induced by the overexpression of the following transcription unit alone, this allele was termed *zwirbelmütze* (*zwim*).

1.9 Aim of this study

The physiological function of APP and its family member proteins still remains enigmatic. Accordingly, the identification of proteins interacting with APP should help to obtain new insights into APP function. The genetic screen using transgenic *Drosophila* expressing human APP enabled a search for such interacting proteins as modifiers of the APP-induced blistered wing phenotype. With this approach, numerous suppressor fly lines of the APP phenotype have been isolated.

This study aims to identify the genes affected in these suppressor fly lines to shed light on APP function in cell adhesion. In the following, it concentrates on the characterization of one of the strongest suppressors found in the screen, an EP-element insertion on the third chromosome, which was termed *zwirbelmütze* (*zwim*). The nature of the interaction between the *zwim* gene product and APP should be revealed. Additionally, the physiological function and expression of this gene during *Drosophila* development should be resolved in order to draw conclusions on its interference with APP function in cell adhesion processes.

Results

2 Results

Previous studies in *Drosophila* have shown that ectopic expression of human APP in the wing imaginal disc interferes with cell adhesion between the epithelial cell layers of the wing, resulting in a blistered wing phenotype (Fossgreen et al. 1998). As both the extracellular and intracellular domain of APP seemed to be necessary for phenotype induction, a signal transduction via APP was suggested. Based on these findings and propositions, a large-scale genetic screen using EP-element mediated mutagenesis was performed to isolate suppressors and enhancers of the APP-induced wing defect. Along with several enhancers, approx. 300 weak and nine strong suppressors were isolated (G. Merdes, unpublished data). The characterization of these modifiers could help to decipher the role of APP in cell adhesion and give new insights into the function of APP during the development of an organism.

2.1 Identification of suppressors of the APP-induced blistered wing phenotype

One advantage of EP-element mediated mutagenesis is that it allows identification of the EP-element integration site and, thus, the corresponding mutated gene through sequencing of the flanking genomic region. Concurrently, depending on the orientation and the insertion site of the EP-element, one can conclude if the EP-element insertion induced a loss-of-function or a gain-of-function mutation.

To recover the flanking sequences, a plasmid rescue was performed. This method takes advantage of the fact that the EP-element has a vector backbone, which can be amplified and propagated in bacteria as a plasmid (Rorth 1996; Rorth et al. 1998; see Material and Methods). The vector backbone comprises an origin of replication, a resistance gene and carries restriction sites for specific enzymes (Fig. 2.1 A). After digestion of genomic DNA with these enzymes, the EP-element and its flanking genomic region were recovered by recircularization. The integration site was identified by sequencing of these plasmids with EP-element specific primers. In a collaborative effort with G. Merdes and H. Ehret, Heidelberg, the adjacent genomic DNA of approx. 300 fly lines that suppressed the APP-induced wing phenotype was isolated using this method and sequenced. For most of the analysed fly lines, a DNA sequence could be obtained. The EP-element insertion site was subsequently identified by aligning the DNA sequence attained from the plasmid rescue with the *Drosophila* genome sequence using the BLAST algorithm. Fig. 2.1 B shows one example of the sequence alignment to identify the chromosomal integration site. The insertion sites and the presumably affected genes of the nine strong suppressors are listed in Table 2.1. The

corresponding genes were found to encode for proteins involved in cell adhesion, calcium signaling, the organization of the cytoskeleton and transcriptional regulation. One of the encoded proteins was uncharacterized.

A

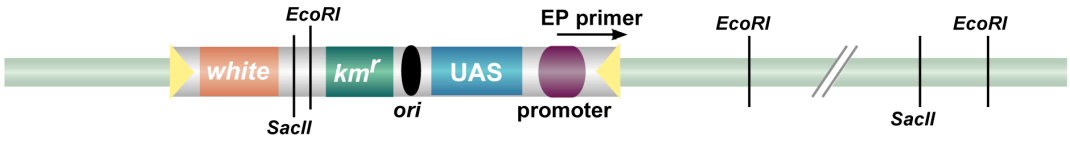

B

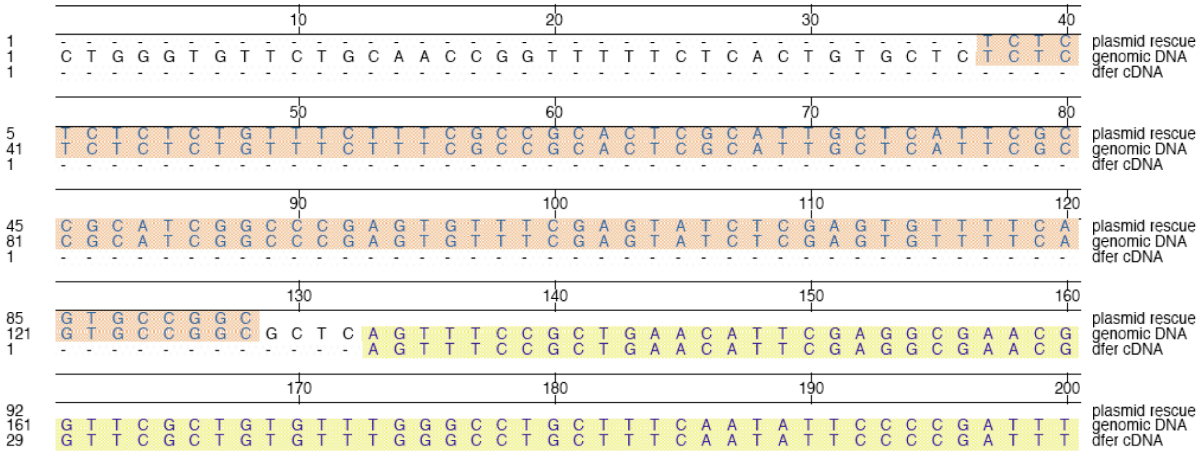

Fig. 2.1 EP-element plasmid rescue and sequence alignment. (A) A plasmid rescue facilitates the identification of the insertion site of an EP-element in the genomic DNA. Following restriction digestion with either EcoRI (i.e. genomic DNA contains statistically every 5 kb an EcoRI restriction site) or SacII, the DNA containing the EP-element vector backbone and the adjacent genomic DNA was isolated and religated to form a bacterial amplifiable plasmid. The neighboring genomic DNA sequence was obtained through sequencing of the plasmid using a specific EP primer. (B) The DNA sequence obtained from the plasmid rescue of one fly line was aligned to the *Drosophila* genome sequence allowing the identification of the chromosomal integration site (sequence identities between plasmid rescue and genomic DNA are highlighted in *tangerine*). In this particular case, the inserted EP-element is in close vicinity to the start of the transcription unit of the gene *dfer* (sequence identities between the genomic DNA and the *dfer* cDNA are highlighted in *yellow*). The plasmid rescue DNA and the genomic DNA are depicted in sense orientation, the *dfer* cDNA sequence in antisense orientation. *white*, marker gene; km^r, kanamycin resistance gene; UAS, upstream activating sequence; *ori*, origin of replication; EcoRI and SacII, restriction sites for the corresponding restriction enzymes.

For some of the genes, fly lines carrying P-element insertions within the same transcription unit were available from the Bloomington *Drosophila* stock center and were used to validate the results of the genetic screen. Crosses with the corresponding P-element insertions suppressed the APP-induced wing phenotype, concluding that the identified genes are the ones affected in the isolated EP-element fly lines and indeed act as suppressors.

Table 2.1 Suppressors of the APP-induced blistered wing phenotype.

Chromosome integration site	Adjacent gene	Protein domains/ Homolog to
X 03A2-3	CG7981 trol (terribly reduced optic lobes)	Perlecan
2L 21B4	CG3660 kismet	ATP-dependent helicase activity
2L 26B3-4	CG9167 krüppel homolog 1	zinc finger transcription factor activity
2L 39A5-6	CG1762 beta^{nu} integrin	Integrin
2R 59B4-6	CG30193-RD	pro-rich
3R 85D15	CG8874 dfer	Fes kinase Fer kinase
3R 85D23	CG9379 blistery	Tensin
3R 86F7	CG17342 lk6	receptor ser/thr kinase
2R 48F1-2	CG8472 calmodulin	Calmodulin

Flies carrying EP-element insertions within or in close vicinity of these genes were found to completely suppress the APP-induced blistered wing phenotype, revealing a wildtype-like wing. The chromosomal integration sites were assigned to neighboring genes, of which the annotated gene (CG) number, the gene name, the vertebrate homolog and putative domain homologies are depicted.

As the examination of all nine identified modifiers of the APP-induced blistered wing phenotype is too complex, we chose to concentrate on the characterization of one of the strong suppressors and resolve its relationship to APP.

2.2 The suppressor *zwirbelmütze* encodes for DFer

One of the strongest suppressors isolated in the screen was an EP-element insertion on the third chromosome of the *Drosophila* genome (Fig. 2.2 A). Because of the striking wing phenotype induced by the overexpression of the adjacent transcription unit (Fig. 2.2 B), which caused twisting of the wing, this allele was termed *zwirbelmütze* (*zwim*). The insertion was viable as homozygous flies carrying both alleles with the inserted EP-element hatched normally. However, flies carrying the EP-element over a balancer chromosome, which is a reorganized chromosome in order to prevent recombination between the same chromosomes, keep the balancer, indicating a slight decrease in viability compared to the wildtype allele.

Fig. 2.2 Genomic transcription unit and amino acid sequence of *Drosophila* DFer protein-tyrosine kinase. (A) The EP-element of the *zwim* fly line (*dfer*^{zwim}) inserted 100 bp upstream of the 5' untranslated region (UTR) and in the same orientation as the *dfer* transcription unit, the arrow displaying its direction. Exons are shown as boxes, split by introns. Dashed lines represent alternative splice sites. Non-coding exons are illustrated in *grey*, coding exons in *green*. (B) Overexpression of the EP-element insertion fly line *dfer*^{zwim} induces strong wing phenotypes resembling a "zwirbel" (in *German*: a twisted or twirled structure). Flies carrying the *zwim* EP-element insertion were crossed to *ap*-GAL4 flies expressing GAL4 in the dorsal part of the wing. Crosses were performed at 28°C. (C) Amino acid sequence alignment of *Drosophila* DFer with human Fes and Fer protein-tyrosine kinase. The *Drosophila* DFer kinase shows high sequence homology to its two mammalian homologs. Conserved amino acid residues are highlighted in *tangerine*.

The EP-element was integrated at chromosomal position 3R 85D15, approx. 100 bp upstream of the 5' untranslated region (UTR) of the gene *dfer,* formerly designated *fps85D* (Table 2.1; Fig. 2.2 A), in the same orientation as the gene. *Dfer* encodes a non-receptor

protein-tyrosine kinase (PTK) with uncharacterized function in *Drosophila*. The gene is located at chromosomal position 85D13-15, extends over 28 kb, and no mutant alleles were recorded.

There are two vertebrate homologs, the Fps/Fes (hereafter referred to as Fes) and the Fer kinase, which were initially identified as proto-oncogenes. Recent studies have implicated these kinases in the regulation of cytoskeletal rearrangements that are mediated by adherens junctions and focal adhesions. In addition, they are involved in inside-out signaling that accompany receptor-ligand, cell-matrix and cell-cell interactions (reviewed in Greer 2002). Expression of the 92 kDa Fes protein is restricted to hematopoietic cells of the monocytic and granulocytic lineages, and to neuronal, epithelial, and vascular endothelial cells (MacDonald et al. 1985; Samarut et al. 1985; Care et al. 1994; Haigh et al. 1996). In contrast to the tissue-specific expression pattern of Fes, the 94 kDa Fer kinase is ubiquitously expressed (Letwin et al. 1988; Pawson et al. 1989). However, Fer has a shorter 51 kDa FerT isoform which is testis-specific (Keshet et al. 1990).

An extended homology was found between the amino acid sequence of the protein encoded by *dfer* and the products of vertebrate *fps* and *fer* (Fig. 2.2 C). DFer displays 38% and 36% identity to human Fes and Fer, respectively, with an overall similarity of 55%. As its vertebrate counterparts, DFer contains an N-terminal Fps/Fes/Fer/CIP4 homology (FCH) domain and three regions of predicted coiled-coil motifs (CC), followed by a central Src-homology-2 (SH2) modular protein domain and a C-terminal catalytic tyrosine kinase domain (Fig. 2.3) (reviewed in Greer 2002; Smithgall et al. 1998). The shorter FerT protein is lacking the N-terminal region, but contains an additional N-terminal 44 amino acid sequence.

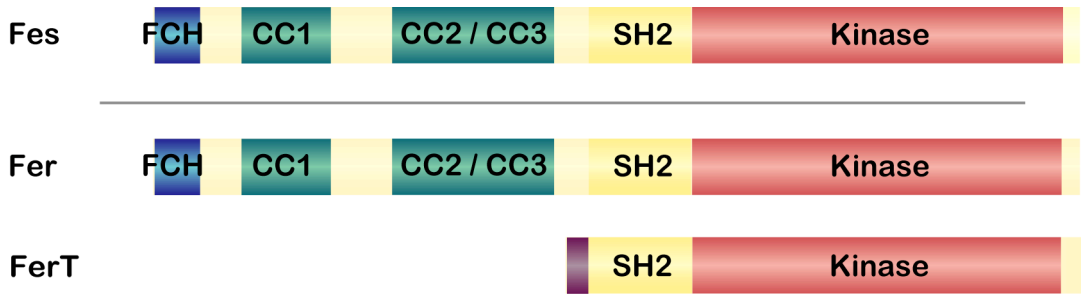

Fig. 2.3 Protein structure of the human Fes and Fer protein-tyrosine kinase. Fes and Fer display similar structural features: The N-terminal FCH (*blue*) and CC (*green*) domains, the SH2 domain (*yellow*), and the catalytic kinase domain (*red*). The shorter FerT protein isoform of Fer kinase lacks the N-terminal domain, but has an additional N-terminal sequence (*violet*). FCH, Fps/Fes/Fer/CIP4 homology; CC, coiled-coil; SH2, Src-homology-2.

Using sequence analysis, no other gene was found with similar features as *dfer*, thus, DFer is the only *Drosophila* homolog to vertebrate Fes and Fer kinase. In close correspondence to mammalian *fer*, *dfer* was initially thought to produce two mRNAs by

different initiation of transcription, and thus two proteins with molecular weights of 92 kDa and 45 kDa and distinctive N-termini (Paulson et al. 1997). In the recent Berkley prediction BDGP 3.1 from the year 2003, however, and also during the course of this study, two more forms of mRNA that arise by alternative initiation of transcription and alternative splicing were predicted. The encode proteins with molecular weights of 144 kDa and 54 kDa, which have not been reported in mammals up to now (Fig. 2.4). Besides, there are differences in the sequence of the previous and the newly predicted versions, and thus in alternative splicing. Comparison revealed that the *Drosophila* genomic *dfer* unit differs in number, size, and arrangement of introns and exons from vertebrate *fes* and *fer* genes.

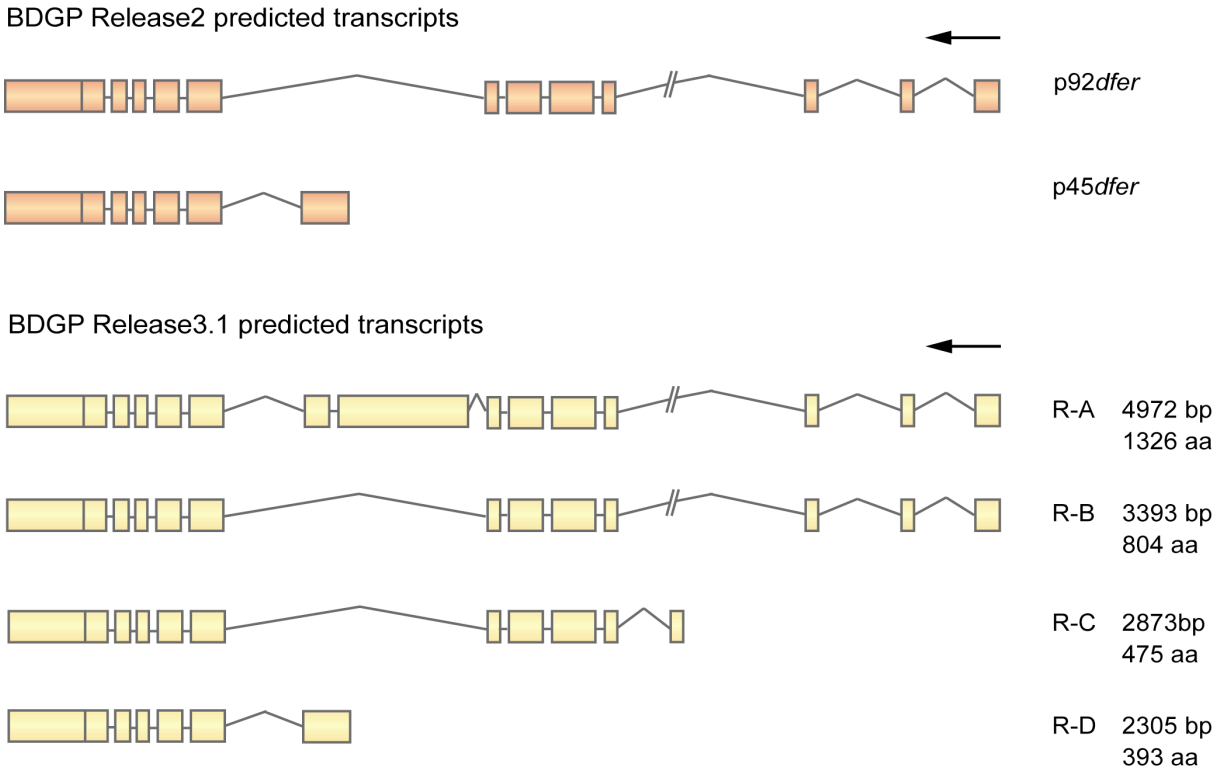

Fig. 2.4 Predicted mRNA transcripts for the DFer kinase. (upper) In the old version of the Berkeley *Drosophila* Genome Project BDGP Release 2.1, two different mRNAs corresponding to the published 92 kDa (p92*dfer*) and 45 kDa (p45*dfer*) DFer proteins were predicted. (lower) The new BDGP 3.1 version predicts four mRNA transcripts, two of them not documented in the literature so far. Arrows mark the direction of transcription. Full boxes represent exons, lines introns. *R-A, R-B, R-C, R-D*, names attributed to the different mRNA transcript isoforms.

The physiological function of DFer in *Drosophila* is entirely unknown. There are only two studies to date, one revealing *dfer* expression throughout the life cycle of *Drosophila*, being transient in some tissues and continuous in others, with prominent expression in imaginal discs, gut, muscle, testes, ovaries, immature blood cells, retina, and other neural tissues (Katzen et al. 1991). The other study found DFer protein to be in part loosely

associated with cytoplasmic membranes and that it is capable of transforming cells (Paulson et al. 1997). Interestingly, when analysing the sequence, there are no motifs that could account for the reported membrane association.

2.3 Functional overexpression analyses of *dfer* in *Drosophila*

2.3.1 *Dfer* cDNA displays the same phenotype upon overexpression as the *dfer*^{zwim} line

Due to the fact that in the *dfer*^{zwim} allele the EP-element inserted close to the 5' UTR of *dfer* and is oriented in the direction of transcription, it is very likely that overexpression of only this gene is induced by GAL4. To exclude a second EP-element insertion in this fly line, Southern blotting was performed on isolated genomic DNA using probes directed against the kanamycin resistance gene of the EP-element, which revealed only one EP-element insertion (data not shown). A first hint that endogenous *dfer* overexpression suppresses the APP-induced phenotype came from crosses using the EP(3)707 fly line (*dfer*^{EP707}) with an EP-element insertion within the same transcription unit identified in another screen (Rorth et al. 1998), showing the same suppression as the *dfer*^{zwim} line (data not shown). To prove that indeed *dfer* is the gene affected in the EP-element fly line, the cDNA of the canonical isoform of *dfer*, i.e. the R-B transcript (the published *p92* kinase form) (Katzen et al. 1991), was cloned into the P-element vector pUASt and transgenic flies were generated by P-element induced germline transformation. These transgenic UAS-*dfer-B* (hereafter referred to as UAS-*dfer* line) flies were crossed to the *apterous*-GAL4 driver line (*ap*-GAL4), an enhancer-trap line that induces transgene expression in the dorsal compartment of the wing imaginal disc. The offsprings displayed the same, but more severe phenotype as the *dfer*^{zwim} EP line (Fig. 2.5 A). In fact, the wing development was massively disturbed. The phenotypic occurrence was extremely variable at 18°C, where GAL4 induced transgene expression is very low, ranging from wings resembling wildtype wings, over vein delta formation at vein L4, up to blistered wings filled with hemolymph. Moreover, the wing hinge of the flies, which is the region that joins the wing and thorax, was deformed, and a held up wing phenotype with flies displaying abnormal wing posture was noticed. Additionally, an upward curvature of the wing was observed caused by a reduced size of the dorsal compartment. Crosses were also carried out at higher temperatures such as 25°C and 28°C, being lethal at 28°C (summarized in Table 2.2). These observations strongly indicate that *dfer* is indeed the gene affected by the *dfer*^{zwim} EP insertion.

2.3.2 *Dfer* cDNA expression suppresses the APP-induced blistered wing phenotype

In order to verify the results obtained from the screen, the generated transgenic UAS-*dfer* fly line was tested for its ability to suppress the APP-induced blistered wing phenotype. APP expression itself caused an edged wing phenotype at 18°C when using the *ap*-GAL4 fly line. *Dfer* expression, however, displays a stronger phenotype than APP, inducing wing blistering and curling. When expressing both transgenes in the wing, suppression of the phenotype was observed (Fig. 2.5 B). The resulting wings were no longer edged but rather slightly curled, revealing a shortening of the dorsal wing layer compared to the ventral wing layer. This can be explained by the stronger *dfer* overexpression induced by the pUASt vector in comparison to the EP line. When performing the same crosses at 25°C, APP actually rather suppressed the *dfer*-induced phenotype, with flies showing reduced phenotypic aberrations compared to *dfer* transgene expression alone. Thus, both the *dfer*^{zwim} EP line and the UAS line are capable of suppressing the APP-induced blistered wing phenotype.

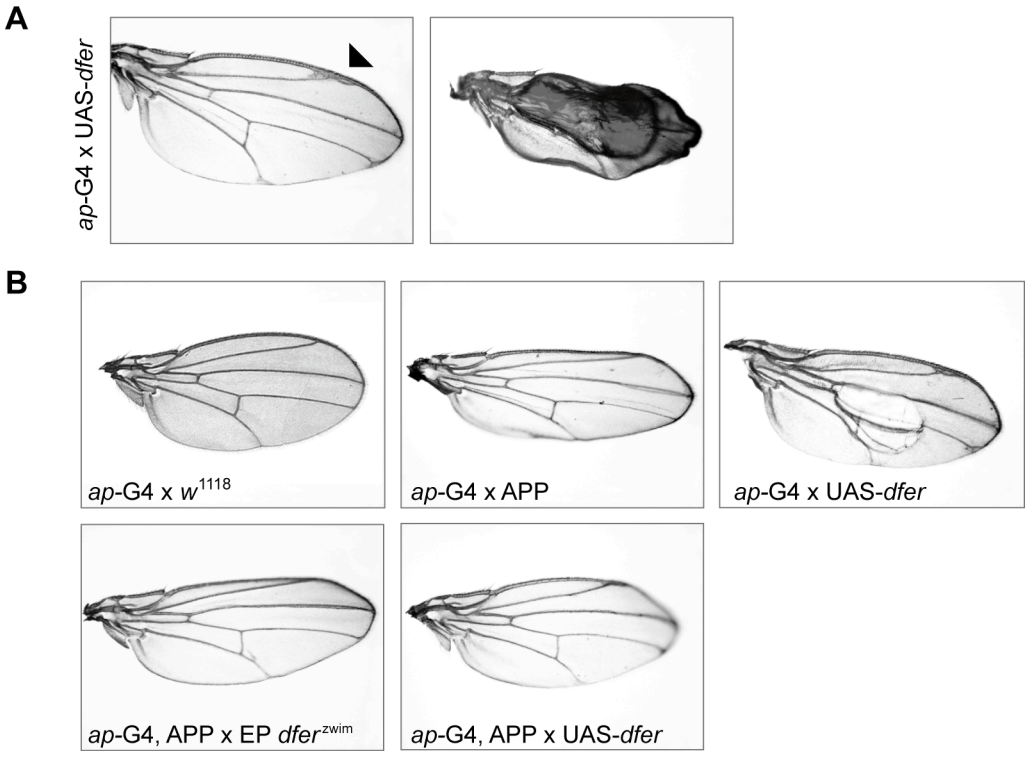

Fig. 2.5 Transgenic *dfer* expression suppresses the APP-induced blistered wing phenotype. (A) Expression of transgenic *dfer* induced by crosses to *ap*-GAL4 lines causes wing defects even at 18°C. Wings display varying phenotypes, having vein broadening (vein deltas) at the end of vein L4 (left, marked by an arrow head) and dark blisters filled with hemolymph (right). (B) Whereas APP expression causes wing edging on the upper and lower border of the wing, *dfer* expression results in wing blistering. Expressing both transgenes simultaneously restores the wildtype-like wing, displaying only slight curling on the wing tip.

2.3.3 *Dfer* cDNA expression does not suppress the APP-induced PNS development defect

Transgenic expression of human APP in *Drosophila* was recently reported to interfere with Notch signaling during PNS development (Merdes et al. 2004). Overexpression of APP induced Notch gain-of-function phenotypes, i.e. cell fate transformations during the mechano-sensory organ development. As *dfer* showed genetic interaction with APP during cell adhesion, it was tested for its involvement in these phenotypes. However, *dfer* overexpression alone using *scabrous*-GAL4, a driver line causing exclusive expression in the sensory organ cell lineage, had no effect on mechano-sensory organ development and did not induce any bristle abnormality. Moreover, when simultaneously expressing *dfer* with APP, the APP-induced phenotypes were not altered (data not shown). In conclusion, though *dfer* overexpression suppresses the APP-induced blistered wing phenotype, it is not involved in the APP-induced PNS development defect and seems to act wing-specifically only on the proposed cell adhesion function of APP.

2.3.4 *Dfer* overexpression analysis during development

Since the overexpression of *dfer* in the dorsal compartment of the wing imaginal disc caused a strong phenotype, the *dfer*^{zwim} EP fly line and the UAS-*dfer* fly line were both crossed to a broad range of GAL4 driver lines, allowing the expression in different tissues and developmental time points, in order to identify additional developmental processes affected. The observed phenotypes upon *dfer* overexpression are summarized in Table 2.2.

Overall, the transgene expression with the UAS-*dfer* line revealed similar but stronger phenotypes compared to *dfer* overexpression from the EP line (Tab. 2.2, Fig. 2.6). Crosses were also performed with the EP(3)707 line from the Rorth Collection and produced the same phenotypes as the *dfer*^{zwim} EP fly line. The wing development seems to be the main developmental process affected upon overexpression. The flies displayed a variety of wing phenotypes, suggesting massive interference with cell adhesion. Other tissues or developmental process appeared not to be influenced, as, for instance, expression with *daughterless*-GAL4 during the embryonic stages did not disturb development and analysis of the embryonic morphology by cuticle preparations revealed normally developed embryos (data not shown). Likewise, expression in neurons using *elav*-GAL4 or in the photoreceptor cells of the eye imaginal discs using *sevenless*-GAL4 caused no phenotypic aberrations even at high temperatures where transgene expression is elevated. Only expression with *GMR*-GAL4 (*glass multiple reporter*), a strong line expressing GAL4 posterior to the morphogenetic furrow of the eye imaginal disc, induced a slight rough eye phenotype. Increasing the dose of the transgene expression in the eye by having two copies of the UAS-

dfer transgene resulted in a rough eye phenotype with irregularly spaced ommatidia and disturbed bristle patterning (data not shown).

2.3.5 *Dfer* overexpression causes Notch and Wingless loss-of-function phenotypes

Although some of the before mentioned crosses resulted in cell adhesion defects in the wing as originally observed for *ap*-GAL4 induced expression, *dfer* expression rather induced wing tissue loss, namely wing margin notching. The most striking phenotypes were observed upon overexpression of *dfer* in the wing pouch induced by crosses to the *scalloped*-GAL4 driver line (*sd*-GAL4) (Fig. 2.6). The same wing defects were obtained when using *69B*-GAL4 (general expression in the wing disc), *engrailed*-GAL4 (in the posterior wing compartment) and *vestigal*-GAL4 (at the wing margin) driver lines (Table 2.2). The severity of the notching of the wing increased with elevated expression level, leading to flies with incompletely developed wing structures and increased pupal lethality. The phenotypes ranged from flies having slight notches, veins with increased width or interveins missing, to flies carrying either sickle-like or fan-shaped wings, or no more than tiny black balloon-like structures with an amorphous mass of the presumptive wing tissue (Fig. 2.6 B).

Table 2.2 Phenotypes caused by overexpression of the *dfer* EP and UAS fly line.

GAL4 fly lines	EP line 28°C	UAS line 28°C	UAS line 25°C	UAS line 18°C
scalloped (wing pouch)	strong notches in the wing, sometimes blisters, vein deformations	partially lethal, strong notches, blisters and balloons 3rd leg pair deformed and shortened	notches, blisters and balloons, vein deformations	some notches
MZ 1580 (ubiquitous 3rd instar)	pupal lethal	lethal, slow development	lethal, slow development	lethal, slow development
a*pterous* (dorsal wing compartment)	partially lethal, blisters, sometimes "zwirbel"	lethal, blisters and "zwirbel" wing hinge deformed	partially lethal, blisters, vein deformations	blisters, deltas and vein deformation, vein broadening
1878 (ubiquitous 3rd instar)	partially lethal some notches vein deltas	lethal, notches, weak flies	partially lethal, notches, vein deformations, deltas, vein broadening	-

69B (embryonic epiderm, imaginal discs)	vein deformations, notches	partially lethal, blisters and ballons	some notches, vein deltas, vein deformations	vein deltas
engrailed (posterior wing compartment)	notches, vein deformations	Notches, vein deformations (veins missing, extra)	notches, vein deformations	vein deltas
vestigal (D/V boundary, wing pouch)	some vein deformations, few slightnotches	some vein deformations 50% notches	-	-
actin 5c (ubiquitous)	partially lethal, vein and wing defects	lethal, slow development	lethal, slow development	lethal, slow development
GMR (eye imaginal disc)	slight defect/ rough eye	slight defect/ rough eye	-	-
twist (embryonic, in imaginal discs)	-	scutellum deformed, blistered wing, vein deformations	n. p.	n. p.
Gal4 ^{332} (imaginal discs)	n. p.	partially lethal, slight notches	n. p.	n. p.
daughterless (embryonic)	-	pupal lethal	wing and vein defects	n. p.
armadillo (low ubiquitous)	-	-	-	-
elav (neuronal)	-	-	-	-
patched (A/P wing boundary)	-	wing curling, some pupal lethal	slight wing curling	n. p.
distalless (wing pouch)	n. p.	pupal lethal, strong notches, balloons	strongly notched veins partially thickened or absent	n. p.
scabrous (sensory organ cell lineage)	-	-	-	-
sevenless (photoreceptor cells in the eye dics)	-	-	-	-

Flies were crossed to various GAL4 driver lines and analysed for phenotypes occurring in the adult fly. Crosses were performed at the indicated temperatures, allowing low GAL4 expression at 18°C and high GAL4 expression at 28°C. *n. p.*, not performed; -, no phenotype.

The loss of wing tissue and the formation of notches, as well as the aberrant wing vein thickening, are reminiscent of loss-of-function mutations in the Notch receptor pathway (reviewed Lai 2004; de Celis 2003). The wing margin defects also resemble late loss of Wingless activity (Couso et al. 1994).

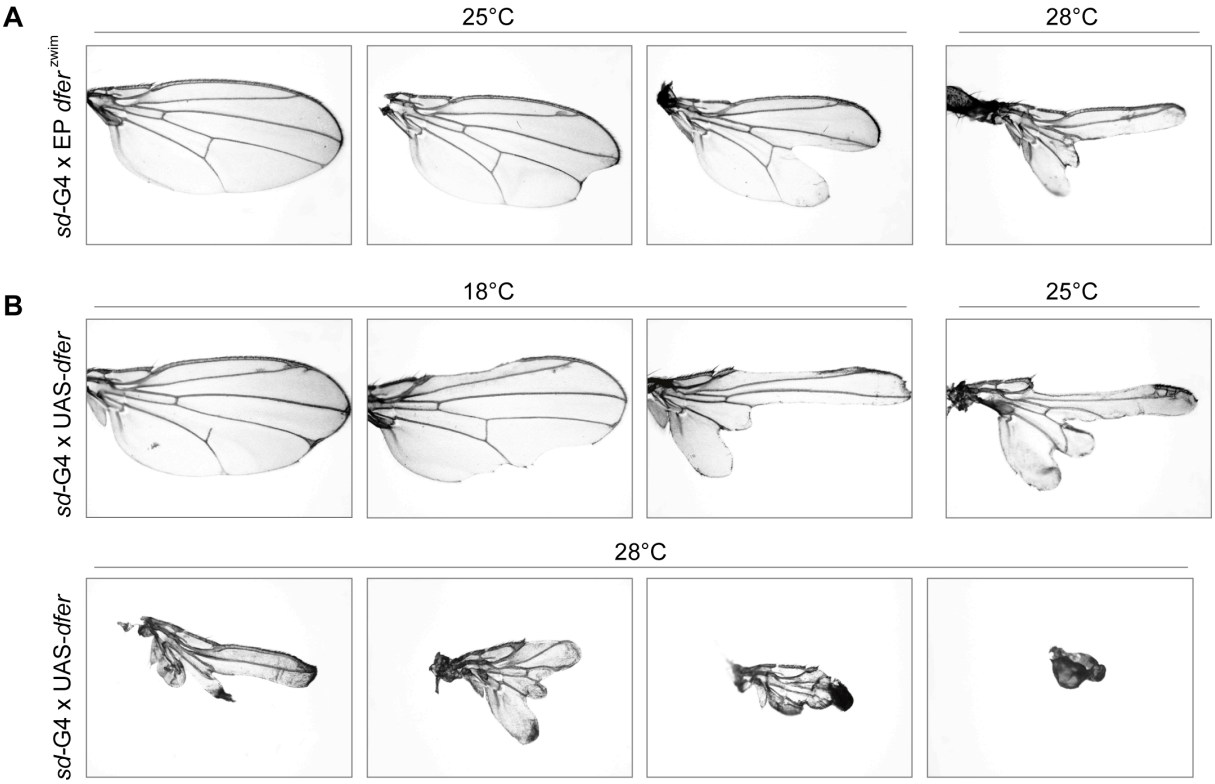

Fig. 2.6 *Dfer* expression in the wing causes margin notches. (A+B) *sd*-GAL4 induced overexpression of the *dfer* gene in the *dfer*^{zwim} EP fly line (A) or the *dfer* transgene in the UAS-*dfer* line (B) results in a variety of wing margin notching phenotypes, being more severe at higher temperatures (indicated).

Very strong overexpression, mediated by elevated transgene expression or an increased dosage of *dfer* expression, led with low frequency to flies displaying a loss of the wing, changes in the structure of the thorax or even wing-to-notum transformations (Fig. 2.7). These transformations, i.e. a replacement of the wing structure by an extra miniature dorsal thorax, are characteristic for *wingless* mutants (Morata and Lawrence 1977; Sharma and Chopra 1976) and mutants of the Wingless signaling pathway such as *armadillo* (Pfeifer et al. 1991). The same effect was observed using the *engrailed*-GAL4 driver line.

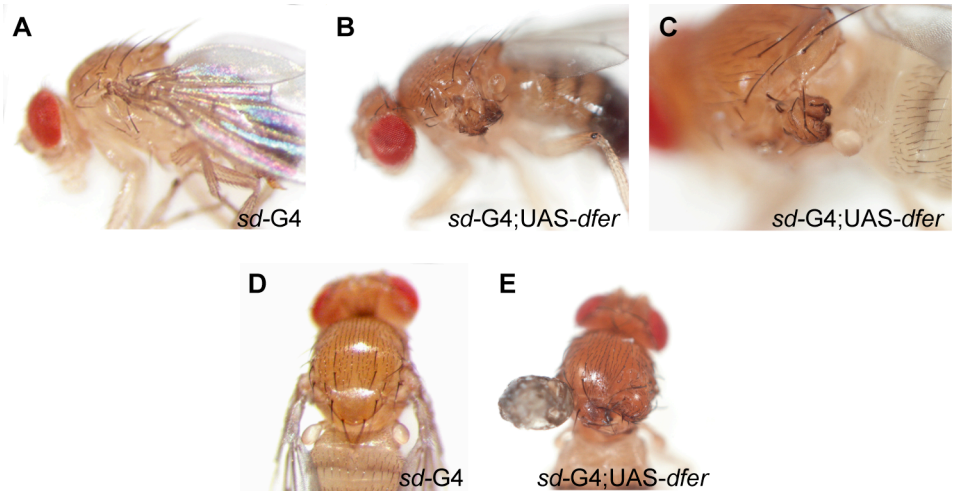

Fig. 2.7 *Dfer* overexpression caused wing-to-notum transformations. Flies carrying two copies of both the *sd*-GAL4 enhancer-trap and the UAS-*dfer* transgene occasionally exhibit a wing-to-notum transformation with an extra miniature thorax forming (B+C) or a spherical deformity in the thorax (E) instead of a wing structure (A+D). Flies were crossed at 25°C.

In summary, overexpression of *dfer* in the wing imaginal disc tissue during wing development causes severe wing and thoracic phenotypes resembling those displayed by loss-of-function mutations of the Notch and Wingless pathways. Both signaling pathways co-operate in wing patterning and are particularly important for the formation of the dorsal-ventral (D/V) boundary (Ng et al. 1996; Milan et al. 2003). Loss of Notch or Wingless signaling leads to a loss of the D/V boundary signal. This could imply that *dfer* overexpression is negatively interfering with these essential developmental pathways.

2.4 Generation and overexpression analyses of *dfer* isoforms and *dfer* mutants

The *dfer* gene is predicted to have several transcriptional isoforms caused by alternative splicing and alternative initiation of transcription. To reveal the functional relationship between these different isoforms, i.e. if they cause the same phenotypes upon overexpression, the *dfer-D* isoform (R-D transcript) was first isolated from a cDNA library and, together with the predicted *dfer-A* (R-A transcript) isoform, cloned into the pUASt vector for transformation of flies (Fig. 2.8). Whereas the overexpression of the small isoform *dfer-D* did not result in any phenotype even at higher temperatures, the long isoform *dfer-A* showed similar phenotypes as *dfer* with wing notching, but also smaller wings (Table 2.3). Additionally, overexpression in the eye induced bristle defects.

To determine whether the kinase activity of DFer is necessary for phenotype induction, different mutant forms were generated (Fig. 2.8). The mammalian Fes and Fer

kinases are proposed to form oligomers in order to be active. The integration of a mutation within the ATP binding domain, namely the amino acid lysine at position 590, by site-directed mutagenesis resulted in a kinase-defective mutant and, moreover, showed a dominant-negative effect on overall Fes kinase activity (Hjermstad et al. 1993; Takashima et al. 2003).

In order to test if the same is true for the *Drosophila* DFer kinase, a putative dominant-negative construct (*dfer-DN*) with a point mutation at the appropriate homologous site, i.e. lysine 571 substitution to arginine (K571R), was generated and transgenic flies were produced. Similarly, only the N-terminal part of the DFer kinase (*dfer-N*) containing the regulatory CC domains needed for oligomerization and lacking the kinase domain, which should also act as a dominant-negative mutant, was cloned into the pUASt vector. Overexpression of the generated constructs UAS-*dfer-DN* and UAS-*dfer-N* using different GAL4 driver lines did not cause any phenotypic aberration even at 28°C. However, co-expression of these constructs with the wildtype *dfer* transgene resulted in a suppression of the phenotype caused by *dfer* overexpression, thus acting dominant-negatively as expected (data not shown). The expression of all generated transgenes was verified upon antibody production against DFer by detecting transgenic protein expression using Western blotting (data not shown).

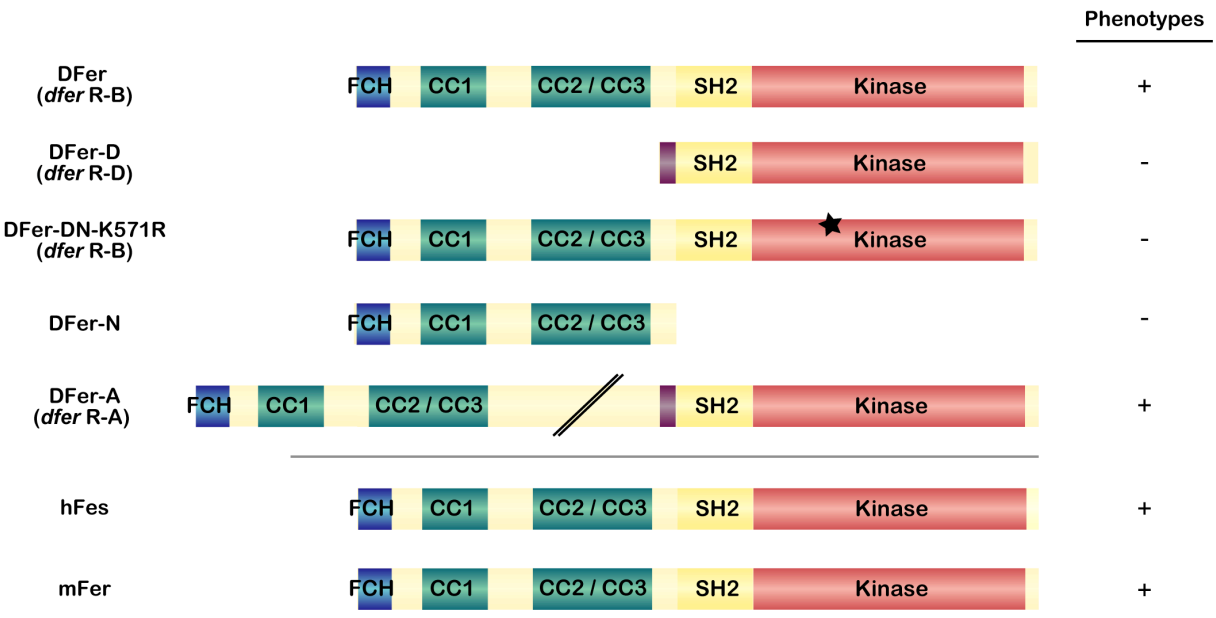

Fig. 2.8 Schematic overview of the transgenic constructs generated. The ability of the transgenic constructs to induce phenotypes in *Drosophila* upon overexpression is indicated. The different protein domains are depicted. The star marks the amino acid K571R substitution.

Taken together, only the two long isoforms of *dfer*, namely R-A and R-B, induce wing-specific phenotypes upon overexpression. The N-terminal domain with the regulating CC motifs and the kinase activity seem to be indispensable for phenotype induction. Additionally,

oligomerization as it occurs in the case of mammalian Fes and Fer kinase might also play a role in regulating the kinase activity of *Drosophila* DFer as co-expression of the *dfer* transgene and the dominant-negative transgenes resulted in a loss of *dfer*-induced phenotype.

2.5 Generation and overexpression analyses of the mammalian homologs of DFer kinase

Since *Drosophila* DFer and the mammalian Fes and Fer kinases exhibit high sequence conservation, and the mammalian homologs were identified as proto-oncogenes, it was interesting to resolve if these mammalian kinases display the same phenotype upon overexpression as their *Drosophila* homolog. Therefore, murine *fer* and human *fes* were cloned into the pUASt vector and transgenic flies were generated (Fig. 2.8). Transgenic protein expression was verified by western blotting and showed comparable expression levels (data not shown). When these flies were crossed to various GAL4 lines for transgene expression, similar phenotypes were induced as by *dfer* overexpression, though producing stronger effects (summarized in Table 2.3). Comparing the severity of obtained phenotypes, mouse Fer appeared to be more potent than human Fes followed by *Drosophila* DFer. Expression of Fer in the eye by *GMR*-GAL4 caused a severe rough eye phenotype with strong reduction in eye size, being dependent on the dose of expression (not shown).

In general, flies carrying the mammalian transgenes died in earlier stages than flies carrying the *Drosophila* transgene, for example, Fer expression with the ubiquitous *actin-5c*-GAL4 line caused larval death in the third instar stage compared to early pupal lethality for *dfer* expression. Additionally, expression with *sd*-GAL4 resulted either in flies dying as early pupae or in stronger wing phenotypes as balloon-like wings or no wings at all. The third leg pair was deformed, leaving flies too weak for pealing out of the pupal case. Fes, however, induced weaker effects than Fer.

Similarly like DFer, the mammalian Fes and Fer kinase were able to suppress the APP-induced blistered wing phenotype when crossed at 25°C. But as APP expression showed weaker phenotype than murine Fer or human Fes expression, APP actually rather suppressed the kinase-induced wing phenotype, revealing flies with reduced phenotypic aberrations (data not shown).

In conclusion, the mammalian Fes and Fer kinase seem to act on the same pathway like their *Drosophila* homolog DFer, since their expression in flies induced similar phenotypes as *dfer* overexpression. In addition, they are capable to suppress the APP-induced wing phenotype, thus interacting with APP in the same way as DFer.

Table 2.3 Phenotypes caused by overexpression of the different transgenic fly lines.

GAL4 fly lines	UAS-dfer line	UAS-dfer-A line	UAS-hfes line	UAS-mfer line
scalloped	partially lethal, strong notches, blisters and balloons	partially lethal, mini wings	partially lethal, strong notches, blisters and balloons	partially lethal, strong notches, blisters and balloons, 3rd leg pair deformed
MZ 1580	lethal, slow development	3rd instar lethal, slow development	3rd instar lethal, slow development	2nd instar lethal, slow development
apterous	pupal lethal, strong blisters and "zwirbel"	pupal lethal, strong blisters, slow development	pupal lethal	pupal lethal
engrailed	posterior notches	posterior wing part curled, wings smaller	pupal lethal, blackened and mini wings	pupal lethal
actin 5c	early pupal lethal, slow development	early pupal lethal, slow development	early pupal lethal, slow development	3rd instar lethal, slow development
GMR	slight defect/ rough eye	slight defect/ rough eye	irregularly spaced eye bristles	rough eye, reduced eye size
twist	small scutellum, shortened thorax	shortened abdomen, cleft in abdomen, with spackles	-	-
daughterless	pupal lethal	pupal lethal	pupal lethal	pupal lethal
elav	-	-	irregularly spaced eye bristles	rough eye
patched	- (wing curling)	-	slight detachment between wing layers	slight detachment between wing layers, some pupal lethal
scabrous	-	n. p.	-	-

Flies were crossed to various GAL4 driver lines and analysed for their phenotypic occurrence in the adult fly. Crosses were performed at 25°C. *n. p.*, not performed; -, no phenotype.

2.6 Analyses of the developmental and spatial expression of *dfer*

2.6.1 *Dfer* is expressed throughout *Drosophila* development

In order to gain insight into the physiological function of the DFer kinase, the expression profile and pattern during *Drosophila* development was analysed on the level of mRNA. Northern blotting was performed on mRNA extracted at various stages of fly development. From all four predicted *dfer* RNA transcripts, the canonical *dfer* isoform with a size of 3.4 kb was the predominant one with expression during all stages of *Drosophila* development (Fig. 2.9). A maternal contribution, however, was not detectable in young 0 to 4 h embryos. Interestingly, the newly predicted large *dfer-A* isoform with a size of 4.9 kb was indeed expressed in *Drosophila*. Expression seemed to be specific for certain developmental stages and tissues as it was only scarcely observed in the pools of 8 to 12 h old embryos and of adult fly heads, but not in pools of total adult fly tissue. Both smaller R-C and R-D transcripts, however, were not detectable.

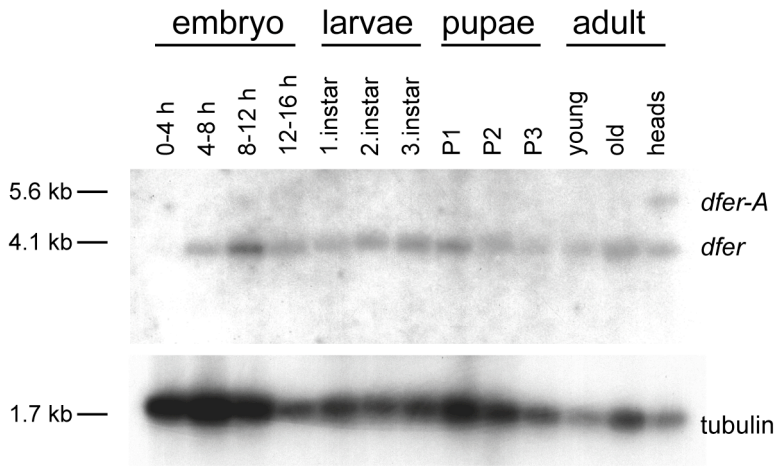

Fig. 2.9 *Dfer* expression during development. The Northern blot shows *dfer* expression during all stages of fly development. The larger *dfer-A* isoform is detectable scarcely at 8-12 h of embryonic development and in extracts from adult heads. mRNA was isolated out of 150 µg total RNA from all developmental stages of *Drosophila* as indicated. A tubulin probe was used as loading control.

2.6.2 Spatial *dfer* expression during embryonic development

To obtain greater resolution and spacial information about the gene expression during the embryonic stages, *in situ* hybridizations were performed. Using probes directed against the full-length transcript of *dfer*, expression was found to be absent during the cleavage stages (stage 1-4). Together with the data obtained from the Northern Blot analysis (Fig. 2.9), it appears that *dfer* expression is zygotic in origin. The expression started at the stage of cellularisation (stage 5, Fig. 2.10 B and C), being predominantly located in the ventral part

of the embryo and in a subset of blastodermal cells, which are presumably vitellophages (yolk nuclei).

During gastrulation, expression was observed in the primordia for the amnioserosa and the proctodeum, and the dorsal epidermis (Fig. 2.10 D, E, F and G). In the stages of germ band elongation, *dfer* expression remained pronounced in the proctodeum and was detectable in the dorsal and ventral epidermis, in somatic muscles, as well as in the mesoderm in a segmental pattern (Fig. 2.10 H, I and J). After germ band retraction was completed (stage 13), expression in the mesoderm appeared to be more uniform and was also observed in the neuroectoderm (Fig. 2.10 K). During dorsal closure in stage 14, *dfer* expression was present in the leading edge cells along the dorsal ridge (Fig. 2.10 L and M). Expression in the cells of the ventral nervous system, presumably the midline glial cells (Fig. 2.10 N, N', O, P and R), continued to the final stages of embryogenesis and expression was also apparent at muscle attachment sites (Fig. 2.10 R), in the tracheal epithelium and the spiracles (Fig. 2.10 Q).

Probes directed specifically against other transcript isoforms of *dfer*, namely against the unique parts of the *dfer-A* transcript and the *dfer-D* transcript, showed a similar expression pattern, being more faint and revealing high background staining (data not shown). The expression of the small *dfer*-D isoform in *Drosophila* is in striking contrast to the expression of the smaller mRNA for the vertebrate FerT kinase, which is restricted to the testis (Keshet et al. 1990; Fischman et al. 1990). However, as the first unique fourteen amino acids of DFer-D are completely identical to the ones found also in the DFer-A form, it cannot be excluded that *dfer*-D is an incorrectly annotated form of the *dfer*-A transcript.

In summary, *dfer* shows zygotic expression during all stages of development, being present in a variety of tissues with changing expression patterns. Most striking is the continuous staining of gut and epidermis, the staining of cells in the ventral nerve cord and the tracheal epidermis, and the enrichment in the leading edge cells of the dorsal epidermis.

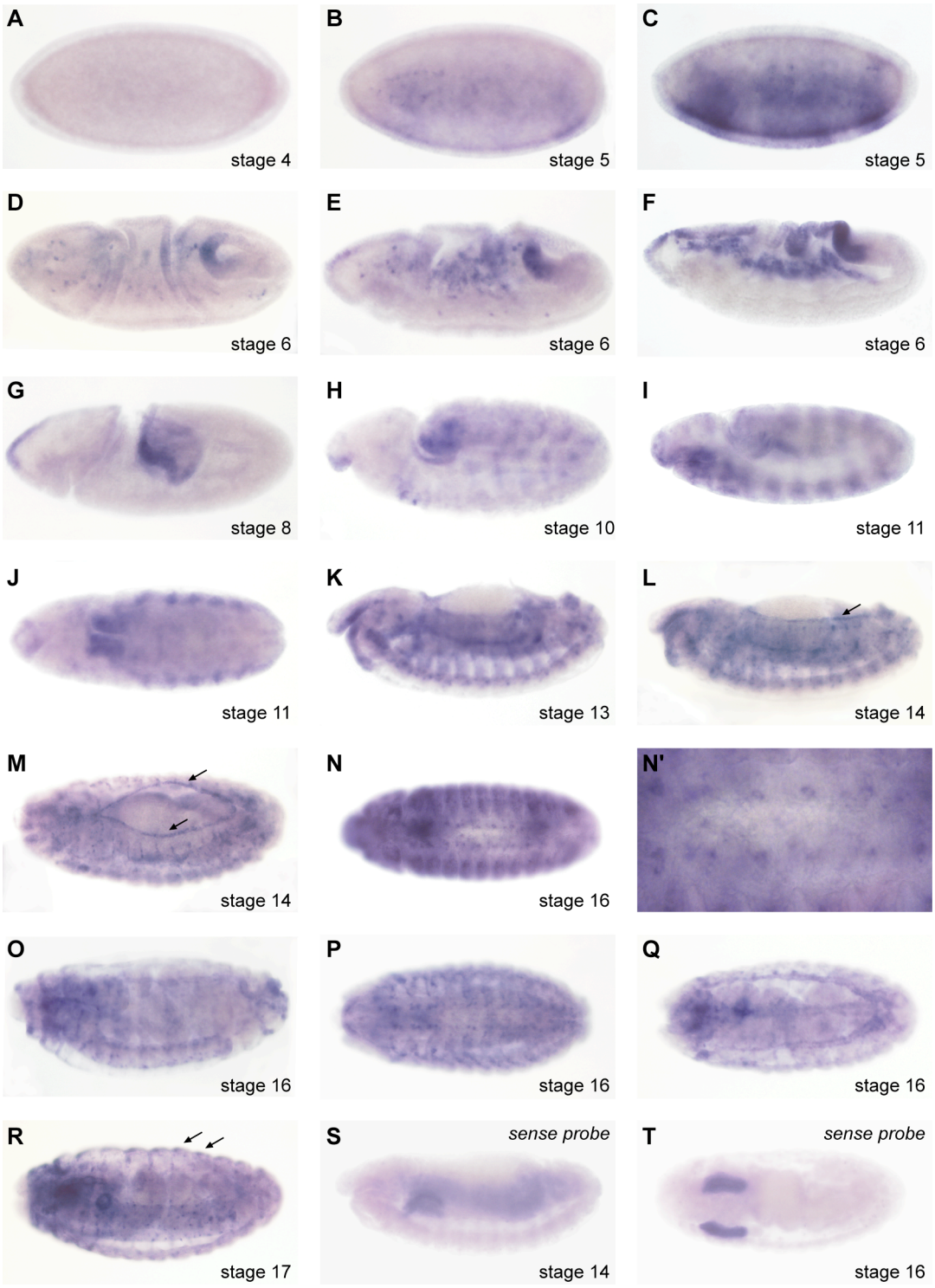

Fig. 2.10 *Dfer* expression during embryogenesis. *Dfer* expression is absent in the syncytial blastoderm (stage 4) (A) and starts in the late cellular blastoderm (stage 5) (B and C). During gastrulation (stage 6-8) (D, E, F and G), expression is detectable in the anlage of the amnioserosa, the hindgut and the dorsal epidermis. Expression continues through germ band elongation (stage 9-11) (H, I and J) and germ band retraction (stage 12-13) (K) and becomes segmental. Following the stages of dorsal closure and head involution (stage 14-15) (L and M), where *dfer* is expressed at the leading edge cells of the dorsal epidermis (arrows), the expression is more general and also detectable in cells of the central nervous system (stage 16-17) (N, N', O, P and R) and in the tracheal epithelium (Q). (R) Expression can also be observed at the muscle attachment sites (arrows). Control *in situ* hybridization with sense *dfer* probes reveal no specific staining (S and T); background staining appeared in the salivary glands (T). Embryos are shown in a lateral view, with anterior to the left. (J, M and Q) are dorsal views, (N and P) ventral views, (N') is an enlargement of (N) showing cells in the ventral nerve cord.

2.7 Generation of DFer antibodies and DFer protein expression analysis

2.7.1 Generation of DFer antibodies and functional testing

Another way to study expression of the *dfer* gene and to verify the results obtained from the Northern blot and the *in situ* hybridization is on the level of protein expression. Despite the high resemblance between the *Drosophila* DFer kinase and the mammalian Fes and Fer kinases, an attempt to detect the overexpressed *Drosophila* DFer kinase in fly head extracts with antibodies directed against conserved regions of the viral v-Fps and the human h-Fes failed and showed only unspecific staining on a Western blot. Concurrently, immunoprecipitation of *in vitro* translated DFer protein using the v-Fps and h-Fes antibodies was unsuccessful. As these antibodies were not able to recognize the *Drosophila* ortholog, a specific DFer antibody had to be produced.

In the first place, expression of the recombinant full-length DFer protein (encoded by the *dfer* R-B transcript) in bacteria was performed and great amounts of protein obtained. However, the protein was completely insoluble, most probably because of the CC domains causing oligomerization and subsequent aggregation and thus insolubility of the protein. The protein was neither soluble in 6M Urea nor in 4M Guanidine hydrochloride and various dialysis protocols were ineffective. As none of the diverse protocols available in the literature led to soluble protein, two different protein fragments of DFer were chosen for expression and tagged with GST in order to produce antibodies (Fig. 2.11 A). One protein fragment, DFer-N, contained the first 128 N-terminal amino acids that are common to the two longer forms DFer and DFer-A. The other fragment, DFer-SK, included the amino acids 362 to 563, forming the SH2 domain and parts of the kinase domain that are found in all DFer kinase forms. The fragments were obtained performing PCR with appropriate primers and cloning these fragments in the pGEX vector for GST tagging and protein expression. Both protein fragments were used jointly for the immunization of two rabbits. The retrieved serum of both rabbits was tested for its specificity on Western Blots with fly head extract from DFer overexpressing *dfer*^{zwim} EP flies and UAS-*dfer* flies using pre-immune serum as a control. A band was detected at the expected height of approx. 92 kDa, which was also visible when performing immunoprecipitation with *in vitro* translated DFer protein (data not shown). Knowing that the sera contained antibodies specifically recognizing the DFer protein, the antibodies were then purified in two steps using protein A-agarose and antigen-antibody affinity chromatography. This strategy allowed the separate treatment of the individual rabbit sera, the removal of GST antibodies, as well as the separate purification of the antibodies produced against the different protein fragments. The obtained purified antibodies were first tested in a Western blot for their ability to recognize overexpressed DFer protein in the fly head (Fig. 2.11 B).

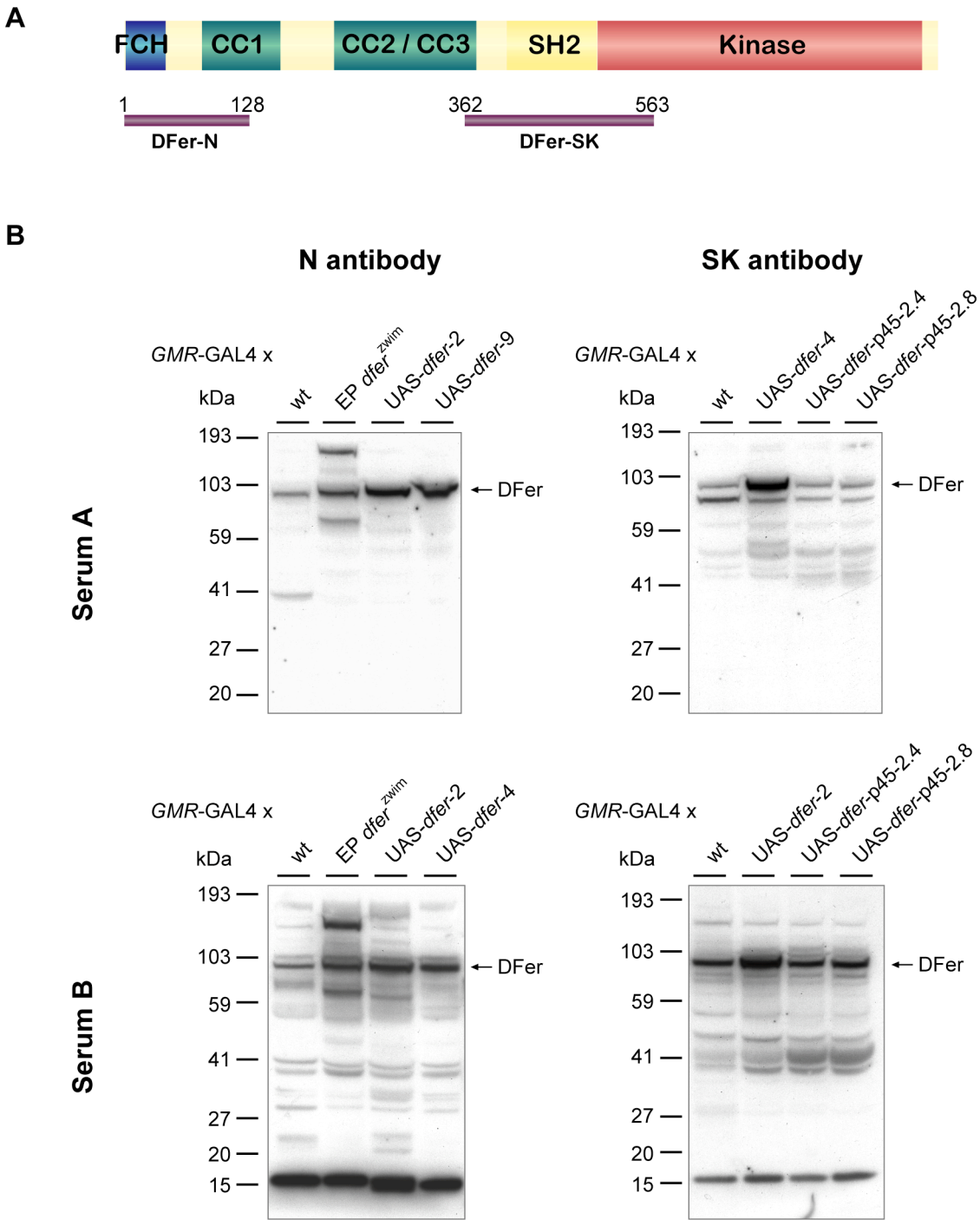

Fig. 2.11 DFer antibody production and testing. (A) The DFer-N protein fragment (amino acids 1 to 128) and the DFer-SK protein fragment (amino acids 362 to 563) were used for the generation of specific DFer antibodies. (B) The purified antibodies were tested by Western blotting. The indicated fly lines were crossed to *GMR*-GAL4 driver lines at 25°C to induce protein expression in the eye. For each cross, protein extract was isolated from 10 fly heads and subjected to SDS-PAGE and Western blotting using the differently obtained antibodies. Serum A and Serum B, separately purified sera from the two immunized rabbits; N antibody, isolated using the DFer-N protein fragment as an antigen for the antigen-antibody affinity chromatography; SK antibody, isolated using the DFer-SK protein fragment as an antigen.

Both antibodies, the N antibody directed against the DFer-N fragment and the SK antibody directed against the DFer-SK fragment, detected a band at approx. 92 kDa that

presumably represents the canonical DFer protein as overexpression with the *dfer*^{zwim} EP line or the UAS-*dfer* line caused a strong increase in the density of this band. Thus, endogenous DFer protein seems to be also present in the fly head. The SK antibody, as expected, recognized in addition a band specifically upon overexpression of the originally described small DFer-p45 kinase form (UAS-*dfer-p45* fly line) at approx. 45 kDa (Paulson et al. 1997). The endogenous form, however, could not be detected, reflecting the low abundance of this isoform. The antibodies were also able to recognize endogenous and overexpressed DFer protein in extracts isolated from embryos and wing imaginal discs (data not shown). Moreover, both antibodies were capable to immunoprecipitate *in vitro* translated DFer protein, DFer protein expressed in cell-culture and DFer protein from embryo extracts (data not shown).

In summary, the generated N antibody and SK antibody recognize specifically the DFer protein expressed upon different conditions in both Western blotting and immunoprecipitation. The SK antibody, as it is generated against a protein fragment containing the SH2 domain and parts of the kinase domain, detects additionally the overexpressed small DFer-p45 protein.

2.7.2 Identification of the long protein form DFer-A

Surprisingly, when overexpressing the endogenous *dfer* transcription unit using the *dfer*^{zwim} EP line and afterwards performing Western blotting on protein extract from fly heads, two additional bands appeared at about 140 kDa and 80 kDa together with the expected DFer protein band (Fig. 2.11 B; Fig. 2.12 A). These bands also emerged when using the *dfer*^{EP707} line causing the same overexpression of the endogenous *dfer* locus. One explanation for the higher band might be an oligomerization of the kinase, which is known for the mammalian Fes and Fer kinase (Craig et al. 1999; Read et al. 1997). However, this is unlikely as these kinases either homotrimerize in the case of Fer kinase, or form pentamers or even higher order oligomers in the case of Fes kinase, and the observed band size would not fit to the expected size range. Phosphorylation of the kinase could also be ruled out since treatment with alkaline phosphatase did not alter the band size, which was also true for the lower 80 kDa band. Knowing the prediction of transcripts from the *dfer* gene, the 140 kDa band would fit to a 144 kDa protein translated from the predicted R-A transcript (DFer-A), whose existence was already verified by the Northern blot analysis (Fig. 2.9). Overexpression of the DFer-A protein using the transgenic UAS-*dFer-A* fly line revealed a band at the same size (data not shown). Thus, the antibodies were able to recognize the long protein form DFer-A upon overexpression of the endogenous locus, although it could not be detected in wildtype flies. The appearing extra 80 kDa band remained unidentified, but

could well be a product of a so far unpredicted *dfer* transcript isoform.

When overexpressing the endogenous *dfer* transcription unit in another tissue like the wing imaginal disc, there were no extra bands of 140 kDa and 80 kDa, no matter if the *dfer*^{zwim} EP line or the *dfer*^{EP707} line was used for overexpression (Fig. 2.12 B). It is quite speculative to assume that there might be factors in the wing, which prevent the expression of a particular transcript isoform or cause its degradation prior to translation, or, the other way around, head-specific factor that favor the alternative splicing. Nevertheless, it is an interesting finding when thinking of the restricted expression of the large *dfer R-A* transcript isoform in the adult fly head but not in the overall adult fly tissue as previously shown in the Northern blot (Fig. 2.9).

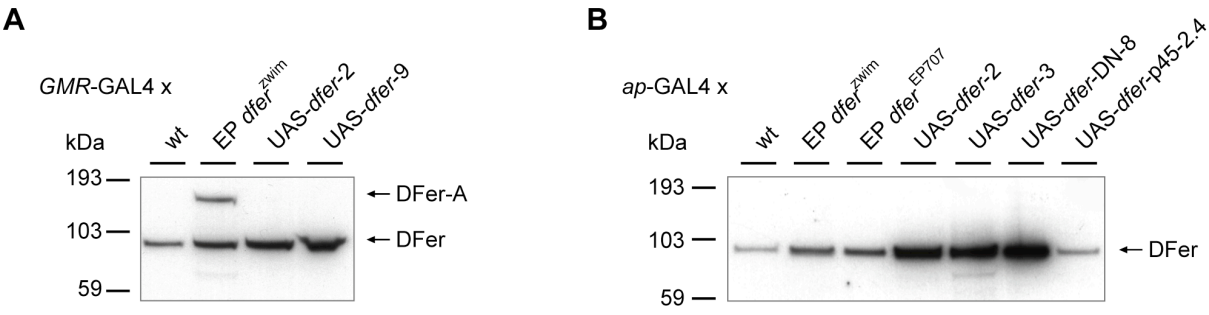

Fig. 2.12 DFer expression in extracts from adult eye and imaginal wing discs. (A) DFer protein expression in the adult eye. The indicated fly lines were crossed to *GMR*-GAL4 driver lines at 25°C. For each cross, protein extract was isolated from 10 fly heads. (B) DFer protein expression in the imaginal wing disc. The indicated fly lines were crossed to *GMR*-GAL4 driver lines at 25°C. For each cross, protein extract was isolated from 20 dissected wing imaginal discs. Protein extracts were subjected to SDS-PAGE and Western blotting using the αDFer N antibody.

2.8 The relationship between APP and DFer interaction

2.8.1 *Dfer* and APPΔCT-GFP

The EP-mutagenesis screen for suppressors of the APP-induced blistered wing phenotypes was based on previous findings that both the extracellular and intracellular domain of APP are necessary for phenotype induction and that APP functions as a signal transduction receptor (Fossgreen et al. 1998). In the course of another study, various deletion constructs of APP were constructed and transgenic flies were generated to map the motifs responsible for blistered wing phenotype induction (Soba 2004). Surprisingly, all deletions and mutations within the C-terminal domain of APP were still able to induce a similar phenotype as wildtype APP, though with variations in phenotype strength. Even the complete truncation of the APP intracellular domain by replacement with GFP in APPΔCT-GFP expressing flies did not abolish phenotype induction (Soba 2004) (Fig. 2.13 C). To test if

dfer overexpression can modify the phenotype induced by APPΔCT-GFP, both constructs were co-expressed in the dorsal wing compartment using *apterous*-GAL4 driver lines (Fig. 2.13 E). Unexpectedly, a suppression of the wing phenotype was observed similar to the wildtype APP construct (see Fig. 2.5 B). As DFer is a cytoplasmic non-receptor kinase and the intracellular domain of APP would be the putative interaction site, the deletion of this domain clearly indicates that DFer and APP cannot interact directly. The nature of the genetic interaction between *dfer* and APP is therefore likely to be indirect, probably through interference with cell-cell adhesion.

2.8.2 DFer overexpression has no effect on APP processing or secretion in cell culture

Having an antibody in hand against the DFer protein allowed a more detailed study of the relationship between APP and DFer. To start with, the effect of DFer co-expression on APP expression and processing was analysed in cell culture. APP N-myc and different *dfer* constructs, namely *dfer*, *dfer-DN* and *dfer-A*, were cloned into a pMT vector, allowing Cu^{2+} inducible high-level expression under control of the metallothionine promoter. S2 cells were transiently co-transfected with myc-tagged APP and the different *dfer* constructs, and following induction and expression, cell lysates were analysed by SDS-Page and Western blotting. Detection with an α–myc antibody recognizing the full-length form and the secreted form of APP showed no effect on APP expression and processing upon co-expression of the different *dfer* constructs though all constructs were expressed (Fig. 2.13 F). Similarly, detection with an α–APP CTF antibody recognizing the C-terminal fragment (CTF) of processed APP showed no effect on APP processing. In particular, no difference in APP expression and APP processing between co-transfections with the active DFer kinase or with the inactive DFer-DN kinase was visible, arguing that the activity of the kinase does not alter APP metabolism. That the kinase was indeed active and able to auto-phosphorylate itself could be shown by detection with an α–phosphotyrosine antibody. However, there was no alteration of APP phosphorylation detectable. Furthermore, when performing a similar experiment in a collaboration with P. Soba, Heidelberg, transiently co-transfecting human COS cells with APP and *dfer*, no effect on APP processing could be found. Moreover, when analysing the APP secretion level upon *dfer* co-expression, no change in the generation of sAPP could be revealed (P. Soba, pers. comm.). Thus, DFer seems to have no effect on APP expression, processing, secretion or phosphorylation in cell culture.

Nevertheless, a direct interaction still might be possible. To investigate this, immunoprecipitation of cell lysate was performed following co-transfection with APP and *dfer*, using an antibody directed against APP. When trying to detect co-precipitated DFer protein

by Western blotting, no protein was found (data not shown). These co-immunoprecipitation experiments have been complicated by unspecific binding of DFer. Vice versa, when using the N antibody for DFer precipitation, no APP was found to be co-precipitated. In conclusion, DFer and APP appear not to interact in a direct way.

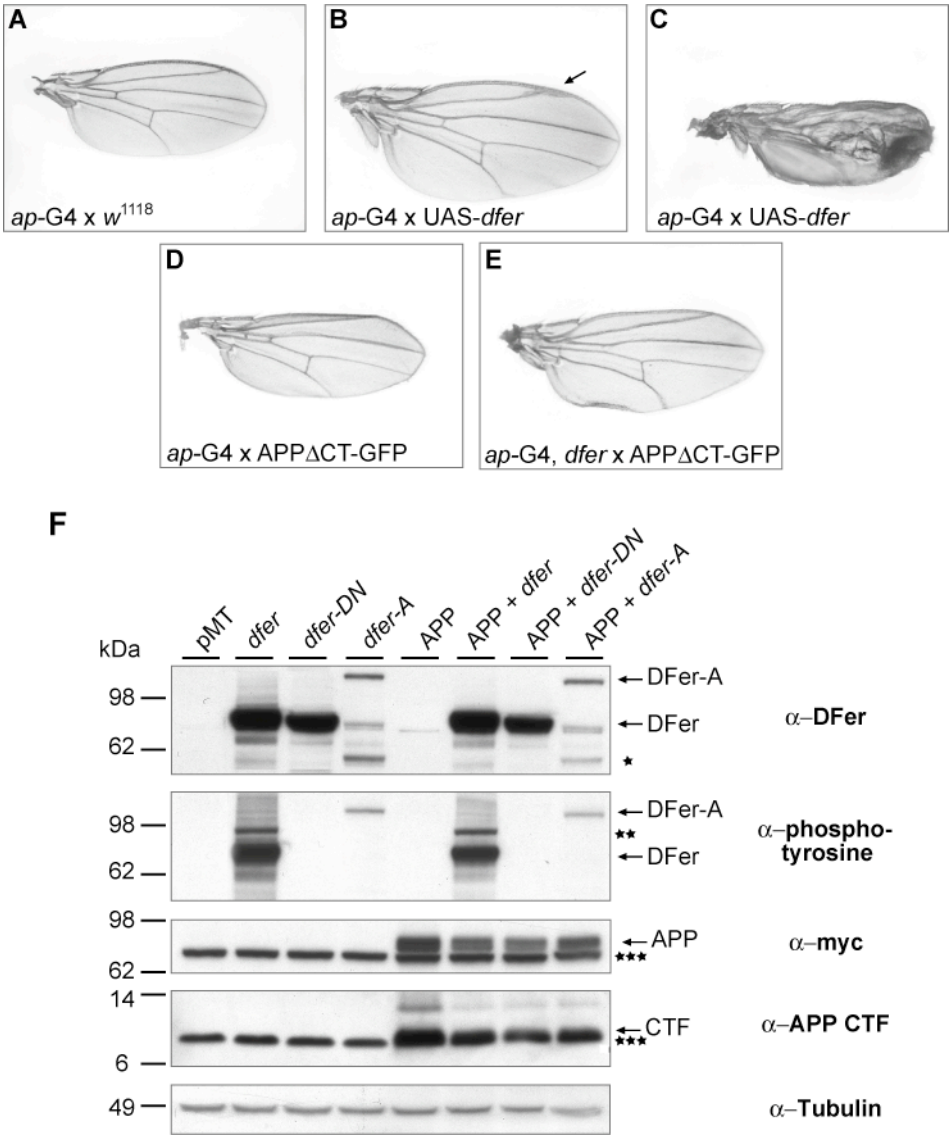

Fig. 2.13 Dfer suppresses the APPΔCT-GFP induced wing phenotype and does not interact directly with APP. (A-E) Interaction between *dfer* and APPΔCT-GFP in the *Drosophila* wing. (F) Co-expression of DFer and APP in S2 cells, analysed for effects on APP processing, phosphorylation and secretion. (A) Wildtype wing. (B+C) Overexpression of *dfer* results in a broad range of wing phenotypes. A weak phenotype (B), with wing vein deltas forming (arrow), and a strong phenotype with blisters (C) are shown. (D) Expression of APPΔCT-GFP results in an edged wing blade. (E) Co-expression of *dfer* and APPΔCT-GFP suppresses the *dfer*-induced phenotypes. Crosses were performed with *apterous*-GAL4 lines at 25°C. (F) Cells were transfected either with APP, *dfer*, *dfer-DN* or *dfer-A* alone, or in combination with APP. Cell lysates were submitted to SDS-PAGE and immunoblotting with either an α–DFer (SK antibody), α-phosphotyrosine, α–myc (APP N-Myc) or α–APP CTF antibody. Equal amounts of protein loading were verified by immunoblotting with an α–Tubulin antibody. One asterisk marks a degradation product of DFer kinase; two asterisks indicate presumably highly phosphorylated DFer protein; three asterisks signify unspecific background bands.

2.8.3 DFer overexpression has no effect on APP processing or phosphorylation *in vivo*

Experiments similar to the ones in cell culture were performed *in vivo* in *Drosophila.* To test if there is a DFer-induced effect on APP phosphorylation or APP processing in *Drosophila*, both proteins were overexpressed in the adult head using the *GMR*-GAL4 driver line. The protein extract was isolated and analysed by Western blotting. As expected, overexpression of DFer kinase with the UAS-*dfer* fly line had neither an effect on APP phosphorylation nor on APP processing (data not shown). The same was true when the study was performed with the dominant-negative inactive kinase form using the UAS-*dfer-DN* fly line for overexpression. Thus, the nature of the interaction between APP and DFer protein is likely to be an indirect one.

2.9 Localization of the DFer protein

2.9.1 Subcellular DFer protein localization

Since DFer and APP seem not to interact together, the further study concentrated on the characterization of *dfer* in *Drosophila*. For the mammalian Fes and Fer kinase, there are several controversial reports about the protein localization within a cell. Some investigators have shown both Fes and Fer kinase to localize to the nucleus (Yates et al. 1995; Hao et al. 1991; Ben-Dor et al. 1999). Others, in contrast, claim that both kinases are excluded from the nucleus. Instead, they find Fes kinase restricted to the trans-Golgi network and other vesicular structures and the Fer kinase in a more diffuse cytoplasmic localization (Zirngibl et al. 2002; Zirngibl et al. 2001). Conversely, both kinases are reported to associate with signaling complexes at the cell membrane (summarized in Greer 2002). The DFer kinase, however, and its smaller p45 kinase form were shown to partially associate with membrane fractions when expressed in cell culture (Paulson et al. 1997).

When analysing the protein sequence of DFer, neither a nuclear localization sequence nor a motif that could account for membrane-association was found. To reveal the cellular localization of the DFer protein in wildtype *Drosophila* flies, immunostainings were performed of salivary glands, which are especially well-suited for localization studies because of their giant cell size. Stainings with the DFer antibody revealed a membrane-association of the DFer protein, co-localizing with the actin cytoskeleton of the cell membranes stained with phalloidin (Fig. 2.14). DFer protein was also found within the cell cytoplasm, presumably in vesicular structures. These observations go along with the previous finding that DFer is in part loosely associated with cytoplasmic membranes (Paulson et al. 1997).

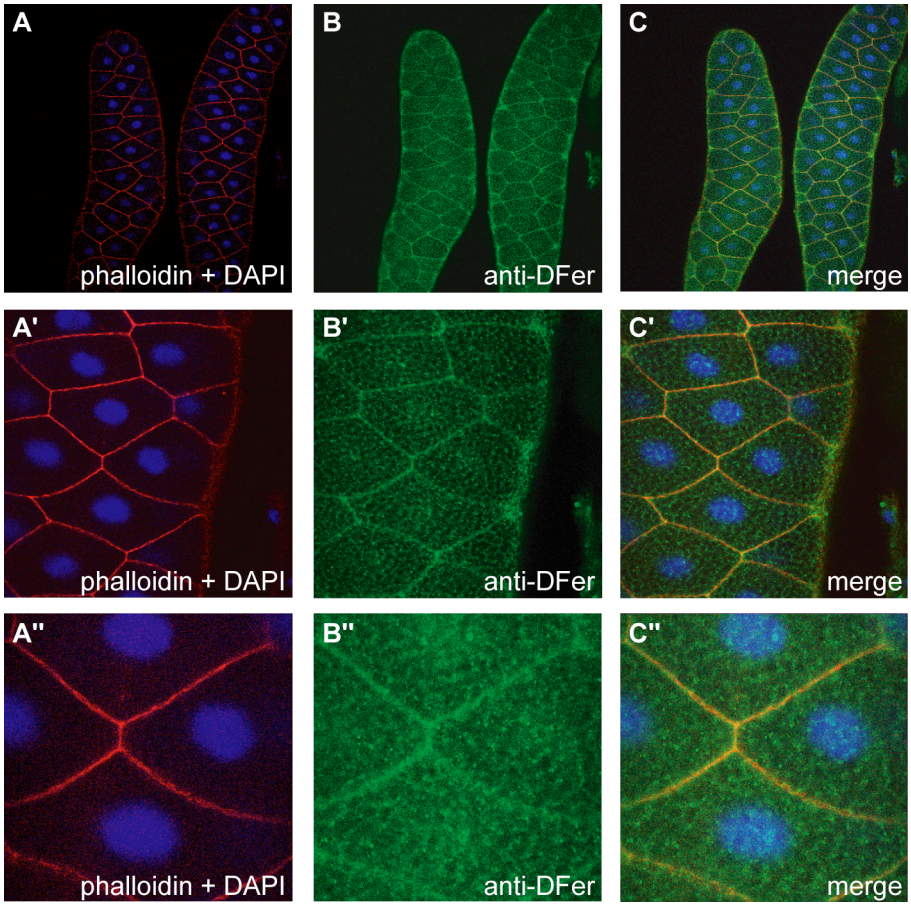

Fig. 2.14 Localization studies of the DFer protein in salivary glands. (A) Salivary glands of wildtype flies were dissected and stained for phalloidin, which marks the actin cytoskeleton along the cell membranes, and DAPI, which marks the DNA in the nucleus. (B) The DFer antibody stains DFer protein along the cell membrane and within the cell. (C) Merge between the phalloidin, DAPI and DFer staining. (A' and A''), (B' and B''), (C' and C'') are higher magnifications of (A), (B) and (C), respectively.

2.9.2 DFer protein localization in *Drosophila* embryos

Next, the question was addressed in which pattern the protein is expressed in the embryos. When staining wildtype embryos for endogenous DFer protein, a clear statement was not possible because the overall staining was very faint and not properly distinguishable from background staining. Besides, differences were observed between the two different antibodies, with the SK antibody revealing a staining at muscle attachment sites, which so far could not be verified to be specific. Nevertheless, the stainings were rather ubiquitous, not revealing any specific expression pattern and appeared to be membrane-associated. Neither using the different DFer antibodies in varying concentrations nor changing the fixation or staining procedures could improve the stainings on wildtype embryos, so the cellular localization of overexpressed DFer was analysed. When overexpressing DFer protein with the UAS-*dfer* line using the *engrailed*-GAL4 (*en*-GAL4) driver line, causing expression in the parasegmental stripes of the embryo, a membrane-association of the overexpressed protein

was evident (Fig. 2.15), which seemed to exclude the nucleus. This simultaneously demonstrated the specificity of the DFer antibody, which immunostained the overexpressed protein in an Engrailed expression pattern.

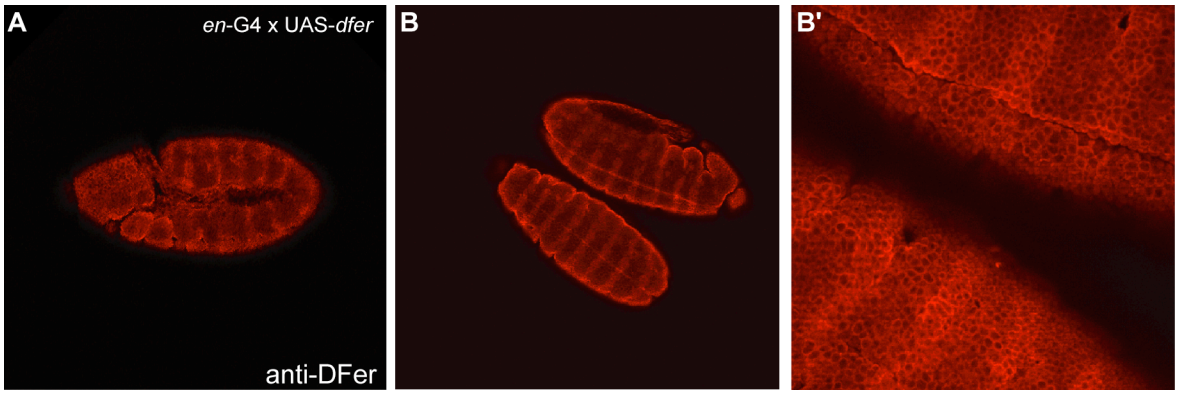

Fig. 2.15 Localization studies of the DFer protein in embryos. (A) DFer overexpression was induced by crossing the transgenic UAS-*dfer* line to an *en*-GAL4 driver line at 25°C. Immunostaining with the DFer antibody was performed on collected embryos, a stage 10-11 embryo is shown, anterior to the left. (B) Ventral view on the DFer staining in *engrailed*-patterned stripes from stage 10-11 embryos, (B') with higher magnification.

In conclusion, it seems that endogenous DFer protein is only weakly but ubiquitously expressed in the embryo and overexpression of the DFer protein visualizes its association with the cell membrane.

2.10 Functional analyses of DFer in larval wing imaginal discs

2.10.1 DFer overexpression affects wing disc morphology

So far, the overexpression of *dfer* was shown to induce strong phenotypes in the adult fly, which are reminiscent of loss-of-function mutations in the Notch or Wingless pathway. Both signaling pathways are required for dorsoventral (D/V) boundary formation during the development of the wing imaginal disc, the larval progenitor cells forming the adult wing, in order to define the dorsal and ventral cell monolayer (Ng et al. 1996, Neumann et al. 1996). As these morphological alterations in the adult wing indicate a profound developmental disturbance, the effect of ectopic *dfer* expression during the wing development, i.e. on the D/V boundary formation, was examined. Therefore, *dfer* was overexpressed in the dorsal wing disc compartment using the *ap*-GAL4 driver line and the wing discs were dissected at the stage of third instar larvae. One of the first observations was the morphological deformation of the wing discs in the *dfer* expressing dorsal part, displaying a shorter but broader notum region and deformed wing pouches (Fig. 2.16 B). When using another GAL4 line, like *sd*-GAL4 with expression in the wing pouch or *en*-GAL4

with expression in the posterior compartment of the wing disc, similar morphological anomalies within the area of *dfer* expression were noticed (data not shown). *Dfer* overexpression, thus, somehow influences the morphology and the development of the wing imaginal disc.

2.10.2 DFer overexpression influences Wingless and Cut expression

Since the overexpression of *dfer* caused strong wing phenotypes resembling Wingless and Notch mutants, the question appeared if *dfer* overexpression interfered with Wingless and/or Notch signaling. In a first step, Wingless expression along the D/V boundary was examined. In wildtype wing discs, Wingless is expressed along the D/V boundary, which will form the wing margin where the dorsal and ventral surfaces of the wing converge (Fig. 2.16 C). Wingless is also expressed in two concentric rings that surround the wing pouch, the inner and the outer ring. These two rings define the wing hinge that attaches the wing to the thorax. In the case of *dfer* overexpression with the UAS-*dfer* line in the dorsal compartment using the *ap*-GAL4 driver line, the Wingless stripe along the D/V boundary changed either to two coupled semicircular halflines (Fig. 2.16 D) or revealed an interruption of the Wingless staining (Fig. 2.16 E). Additionally, the inner ring staining around the wing pouch was missing, concomitant with the observed deformations of the wing hinge (del Alamo Rodriguez et al. 2002). The impairment of Wingless staining along the D/V boundary was also observed when overexpression was induced with *sd*-GAL4 or *en*-GAL4 driver lines (Fig. 2.17). The examination of different focal planes through the wing imaginal disc showed that the Wingless staining along the D/V boundary was indeed disrupted (Fig. 2.17 B').

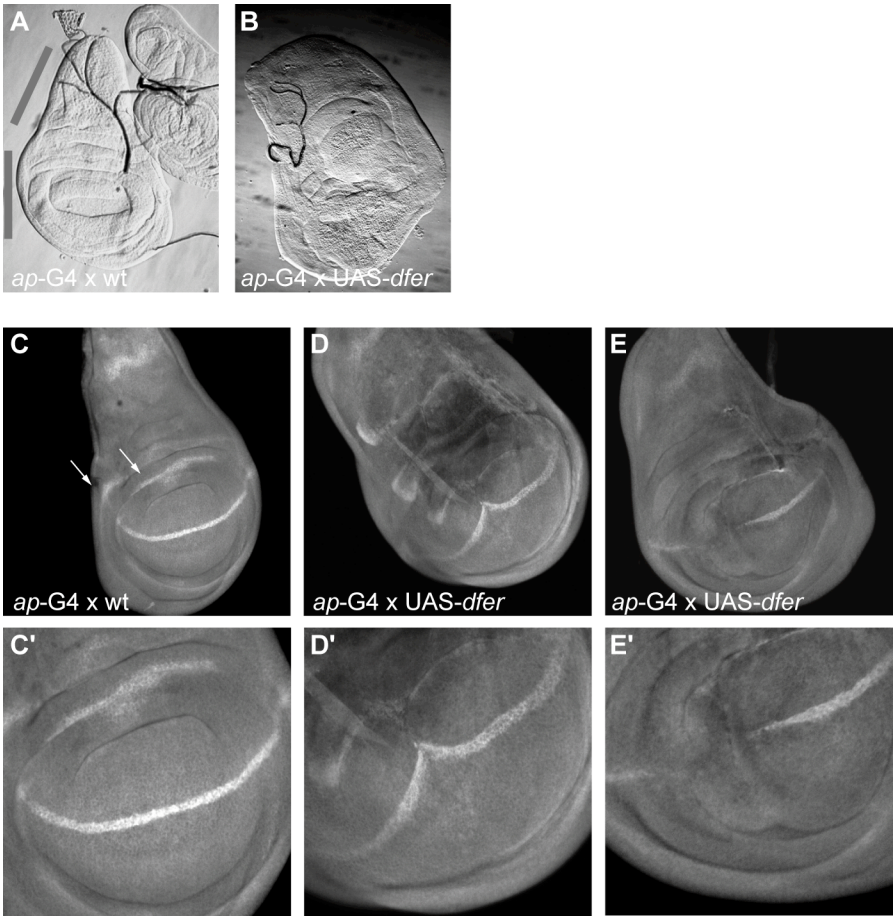

Fig. 2.16 *Dfer* overexpression causes morphological deformations and aberrant Wingless staining in the wing imaginal disc. (A) Phase contrast pictures of a wildtype third instar imaginal wing disc and (B) a *dfer* overexpressing wing disc. Grey bars indicate the notum (upper) and the wing pouch (lower). (C) Wingless staining along the D/V boundary in a wildtype wing disc and (D and E) *dfer* overexpressing wing discs. (C'), (D') and (E') are the respective magnifications. Anterior is to the left. The arrows indicate the inner and outer ring of Wingless expression. Crosses were performed as indicated with *ap*-GAL4 driver lines crossed to wildtype (wt) flies or transgenic UAS-*dfer* flies at 25°C.

Performing the same crosses with induced overexpression of the dominant-negative kinase-inactive form using the transgenic UAS-*dfer-DN* line did neither disturb the wing imaginal disc morphology nor abrogate the Wingless staining (Fig. 2.17 C). The outcome was the same for all of the three different GAL4 driver lines used (*en*-GAL4, Fig. 2.17; *sd*-GAL4 and *ap*-GAL4, data not shown).

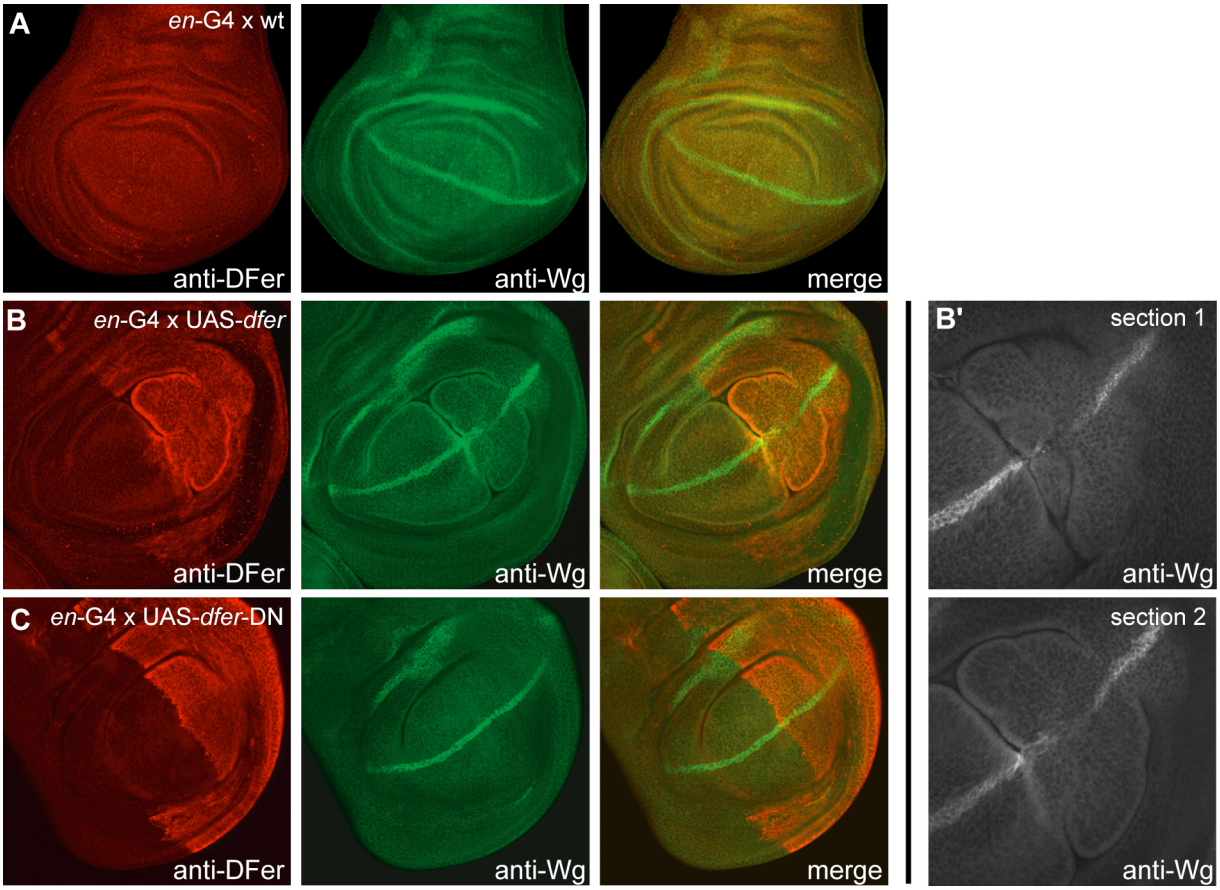

Fig. 2.17 Overexpression of *dfer* but not of the kinase-inactive transgene *dfer-DN* disrupts Wingless staining. (A) In wildtype wing discs, Wingless is expressed along the D/V boundary visualized by staining with anti-Wingless (anti-Wg) antibody (middle). Endogenous DFer expression is detected with the anti-DFer antibody (left). Anti-Wg and anti-DFer staining were merged (right). (B) In a *dfer* overexpressing wing disc, Wingless staining is disrupted in the posterior part of the wing pouch. (C) When overexpressing the kinase-inactive form DFer-DN in the posterior part of the wing pouch, Wingless staining remains persistent along the D/V boundary. (B') Two different sections within the wing pouch are presented showing disturbed Wingless staining. Anterior is to the left, dorsal to the top. Only the wing pouch section is depicted. Crosses were performed as indicated with *en*-GAL4 driver lines crossed to wildtype (wt) flies or transgenic UAS-*dfer* flies expressing DFer kinase or UAS-*dfer-DN* flies expressing kinase-inactive DFer-DN protein at 25°C.

Taken together, the kinase activity of overexpressed DFer is essential not only for adult wing phenotype induction but also for the disturbed appearance of the wing disc morphology and the disruption of the Wingless staining along the D/V boundary.

As Wingless is a morphogen required for boundary formation and its expression is induced by Notch signaling (reviewed in Tabata and Takei 2004), the Notch pathway might be the main pathway affected upon *dfer* overexpression. Notch signaling can be indirectly monitored by immunostainings of the product of one of the target genes, e.g. Cut. Cut is a homeobox-containing transcription factor, whose expression is induced upon Notch activation at the D/V boundary, however, Wingless signaling is also indirectly required (Micchelli et al. 1997). Stainings were performed on third instar wing discs upon overexpression of the active DFer and inactive DFer-DN kinase to see if there was an

influence on Cut expression. Indeed, as already observed for Wingless, Cut expression was abrogated upon DFer overexpression along some parts of the D/V boundary when using *en*-GAL4 driver lines, or showed the typical semicircular halflines in the case of *ap*-GAL4 driver lines (Fig. 2.18). In contrast, wildtype discs displayed normal Cut expression in a stripe along the D/V boundary. Overexpression of the kinase-inactive DFer-DN protein, however, did not alter this Cut expression pattern. These results suggest that DFer can interfere with Notch signaling along the D/V boundary.

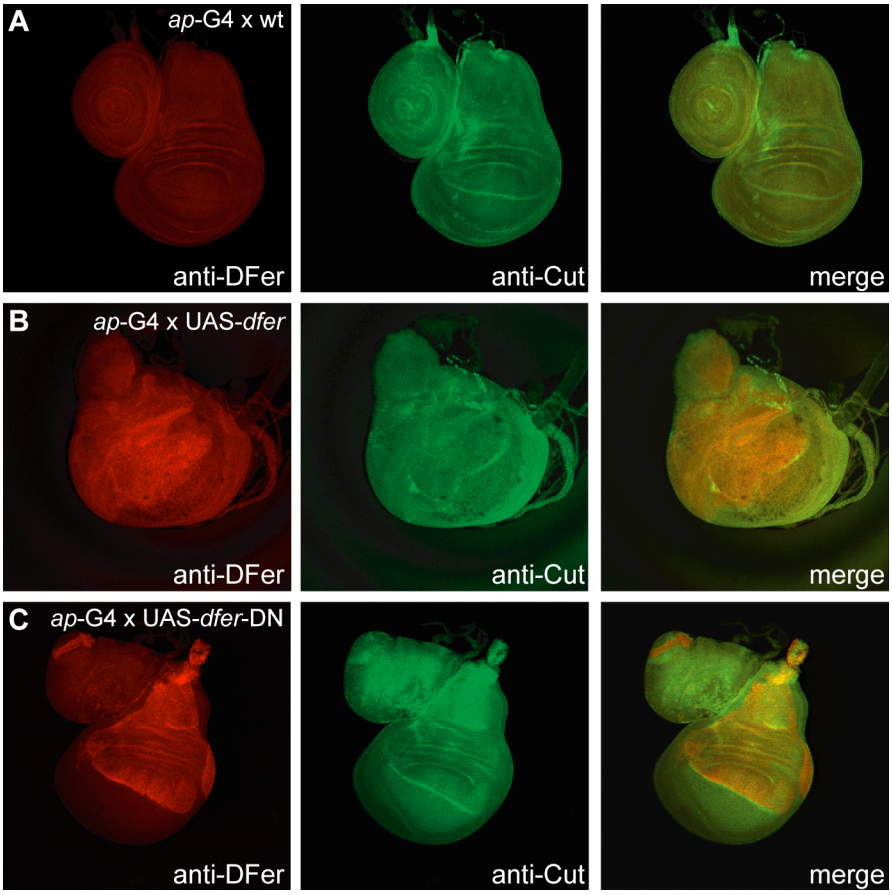

Fig. 2.18 *Dfer* overexpression affects Cut staining. (A) In wildtype wing discs, Cut expression along the D/V boundary was visualized by staining with the anti-Cut antibody (middle). (B) In a *dfer* overexpressing wing disc, Cut staining reveals two semicircular lines along the D/V boundary. DFer expression is visualized in the dorsal part of the disc. (C) Overexpression of the kinase-inactive form DFer-DN in the dorsal compartment results in the regular Cut staining along the D/V boundary. Anterior is to the left. Crosses were performed as indicated with *ap*-GAL4 driver lines crossed to wildtype (wt) flies or transgenic UAS-*dfer* flies expressing DFer kinase or UAS-*dfer-DN* flies expressing kinase-inactive DFer-DN protein at 25°C.

Another Notch target gene is the selector gene *vestigial* (*vg*). The activity of Wingless and Notch in the wing margin leads to the expression of *vg* through the activation of the *vg* boundary enhancer (*vg* BE-lacZ) along the D/V boundary (Kim et al. 1996; Williams et al. 1994). Therefore, to verify the interference with Wingless and Notch signaling along the wing margin, stainings were performed upon *dfer* overexpression for *vg* boundary enhancer

activation (*vestigial* intron2) (Neumann et al. 1996). Reflecting the previous observations, the activation of the *vg* boundary enhancer was partially lost upon overexpression of *dfer* (data not shown). Thus, DFer kinase seems to interfere with Notch signaling in the wing imaginal disc, and in this way abrogates the expression of the Notch targets Wingless, Cut and Vestigial. Nevertheless, it still remains to be clarified, why Wingless, Cut and Vestigial expression are lost upon *dfer* overexpression during wing development.

A key component of the Wingless pathway is β-catenin, a cytoplasmic protein that plays also an essential role in calcium-dependent intercellular adhesion mediated by cadherins (reviewed in Gottardi et al. 2001; Nelson and Nusse 2004). In the Wingless pathway, binding of Wingless to its receptor prevents β-catenin degradation, causing its stabilization and accumulation in the cytoplasm and translocation to the nucleus where it acts as a transcriptional cofactor. For cell-cell adhesion, β-catenin binds to cadherin adhesion receptors and acts as a structural adaptor protein linking cadherins to the actin cytoskeleton. The mammalian Fer kinase was reported to be in a complex with β-catenin and overexpression of Fer in fibroblasts correlated with increased phosphorylation of β-catenin (Li et al. 2000; Arregui et al. 2000; Rosato et al. 1998). The *Drosophila* β-catenin homolog, Armadillo, is also part of the Wingless pathway. As Wingless expression is affected upon *dfer* overexpression, Armadillo might be a candidate for direct interaction with the DFer kinase. Armadillo protein levels in wing imaginal discs were analysed upon overexpression of *dfer* in a broad stripe along the anterior/posterior (A/P) boundary using the *patched*-GAL4 driver line. In wildtype discs, Armadillo accumulated in two stripes flanking the D/V boundary (Fig. 2.19 A and B). In discs overexpressing *dfer*, it appeared as if Armadillo was especially enriched in the cells directly adjacent to DFer expressing cells along the A/P boundary (Fig. 2.19 C). Additionally, it seemed as if the expression in the intersection of the A/P and D/V boundary was increased. Yet it is not clear, if this reflects increased amounts of stabilized cytoplasmic or cadherin-associated Armadillo. Dissecting more discs, however, showed that occasionally the same intensified pattern for Armadillo staining emerged also in the case of wildtype wing discs and in discs overexpressing the kinase-inactive form DFer-DN (Fig. 2.19 B and D). Indeed, a high variability of Armadillo staining in wildtype discs can be found in the literature (Zeng and Verheyen 2004; Mohit et al. 2003). Nevertheless, this enrichment of Armadillo along the edges of the A/P border seemed to be more pronounced in the case of *dfer* overexpression. With these contradicting results, no conclusions can be drawn for a direct interplay between DFer and Armadillo in the phenotypes caused upon *dfer* overexpression.

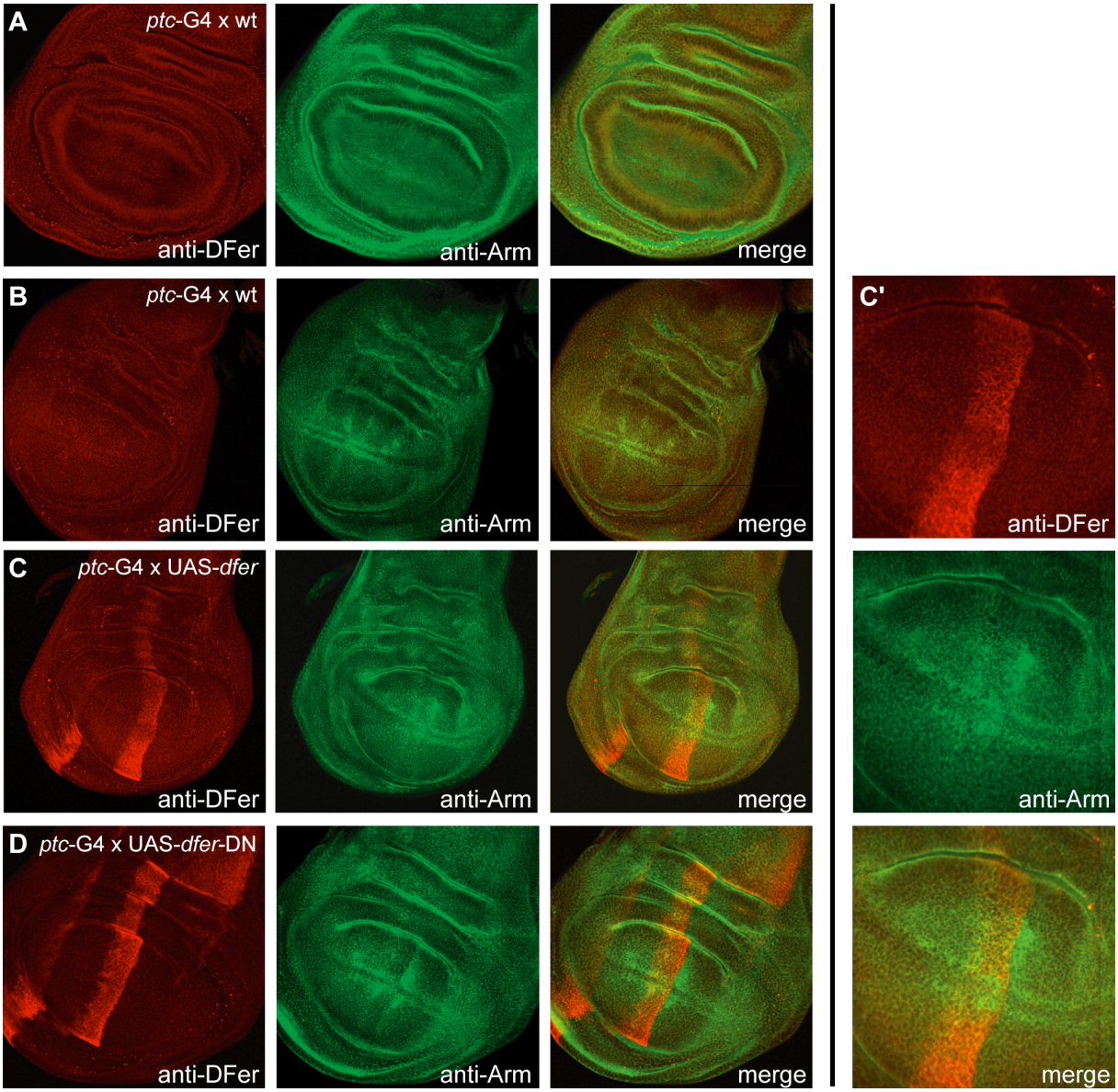

Fig. 2.19 *Dfer* overexpression and Armadillo staining. (A and B) In wildtype wing discs, endogenous DFer expression is detected with the DFer antibody (left). Armadillo (Arm) is expressed in two stripes flanking the D/V boundary visualized by staining with the anti-Arm antibody (middle). The staining is very variable and can be faint as in (A) or strong as in (B). Additionally, Arm staining can be occasionally visualized along the A/P boundary (B). Anti-Arm and anti-DFer stainings were merged (right). (C) In a *dfer* overexpressing wing disc using *ptc*-GAL4, where DFer expression is apparent in a broad stripe along the A/P boundary driver lines, Arm staining appears to be enriched along the border of DFer expressing areas and shows expression at the intersection of the two boundaries (arrow). (D) The enrichment along the A/P boundary can also be found in discs overexpressing the kinase-inactive form DFer-DN. Anterior is to the left, only the wing pouch of the imaginal discs is shown. Crosses were performed as indicated with *patched*-GAL4 (*ptc*-GAL4) driver lines crossed to wildtype (wt) flies or transgenic UAS-*dfer* flies expressing DFer kinase or UAS-*dfer-DN* flies expressing kinase-inactive DFer-DN protein at 25°C. (C') is a magnification of (C).

2.11 Genetic interaction partners of *dfer*

Dfer overexpression obviously acts on a specific developmental pathway causing wing blistering and wing margin notching in the adult fly. To elucidate the affected pathways and to identify possible interacting factors, a search for dominant genetic modifiers of the *dfer*-induced phenotypes was performed. Two different fly lines were used for the genetic interaction assay, one displaying the wing blistering and the other the wing notching phenotype. Therefore, a UAS-*dfer* transgene was recombined onto the *ap*-GAL4 chromosome to get a stable fly line allowing permanent expression of *dfer* in the dorsal part of the wing causing wing blistering. These crossings resulted in *ap*-GAL4, UAS-*dfer*/*Cyo* flies, dedicated as *ap*G4-*dfer*. To obtain the second fly line, *sd*-GAL4 was crossed in to the transgenic UAS-*dfer* flies, resulting in flies with stable expression of *dfer* in the wing pouch and thus wing notching. This fly line with the genotype *sd*-GAL4; UAS-*dfer*/*BcG* was abbreviated *sd*G4-*dfe*r. With these two lines and two different wing phenotypes, respectively, several crosses were carried out to fly lines with gain- or loss-of-function mutations in genes encoding known members of various developmental pathways, to identify factors that either enhance or suppress the *dfer*-induced wing phenotypes. Additionally, fly lines with mutations in several genes, which were reported to interact with or be in the same pathway as the mammalian Fes and Fer kinase, were also analysed, e.g. p120catenin and β-catenin (Rosato et al. 1998; Piedra et al. 2003), Phosphatidylinositol-3 kinase (PI3K) (Iwanishi et al. 2000; Jiang et al. 2001), Ras, Rho, and Cdc42 (Li and Smithgall 1998), Cortactin (Kim and Wong 1998; Craig et al. 2001; Fan et al. 2004), N-Cadherin and β-Integrin (Arregui et al. 2000; Li et al. 2000), Jun N-terminal kinase (JNK) (Li and Smithgall 1998) and Rac1 (Vastrik et al. 1999). Some of the crosses are listed in Table 2.4.

Table 2.4 Phenotypes of the crosses for genetic interaction.

Overexpression and mutant lines	apG4	apG4-*dfer*	sdG4	sdG4-*dfer*
kept at 18°C				
w^{1118}	-	slight VD, vein deltas	-	slight notches
UAS-*dfer*-DN	-	wildtype-like wing	-	slight notches
UAS-*Abl*	slight VD macrochaete clustered	dead pupae, 4 hatched with thorax deformation	-	strong VD, slight notches
UAS-Abl^{DN}	slight VD	dead pupae, some hatched with mini thorax	-	mini wings and blisters

abl^{3}	-	blisters and balloons	-	strong notches, broad veins
UAS-*wg*	dead pupae	dead pupae	dead pupae	dead pupae
N^{55e11}	-	slight notches	-	slight notches
H^{P8}	-	-	small interruptions in veins	-
UAS-*H*	split thorax, wing balloons	split thorax, wing balloons, dead pupae	small wings, notches	notches (very thin)
UAS-*Su(H)*	dead pupae	dead pupae	blackened blisters, broadened wing, veins missing	blackened blisters, broadened wing, veins missing (all stronger)
EGFR^{f2}	-	-	-	slight notches
kept at 25°C				
w^{1118}	-	slight blistery to black blisters	-	blistery, notches
β1-int Df Exel	-	blistery	-	notches
β1-int Df	-	strong black balloons	-	strong notches, balloons
p120ctn Df Exel	-	weak blisters	-	notches
p120ctn Df	-	dead pupae	-	notches, balloons
ras82D Df	-	dead pupae, blisters	-	dead pupae, notches
ras64B Df Exel	-	weak blisters	-	slight notches
ras64B Df	-	pupal lethal	-	blisters, vein broadening, some missing, notches
Stat92E Df	-	slight blisters	-	slight notches
Stat92E Df Exel	-	blisters	-	slight notches
rac1 Df	-	dead pupae	-	strong notches
cdc42 Df		black balloons, dead pupae, thorax deformed	-	dead pupae
GSK3β	-	dead pupae, mini wings, blisters	n.p.	n.p.
sgg^{1}	-	dead puape		tiny balloons

wg^{spd}	-	blisters	-	notches
wg$^{1-17}$	-	black blisters	-	notches
ap^{ts78j} *wg*	-	black blisters, dead pupae	-	notches, blistery
arm^{1}	-	black balloons, dead pupae	-	black balloons
PI3K Df	-	slight blisters	-	slight notches
Ncad Df	-	strong blisters, dead pupae	-	black balloons, dead pupae
Ncad Df Exel	-	black blisters, mini wings	-	strong notches, balloons
shg^{2}	-	black blisters, weak flies		balloons
Abl^{3}	-	dead pupae	-	dead pupae
bsk Df	-	black blisters, dead pupae	-	notches, balloons
hep^{1}	-	wildtype-like	-	wildtype-like
hep^{75}	-	wildtype-like	-	wildtype-like
EP *cortactin*	-	dead pupae	-	black balloons
cortactin Df	-	dead pupae	-	dead pupae
cortactin^{M7}	-	slight blisters	-	notches

Df, deficiency lines; *Df Exel*; deficiency lines from Exelixis, Inc.; *n.p.*, not performed.

One drawback of the genetic interaction assay was the broad variety of the phenotypic severity induced by the overexpression of *dfer* itself. Therefore, a clear of suppression or enhancement could not be scored. It appeared that only mutations in *hemipterous*, the *Drosophila* JNK homolog, were able to suppress the phenotypes. Several genes were found to enhance them. Genetic interactions could be observed for genes involved in cadherin-mediated cell-cell adhesion (*p120 catenin*, *N cadherin*), ras and cdc42 GTPases, Wingless pathway components (*shaggy*, the GSK3β homolog; *armadillo*) and the tyrosine kinase *abelson*. The deficiency line of the *cortactin* gene seemed to enhance the phenotype by revealing pupal lethality. An interaction with cortactin was already reported from the group of J.M. Bishop, San Francisco, working also on *dfer* (Abstract Hill et al. 2004). However, when investigating in more detail and using a newly generated *cortactin* mutant fly line, genetic analysis showed no interaction with *dfer* (Somogyi and Rorth 2004).

2.12 Generation and identification of *dfer* mutant alleles

In order to determine the role of *dfer* during normal *Drosophila* development, loss-of-function mutations in the *dfer* locus had to be generated. One possible method is imprecise P-element excision by the reintroduction of a transposase source to create deletions in the EP-element flanking genomic region, which can range from a few bp up to several kb (Salz et al. 1987; Tsubota and Goodwin 1990). In the case of the *dfer*^{zwim} EP fly line, the EP-element inserted approx. 100 bp upstream of the 5' UTR of the *dfer* gene. Hence, a deletion of the flanking region could possibly delete a substantial region of the *dfer* transcription unit, resulting in a *dfer* mutant fly.

During the course of this study, two such P-element excision screens were performed (Fig. 2.20). They were further complicated by the fact, that for the genomic *dfer* region (*dfer* is mapped to the cytological position 85D13-15) no deficiency fly lines exist, i.e., fly lines that harbor huge deletions within their genome removing the *dfer* transcription unit. Initially, the screen was based on the assumption that *dfer* mutant flies heterozygous over a deficiency line die. Accordingly, these fly lines would have been used to screen the flies from the F2 generation isolated with an EP-element excision for lethality. Although several deficiency fly lines should supposedly exist with deletions attributed to the region of interest according to the cytological mapping and to information available on FlyBase, analyses of thirteen putative deficiency lines by PCR and Southern blotting revealed that they still carried the *dfer* gene and were not deficient for this particular genomic region as stated (data not shown). These findings were confirmed by the group of Andrea Brand, Cambridge, working on the same gene (M. Murray, pers. comm.). Thus, the screens had to be adjusted and isolated fly lines with EP-element excisions analysed for lethality.

Both screens were conducted using the homozygous *dfer*^{zwim} EP fly line, which was crossed to flies carrying a transposase source. In the first screen (Fig. 2.20 A), 550 male flies were independently isolated, discriminated by the loss of the EP-element marker gene *white*. With these fly lines, stocks were established by crosses to balancer lines and then screened for lethality. Of these, 37 fly lines were homozygous lethal and were further examined by PCR and Southern blot analyses. The examination of the obtained fly lines was far more complex than expected. As anticipated, some of the lines still carried parts of the imprecisely excised EP-element, had deletions upstream of *dfer* or only a few bp deletions flanking the original site of EP-element insertion. These results were obtained mainly by PCR analysis of the EP-element flanking region, and changes were identified by sequencing the obtained PCR fragments (see also Fig. 2.21 B and C). When analysing viable fly lines from the same screen, only wildtype-like fragments were obtained, arguing for a *dfer* mutation being lethal. Several lethal fly lines, however, still revealed wildtype-like fragments in the PCR analysis. Yet, sequencing of these uncovered bizarre sequence inversions or other types of complex

rearrangements, which could have probably led to the lethality of the homozygous flies. A few fly lines with their summarized characterization are depicted in Table 2.5. Only one fly line, *dfer*$^{\Delta 252}$, which will be discussed in the following section, carried a 712 bp deletion, removing the first exon of the *dfer* gene. The translation start site of *dfer*, however, is positioned within the second exon. Consequently, the *dfer*$^{\Delta 252}$ mutant could possibly still express functional *dfer*.

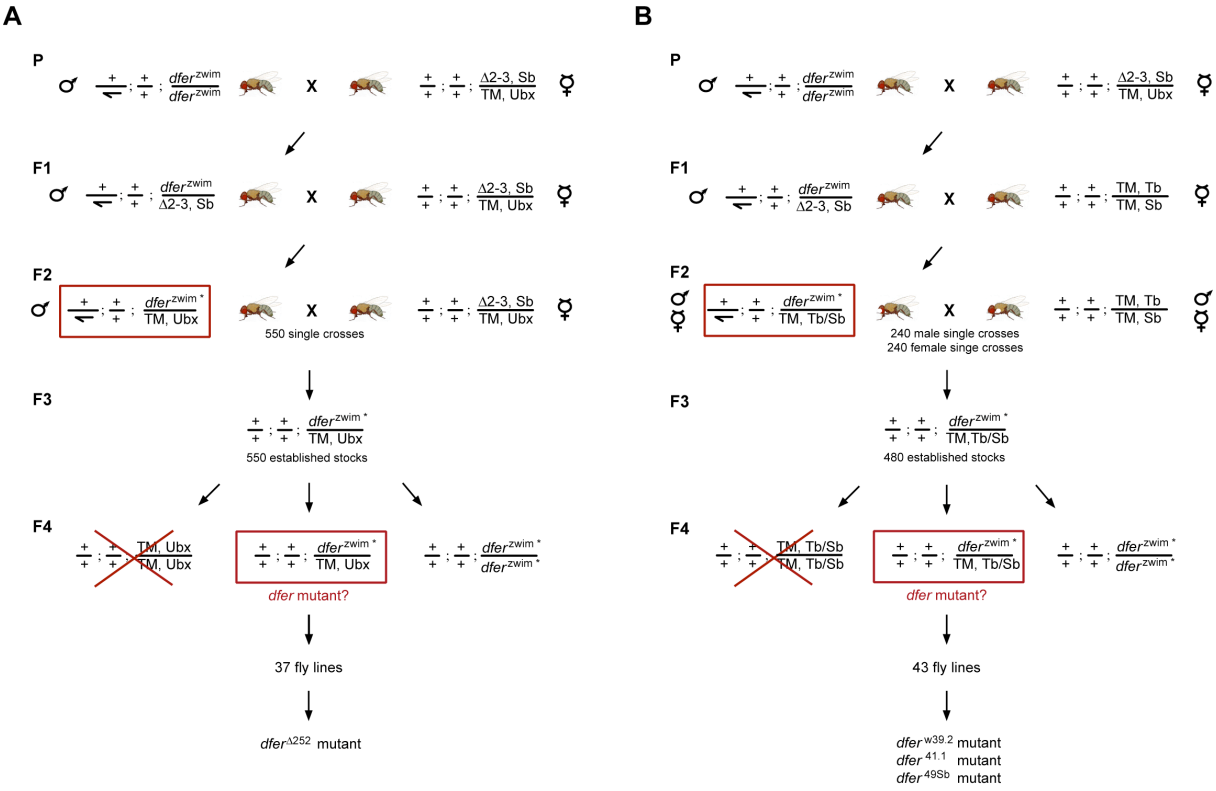

Fig. 2.20 Schematic outline of the two transposase-mediated imprecise P-element excision screens. (A) In the first screen, homozygous *dfer*^{zwim} EP-element flies were crossed to flies carrying a transposase source (Δ2-3). Flies of the F1 generation consequently carried both the transposase and the EP-element. These flies were crossed to a balancer line and the offspring in the F2 generation were screened for the absence of the EP-element marker gene *white* (e.g. flies, which lost their EP-element, with white-colored eyes). 550 independently obtained males were identified and balanced to establish genetically identical stocks. Their progeny in the F4 generation were screened for flies, which were not able to become homozygous, being presumptive *dfer* mutants. Flies being homozygous for the balancer die early in development. 37 independent fly lines were isolated and screened by PCR and Southern blot analysis for deletions in the *dfer* gene. One mutant fly line *dfer*$^{\Delta 252}$ was identified, carrying a small deletion in the gene. (B) The second screen was conducted similarly to the first screen, however, in the F1 generation, flies were crossed to a different balancer line to simplify the screening procedure. In addition, both male and female flies with an EP-element excision were used for the next crossings to exclude a possible influence on male fertility. Consequently, independently obtained 240 males and 240 virgins of the F2 generation were balanced and their progeny screened. 43 independent fly lines were isolated thereof and the three fly lines *dfer*$^{w39.2}$, *dfer*$^{41.1}$ and *dfer*^{49Sb} were confirmed by genomic analysis to have the *dfer* gene deleted. *TM*, Third Multiple Balancer; *Sb*, *Tb* and *Ubx* are marker genes. The asterisk marks the chromosome with the excised EP-element.

To isolate a deletion, which covers a greater part of the *dfer* gene, a second P-element excision screen had to be performed. This one was similar to the first screen but comprised a few changes, such as the use of another balancer line to facilitate the screening procedure. Additionally, upon the observation of male sterility in a high percentage of the F2 males in the first screen (10.7%/59 males), concerns were raised that mutations of the *dfer* gene could possibly result in male sterility and prevent the identification of a mutant. Thus, flies of both genders with excised EP-element were used to screen the F2 generation for deletions (Fig. 2.20 B). In total, 480 fly stocks with excised EP-element were established and tested for lethality. 43 lethal fly lines were isolated and further tested for deletions, 18 of them displayed pupal lethality; a few of these lines are summarized in Table 2.5. This screen, combined with other methods, let to the identification of the three mutants $dfer^{w39.2}$, $dfer^{41.1}$ and $dfer^{49Sb}$, which will be characterized in detail in the following sections.

Table 2.5 Analysis of some of the isolated *dfer* alleles.

	Allele	Viability	PCR product	EP-element excised?
1st screen	$dfer^{\Delta 179}$	lethal	no product	yes
	$dfer^{\Delta 252}$	viable	no product	yes
	$dfer^{\Delta 259}$	lethal	1.1 kb longer product	no
	$dfer^{\Delta 297}$	lethal	no product	no
	$dfer^{\Delta 308}$	lethal	no product	no
	$Dfer^{\Delta 310}$	lethal	40 bp longer product	yes
	$dfer^{\Delta 350}$	lethal	200 bp shorter product	yes
2nd screen	$dfer^{15.2}$	viable	longer product	yes
	$dfer^{17.2}$	lethal	wt product	yes
	$dfer^{w39.2}$	lethal	no product	yes
	$dfer^{39.3}$	lethal	no product	no
	$dfer^{40.2}$	lethal	product	yes
	$dfer^{41.1}$	lethal	no product	yes
	$dfer^{49Sb}$	lethal	no product	yes

Mutant fly lines were analysed for their viability. PCR analysis of the genomic region flanking the original EP-element insertion site revealed either no products (corresponding to a deletion or the presence of the EP-element) or PCR products of varying sizes (corresponding to the wildtype intact genomic DNA sequence, or in case of longer or shorter PCR products, rearranged DNA sequences). The presence of the EP-element was also tested by PCR with EP-element specific primers. Mutant fly lines that were further analysed are highlighted.

2.13 Functional analysis of the *dfer*$^{\Delta 252}$ mutant

2.13.1 Identification of the *dfer*$^{\Delta 252}$ mutant

The first P-element excision screen led to the identification of the *dfer*$^{\Delta 252}$ mutant. The isolated mutant flies were crossed to the original *dfer*^{zwim} EP line to facilitate genomic analysis by circumventing the wildtype allele. The deletion in the *dfer*$^{\Delta 252}$ mutant was mainly identified by single fly PCR analysis, using primers constructed upstream and downstream of the initial EP-element insertion site in the *dfer*^{zwim} line (Fig. 2.21 B and C). With this, a shorter PCR product compared to the wildtype allele was obtained, and sequencing this fragment confirmed the deletion of the genomic DNA flanking the 3' site of the EP-element and its complete excision. The *dfer*$^{\Delta 252}$ fly line carries a small 712 bp deletion, which removes the first exon and the first intron of the *dfer* gene, leaving the translation start site located in the second exon untouched (Fig. 2.21 A).

2.13.2 *dfer*$^{\Delta 252}$ is viable and expresses DFer

Since the deletion in the *dfer*$^{\Delta 252}$ mutant left the translation initiation site of the *dfer* gene untouched, the fly line could possibly still reveal normal *dfer* function. Indeed, although this line was originally identified as a lethal line in the performed screen, it proofed to be semi-lethal, as homozygous mutant individuals were recovered, though with a low frequency. Additionally, these homozygous flies were fertile, but developed slower with a three days delay in development compared to heterozygous controls. The adult flies were apparently morphologically normal, and no pupal lethality could be observed. When testing for embryonic lethality, however, it was found that only 85.1% (n = 1382) of the larvae hatched.

To test if the decreased embryonic viability is due to a reduced expression of *dfer*, *in situ* hybridizations on homozygous *dfer*$^{\Delta 252}$ embryos were performed (Fig. 2.22 A). Surprisingly, the expression of *dfer* mRNA was detectable in all major stages of embryonic development and seemed to be undisturbed compared to the wildtype situation (see Fig. 2.10). Similar to the mRNA expression, DFer protein expression was still present though the level of expression was reduced (Fig. 2.22 B). The decrease in expression in the *dfer*^{D252} mutant was comparable to the one observed in the *dfer*^{zwim} EP line.

Taken together, although the *dfer*$^{\Delta 252}$ line carries a small deletion of the *dfer* gene, flies are still homozygous viable and fertile, express *dfer*, and show no obvious adult phenotypes.

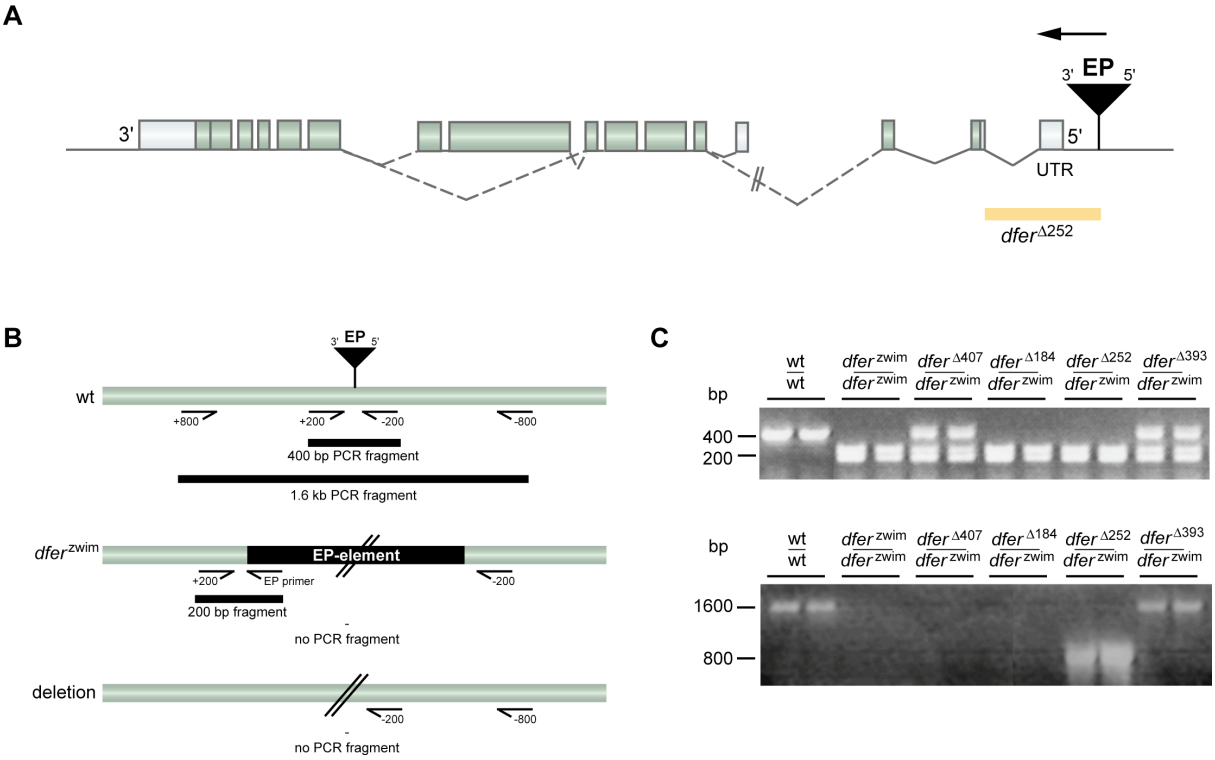

Fig. 2.21 PCR analysis and identification of the mutant *dfer*$^{\Delta 252}$ fly line. (A) The deletion in the *dfer*$^{\Delta 252}$ mutant removes 712 bp directly downstream of the original EP-element insertion site, eliminating the first exon and intron structure. The start site of translation is located within the second exon. Exons are represented as boxes, split by introns. Dashed lines represent alternative splice sites. Untranslated regions are illustrated in *light grey*, coding regions in *dark grey*. The deleted region is indicated in *yellow*. (B and C) PCR analysis of different mutant *dfer* fly lines recovered from the first excision screen. Putative mutant flies were crossed to the original *dfer*^{zwim} EP line to allow genomic analysis by PCR and Southern blotting. (B) Single fly PCR was used as a method with primers located 200 bp and 800 bp upstream and downstream of the EP-element insertion site. In the wildtype situation, or for precise EP-element excisions, fragments with sizes of 400 bp and 1.6 kb, respectively, are obtained. Flies carrying the original EP-element insertion, which has a size of approx. 10 kb, do not reveal a PCR product under these conditions. Using an EP-element specific primer located in the 3' terminal repeat of the element and the downstream genomic primer, fragments are obtained, revealing the presence of the EP-element. If flies carry a deletion removing substantial parts of the flanking genomic region, smaller or no PCR fragments are produced. (C) Single fly PCR analysis with the 200 bp primer pair (top) or 800 bp primer pair (bottom) upstream and downstream of the EP-element insertion site. In the upper PCR analysis, the EP-element specific primer was used additionally, allowing the visualization of the *dfer*^{zwim} EP allele. The mutant *dfer*$^{\Delta 252}$ line does not reveal a PCR product, when using the 200 bp primer pair as these regions are deleted. PCR using the 800 bp primer pairs generates a smaller product of approx. 900 bp, which was subcloned and subsequently sequenced. Two independent flies per fly line were examined separately.

2.13.3 *dfer*$^{\Delta 252}$ displays defects during embryonic morphogenesis

Given that the *dfer*$^{\Delta 252}$ line is still able to produce *dfer* mRNA and protein, it is quite unexpected to obtain embryonic lethality, though with a low penetrance. In order to reveal any defect during embryonic morphogenesis, the cuticle of the dead mutant embryos, which is secreted by the epidermal epithelium, was closer examined. Generally, the major source of dead embryos are unfertilized embryos. When analysing the mutant *dfer*$^{\Delta 252}$ line by preparation of the larval cuticle, however, a range of different phenotypes was observed affecting a major morphogenetic event in the embryo, the dorsal closure (Fig. 2.22 C-H). Dorsal closure is initiated immediately after germ band retraction, where the caudal end of the embryo retracts to its final position (Martinez Arias 1993). During dorsal closure (embryonic stage 13 to stage15), coordinated changes in cell shape and cellular movements occur to enclose the embryo and cover the hole in the dorsal epidermis occupied by an epithelium called the amnioserosa (reviewed in Schock and Perrimon 2002; Campos-Ortega and Hartenstein 1985). The movement of the two lateral epidermal sheets towards the dorsal midline is directed by the dorsal most row of epidermal cells, which is known as the leading edge, that are in contact with the amnioserosa (Jacinto et al. 2000). The process involves dynamic reorganization of the actin cytoskeleton, which is regulated by a network of interacting signaling molecules. At the center is the JNK cascade acting at the leading edge of the migrating epidermis. JNK activation triggers signaling by the Decapentaplegic pathway and interacts with the Wingless pathway (reviewed in Harden 2002; Jacinto et al. 2002, Kaltschmidt et al. 2002). Head involution accompanies dorsal closure from stage 14 on and is a complex movement during which most head structures are displaced from the surface into the interior of the embryo (Campos-Ortega and Hartenstein 1985). Numerous mutants have been identified in which dorsal closure fails, leading to a dorsal hole in the larval cuticle caused by a detachment of the amnioserosa from the epidermis.

The characterized phenotypes of the examined *dfer*$^{\Delta 252}$ mutant are summarized in Table 2.6. Mutant flies exhibited various defects in the morphogenetic processes dorsal closure and head involution that range from dorsal holes to missing head structures (Fig. 2.22 D-H). Approximately 5.4% of the mutants displayed dorsal closure defects with holes in the dorsal epidermis, approx. 5.8% failed to complete head involution and 7.4% showed both dorsal and head defects. Only 0.8% exhibited germ band retraction defects, whereas 15.7% had other unspecifiable defects, resulting in darkened embryos dying during early embryogenesis. The other embryos were unfertilized or wildtype in appearance with no obvious phenotype.

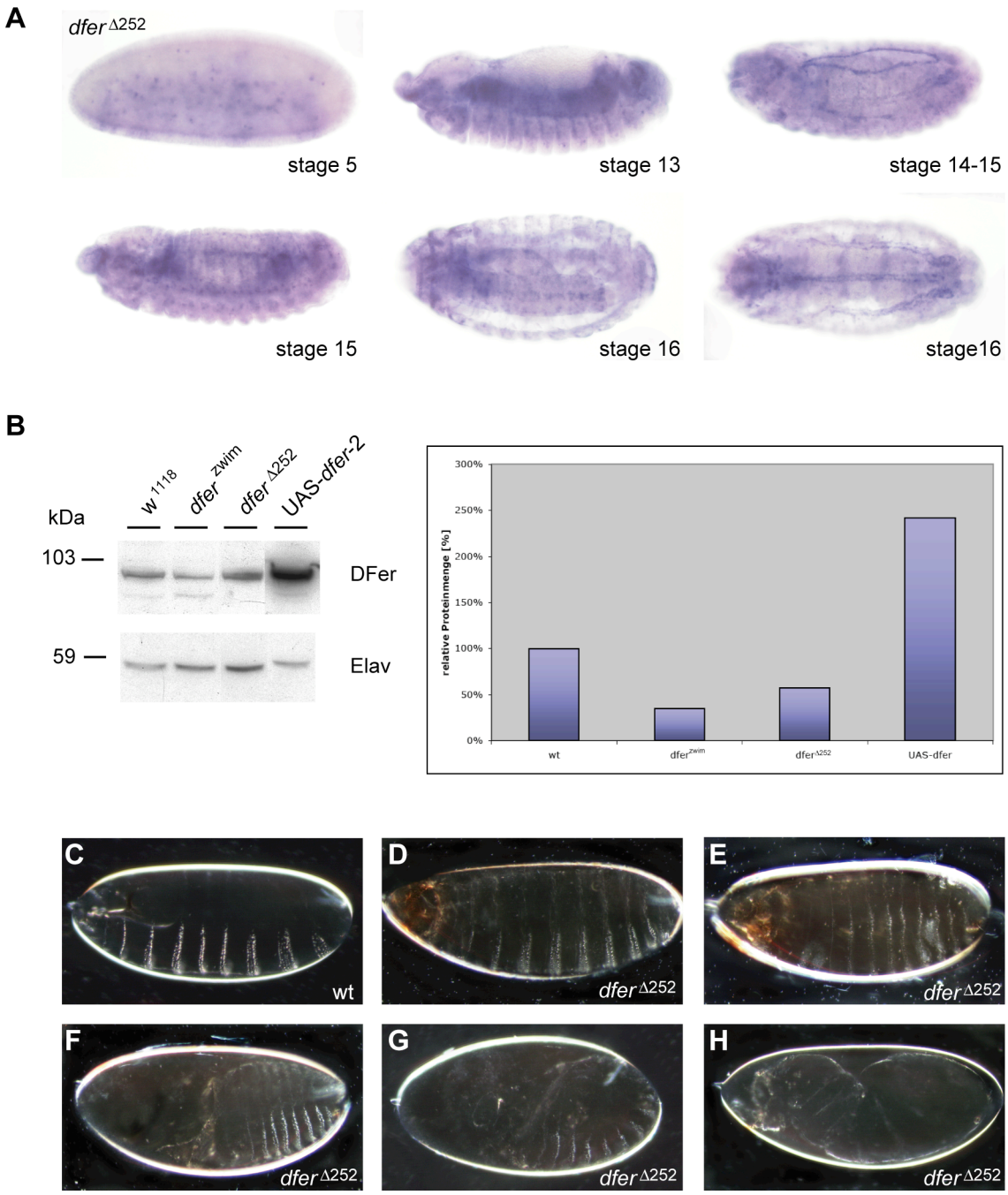

Fig. 2.22 *Dfer* expression analysis and embryonic phenotypes of the *dfer*$^{\Delta 252}$ mutant. (A) mRNA expression in homozygous *dfer*$^{\Delta 252}$ mutant embryos visualized by *in situ* hybridization. Only the stages with the most prominent expression patterns of *dfer* expression are shown. Expression starts at the stage of cellularisation (stage 5) and continuous as in the wildtype situation. During germ band retraction (stage 13), expression is detectable in a segmental pattern and in the neuroectoderm. Following the stages of dorsal closure and head involution (stage 14-15), where *dfer* is expressed at the leading edge cells of the dorsal epidermis, the expression is present in the CNS and becomes more general (stage 15; stage 16, middle). Expression can be also found in the tracheal epithelium (stage 16, right). Embryos are shown in a lateral view, with anterior to the left. (stage 16, right) is a dorsal views. (B) DFer protein expression analysis by Western blotting and quantification thereof. The *dfer*$^{\Delta 252}$ mutant shows decreased DFer protein levels, similar to the ones obtained from the *dfer*^{zwim} EP line. DFer overexpression results in an increasing level of protein expression. Elav expression represent the protein loading control. (C-H) Embryonic cuticle preparations. (C) Wildtype embryo. Note alternating denticle bands and naked cuticle on the ventral epidermis (bottom). (D-H) The range of phenotypes in dead homozygous *dfer*$^{\Delta 252}$ embryos observed. Displayed are (D) head defects with a dorsal hole (arrow), (E) head involution defects, (F) dorsal closure and head involution defects, (G) germ band retraction defects, and (H) massively disturbed morphogenesis. Anterior to the left.

Table 2.6 Percentage of dead *dfer*$^{\Delta 252}$ embryos with defects in epithelial morphogenesis.

Genotype	Unferti-lized	Wildtype -like	Dorsal closure	Head involution	Dorsal & head defects	Germ band retraction	Other defects	*n*
w^{1118}	100	-	-	-	-	-	-	81
dfer$^{\Delta 252}$	48.8	15.7	5.4	5.8	7.4	0.8	15.7	121

Data is shown as percentage of counted embryos.

Nevertheless, as the *dfer*$^{\Delta 252}$ line does not remove the entire *dfer* gene and still expresses *dfer*, only a null mutation would confirm the possible involvement of *dfer* in the process of dorsal closure.

2.14 Functional analysis of the *dfer*^{del1} mutant and the mutants *dfer*$^{w39.2}$, *dfer*^{49Sb} and *dfer*$^{41.1}$

Despite the extensive PCR and Southern blotting analyses, a fly line carrying a null mutation of the *dfer* gene was not identifiable by conventional methods. Therefore, a collaboration was started with M. Murray from the group of Andrea Brand, Cambridge, who was also working on the *dfer* gene. Similarly, they also encountered great problems trying to create deletions within the gene. Four imprecise excision screens using the *dfer*^{EP707} fly line and the Mz465 line failed to identify a *dfer* mutation. In two following male recombination screens, they managed to isolate one mutant, *dfer*^{del1} (Abstract Murray et al. 2001). The mutant contains an overall deletion of approx. 50 kb, removing the entire *dfer* transcription unit. However, four adjacent genes are additionally deleted. The line is homozygous lethal and preliminary analysis revealed defects in both CNS development and dorsal closure. Yet, more information about the nature of these defects was not available. The dorsal closure phenotype could be partially rescued by expressing the cDNA of the canonical *dfer* transcript, but not the neuronal phenotype. The *dfer*^{del1} mutant was kindly provided by the Brand group and used to continue with the characterization of *dfer* function. Therefore, first the mutant had to be further analysed.

2.14.1 The *dfer*^{del1} mutant has several genes deleted and displays lethality in all major stages of development

The Brand laboratory used P-element induced male recombination to generate the *dfer*^{del1} mutant. The event of male recombination happens upon P-element excision and produces flanking deletions in the immediate vicinity of the P-element by double strand DNA

breaks and concomitant DNA repair (Preston et al. 1996). An enhancer-trap fly line called Mz465 from J. Urban and G. Technau, Mainz, served as a starter line. This fly line carries a GAL4 P-element upstream of the *dfer* 5'UTR and expresses GAL4 in particular pioneer neurons of the embryonic CNS (Hidalgo and Brand 1997). GAL4 expression starts from about stage 12 in some pioneer neurons and continues through embryogenesis. The expression can be variable; scattered cells are found varying between segments and can be detected throughout the development of the CNS. According to the information of the Brand group, the deletion in the *dfer*^{del1} mutant removed a region of approx. 50 kb, deleting at least three additional genes together with the entire *dfer* transcription unit (Fig. 2.23). However, as it was generated by male recombination, the original pGawB P-element insert is still retained and functions as a GAL4 driver. To start with, the deletion had to be confirmed and mapped by PCR. As the deletion in the *dfer*^{del1} mutant was homozygous lethal, flies were first crossed to *dfer*^{zwim} EP flies do facilitate the PCR analysis. Using primers directed against different regions of the presumably deleted region and the flanking areas thereof, the deletion could be verified. Taken together, additionally to the *dfer* gene, the four predicted proximal genes CG8129, CG18473, CG33187 and CG33188 were deleted in the mutant. The gene further downstream, CG8121, which encodes a putative amino acid transporter, was not affected. There are no studies published concerning these genes. As they are uncharacterized, it remains unknown whether they are essential genes.

The Brand group attributed a dorsal closure and neuronal embryonic phenotype to the mutant. Thus, one would expect the *dfer*^{del1} mutant to die during embryonic stages. Surprisingly, analysis uncovered lethality at all stages of development, with flies being mainly larval lethal. Homozygous larvae had a prolonged development and needed about two to three days longer for their development. When taking homozygous larvae, approx. 12.3% (n = 65) of them developed even to adulthood. However, they were not able to eclose. Dissection of these pharate adults revealed an abnormal orientation of the abdominal segments, with the abdomen being twisted and split by a cleft (Fig. 2.25 A). Additionally, the patterning of the bristles on the abdomen was disturbed showing changed polarity.

Crosses of the *dfer*^{del1} mutant line to the *dfer*$^{\Delta 252}$ line revealed trans-homozygous flies, carrying both the *dfer*^{del1} and *dfer*$^{\Delta 252}$ mutant allele. These flies were morphologically normal and fertile, providing a first hint for *dfer* mutations being not lethal.

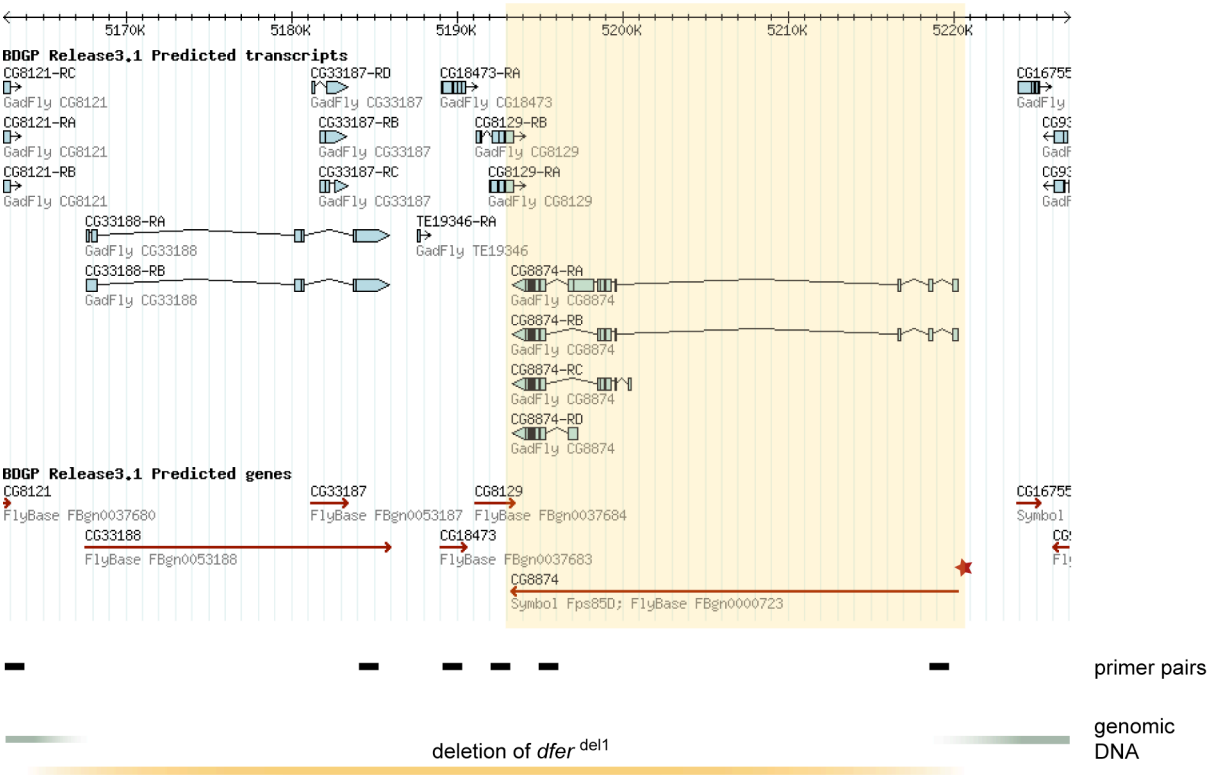

Fig. 2.23 Genomic region of the deletion in the *dfer*^{del1}mutant. The deletion in the *dfer*^{del1} mutant is caused by male recombination of the original Mz465 line; its P-element is represented as a star in the 5'UTR region of the *dfer* gene. A region of approx. 50 kb is removed in the mutant, including the entire *dfer* gene (region highlighted in *yellow*), and the downstream genes CG8129, CG18473, CG33187 and CG33188. The gene CG8121 is still present. The genomic region is taken from the HDFlyArray webpage (hdflyarray.zmbh.uni-heidelberg.de). The deletion is indicated in *yellow*, the breakpoints on both sides are imprecisely mapped. The respective primer pairs used for PCR mapping are shown as black boxes.

2.14.2 Expression analysis of the deleted genes in the *dfer*^{del1} mutant

The *dfer*^{del1} mutant displayed homozygous lethality, and neuronal and dorsal closure phenotypes were reported. Bearing in mind that any phenotype could be attributed to mutations in the other genes CG8129, CG18473, CG33187 and CG33188, these predicted genes had to be examined in more detail.

The two genes CG8129 and CG18473 appear to be involved in metabolic processes. Whereas the predicted gene CG8129 encodes a product with threonine ammonia-lyase activity (469 amino acids) and is putatively involved in amino acid biosynthesis, CG18473 encodes a protein with hydrolase activity (i.e. aryldialkylphosphatase activity, 350 amino acids) involved in unknown biological processes. A P-element insertion line in the CG8129 locus is available, being viable and fertile.

The gene CG33188 encodes a small zinc finger protein of approx. 200 amino acids, which is putatively involved in perception of sound as interfered from electronic annotation. The gene was found in a differential embryonic head cDNA screen for developmentally

regulated *Drosophila* neural precursor genes, but was not further investigated (Brody et al. 2002). It is comprised of an AN1-like and an A20-like zinc finger domain and is thus homologous to mammalian AWP1, a novel protein that is expressed during early mammalian development (Duan et al. 2000). Within the transcription unit, i.e. within an intron of the gene CG33188, an additional gene is predicted, CG33187. It encodes for a 314 and 372 amino acid protein, respectively, with no homologies to other proteins. Similar to CG33188, it was also found in the differential embryonic head cDNA screen. Therefore, CG33187 might be envisioned as a CG33188 splice variant. Indeed, in previous predictions, the two genes were annotated to be one gene. Thus, the gene CG33187 was regarded as part of the CG33188 gene and referred to as CG33188. There are P-element insertion lines within the original CG33188 transcription unit available, which are recessive lethal.

To investigate the potential cellular function of these genes, their expression during embryonic stages was analysed by *in situ* hybridization. For the gene CG8129, no specific staining was detectable, either reflecting a low abundance of the transcript such that it is below the detection rate or the absence of the transcript during embryogenesis (Fig. 2.24 A). As it is a putative threonine dehydratase, it might well be only expressed in later stages during larval or pupal development. While no expression was observed for the gene CG18473 during early stages, it was expressed in the Malpighian tubules (evaginations of the hindgut) from stage 14 onward (Fig. 2.24 B). This would fit to the assumption of CG18473 being a hydrolase, which could act specifically in the metabolism of Malpighian tubules. The gene CG33188, however, revealed a neuronal staining starting with the first and second wave of neuroblast formation (Fig. 2.24 C). Expression continued through all stages of CNS development until the ventral nerve cord was fully condensed. Thus, CG33188 is a neuronal gene. Due to the presence of zinc finger domains and therefore putative DNA binding capacity, it might well act as a transcription factor being involved in the neurogenesis of *Drosophila*. In the $dfer^{del1}$ mutant, the characteristic expression patterns of these three genes and of *dfer* were, as expected, absent (Fig. 2.24 D).

As distinct hybridization patterns observed at different developmental stages may hint to possible functions and lethality of a gene, it cannot be excluded that especially the presumably neuronal Gene 33188 might be essential for *Drosophila* development and thus causing the neuronal phenotype and the lethality in the $dfer^{del1}$ mutant.

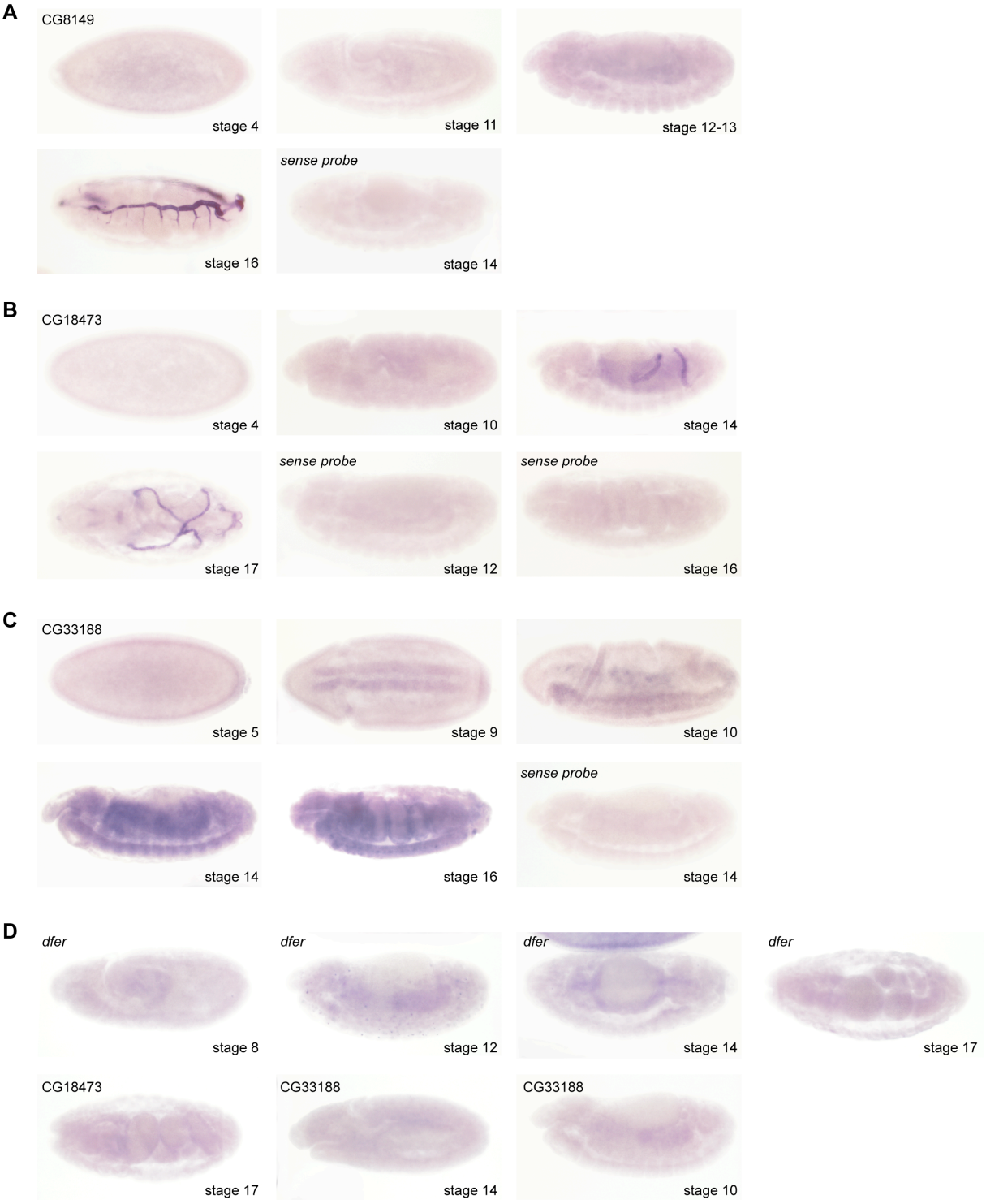

Fig. 2.24 Expression pattern of the genes CG8129, CG18473 and CG33188 in the *Drosophila* wildtype embryo and in the *dfer*^{del1}mutant. (A-C) Wildtype embryo. (D) *dfer*^{del1} mutant embryo. (A) Expression of the gene CG8129 is not detectable during embryogenesis. Stage 16 shows tracheal background staining. (B) The Gene CG18473 is expressed in the Malpighian tubules from stage 14 on. (C) CG33188 is expressed during neurogenesis. At stage 9, expression is apparent in the neuroblasts segregated from the ventral neurogenic region during the two waves of neuroblast delamination and continued during neuronal differentiation and ventral nerve cord condensation until the end of embryogenesis. (D) The characteristic expression pattern of *dfer*, with expression in the hindgut primordial, in the CNS and during dorsal closure, is absent in the *dfer*^{del1} mutant. See also Fig. 2.10. Similarly, there is no expression of the genes CG18473 and CG33188 in the mutant. For all stainings, control *in situ* hybridizations with sense probes were performed. Embryos are shown in lateral view, anterior is to the left. (B, stage 17) is a dorsal view, (C, stage 9; D, *dfer* stage 14) are ventral views.

2.14.3 Identification of the *dfer*$^{w39.2}$, *dfer*^{49Sb} and *dfer*$^{41.1}$ mutant

As the *dfer*^{del1} mutant harbors a large deletion covering at least three additional genes, of which at least one might be essential for *Drosophila* development, a new mutant which specifically deletes only the *dfer* gene had to be isolated. Having the homozygous lethal *dfer*^{del1} mutant allowed a new screening method for the identification of another *dfer* mutant, which should be identifiable by trans-homozygous lethality.

Two approaches were used: Since *dfer* displayed transcriptional expression in glial cells (C. Klämbt, pers. comm.), one idea was to cross the *dfer*^{del1} line to mutants in glial cell development and to screen for flies which were not able to get trans-homozygous. In a saturating EMS mutagenesis screen performed in the laboratory of C. Klämbt, Münster, 330 different fly lines with mutations on the 3rd chromosome affecting the midline glial cell development and thus the embryonic CNS axon pattern were previously isolated (Hummel et al. 1999; Klambt et al. 1997). These 330 lines were therefore crossed to the *dfer*^{del1} mutant and the progenies were screened for trans-homozygous lethality. However, no line meeting this condition was found, pointing either to *dfer* being not lethal or playing no essential role in glial cell development.

In the second approach, the putative mutant fly lines obtained from the two already described imprecise P-element excision screens were closer examined. Therefore, the *dfer*^{del1} mutant fly line was crossed to the 37 fly lines isolated from the first screen and the 43 fly lines from the second screen, and the progenies were screened for homozygous lethality. Three lines from the second screen meeting this condition, *dfer*$^{w39.2}$, *dfer*^{49Sb} and *dfer*$^{41.1}$, could be identified. Crossing between each other proved that they are all within one complementation group. PCR analysis was performed to map the extent of the deletion. Surprisingly, all three genes harbored the same deletion as the *dfer*^{del1} mutant, removing not only the *dfer* locus but also the proximal genes CG8129, CG18473 and CG33188. Similar problems were also encountered in the laboratory of A. Brand, Cambridge, as they were only able to obtain several large deletions comparable to the one of the *dfer*^{del1} mutant, but none removing *dfer* only (M. Murray, pers. comm.). Presumably, the chromosomal arrangement somehow prevents the creation of small deletions into the *dfer* gene, allowing only very large deletions. However, these deletions thereby remove the neighboring proximal genes as well. The identification of these three *dfer*$^{w39.2}$, *dfer*^{49Sb} and *dfer*$^{41.1}$ mutant fly lines argued also for a lethality caused by the CG33188 gene, which was in all three cases deleted.

2.14.4 CG33188 is causing the lethality of the *dfer*^{del1} mutant and the *dfer*$^{w39.2}$, *dfer*^{49Sb} and *dfer*$^{41.1}$ mutants

Crosses of the mutants to each other caused lethality in trans-homozygous progeny. With a very low frequency of less then 5-10%, however, trans-homozygous flies, so-called escapers, hatched with an abdominal phenotype similar to the one observed from homozygous *dfer*^{del1} mutant pharate adults (Fig. 2.25 A and B). These flies also displayed a reduction in body size compared to heterozygous controls of the same age and gender, but were still fertile (Fig. 2.25 C). In order to find out if these phenotypes are due to the loss of the CG33188 gene, EP-element insertion fly lines within this gene were tested. Two available fly lines, EP(3)3270, with an insertion within an intron in counter direction being recessive lethal, and EP(3)0632, with an insertion upstream of the 5'UTR of the gene in the same orientation being semi-lethal, were used for the crossings (Fig. 2.25 E). Indeed, crosses of the EP(3)3270 to the different *dfer* mutants revealed trans-homozygous escapers with the characteristic cleft in the abdomen (Fig. 2.25 D). For the crosses with the EP(3)0632 line, homozygous flies hatched with no obvious phenotype. The discrepancy between these two EP fly lines can be explained by the fact that the EP(3)3270 line with its insertion in the intron acts as a mutant of the CG33188 gene being also recessive lethal, whereas the EP(3)0632 line located in the 5'UTR has no strong effect on the CG33188 gene expression. Crosses of these EP lines to various GAL4 driver lines revealed no phenotypes. In summary, the neuronal CG33188 seems to be an essential gene, with its deletion causing the lethality of the *dfer* mutants.

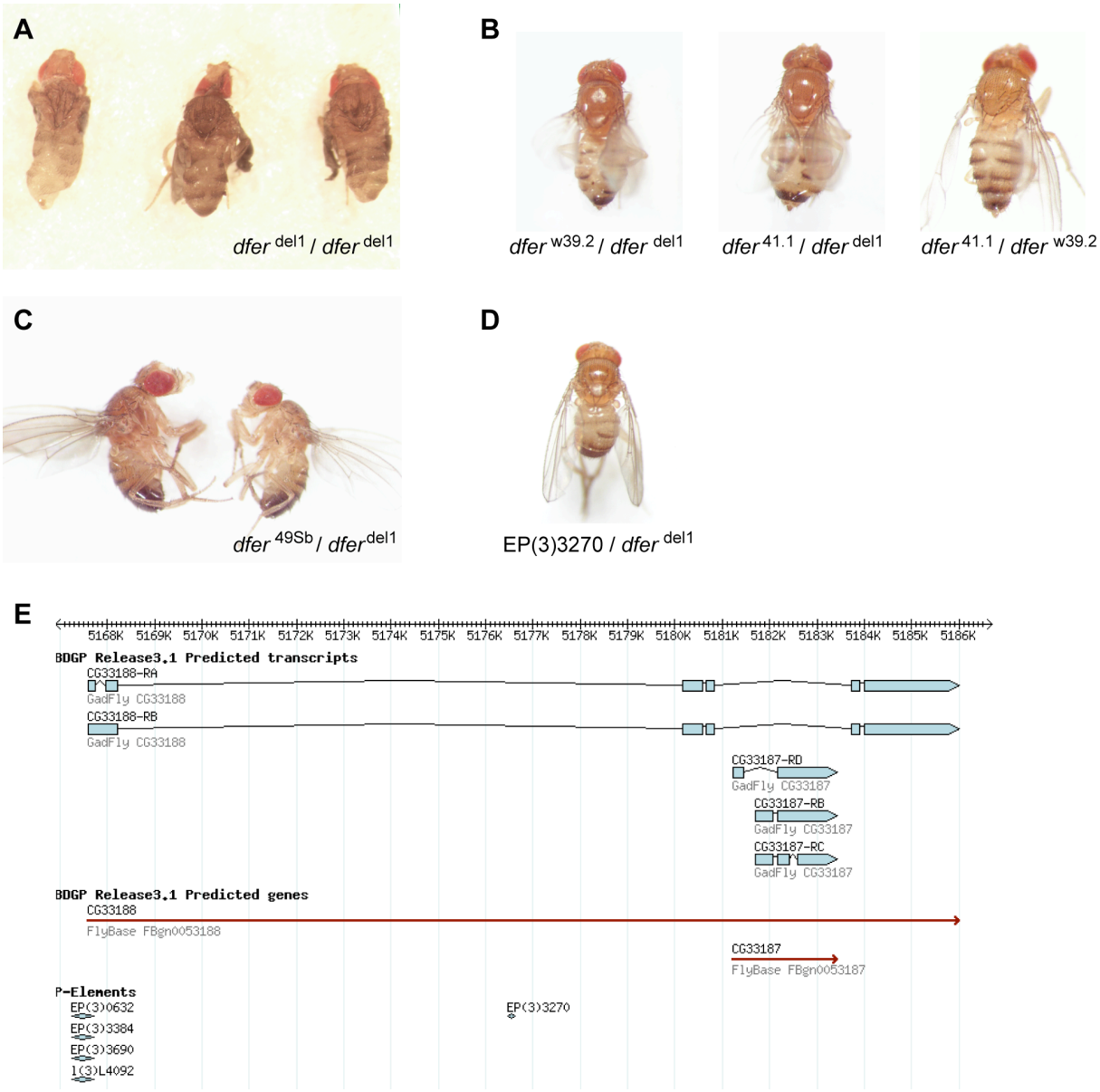

Fig. 2.25 Phenotypes of *dfer* mutant flies caused by the gene CG33187. (A) Homozygous mutant *dfer*^{del1} pharate adults that fail to eclose display an abnormal patterning of the abdominal segments, the abdomen being split by a cleft. (B) Crosses of the *dfer*^{del1} mutant to the *dfer*$^{w39.2}$, *dfer*^{49Sb} and *dfer*$^{41.1}$ mutants, or crosses within these, result with very low frequency in hatching trans-homozygous flies showing the same characteristic cleft in the abdomen. (C) Trans-homozygous flies (right) have smaller body sizes than heterozygous control flies (left) of the same age and sex. (D) Crosses of the EP(3)3270 line to the *dfer*^{del1}mutant result in lethality and reveal escapers with the abdominal phenotype. (E) The transcription units of CG33188 and CG33187 (taken from HDFlyArray). The EP-element insertion lines within these genes are depicted.

2.15 Analysis of *dfer* RNAi *in vivo*

Another approach to examine loss-of-function phenotypes of particular genes is the induction of RNA interference (RNAi), where the presence of double-stranded RNAs (dsRNA) causes the sequence-specific posttranscriptional silencing of a corresponding gene (reviewed in Mello and Conte 2004). Injection of dsRNA into *Drosophila* embryos silences

gene activity effectively, but its effect is transient and not inherited into the next generation (Kennerdell and Carthew 1998; Misquitta and Paterson 1999). To circumvent this problem, different methods have been developed for *in vivo* applications by using the UAS-GAL4 system to express dsRNA stably in transgenic *Drosophila*.

One method is based on a transgene that is symmetrically transcribed from opposing promoters (Giordano et al. 2002). Two convergent arrays of UAS sequences drive the dsRNA production by simultaneous transcription of sense and antisense strands. Using the *Sym*-pUASt vector containing these bidirectional UAS sites, flies were established expressing the first 1413 nucleotides of *dfer* (encoding approx. the first 400 amino acids of DFer) as dsRNA to mediate RNAi. In order to test their functionality, flies were crossed to lines overexpression *dfer* in the dorsal wing compartment (using *apterous*-GAL4) or in the wing pouch (using *scalloped*-GAL4), inducing blistery wings or wing notching, respectively. In both cases, the simultaneous expression of the *dfer* dsRNA led to a repression of the *dfer*-induced phenotypes (Fig. 2.26 F), showing efficient RNAi-mediated downregulation of the *dfer* mRNA. *Sym-dfer*-N flies were then crossed to different GAL4 lines to downregulate *dfer* in various tissues during different developmental time points. Surprisingly, no loss-of function phenotypes could be detected. One reason for this might be that RNAi mediated by the *Sym*-pUASt vector might be inefficient, thus leaving small amounts of mRNA which remain functional.

The newly designed pWIZ vector was reported to be very effective in inducing dsRNA-mediated RNAi *in vivo* (Lee and Carthew 2003) and was therefore utilized to exclude possibly missed RNAi-induced phenotypes. The pWIZ vector allows the cloning of a transgene containing inverted repeats separated by a functional intron to enhance the stability of inverted-repeat sequences and to produce splice-activated dsRNA. A length of 450 to 600 bp, which was shown to be most efficient for RNAi (Reichhart et al. 2002), was chosen to generate different constructs covering either nucleotides encoding for a fragment specific to the N-terminal domain (RNAi-*N*) or the SH2 and kinase domain (RNAi-*SK*) of DFer, or for the unique part of the longer DFer-A protein (RNAi-*long*) (Fig. 2.26 A). Transgenic flies were established and checked for their ability to suppress the *dfer*-induced overexpression phenotypes in the wing upon co-expression (Fig. 2.26 B-E). Flies producing dsRNA from RNAi-N or RNAi-SK constructs were able to suppress the phenotype much stronger than the previously used *Sym-dfer*-N line, resulting in a wildtype-like wing. As expected, dsRNA produced by RNAi-long did not show suppression as it specifically affects the *dfer-A* transcript. However, when crossing these flies to different GAL4 lines to monitor RNAi-induced phenotypes, similarly to *Sym-dfer*-N, no effect could be detected. Even an increase of dsRNA expression at higher temperatures caused no phenotypic occurrence. Embryonic stages were of particular interest to confirm the specificity of the observed dorsal

closure phenotypes from the *dfer*$^{\Delta 252}$ mutant. RNAi during embryogenesis using embryonic or maternal GAL4 lines, however, could also not induce phenotypes.

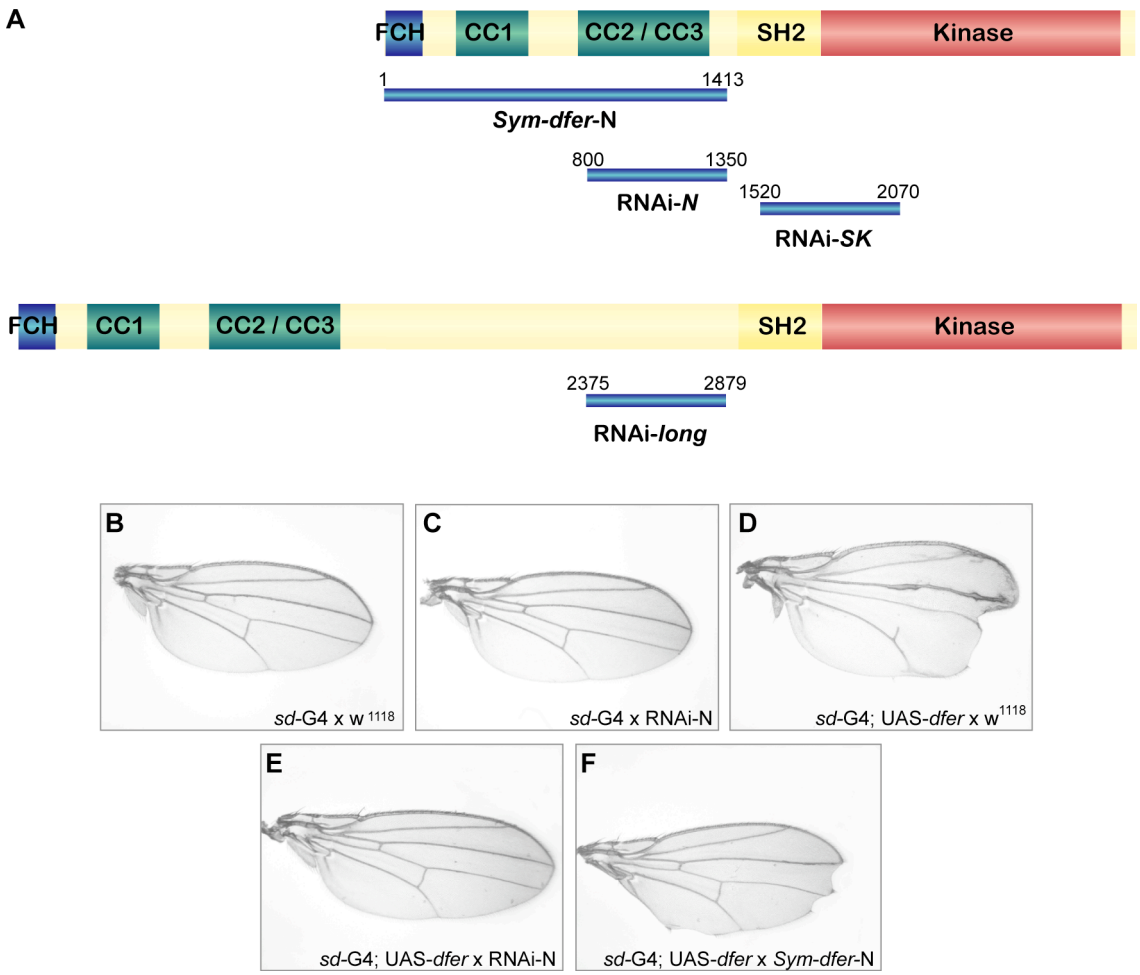

Fig. 2.26 RNAi constructs and suppression of the *dfer*-induced wing phenotype by transgene-mediated RNAi. (A) Several RNAi constructs were generated. *Sym-dfer*-N encodes for the first 1413 nucleotides of *dfer* and was cloned into the *Sym*-pUASt vector. RNA-*N* and RNAi-*SK* encode the nucleotides 800-1350 and 1520-2070, respectively, of *dfer*. RNAi-*long* encodes the nucleotides 2375-2879 of the longer *dfer-A* transcipt. All three constructs were cloned into the pWIZ vector for transgene-mediated RNAi. (B-F) Suppression of the *dfe*r-induced wing notching defect. All crosses were performed with scalloped-GAL4 at 25°C. (B) Wildtype wing. (C) Expression of *dfer* dsRNA, in this case by the RNA-*N* construct, does not result in a phenotype. (D) An intermediate phenotype upon *dfer* overexpression is shown with wing notching, vein broadening and missing interveins. (E) Co-expression of the RNA-*N* dsRNA results in a complete suppression of the *dfer*-indcued wing phenotype. (F) Co-expression of the *Sym-dfer*-N dsRNA partially suppresses the *dfer*-indcued wing phenotype.

In fact, transgenic RNAi-mediated gene silencing during embryogenesis has been described independently by several persons to be not functional (G. Merdes, pers. comm.). To increase the dosage of expressed dsRNA, two alleles of each construct were recombined and tested with different GAL4 lines at an elevated temperature of 29°C. Surprisingly, the progenies revealed pupal lethality. When using a control line carrying a construct producing *f:nec* dsRNA mediating RNAi and normally causing forked bristles and hairs (Reichhart et al.

2002), flies showed again lethality at 29°C. Thus, the elevated dsRNA production during larval and pupal development seems to interfere with the RNAi machinery causing lethality.

In conclusion, using two independent approaches to knock down the *dfer* gene by transgenic RNAi-mediated silencing, no obvious mutant phenotype could be observed. It still can be envisioned that small amounts of mRNA escaping the RNAi mechanism retain *dfer* function, preventing the detection of phenotypic disturbances. Nevertheless, together with the results obtained with the different *dfer* mutants, these data argue for *dfer* being a non-essential gene.

2.16 Genomic rescue constructs for *dfer* and the genes CG8129, CG18473 and CG33188

2.16.1 Generation of genomic rescue constructs and transformation of flies

All isolated *dfer* mutants carry deletions removing not only the *dfer* gene, but also the three proximal genes CG8129, CG18473 and CG33188. To analyse the function of one gene, however, effects of other genes have to be excluded. Genomic rescue constructs can be used to reintroduce missing genomic regions and thus omitted genes. In this way, transgenic flies could be generated containing the genomic region of the missing CG8129, CG18473 and CG33188 genes, which would be then introduced into the mutant flies in order to obtain flies lacking only *dfer*. Vice versa, a genomic rescue constructs for *dfer* could confirm that the observed lethality and abdominal phenotypes were specific to one of the three other deleted genes (Fig. 2.27).

Thus, two genomic rescue transgenes had to be generated. In practice, this approach was hindered by the large size of the genomic region, given by the technical size limits of the cloning procedure, and the *Drosophila* transformation protocols that were employed. The genomic fragments were obtained from BACs isolated from a BAC library of the second and third chromosome of *Drosophila* (Hoskins et al. 2000). For the *dfer* genomic rescue, the entire 28 kb of the *dfer* transcription unit were cloned. Additionally, 8 kb upstream of the *dfer* transcription start including the presumable promoter region were included into this fragment. The whole region could be excised as an FseI fragment with a total length of 38 kb. The construct for the genes CG8129, CG18473 and CG33188 contained their open reading frames within 26 kb and extended 4 kb upstream of the gene CG33188 to include the presumptive promoter region. The entire region could be excised from a BAC as a 30.4 kb fragment using the SphI restricition enzyme (Fig. 2.27; Fig. 2.28 A). As these genomic regions were extremely large, cosmid vectors that allow cloning of large genomic fragments were the favorite tools. To mediate germ line transformation in *Drosophila*, the cosmid had to

additionally incorporate the terminal repeats of a P-element and include the *Drosophila white* gene as a marker. The P-element cosmid vector pCosPer (Steller and Pirrotta 1985; Pirrotta 1988) met these conditions, but had to be first modified in several ways before it could be used for the cloning procedure (see Material and Methods). The modifications resulted in pCosPer-ASF and pCosPer-45(-S)-L/ASF cosmid vectors, which were used for the cloning of the isolated and purified FseI fragment containing the *dfer* gene and the SphI fragment containing the other three genes, respectively (Fig. 2.28 B).

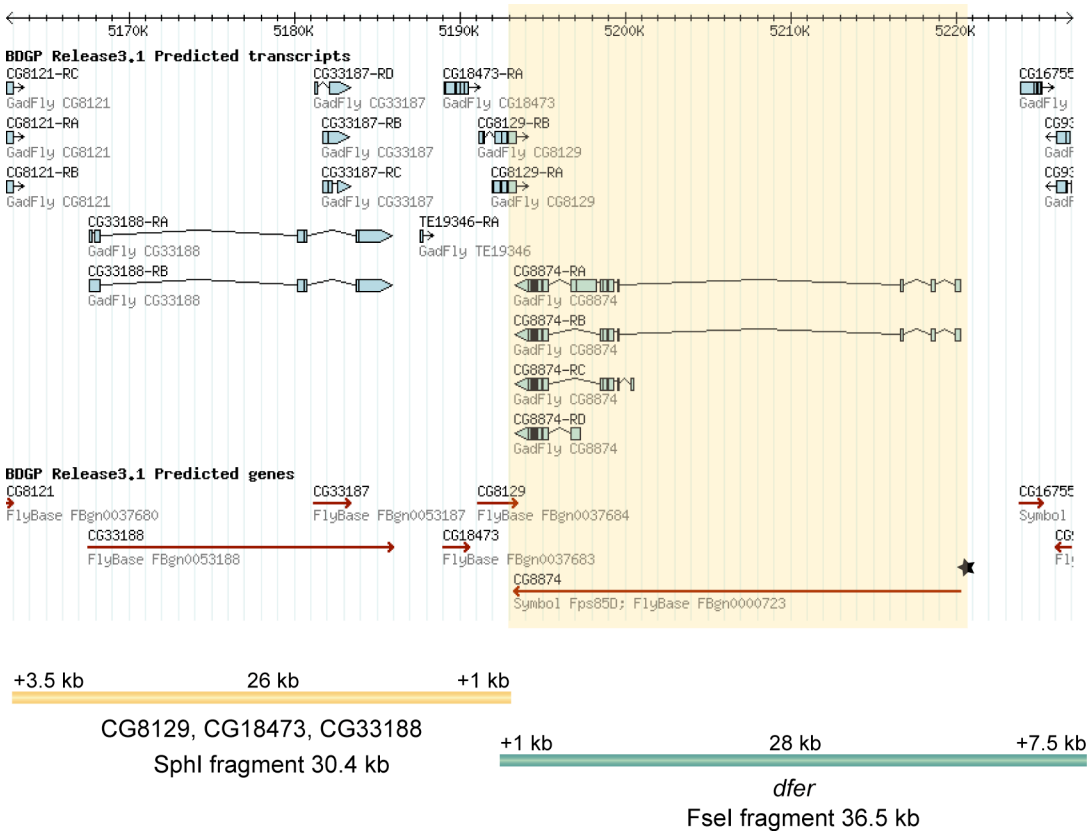

Fig. 2.27 Genomic rescue constructs for *dfer* and the genes CG8129, CG18473 and CG33188. The genomic region of these genes is shown (taken from HDFlyArray). The 36.5 kb FseI fragment contains the 28 kb of the *dfer* locus and some 8 kb flanking the upstream region, as well as an additional 1 kb downstream. The 30.4 kb SphI fragment includes the transcription units of the genes CG8129, CG18473 and CG33188, which spans a region of approx. 27 kb. 4 kb upstream of CG33188 and 1 kb downstream of CG8129 were additionally included.

The two constructs were isolated from BACs and cloned into their respective cosmid vectors. Following phage packaging and infection of bacterial cells, positive cosmids containing the genomic rescue regions were isolated, amplified and purified. As the resulting genomic cosmids had large sizes with 41.9 kb and 48 kb, respectively, P-element mediated germ line transformation was impeded. Due to problems with the high viscosity of the DNA solutions and therefore the increased amount of dying embryos following injection, up to 6.500 embryos had to be injected for one genomic rescue construct (Fig. 2.28 C). For the

dfer genomic rescue, 16 transformants identified by their eye color could be obtained. PCR analysis to check the integrity of the inserted DNA revealed that only 9 of them carried the entire genomic region. The insertions were mapped to the different chromosomes. Transgenes for the *dfer* genomic rescue could be found on all three chromosomes.

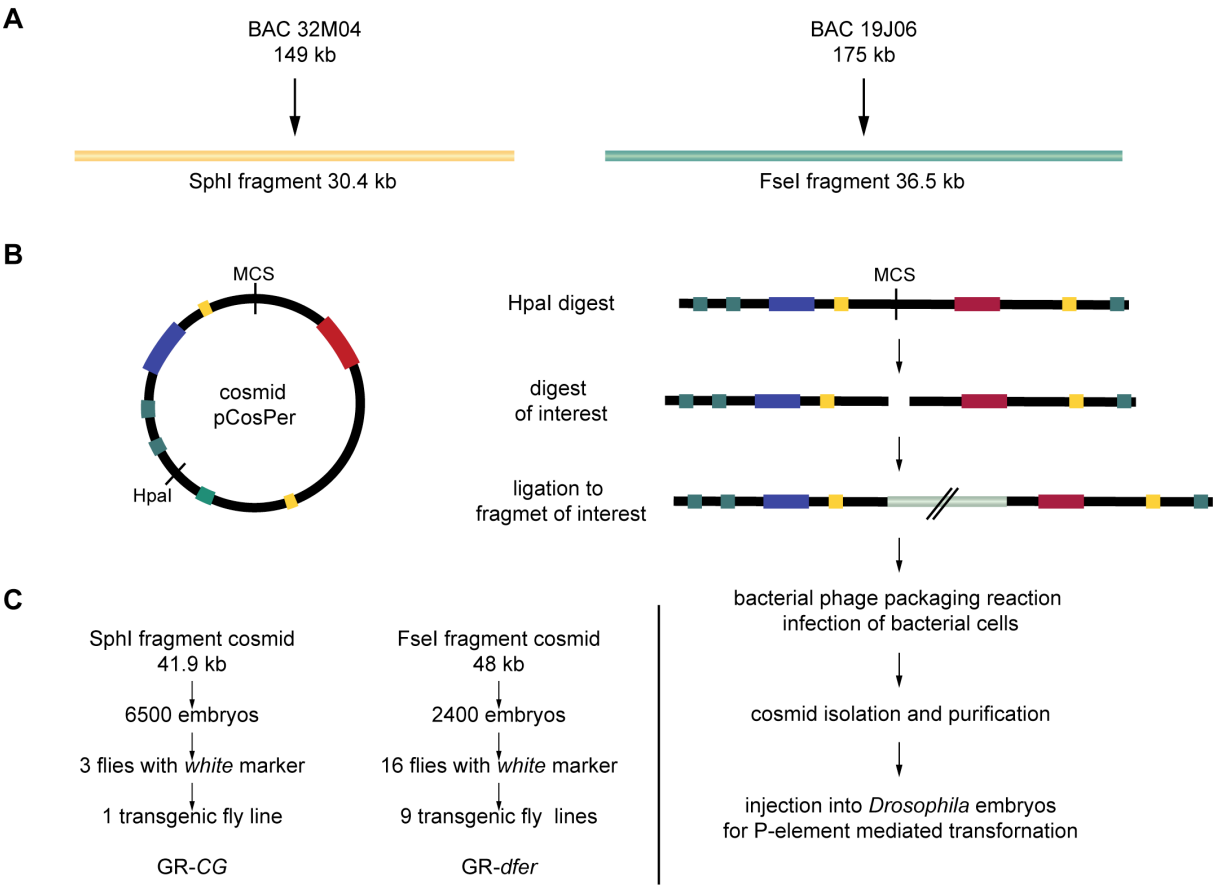

Fig. 2.28 Generation of the genomic rescue constructs by cosmid phage packaging and transformation of flies. (A) The 30.4 kb SphI fragment containing the genes CG8129, CG18473 and CG33188 was obtained by digestion of BAC 32M04. The 36.5 kb FseI fragment including the *dfer* gene was obtained by digestion of BAC 19J06. The fragments were isolated by pulsed field gel electrophoresis, extracted from the agarose and subsequently purified. (B) Outline of the cosmid cloning. Derivatives of the P-element cosmid vectors pCosPer were used for the cloning of the genomic rescue constructs. Following the cloning procedure, positive cosmids containing the desired genomic region were identified and used for P-element mediated transformation of *Drosophila*. *Green* boxes in the cosmid vector represent the *cos*-sites, *yellow* the P-element sites, *blue* the Ampicillin resistance gene, and *red* the *white* marker gene. (C) The resulting cosmids with sizes of 41.9 kb for the genes CG8129, CG18473 and CG33188 and of 48 kb for the *dfer* gene were injected into 6500 and 2400 *Drosophila* embryos, respectively, for germ line transformation. For the three genes, only 3 flies were obtained carrying the *white* marker of the cosmid, but of these only one fly line carried the entire genomic rescue construct identified by PCR analysis. For the *dfer* gene, 16 flies were obtained with the marker gene, of which 9 fly lines were transgenic for the *dfer* genomic rescue construct. GR-*CG*, genomic rescue for the genes CG8129, CG18473 and CG33188; GR-*dfer*, genomic rescue for the *dfer* gene.

The transformation of the genomic rescue for the genes CG8129, CG18473 and CG33188, however, resulted only in three transgenic flies despite the huge number of injected embryos. Moreover, of these three flies, only one contained the entire construct. Mapping revealed that the insertion of the genomic rescue was on the third chromosome, which complicated the analysis as it also contains the original *dfer* locus and the locus for the three other genes.

2.16.2 The *dfer* genomic rescue does not rescue the lethality of the *dfer* mutants

Having several fly lines containing the genomic rescue of the *dfer* locus, these flies were crossed to the *dfer* mutants to decipher the contribution of each gene to the observed phenotypes. The presence of the *dfer* genomic rescue construct in *dfer* mutants, however, failed to rescue the lethality. This observation provides final evidence for *dfer* being not involved in the lethality of the mutants and, concurrently, *dfer* being a non-essential gene.

2.16.3 The genomic rescue for the genes CG8129, CG18473 and CG33188 rescues the lethality of the *dfer* mutants

Only one transgene carrying the genomic rescue of the genes CG8129, CG18473 and CG33188 was obtained with an insertion on the third chromosome. Since the genes to be analysed are also located on the third chromosome, lines with new insertion sites on other chromosomes were tried to be isolated in a precise P-element excision screen. Similarly to the imprecise P-element excision screens, the transgenic fly line GR-CG$^{53.1}$ was crossed to a transposase-supplying fly line to induce the excision and the subsequent reinsertion of the genomic rescue construct. Putative chromosomal mobilizations of the insert were identified by a change in eye color intensity. Of these, 390 males were isolated and established as stocks. PCR analysis of them revealed that the genomic rescue DNA construct jumped precisely, resulting in flies with an integer construct (Fig. 2.29 A). When mapping the chromosomal insertion sites, however, all of the newly inserted genomic rescues had jumped only locally and were still located on the third chromosome. This phenomenon can only be explained by a finding, that, when mobilized in females, P elements transpose at high frequency into genomic regions close to the original site of insertion within 100 kb (Sentry and Kaiser 1992).

Another possibility to combine the genomic rescue construct with the *dfer*^{del1} mutant is the recombination of the third chromosome resulting in flies carrying both genomic rescue and deletion of the genes. However, as both lines (the GR-CG$^{53.1}$ and the *dfer*^{del1} mutant)

carry the *white* gene as a marker, there was no marker available to identify flies with successful recombination events. Thus, a screen for recombinants was performed. Following the crosses of GR-CG$^{53.1}$ to the *dfer*^{del1} mutant, 52 males of the F1 generation were crossed to balancer lines and analysed for a recombination event by PCR. In parallel, these lines were also crossed to the *dfer*^{del1} mutant. 19 of these lines revealed flies becoming homozygous for the *dfer*^{del1} deletion. When analysing the genomic DNA for recombination by PCR, these 19 lines indeed contained the genomic rescue, thus carrying both the genomic rescue construct and the *dfer*^{del1} deletion (Fig. 2.29 A). The lines are referred to as *dfer*$^{del1/GR-CG}$ lines. The presence of a single copy of the genomic rescue construct DNA for the genes CG8129, CG18473 and CG33188 rescues the *dfer*^{del1} mutant lethality and results in homozygous *dfer*^{del1} mutant flies. These findings indicate that the lethality and the observed lethality of the *dfer*^{del1} mutant are specific to the loss of one of the three gene functions, presumably of the gene CG33188. Having the *dfer*$^{del1/GR-CG}$ lines allows now to study the effect of the single loss of the *dfer* gene. That the *dfer* gene was indeed deleted and thus no DFer protein expressed could be verified by Western blotting (Fig. 2.29 B).

2.16.4 Analysis of the *dfer*$^{del1/GR-CG}$ mutants

Since fly lines were now available, which were only mutant for the *dfer* gene and homozygous viable, these *dfer*$^{del1/GR-CG}$ lines were further examined. Apparently, no adult phenotypes were noticeable. However, a first test of the embryonic viability showed a significant reduction summarized in Table 2.7. The rate of embryonic viability was similar to the one previously observed for the *dfer*$^{\Delta 252}$ mutant with the small *dfer* deletion, ranging between approx. 71.4% to 85.4%.

Table 2.7 Embryonic viability of the different *dfer*$^{del1/GR-CG}$ mutants.

Fly line	Viability	*n*
w^{1118}	94.6%	1089
dfer$^{\Delta 252}$	87.3%	801
dfer$^{del1/GR-CG1}$	71.4%	971
dfer$^{del1/GR-CG2}$	85.2%	826
dfer$^{del1/GR-CG6}$	85.4%	707

Three of the rescued lines were representatively examined.

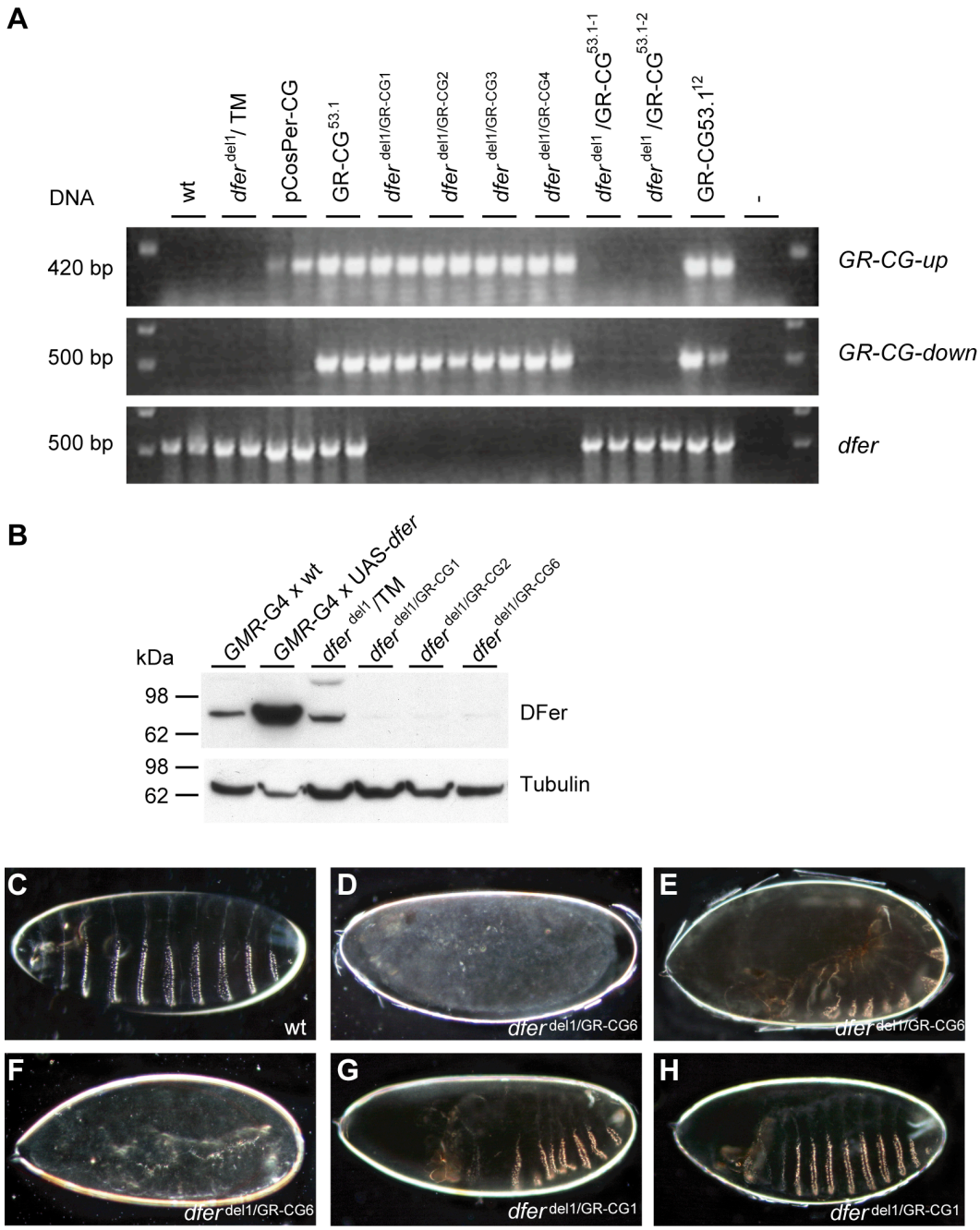

Fig. 2.29 Identification and analysis of rescued *dfer*$^{del1/GR-CG}$ mutants. (A) PCR analysis of flies carrying the CG genomic rescue construct. Genomic DNA was isolated from different fly lines and analysed for the presence of the CG genomic rescue construct by testing for the transition between the end of the genomic rescue fragment and the flanking cosmid sequence from both sides of the fragment (*GR-CG-up* and *GR-CG-down*), and for the absence of the genomic *dfer* region (*dfer*). For each fly line, two flies were separately tested. Note that in the recombinant flies the CG genomic rescue construct DNA is present, whereas the genomic *dfer* region is deleted. (B) DFer protein expression analysis. Protein extract from fly heads were isolated and subjected to SDS-PAGE and Western blotting (DFer SK antibody was used). *dfer*$^{del1/GR-CG}$ flies carrying the genomic rescue do not show DFer protein expression. *wt* flies and UAS-*dfer* flies were crossed to the GMR-GAL4 driver at 25°C. (C-H) Embryonic cuticle preparations. (C) *wt* embryo. (D-H) Phenotypes of the rescued *dfer*$^{del1/GR-CG}$ embryos. (D) Unspecifiable early embryonic defect. (E) Germ band retraction defect. (F) Strong dorsal closure phenotype, leaving the embryo dorsally completely open. (G) Head involution and dorsal closure defect. (H) Head involution defect. *wt*, wildtype flies; *dfer*^{del1}/TM, deletion over a balancer chromosome; pCosPer-CG, CG genomic rescue cosmid; GR-CG$^{53.1}$, original CG genomic rescue fly line; *dfer*$^{del1/GR-CG1-6}$, recombinant flies carrying both the CG genomic rescue and the *dfer*^{del1} deletion; *dfer*^{del1}/GR-CG$^{53.1\ 1-2}$, non-recombinant fly line; GR-CG53.1^{12}, fly line with jumped CG genomic rescue; -, no DNA.

In order to confirm that the observed dorsal closure phenotypes of the *dfer*$^{\Delta 252}$ mutant were specific to the loss of *dfer* function, the lethal rescued embryos were also analysed by cuticle preparations (Fig. 2.29 C-H; Table 2.8). Indeed, only approx. 70% of the examined different lethal *dfer*$^{del1/GR\text{-}CG}$ embryos were unfertilized eggs or wildtype-like larvae, which failed to hatch. The other embryos displayed various dorsal closure phenotypes and head involution defects (Fig. 2.29 G and H). Some had very strong effects and were even entirely dorsally open (Fig. 2.29 F), whereas others showed defects already during germ band retraction (Fig. 2.29 E). A few embryos died early with unspecifiable defects (Fig. 2.29 D). These findings together with the previous observations with *dfer*$^{\Delta 252}$ mutant support a role of *dfer* in embryogenesis during dorsal closure and head involution.

Table 2.8 Percentage of dead *dfer* mutant embryos with defects in epithelial morphogenesis.

Genotype	Unfertilized	Wildtype-like	Dorsal closure	Head involution	Dorsal & head defects	Germ band retraction	Other defects	*n*
w^{1118}	41.7	41.7	-	8.4	-	-	8.4	12
dfer$^{del1/GR\text{-}CG1}$	53.5	19	3.5	8.6	1.7	1.7	12.0	58
dfer$^{del1/GR\text{-}CG2}$	44.1	23.5	-	11.8	-	5.9	14.7	34
dfer$^{del1/GR\text{-}CG6}$	70	3.6	7.1	5.4	-	5.4	9.0	56

Data is shown as percentage of dead embryos. Note that the high percentage of *wt* embryos with defects represent only one single embryo for each defect and is dependent on the low total number of obtained lethal *wt* embryos. *Other defects* refers to unspecifiable early embryonic defects.

Discussion

3 Discussion

This study reports nine putative interaction partners of APP, which were identified as modifiers of the APP-induced blistered wing phenotype in *Drosophila*. Further analysis of one of the modifiers, the protein-tyrosine kinase DFer, revealed an indirect interaction between APP and *dfer*, presumably caused by interference with cell adhesion. It could be shown that DFer is similar in structure and functional regulation to its vertebrate homologs Fes and Fer kinase. Moreover, overexpression and mutant analysis pinpoint to a similar function in adhesion-dependent signaling pathways during *Drosophila* development.

3.1 Suppressors of the APP-induced blistered wing phenotype

One of the numerous functions attributed to APP is an involvement in cell adhesion. Previous work has shown that the expression of human APP during *Drosophila melanogaster* wing development leads to cell adhesion defects visible as wing blisters (Fossgreen et al. 1998). Wing blisters are generally caused by disruption of the integrin-mediated cell adhesion or interference with integrin signaling between the two cell layers forming the wing epithelium (Brown et al. 2000). Together with the finding that the phenotype induction is dependent on both the intra- and extracellular domain of APP (Fossgreen et al. 1998), this suggests a receptor-like function of APP in the regulation of cell adhesion and an interaction with evolutionarily conserved protein partners involved in the cell adhesion of the two wing epithelia. Since the blistered wing phenotype represents an easy accessibly feature and the pathways during wing development of *Drosophila* are well characterized and highly conserved, a dominant modifier screen was performed to identify novel interactors of APP that could shed light on its function in cell adhesion and might provide new clues regarding other aspects of APP function (G. Merdes, unpublished data).

This work presents the results of the screen, where approx. 300 weak suppressors and nine strong suppressors of the APP-induced wing phenotype could be isolated along with several enhancers (G. Merdes, unpublished data). In a collaborative effort with H. Ehret and G. Merdes, Heidelberg, all genetic modifiers of the phenotype were identified. Here, the focus is mainly laid on the nine strong suppressors to ensure the specificity of the genetic interaction with APP. Since APP expression interferes with cell adhesion, mutations were anticipated in several known loci implicated in cell adhesion during *Drosophila* wing development. As expected, some components were found, in particular *blistery*, the *Drosophila tensin* ortholog, and the *beta*^{nu} *integrin* subunit, that are directly involved in cell adhesion. This proves the principle of the performed enhancer/suppressor screen in identifying factors relevant for cell adhesion. Thus, it can be predicted that some of the novel

loci might encode important components of cell adhesion that interact with APP.

The genes corresponding to the suppressors can be classified in four categories: proteins involved in cell adhesion, in calcium signaling, in the organization of the cytoskeleton, and in transcriptional regulation. One isolated gene encodes the *beta*^{nu} *integrin* subunit, a new uncharacterized integrin. So far, no mutation in this gene could be identified. Integrins are involved in several fundamental cell-biological processes during development, including cell migration, differentiation and proliferation by acting as a signal receptor, and formation of strong adhesive junctions between the extracellular matrix and the cellular cytoskeleton (reviewed in Watt 2002; Brower 2003; Bokel and Brown 2002; Brown et al. 2000). Besides in the adhesion between the two wing epithelial layers (Wilcox et al. 1989; Brown et al. 2000), integrins obviously play essential roles in the *Drosophila* nervous system. Several studies uncovered novel functions in axon growth cone guidance (Hoang and Chiba 1998; Billuart et al. 2001; Stevens and Jacobs 2002), short-term memory and synaptic plasticity (Beumer et al. 2002; Rohrbough et al. 2000; Beumer et al. 1999). Interestingly, APP has also been implicated in various processes regulating neuronal activity, such as neurite outgrowth, neuronal plasticity and memory (reviewed in Turner et al. 2003). A scenario could be envisioned in which APP interferes with integrin-mediated cell adhesion in the *Drosophila* wing, but possibly cooperates with integrin signaling in the nervous system, establishing a functional relationship between these two molecules and/or their pathways. In this respect, it is intriguing that APP has been found to colocalize with β1-Integrin subunits in primary neurons (Storey et al. 1996; Yamazaki et al. 1997) and to associate with the adaptor protein Fe65 and β1-Integrin at dynamic focal complexes (Sabo et al. 2001). This is further supported by the finding of another typical constituent of focal cell adhesion complexes in the screen, the *Drosophila* ortholog of *tensin*, *blistery.* The protein is implicated in linking integrins to the cytoskeleton and signaling pathways (reviewed in Geiger et al. 2001). In *Drosophila*, it was recently identified and reported to both mediate and stabilize the link between integrins and the cytoskeleton (Torgler et al. 2004; Lee et al. 2003).

Another suppressor of the APP phenotype is *trol* (*terribly reduced optic lobes*) that codes for *Drosophila* perlecan, a large multidomain heparan sulfate proteoglycan originally identified in extracellular matrix structures of mammals. Trol participates in neuroblast cell division and proliferation by modulating FGF and Hedgehog signaling (Park et al. 2003; Voigt et al. 2002). As APP was observed to interact with Perlecan in mammals (Narindrasorasak et al. 1991), it might suppress the APP induced blistered wing phenotype via direct interaction, strengthening the assumption of a ligand-based mechanism of APP interference with cell adhesion and a possible role in neuronal adhesion. Consistent with this notion, several other extracellular matrix molecules are known to associate with APP, like heparin, laminin and collagen (Multhaup et al. 1995; Williamson et al. 1995; Kibbey et al. 1993; Beher et al. 1996).

Indeed, a new mouse model with a triple knockout of all three APP family members, i.e. APP, APLP1 and APLP2, provides evidence for a crucial role of the APP family members in neuronal adhesion and the survival of neuronal cells, with mice displaying a phenotype resembling human type II lissencephaly with cortical dysplasias and a partial loss of cortical Cajal Retzius cells (Herms et al. 2004). Additionally, with F-Spondin, a first ligand for APP has been found that modulates APP cleavage (Ho et al. 2004). F-Spondin is a secreted signaling molecule that impairs binding of cells to the extracellular matrix and is implicated in neuronal development and repair.

The identification of calmodulin as one of the suppressors provides evidence for a role of calcium signaling in APP function. Calcium is one of the most important intracellular messengers in the brain, being essential for neuronal development, synaptic transmission and plasticity, and the regulation of multiple metabolic pathways. Additionally, extracellular calcium ions regulate the adhesive activity of cadherins and cytoplasmic signaling events thereof (reviewed in Tepass et al. 2000). Cadherins are transmembrane molecules mediating cell-cell adhesion through homophilic interactions (Vleminckx and Kemler 1999). In *Drosophila*, they are also essential for the formation of the wing by connecting the cells within one monolayer and mediating growth and patterning (Cho and Irvine 2004; Rodriguez 2004; Clark et al. 1995). Removal of calcium ions leads to a disordered cadherin structure, dysfunction of cadherin-mediated cell-cell adhesion and signaling, and concurrently to a disruption of the wing structure. It could be envisioned that APP expression might interfere with these processes, and thus causing wing blistering. Associations between Alzheimer's disease and perturbed cellular calcium homeostasis have been established in studies of patients, animal models and cell culture systems, where neurons render vulnerable to excitotoxicity and apoptosis (reviewed in Mattson 2002; Chan et al. 20002). Calmodulin itself acts as a ubiquitous calcium sensor/receptor protein and is engaged in almost all intracellular calcium events. With respect to APP, calmodulin functions as an activator and component of the calcium/calmodulin-dependent protein kinase II (CaMKII), a serine/threonine kinase implicated in APP phosphorylation *in vitro*, which was recently found to colocalize with Aβ depositions in the pathological brain (Wang et al. 2005). The finding of calmodulin as a genetic interactor of APP would raise the question whether APP phosphorylation by the CaMKII is an important event for APP mediated function in cell adhesion.

In fact, APP processing and signaling events can be regulated by phosphorylation and phosphorylation-dependent events (reviewed in da Cruz e Silva et al. 2004). APP has several well-defined phosphorylation sites within the intracellular domain and a number of kinases have been implicated in the phosphorylation, for example the serine/threonine protein kinase Cdk5 that phosphorylates the mature form of APP specifically at Thr-668 in neurons (Iijima et al. 2000). Phosphorylation seems to influence the specificity and affinity of

cytosolic binding partners, as, in the particular case of Thr-668, phosphorylation prevents the binding of Fe65, whereas the binding of X11 and mDab1 is unaffected (Ando et al. 2001). Simultaneously, phosphorylation alters APP processing (Ando et al. 2001; Lee et al, 2003) and causes structural changes (Ramelot and Nicholson 2001), possibly inducing a conformational switch that alters the binding to APP interacting proteins. These might be themselves modified by phosphorylation, providing an additional step of regulation. Interestingly, two kinases, the serine/threonine protein kinase Lk6 and the protein-tyrosine kinase DFer, were among the interactors identified in the screen. Both kinases are uncharacterized in *Drosophila,* and for Lk6 no mammalian homolog is known. DFer has two mammalian homologs, the Fes kinase and the Fer kinase. These non-receptor protein-tyrosine kinases have been implicated in the regulation of cell-cell and cell-matrix interactions that are mediated by adherens junctions and focal adhesions. Additionally, they are involved in the signaling between receptor complexes, possibly through a role in the regulation of cytoskeletal rearrangement (reviewed in Greer 2002). The attributed functions of these kinases in cell adhesion raise the possibility of a role of DFer in the APP-induced interference with cell adhesion, possibly via direct phosphorylation of APP or APP binding proteins.

The interactions with the genes *kismet* and *kruppel homolog 1* are somehow surprising as they encode for nuclear proteins involved in transcriptional regulation. Kismet is a member of the trithorax group and functions as a chromatin-remodeling ATPase (Daubresse et al. 1999). Kruppel homolog1 is a zinc finger transcription factor and acts as a modulator of the expression of many ecdysone regulated genes during *Drosophila* metamorphosis (Pecasse et al. 2000; Beck et al. 2004). During embryogenesis, however, its expression is restricted to neurons and essential for early development (Beck et al. 2004). Together with the fact that it was isolated in a gain-of-function screen in the embryonic CNS of *Drosophila* (McGovern et al. 2003), this pinpoints to a role of Kruppel homolog 1 in axon guidance or CNS development. Though these proposed functions correlate well to functions ascribed to APP, the two identified genes involved in transcription processes and chromatin remodeling represent rather unexpected candidates for suppression of the wing phenotype. Nevertheless, there is evidence for a potential role of APP in transcriptional regulation via nuclear signaling. Complexes containing the A^{ID}, Fe65 and TIP60, a Histone-Acetyl-Transferase, or A^{ID}, Jip1b and TIP60, were found in the nucleus (Cao et al. 2001; Scheinfeld et al. 2003) and even induced gene expression of APP-effector genes (von Rotz et al. 2004). Yet, there is still controversy in regard to nuclear translocation of the A^{ID} (Cao et al. 2004; Muresan et al. 2004). A recent study, however, uncovered a complex including A^{ID}, Fe65 and Tip 60 together with the nucleosome assembly factor SET at the promoter region of a target gene (Telese et al. 2005). Thus, a connection can be made between APP and transcriptional regulation requiring chromatin remodeling. The ability of these two genes to suppress the

APP-induced wing phenotype suggests that the interference of APP with cell adhesion cannot be only attributed to one signaling pathway, but rather multiple pathways, which are already reflected by the numerous proposed functions of APP.

In summary, the enhancer/suppressor mutagenesis screen enabled the identification of putative novel players in the APP induced interference with cell adhesion between the two epithelial wing layers. The goal remaining is to elucidate the function of these nine proteins with respect to APP function, signaling pathways affected by APP interference, and cell adhesion.

3.2 The DFer kinase and APP do not interact directly

From the nine promising suppressors identified in the screen, this study focused then on the further functional characterization of one of the genetic interactors, the DFer kinase, for several reasons: (i) The mammalian homologs Fes and Fer kinase have attributed functions in cell adhesion processes and cytoskeletal arrangements. A role in cell adhesion in *Drosophila* is therefore likely. (ii) As DFer is a protein-tyrosine kinase, a direct link may exist between APP and DFer, with DFer possibly phosphorylating APP, its binding partners, or other components downstream of APP. (iii) The overexpression of the endogenous *dfer* transcription unit alone induced a striking wing phenotype, supporting a role in cell adhesion and naming the allele *zwirbelmütze* (*zwim*). (iv) One of the observed overexpression phenotypes in the wing were Notch loss-of-function defects. Intriguingly, APP was shown to interfere with the Notch signaling cascade, inducing Notch gain-of-function during neuronal development (Merdes et al. 2004). (v) The *Drosophila* DFer is still uncharacterized. Consequently, this study would provide important clues to decipher the molecular function of DFer.

Although the suppression of the APP-induced wing phenotype could be verified with a transgene co-expressing the *dfer* cDNA, which proved the genetic interaction between these two genes, further experiments revealed that it is of an indirect nature. It could be shown that *dfer* overexpression does neither alter the APP expression level, APP processing nor APP phosphorylation *in vivo* in the *Drosophila* organism. Moreover, co-transfection experiments with human and *Drosophila* cells similarly proved that *dfer* expression has no effect on APP metabolism, processing, phosphorylation and secretion. Another indication for indirect interaction came from co-immunoprecipitation experiments with antibodies directed against either DFer or APP, which failed to detect interacting APP or DFer, respectively. Likewise, DFer had no effect on the reported interference of APP with Notch signaling during PNS development (Merdes et al. 2004).

The obtained data corresponds nicely to the novel and surprising finding that the

intracellular domain of APP is dispensable for wing phenotype induction, as APP constructs with mutations in the intracellular domain and even a complete truncation of this domain did not abolish the phenotype (Soba 2004). The obvious discrepancy to the previous findings (Fossgreen et al. 1998) can be explained by the fact that the novel construct lacking the intracellular domain was fused to GFP (APPΔCT-GFP). Improper membrane retention of the original APPΔCT construct might have been the reason for not observing a phenotype in the past. Thus, the assumption of APP interfering with cell adhesion in a receptor-like fashion via a signal transduction mechanism seems now unlikely. According to the observations, proper membrane anchoring of APP seems to be a crucial and sufficient requirement for blistered wing phenotype induction, while the intracellular domain is dispensable. In the light of these findings, it is interesting to find *dfer* still genetically interacting with and thereby suppressing the phenotype of the C-terminally deleted APPΔCT-GFP construct similar to the full-length APP construct. This genetic interaction between the cytoplasmic DFer kinase and the APP protein with the deleted intracellular domain argues strongly for an indirect interaction between these two proteins, as the APP cytoplasmic domain represents the only possible side of interaction.

Taken together, the nature of the genetic interaction between *dfer* and APP is likely to be one produced by secondary effects caused through general interference with cell adhesion. One could envision that DFer acts on an additional pathway mediating cell adhesion by phosphorylating another unknown protein and thereby suppressing the APP induced effect on cell adhesion.

3.3 DFer kinase is similar to vertebrate Fes and Fer kinase in structure and function, but differs in expression

This work describes the DFer kinase, a non-receptor PTK, which is the only *Drosophila* protein to share strong structural and sequence similarity with the mammalian Fes and Fer kinases, baring 36% and 38% sequence identity, respectively. *Drosophila dfer* is a closer homolog to *fer* than to *fes* because of two reasons. First, it is reported to direct the expression of both a long p92Dfer and short a p45Dfer isoform in close correspondence to *fer* (Paulson et al. 1997). Additionally, DFer is rather ubiquitously expressed like Fer kinase (Letwin et al. 1988; Pawson et al. 1989) and does not show the restricted expression pattern of Fes (MacDonald et al. 1985; Samarut et al. 1985; Care et al. 1994; Haigh et al. 1996). Activating mutations of both vertebrate kinases can mediate cellular transformation, and *fes* has frequently been isolated as a retroviral oncogene that encodes fusion proteins comprising sequences from Fes and the viral Gag protein (Groffen et al. 1983). Expression of these fusionproteins in transgenic mice induces tumors in lymphoid and mesenchymal

tissues, as well as cardiac and neurological abnormalities (Yee et al. 1989a; Yee et al. 1989b). However, despite the identification of several important signaling proteins as putative targets, like p120RasGAP (Ellis et al. 1990), PI3K (Iwanishi et al. 2000), breakpoint cluster region (BCR) (Maru et al. 1995) and signal transducer and activator of transcription 3 (STAT3) (Garcia et al. 1997), it is not yet understood how this oncoprotein causes cellular transformation. To date, an association to human malignancies has not been reported.

Here, using the UAS/GAL4 system, evidence is provided for DFer kinase affecting multiple signaling pathways upon overexpression in *Drosophila,* resulting in a variety of different phenotypes. Surprisingly, overexpression of DFer in the developing *Drosophila* wing revealed not the overgrowth or transformation of tissue expected for an oncogene, but rather a loss of tissue resulting in wing margin notches in one phenotype, which are reminiscent to Notch loss-of-function mutations. This is in contrast to previously reported studies, where *Drosophila* DFer kinase had oncogenic transforming capacity when overexpressed in fibroblasts, although vertebrate *fer* has not yet been isolated as a retroviral oncogene (Paulson et al. 1997). Similarly, the smaller form p45DFer (corresponding to the *dfer*-D transcript) was initially also described to transform cells. *In vivo*, however, overexpression of this form in *Drosophila* seems to have no effect by any means. This discrepancy might be explained by the fact that in the context of a living organism, overexpression might cause different effects than in cell culture, as activation of the same pathways might still lead to different outcomes. It cannot be excluded that the pathway affected upon overexpression of DFer in *Drosophila* might be the unresolved one leading to cellular transformation. Obviously, the intrinsic kinase activity is indispensable for phenotype induction as proved by expression of a kinase-inactive form that could not induce a phenotype. Moreover, the N-terminal domain with its FCH domain and CC motifs seems to be crucial as well, suggesting a regulatory function of this domain and/or interactions with substrates or other proteins.

There is emerging evidence that DFer kinase utilizes a regulatory mechanism similar to the mammalian forms. The CC domains of Fes and Fer protein-tyrosine kinase direct homotypic oligomerization, resulting in the formation of trimers in the case of Fer (Craig et al. 1999), and pentamers or higher-order oligomers in the case of Fes (Read et al. 1997). Oligomerization of these kinases potentiates *trans*-autophosphorylation, implicating an autoregulatory function. Here, co-expression of the kinase-inactive form of DFer together with the wildtype form suppressed the overexpression phenotypes, suggesting that it acts in a dominant-negative fashion by titrating the overexpressed functional DFer protein. Conclusively, DFer kinase might oligomerize analogous to their vertebrate counterparts in order to be active. Indeed, intrinsic tyrosine kinase activity identifiable as autophosphorylation of the expressed kinase could be observed and it is tempting to speculate that an overexpression of this kinase results in an autoactivation. Another

indication for DFer oligomerization came from the observation that the expression of just the N-terminal domain containing the CC motifs necessary for oligomerization produced no phenotype by itself, but when co-expressed with the wildtype form, suppressed the induced phenotype.

That indeed the function of the DFer kinase and its vertebrate homologs is conserved can be concluded from experiments with ectopic expression of the human Fes and the murine Fer protein in *Drosophila*. Similarly to DFer, the vertebrate kinases induced the same phenotypes with subtle differences, though being more severe. This provides further evidence not only for a functional relationship between the *Drosophila* and the vertebrate kinases affecting the same developmental pathway, but also that this might reflect the yet unknown pathway leading to transformation.

Alternative initiation of transcription and alternative splicing *in vivo* has been described for the mammalian *fer* gene, resulting in the two forms *fer* and the testis-specific shorter *ferT* (Fischman et al. 1990) (Fig. 3.1). In the course of this study, evidence emerged that *dfer* is also subjected to alternative splicing and alternative initiation of transcription. The existence for three of the four transcripts predicted by the *Drosophila* genome annotation could be verified *in vivo*. Surprisingly, a large transcript of approx. 5 kb is produced in addition to the already reported canonical *dfer* form, corresponding to an novel predicted mRNA isoform called *dfer-A*. This is the first time that such a transcript was shown to exist and stands in contrast to the situation in mammals, were expression of a larger transcript is absent. The resulting DFer-A protein with 140 kDa contains an extra proline/serine rich domain between the N-terminal CC domain and the SH2 domain. The *dfer-A* transcript could be detected only at a certain stage during embryonic development, i.e. in 8-12 h old embryos, where morphogenic movements like germ band retraction, dorsal closure and head involution take place, and specifically in the adult fly head. Interestingly, when inducing the overexpression of the endogenous locus, expression of the DFer-A protein could only be found in the adult head and not in wing imaginal discs, suggesting a head-specific regulation of *dfer-A* expression. The *in vivo* existence of *dfer-A* is further supported by the finding that this form is functional upon transgenic overexpression and induces phenotypes similar to the canonical *dfer* form.

The smallest predicted form *dfer-D*, which is homologous to *ferT* and has been already reported in the literature as p45*dfer* (Paulson et al. 1997), could be isolated from a cDNA library, suggesting an expression *in vivo*. However, overexpression of the endogenous *dfer* locus did nor result in detectable DFer-D protein expression. Conversely, using a probe specific to *dfer-D*, expression of this transcript was detectable during embryogenesis in a similar pattern as *dfer*. This is in clear contrast to the expression of *ferT* in mammals, which is restricted to the testis (Fischman et al. 1990; Keshet et al. 1990). Nevertheless, it remains

to be clarified if *dfer-D* is indeed expressed in the testis of *Drosophila* and produces a functional protein as well. Moreover, as the first fourteen amino acids are identical to the ones in the DFer-A protein and the nucleotide sequence is part of the open reading frame of the long *dfer-A* form, it cannot be excluded that this transcript represents only an incorrectly annotated form.

Similarly, the predicted *dfer-C* form might be incorrectly annotated as its expression could not be verified in this study. In agreement with this is the observation that *dfer-C* is a part of the open reading frame of the canonical *dfer* form.

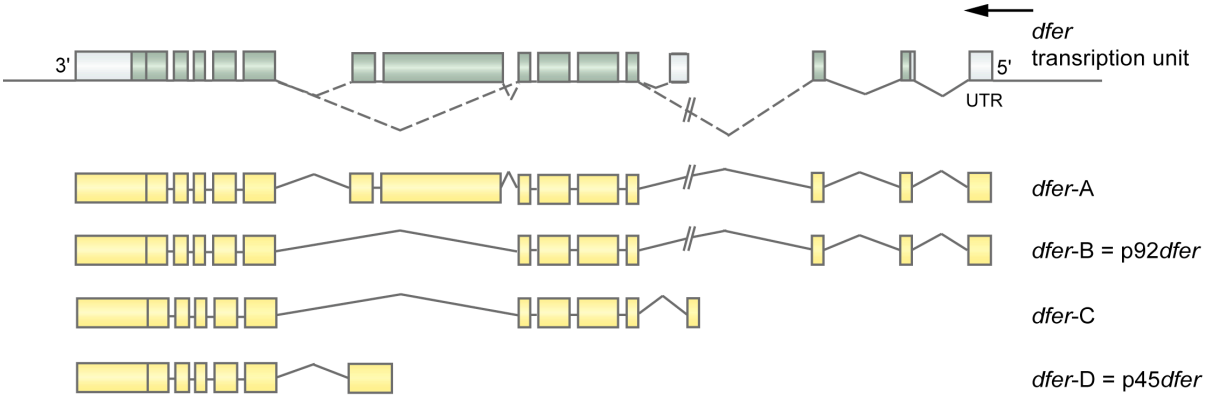

Fig. 3.1 The various *dfer* transcript isoforms. The genomic region of *dfer* is shown, with coding exons illustrated in *green*, non-coding exons in *grey*. Dashed lines represent alternative splice sites. Four different *dfer* transcripts are annotated (exons in *yellow*). Expression of *dfer*-A and *dfer*-B *in vivo* could be verified.

Additionally, it could be shown that the canonical *dfer* form is expressed throughout all developmental stages in *Drosophila* and is entirely of zygotic nature as no maternal contribution was detectable. During embryogenesis, expression could be found in various tissues that undergo morphological changes, most prominently in the proctodeum, the somatic muscles, the CNS, the cells forming the leading edge at the stage of dorsal closure, and at muscle attachment sites. The expression pattern correlated largely with previous observations (Katzen et al. 1991). Moreover, it has striking similarities to the distribution of integrin and extracellular matrix proteins. Interestingly, immunostainings with one of the generated antibodies directed against parts of the SH2 domain and the kinase domain revealed DFer protein localization at the sites of muscle attachment. However, as other produced antibodies resulted only in faint ubiquitous staining of the embryo, it remains to be clarified if control stainings with *dfer* mutant embryos reveal a loss of this pattern, thus verifying its specificity.

3.4 *Dfer* overexpression phenotypes – closing in on the biological function of DFer

The physiological function of DFer in *Drosophila* is entirely unknown. Similarly, it is still unresolved for the vertebrate Fes and Fer kinase. Several growth factors, cytokines and immunoglobulins, after engaging their receptors, were shown to induce the activation of cellular Fes and Fer. Both kinases have also been implicated in the regulation of cell-cell and cell-matrix interactions that are mediated by adherens junctions and focal adhesions, particularly in the cells of the hematopoietic system. More recent insights implicated these kinases in crosstalk between receptor complexes, possibly through a role in the regulation of cytoskeletal rearrangement by cadherins and integrins (reviewed in Greer 2002; Li et al. 2000; Arregui et al. 2000). However, the significance of these findings *in vivo* is still unclear, as most of the studies were performed with mammalian cells in culture.

3.4.1 The interference with cell adhesion

In this study, the UAS/GAL4 expression system was utilized to express *dfer* and analyse its function *in vivo*. Overexpression of DFer results in pupal lethality when ubiquitously expressed. More restricted expression in the wing imaginal disc gives phenotypes such as wing blistering, which is associated with defects in integrin-mediated signaling pathways in *Drosophila*. These results, together with the membrane-associated localization of the DFer protein within the cell, imply a potential role for Dfer in adhesion during development. Integrins have been found to be essential for diverse developmental functions in the fly, not only acting as simple mediators of cell adhesion between two layers of cells, particularly at muscle attachment sites and between the two surfaces of the developing wing, but also in the transduction of biochemical signals across the cell membrane and the regulation of cellular functions such as cell migration and gene expression during differentiation (Bokel and Brown 2002; Brower 2003). In this context, it is remarkable that endogenous *dfer* could also be detected at the muscle attachment sites, though formal proof is lacking. Consisting with an accessory involvement of *dfer* in integrin-mediated adhesion, it could be shown that the *dfer*-induced wing blister phenotype is enhanced in a heterozygous integrin mutant deficiency background, thus indicating a genetic interaction between *dfer* and integrin in the wing.

The pupal lethality induced by the ubiquitous expression of Dfer and the wing blistering are also reminiscent of the phenotype associated with DFak56 overexpression, the *Drosophila* focal adhesion kinase (FAK), which additionally disrupts muscle attachment (Palmer et al. 1999; Grabbe et al. 2004). FAK is another non-receptor protein tyrosine kinase

localized to focal adhesions and an intracellular mediator of integrin signaling. Integrin engagement recruits the FAK to focal contacts and increases its kinase activity. FAK then forms a signaling complex with Src tyrosine kinases resulting in further tyrosine phosphorylation of FAK and other associated proteins (e.g. p130Cas and paxillin), and subsequently the recruitment of multiple cellular components (reviewed in Gelman 2003; Parsons 2003). In contrast to its vertebrate homolog, where ablation of *fak* in mice produces embryonic lethality (Ilic et al. 1995), DFak56 is not essential for integrin function in adhesion, migration or signaling *in vivo*, revealing animals that are viable and fertile (Grabbe et al. 2004). As *dfer* mRNA expression has a widely overlapping expression pattern to *dfak56* with elevated expression in the central nervous system and at segmental junctions, and displays comparable phenotypes upon overexpression, DFer might play a role in the negative regulation of integrin adhesion similarly to DFak56 (Grabbe et al. 2004). A genetic connection might be revealed when analysing flies mutant for both *DFak56* and *dfer*.

This possibility is further supported by studies of Fer in cell culture that indicate a function of Fer in the regulation of cell adhesion and migration through effects on adherens junctions and focal adhesions. In one study, trojan peptides that included either a neuronal (N)-cadherin juxtamembrane sequence or its β-catenin binding sequence disrupted adherens junctions, and this correlated with a loss of N-cadherin-Fer interaction mediated by Fer association to p120catenin (Arregui et al. 2000; Chen et al. 2003; Kim and Wong 1995). The β-catenin binding sequence peptide caused Fer to dissociate from N-cadherin in a complex with p120catenin and β-catenin, which correlated with loss of N-cadherin interaction with protein-tyrosine phosphatase 1 B (PTP1B), and enhanced tyrosine phosphorylation of β-catenin. By contrast, peptides that included the N-cadherin juxtamembrane sequence caused Fer to dissociate from N-cadherine alone, although the domain mediating this interaction has not yet been determined. Once dissociated, Fer then appeared in a complex with FAK, which correlated with a disruption of focal adhesions and reduced tyrosine phosphorylation of the docking protein p130Cas. This dissociation of Fer from adherens junctions and reduced cadherin- and integrin-mediated adhesion could also be observed in another study after addition of neurocan, an endogenous regulator of N-cadherin (Li et al. 2000). These observations indicate that Fer might regulate the adherens junctions through interaction with, and/or tyrosine phosphorylation of adherens junctions components, including PTP1B, p120catenin and β-catenin, and that Fer might mediate crosstalk between adherens junctions and focal adhesions. Similarly, overexpression of Fer in fibroblasts was also reported to cause reduced cell adhesion to the substrate, which correlated with decreased tyrosine phosphorylation of FAK-associated p130Cas, leading to a reduced integrin-mediated adhesion, and increased tyrosine phosphorylation of both p120catenin and β-catenin, leading to reduced cadherin-mediated adhesion (Rosato et al. 1998). Fer might function in the

activation of a protein-tyrosine phosphatase that mediates the dephosphorylation of FAK and p130Cas and other focal-adhesion proteins observed on loss of integrin attachment. For cadherin-mediated adhesion, it was shown that Fer appears to play opposing roles. It normally maintains the stability of the cadherin-cytoskeleton link through phosphorylation of PTP1B, which then binds to the cytoplasmic domain of cadherins (Xu et al. 2004; Rhee et al. 2001) and dephosphorylates β-catenin, thereby stabilizing cadherin-mediated adhesion (Balsamo et al. 1996; Balsamo et al. 1998; Rhee et al. 2002, Xu et al. 2002). When activated, Fer decreases the stability of this linkage by directly phosphorylating β-catenin and reducing its affinity for α-catenin (Piedra et al. 2003). A similar role could be envisioned for DFer kinase, mediating the crosstalk between focal adhesions and adherens junction, which finally leads to a reorganization of the cytoskeleton (Fig. 3.2).

An involvement in cortactin phosphorylation as found for Fer kinase can also be postulated for DFer (Fig. 3.2). Cortactin has been implicated in the cytoskeletal reorganization by directly influencing the actin polymerization that accompanies cell migrations and vesicular transport, and it has been found to localize to lammelopodia (Uruno et al. 2001; Weaver et al. 2001; Kaksonen et al. 2000). Tyrosine phosphorylation of cortactin inhibits its actin crosslinking activity and promotes its proteolytic degradation (Huang et al. 1997). Although tyrosine phosphorylation has been largely attributed to the activity of Src and Fyn kinases, Fer also plays a role as studies with *fer* mutant embryonic fibroblasts showed (Craig et al. 2001). In addition, Fer was identified as a candidate in actin depolymerization-induced tyrosine phosphorylation of cortactin (Fan et al. 2004). In agreement with this, genetic interactions studies in *Drosophila* using the *dfer*-induced wing blistering phenotype revealed an enhancement upon cortactin overexpression. However, no interaction could be observed with a cortactin mutant, which is viable and fertile (Somogyi and Rorth 2004). Nevertheless, it should be mentioned that the experiment was performed in a heterozygous cortactin mutant background and it remains to be investigated, if an interaction can be revealed in a homozygous mutant background. Similarly, studies with *dfer* and *cortactin* double mutants might help to elucidate their relationship.

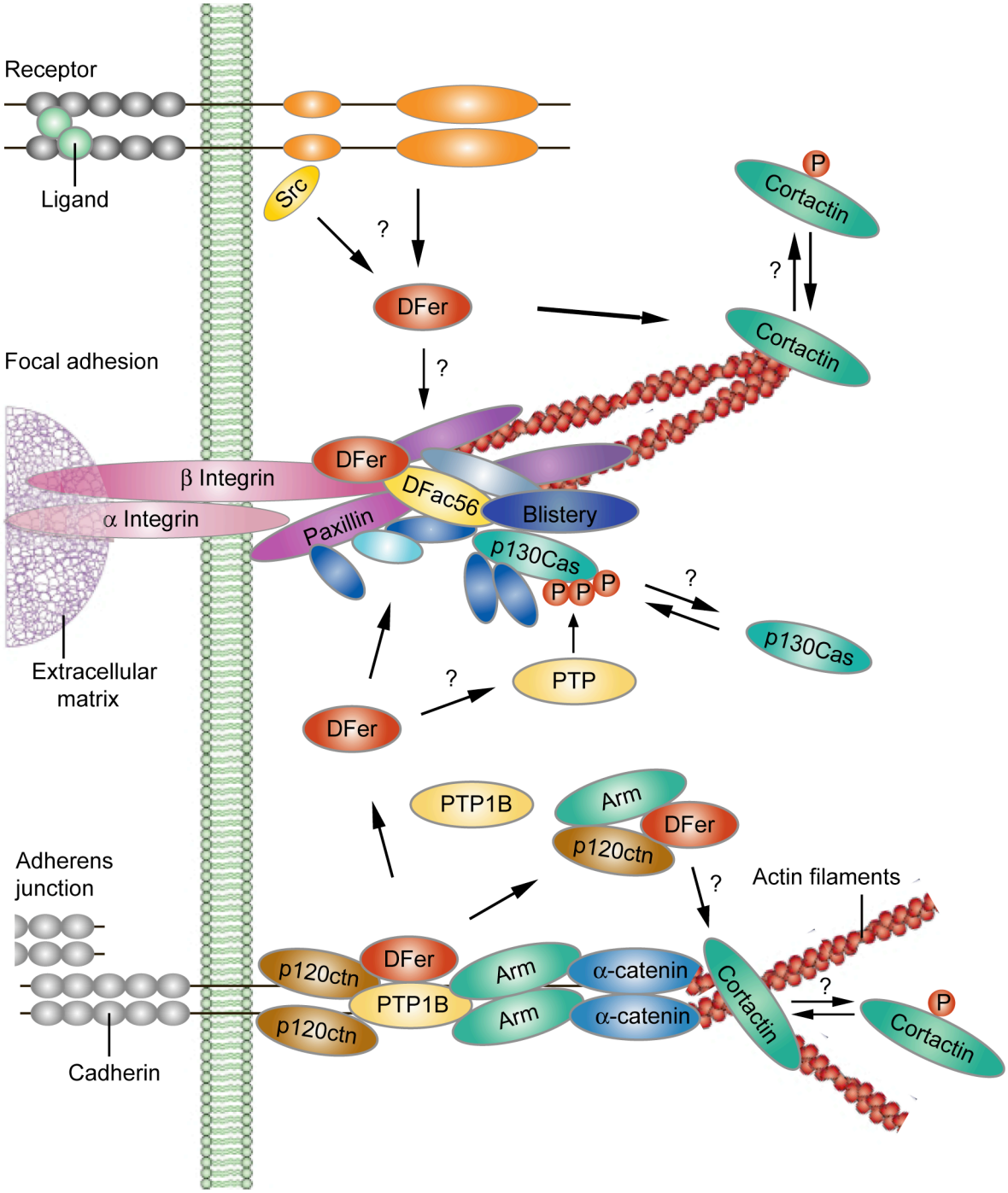

Fig. 3.2 Hypothetical involvement of DFer in the crosstalk between different receptor systems. The engagement of an unknown receptor could activate DFer. This might involve phosphorylation of the receptor itself or an associated kinase that leads to DFer activation. A scenario could be envisioned where DFer phosphorylates cortactin, which leads to changes in the cytoskeleton and regulation of integrin or cadherin affinity towards their extracellular substrates. DFer might then participate in the regulation of focal adhesions and integrin signaling, possibly through a role in the regulation of a focal adhesion associated protein tyrosine phosphatase. DFer that is released from the adherens junctions, where it is possibly bound to p120ctn and PTP1B, might also contribute to the reorganization of the cytoskeleton through putative substrates including PTP1B, Armadillo (Arm), p120catenin, and cortactin. Adapted from (Greer 2002).

Various other genetic interactions with the *dfer* overexpression phenotype could be observed, all pointing to a role of DFer in modulating cell adhesion. Among the modifiers

attributed to integrin function is Abelson, a non-receptor tyrosine kinase whose activity and localization is regulated by integrins in order to coordinate cytoskeletal rearrangements (reviewed in Hernandez et al. 2004; Lewis et al. 1996; Lewis and Schwartz 1998). In *Drosophila*, Abelson is most abundant in the CNS of the developing fly, where it regulates axonal outgrowth and fasciculation (reviewed in Lanier and Gertler 2000). It is also required for the normal morphogenesis and movement of epithelial cells (Grevengoed et al. 2001; Grevengoed et al. 2003). p120catenin belongs to the genetic interactors involved in cadherin-mediated cell adhesion. p120catenin gets phosphorylated by Src tyrosine kinases that increases its affinity to the cytosolic region of cadherins, providing a link between β-catenin, Fer and PTP1B. Recently, a direct interaction between p120catenin and Fer was reported (Piedra et al. 2003), leading to the hypothesis that these two proteins might also directly interact in *Drosophila*. In fact, *Drosophila* p120catenin is not essential in the developing embryo (Myster et a. 2003; Pacquelet et al. 2003). However, null mutations in *Drosophila* p120catenin cause subtle dorsal closure defects and enhance mutations in DE-cadherin and Armadillo (*Drosophila* β-catenin homolog) (Myster et al. 2003), suggesting an important role in regulating cadherin-mediated adhesion. One aspect of this regulatory role might well be to act as an adaptor of the DFer tyrosine kinase.

Taken together, the results imply an accessory role of DFer in modulating adhesion-dependent signaling pathways *in vivo* during *Drosophila* development. It is obvious that further experiments will be required to understand the exact role of *dfer in vivo*.

3.4.2 The interference with Notch and Wingless signaling

The observation that *dfer* overexpression during *Drosophila* wing development causes also a wing margin notching phenotype implies a role in Notch and Wingless signaling. Notch and Wingless signaling pathways organize the D/V axis, including patterning along the presumptive wing margin (reviewed in Tabata and Takei 2004; Irvine and Rauskolb 2001; Irvine 1999). Wingless is activated by Notch signaling along the D/V boundary of the wing imaginal disc and acts as a morphogen to organize gene expression and cell growth (see also Introduction, Section 1.7). The data presented here argues for an interference with Notch rather than Wingless signaling. Immunostaining experiments of wing imaginal discs showed that the Wingless expression pattern along the D/V boundary was disrupted and the inner ring of Wingless expression around the wing pouch missing. However, as Cut and Vestigial, two target genes of Notch, revealed similar abrogation, it is quite likely that Notch signaling is affected. Nevertheless, one should bare in mind that *vestigial* is also regulated by Wingless and *cut* needs indirect input of Wingless (Neumann and Cohen 1996; Micchelli et al. 1997; Kim et al. 1996; Williams et al. 1994). To complicate matters further, a complex

interplay exists between these signaling cascades with regulatory feedback mechanisms. For instance, Wingless induces expression of the Notch ligands Serrate and Delta in nearby dorsal and ventral cells. Serrate and Delta signal back to activate Notch and thereby maintain Cut and Wingless expression. Cut in turn promotes expression of Wingless and inhibits expression of Serrate and Delta (Micchelli et al. 1997; Neumann and Cohen 1996; De Celis and Bray 1997).

The observed defects in the adult eye structure and the deformations in the third leg pair upon *dfer* overexpression could also well represent interferences with the Notch receptor pathway. Analysis of Notch loss-of-function mutants indicated that Notch activation regulates eye growth and patterning. Dependent on the time of interference, mutants show an irregular spacing of the ommatidia and a reduction in the size of the eye (reviewed in Voas and Rebay 2004; Baker and Zitron 1995; Papayannopoulos et al. 1998), phenotypes also observed upon overexpression of *dfer* and the vertebrate homologs *fes* and *fer*. Likewise, the elimination of Notch signaling in the leg results in fusions between leg segments and a reduction of leg growth (Shellenbarger and Mohler 1978; de Celis et al. 1998; Bishop et al. 1999; Rauskolb and Irvine 1999; Rauskolb und Irvine 1999).

Although unlikely, a direct effect on Wingless signaling cannot be excluded, as wing-to-notum transformations observed upon *dfer* overexpression strongly correlate with mutations in *wingless* mutants (Morata and Lawrance 1977; Sharma and Chopra 1976) and mutants of the Wingless signaling pathway such as *armadillo* (Pfeifer et al. 1991). As already mentioned, β-catenin was shown to associate with and to be phoshorylated by Fer kinase, and represents a potential target of DFer in the Wingless pathway. However, the complete loss of wing structures can also be found in mutants for the wing-specific genes *apterous* (Cohen et al. 1992), *vestigial* (Williams et al. 1991) and *scalloped* (Campbell et al. 1992). Additionally, evidence is provided that rather Wingless expression than Wingless signaling is affected. Armadillo is an essential component of the Wingless signaling pathway, activating target gene transcription together with lef/TCF/pangolin transcription factor (van de Wetering et al. 1997; Brunner et al. 1997; reviewed in Seto and Bellen 2004). Here, no obvious influence on Armadillo expression and stability could be observed in the wing imaginal disc upon *dfer* overexpression, arguing against an effect on Wingless signaling. Similarly, *dfer* overexpression in the embryo seems not to alter the patterning of the denticle bands of the cuticle, which is a paradigm for *wingless* mutants and mutants of the Wingless signaling pathway, usually resulting in a formation of extra rows of denticles (Payre et al. 1999).

Nonetheless, Armadillo as a putative target of DFer represents also a connection between Wingless signaling and cadherin-mediated cell adhesion (reviewed in Nelson and Nusse 2004; Pfeifer and Wieschaus 1990; Pfeifer et al. 1991). Although its signaling activity is independent of its role in cadherin-mediated cell adhesion (Heasman et al. 1994; Pfeifer et

al. 1994) and distinct molecular forms were recently proposed for adhesion and transcriptional processes (Gottardi and Gumbiner 2004), both activities take place in the same cell, and overexpression of cadherin was shown to inhibit β-catenin signaling (Heasman et al. 1994; Funayama et al. 1995; Sanson et al. 1996). However, as no effect was observed on Armadillo expression, it can be, at least in this context, ruled out as a DFer target.

Another interesting finding is the genetic interaction of *dfer* with components of the JNK pathway. Recently, a connection between the JNK and Wingless pathway, which is already well established for the process of dorsal closure in the *Drosophila* embryo (Kaltschmidt et al. 2002; McEwen et al. 2000), was reported also for the wing (Ryoo et al. 2004; Mirkovic et al. 2002). JNK activation in the wing goes hand in hand with apoptosis to activate signaling cascades for compensatory proliferation. Similarly, reduction of Wingless signaling not only impaired compartment and clonal growth but increased cell death (Giraldez et al. 2003). Intriguingly, the low frequency of *dfer* expressing clones generated by mosaic analysis (data not shown) suggest that these cells are eliminated very early, possibly via apoptosis mediated by JNK activation. Consistent with this observation, vertebrate Fes kinase was reported to transform fibroblasts by inducing extracellular signal-regulated kinases (ERK) and JNK activation (Li and Smithgall 1998). Though experiments showing directly JNK activation or apoptosis were not conducted so far, it is a feasible possibility. In this context, it is interesting that the *Drosophila* Tensin homolog Blistery was shown to interact with components of the JNK signaling pathway during wing development (Lee et al. 2003; Torgeler et al. 2004). Blistery overexpression increased JNK activity and induced apoptotic cell death. Interestingly, *blistery* null mutations display wing blistering as a failure of integrin-mediated cell adhesion. It remains to be investigated if JNK activation and apoptosis are involved in the *dfer* phenotypes.

Wingless expression, however, was shown to be also essential for other developmental aspects of the *Drosophila* wing. More recently, it has become clear that normal wing development is also dependent upon signaling along the proximodistal axis (Liu et al. 2000; del Alamo Rodriguez et al. 2002). An initial subdivision in the wing is effected by signaling from the A/P and D/V compartment boundaries, which promote expression of *scalloped* and *vestigial*, that encode subunits of a heterodimeric transcription factor in the wing pouch (Halder et al. 1998; Klein and Martinez Arias 1998; Simmonds et al. 1998). This subdivides the wing into distal cells, which give rise to the wing blade, and surrounding cells, which give rise to proximal wing and wing hinge structures, being partially dependent on the signaling from the distal Scalloped-Vestigial expressing cells to more proximal cells (Liu et al. 2000). A key target of this signaling is Wingless, which is necessary and sufficient to promote growth of the proximal wing (Neumann and Cohen 1996; Klein and Martinez Arias 1998).

Within this context, there is also a connection between Wingless and cadherins. Two of the *Drosophila* cadherin like proteins, Fat and Dachsous, have roles in imaginal development in a complex interplay with Four-jointed, a Golgi-associated transmembrane protein, and Dachs, and unconventional myosin (Matakatsu et al. 2004; Buckles et al. 2001; Cho and Irvine 2004; Strutt et al. 2004; Clark et al. 1995; Mahoney et al. 1991). Mutations in these genes produce a number of phenotypes that can be interpreted as being due to effects on cell adhesion, e.g. strong *dachsous* mutations result in adults with abnormally shaped legs and wings (Waddington 1943; Clark et al. 1995; Held et al. 1986). Besides the finding that these genes organize planar cell polarity in the wing (Adler et al. 1998; Matakatsu and Blair 2004) with Dachsous forming a proximal to distal gradient, a new study revealed that they also influence the expression of Wingless in the proximal wing, being required for the initiation of Wingless expression (Cho and Irvine 2004). This leads to the hypothesis that DFer might actually act on the signaling mediated by the Fat and Dachsous protocadherins, thereby causing an interference with the initiation of Wingless expression, which would explain the lacking Wingless expression along the D/V boundary (Fig. 3.3). In this respect, it is of great interest that *four-jointed* was shown to be not only regulated downstream of Notch activation, but that it can also induce expression of the Notch ligands, Serrate and Delta, and may thereby participate in a feedback loop with the Notch signaling pathway (Buckes et al. 2001). Thus, a proposed interference of DFer with these proteins involved in the P/D growth and patterning of the wing could indirectly act similarly on Notch activation itself, leading to a loss of expression of the Notch target genes, which is observed upon *dfer* overexpression.

Moreover, the finding that Four-jointed is also required for the segmentation and growth of the *Drosophila* leg, for ommatidial polarity in the eye and epithelial planar polarity in the wing and abdomen (Waddington 1943; Villano and Katz 1995; Brodsky and Steller 1996; Zeidler et al. 1999; Zeidler et al. 2000), might be in agreement with the observed phenotypes in the *Drosophila* adult eye and third leg pair upon *dfer* overexpression. As all of these processes involve dynamic changes in the actin cytoskeleton (Fristrom et al. 1993; Eaton 1997; Mlodzik 1999), DFer might play a role in the regulation of the cytoskeleton by being engaged downstream of the protocadherins. Interestingly, *abelson* was found to interact with *four-jointed* (Buckles et al. 2001).

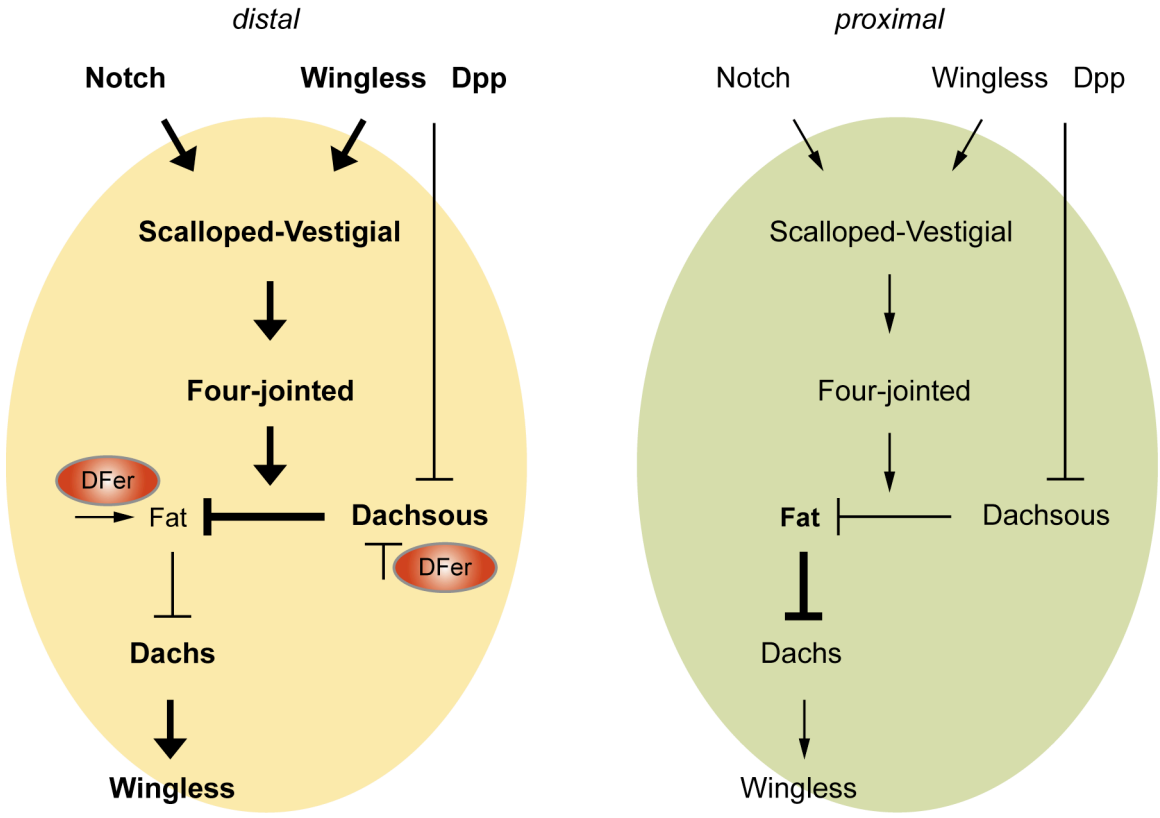

Fig. 3.3 Hypothetical involvement of DFer in the distal to proximal signaling in the wing. Scalloped-Vestigial transcription complexes specify the distal wing fate and are regulated by Notch, Wingless and Decapentaplegic (Dpp) signaling. In the distal cell, Scalloped-Vestigial in turn regulates Four-jointed expression. Four-jointed acts as a modulator on Dachsous and Fat interaction, where Dachsous normally inhibits Fat activity. Thus, Dachs can promote Wingless expression. In the proximal cell, Fat is active and inhibits Dachs, thereby reducing Wingless expression. DFer might possibly act negatively on Dachsous or positively on Fat in the distal cells, thus interfering with their signaling and concomitantly inhibiting Wingless expression. It should be mentioned that the interactions among these proteins are still not revealed and highly speculative. Additionally, they occur also within one cell. High concentrations of one protein or high activity of it are highlighted.

3.5 *Dfer* is a non-essential *Drosophila* gene

The strong *dfer* overexpression phenotypes suggested an important role of DFer kinase in cell adhesion processes, leading to the assumption that mutations of *dfer* might be lethal. This study, however, reports that *dfer* function is not essential for overall viability in *Drosophila*. This is sustained by two observations: First, transgene-mediated RNAi against different regions of *dfer* did neither induce lethality nor an obvious phenotype. Second, the generated *dfer* mutant flies are both viable and fertile. This is supported by recent genetic studies in mice that similarly demonstrated a non-essential role for Fes and Fer kinase in mammals (Senis et al. 2003; Craig et al. 2001; Zirngibel et al. 2002; Senis et al. 1999; Hackenmiller et al. 2000). The discovery came as a surprise since a number of diverse signaling pathways downstream of Fes and Fer kinase were previously identified. However, mice targeted with a kinase-inactivating mutation of *fer* were reported to be viable and fertile,

and show only subtle defects in the degree of cortactin phosphorylation (Craig et al. 2001). Transgenic mice with a kinase-inactivating mutation of *fes* developed normally as well, with no obvious defects. Yet, a subtle influence on the amount of myeloid cells and lymphoid cells was detected, however, with conflicting observations dependent on the approach for targeting the mutation (Zirngibel et al. 2002; Senis et al. 1999; Hackenmiller et al. 2000). Though redundant roles were proposed for these kinases, double knockouts harboring kinase-inactivating mutations in both *fes* and *fer* have been recently generated and were viable and fertile. However, they display subtle effects on hematopoiesis (Senis et al. 2003).

The non-essential nature of *dfer* in *Drosophila* perhaps partially explains why extensive attempts to target *dfer* through various methods have been so far unsuccessful in several groups, since the general assumption has been that such mutants would be lethal. Another reason why the genetic screening initially failed is the presumably compacted chromatin structure at the *dfer* locus, which allows only small or very large deletions. This is in consistence with the fact that none of deficiency fly lines map to this region. In this work, both a mutant with a small deletion named $dfer^{\Delta 252}$ and three independently obtained mutants with large deletions ($dfer^{w39.2}$, $dfer^{41.1}$ and $dfer^{49Sb}$) covering a 50 kb region and thereby removing three neighboring genes could be isolated. In this context, it is intriguing that the laboratory of A. Brand isolated in five separately performed screens only one mutant with a small deletion and nine mutants with similar large deletions spanning over 50 kb, and removing the same adjacent genes. The fact that only mutants with the large deletion were homozygous lethal strongly suggested that one of the *dfer* neighboring genes was essential for *Drosophila* development. By genetic analysis of these genes, it could be shown here that CG33188, a gene with formerly uncharacterized function, encodes a neuronal transcription factor critical for *Drosophila* development. Similarly, when integrating a genomic rescue construct containing these three missing genes into the *dfer* mutants with the large deletions, resulting in $dfer^{del1/CG}$, the previous recessive lethality could be rescued. In contrast, a genomic rescue harboring the *dfer* transcription unit was not able to rescue the lethality.

Of great interest is the finding that both kinds of mutants, $dfer^{\Delta 252}$ with the short deletion and $dfer^{del1/CG}$ with the rescue construct for the three missing genes, display elevated embryonic lethality with a dorsal closure phenotype, though with low penetrance. The phenotype correlates strongly with the data from *in situ* hybridizations, where *dfer* mRNA was shown to be strongly expressed at the leading edge cells during the process of dorsal closure in the embryo. It is interesting to note that during dorsal closure an accumulation of phospho-rich structures in the leading edge cells can be observed, which is not visible during germ band retraction (Harden et al. 1996). These probably represent sites where adherens junctions and focal adhesions contribute to the organization of the leading edge cytoskeleton. Remarkably, *dfer* expression was shown to be enriched in the cells at the leading edge only

at the time of dorsal closure and would therefore correspond nicely to the observed *dfer* mutant phenotypes. A scenario could be envisioned in which DFer might somehow associate with cell adhesion processes driving dorsal closure. In remains to be clarified if the surviving mutant embryos display subtle defect or a delay in dorsal closure.

In this respect, it is intriguing that *Drosophila* p120catenin is similarly not essential for fly development, but plays a supporting role in cell adhesion during dorsal closure (Myster et al. 2003; Pacquelet et al. 2003). *p120catenin* null mutations, like *dfer* mutations, cause subtle dorsal closure defects. As vertebrate p120catenin was shown to be associated with and phosphorylated by Fer kinase (Piedra et al. 2003), it is tempting to assume a similar direct interaction in *Drosophila*. It remains to be investigated, if the combination of these two null mutations would enhance the phenotype strength. Moreover, according to the hypothetical involvement in regulating cadherin-mediated cell adhesion, it would be interesting to reveal if mutations in DE-cadherin or Armadillo are also able to enhance the phenotypes.

Similarly, the relationship of DFer to JNK signaling and Wingless signaling during the process of dorsal closure remains elusive. The JNK cascade acts at the leading edge of the migrating epidermis. It triggers signaling by the TGF-β superfamily member Decapentaplegic and interacts with the Wingless pathway, in order to regulate the cytoskeletal reorganization and cell shape changes (reviewed in Jacinto et al. 2002). The Armadillo-dependent Wingless signaling was also reported to be required for the polarization of the epidermal cells during dorsal closure (Morel and Martinez Arias 2004). Interestingly, Abelson kinase is involved in the regulation of epithelial morphogenesis in *Drosophila* as well, where it regulates adherens junction stability and actin organization (Grevengoed et al. 2001; Grevengoed et al. 2003). Combined mutant analysis will provide more clues about DFer interactions with these pathways.

With respect to integrin-dependent processes, it will be interesting to analyse if *dfer* is required for the proper development of embryonic tissues, especially at sites with particularly high levels of *dfer* expression, like muscle attachment sites. For instance, null mutations of *Drosophila* DFak56 are viable and fertile in contrast to the vertebrate homolog FAK, revealing a non-essential function of DFak56 for integrin adhesion or signaling (Grabbe et al. 2004). However, mutants display subtle muscle attachment defects and overexpression resulted in wing blistering, similarly to *dfer* (Palmer et al. 1999).

The non-essential nature of the dfer mutants and their phenotypes in dorsal closure processes imply an accessory role of DFer in modulation of cell adhesion. It is obvious that further experiments will be required to understand the exact role of DFer in such processes *in vivo*.

3.6 Conclusion and outlook

In summary, several putative interaction partners of APP in its adhesion or signaling function during *Drosophila* wing development were identified. The study of one of them, DFer protein-tyrosine kinase, revealed an indirect nature of interaction *in vitro* and *in vivo*. The functional characterization of the DFer kinase implies a role in adhesion-dependent signaling pathways *in vivo* during *Drosophila* development. This is evident from overexpression and mutant analysis. Overexpression of the kinase in *Drosophila* resulted in phenotypes associated with defects in integrin- and cadherin-mediated signaling pathways, as well as in Notch and Wingless signaling pathways. Null mutations similarly pinpoint to a function in cadherin-mediated cell adhesion during epithelial morphogenesis in the *Drosophila* embryo.

The further analysis of the *dfer* mutant will broaden the perspective on DFer function in cell adhesion processes. Future studies should take the numerous *Drosophila* mutants into account that are involved in these processes. In particular, the combination with mutants of the cadherin-associated gene *p120catenin,* the integrin-associated *DFak56*, the protocadherins *dachsous* and *fat*, the wingless gene *armadillo*, the tyrosine kinase *abelson* and other genes involved in dorsal closure processes should reveal functional interactions by modifying the *dfer* mutant phenotype. Similarly, the role of the JNK pathway within the *dfer* overexpression and mutant phenotypes should be investigated. The combination of several mutations will help to genetically define which genes and pathways overlap in function and reveal the contribution of Dfer in the regulation of these signaling pathways. Finally, resolving DFer function will give new insights on its interference with APP function in cell adhesion during *Drosophila* wing development.

Material and Methods

4 Material

4.1 Molecular Weight Markers

DNA Molecular Weight Marker III	Roche
DNA Molecular Weight Marker IV	Roche
DNA Molecular Weight Marker VI	Roche
Low Range PFGE Marker	New England Biolabs (NEB)
Protein Standard Broad Range	NEB
SeeBlue Plus 2 Prestained	Invitrogen
1 kb DNA Ladder	NEB

4.2 Enzymes

Benzonase	Merck
Calf Intestinal Alkaline Phosphatase (CIP)	NEB
DNAse	Roche
DNA-Polymerase-I	NEB
GELase, Agarase	Epicentre, Madison, USA
Lysozyme	Roche
Mung Bean Nuclease	NEB
Proteinase K	Roche
Pwo-Polymerase	Roche
Restriction enzymes	NEB / Roche
Reverse Transcriptase	Promega
RNAse A	Roche
RNAse H	Gibco
RNasin, Ribonuclease-Inhibitor	Promega
Shrimp Alkaline Phosphatase (SAP)	Roche
Sp6-RNA-Polymerase	Roche
Taq-Polymerase	Qiagen / Roche
T4-DNA-Ligase	NEB / Roche
T3-RNA-Polymerase	Roche
T7-RNA-Polymerase	Roche

4.3 Antibodies

Antigen	Source	Obtained from	WB	IP	IS
hAPP 22C11	mouse	K. Beyreuther	1:10.000	-	-
hAPP 22C13	rabbit	K. Beyreuther	1:10.000	-	-
hAPP 22734	mouse	G. Multhaup	-	5	-
Armadillo	mouse	DSHB	-	-	1:10
Cut	mouse	DSHB	-	-	1:200
Elav	mouse	DSHB	1:1.000	-	1:10
DFer-N (A)	rabbit	generated during thesis	1:5.000	2	1:200
DFer-N (B)	rabbit	generated during thesis	1:5.000	2	1:200
DFer-SK (A)	rabbit	generated during thesis	1:5.000	2	1:200
DFer-SK (A)	rabbit	generated during thesis	1:5.000	2	1:200
hFpsQE	rabbit	P. Greer	1:1.000	-	1:100
Human Fes	rabbit	Upstate biotechnology	1:1.000	-	-
v-Fes	mouse	Oncogene Research	1:1.000	-	-
myc	rabbit	Santa Cruz	1:1.000	-	-
Phosphotyrosine	mouse	Cell Signaling	1:10.000	-	-
Tubulin	mouse	Sigma	1:5.000	-	-
V5	mouse	Invitrogen	1:5.000	-	-
Wingless	mouse	DSHB	-	-	1:10
DIG-Fab AP		Roche	1:10.000 (SB)	-	1:2.000 (in situ)
Phalloidin-Alexa546	-	Molecular Probes	-	-	1:1.000
α-rabbit Cy3	goat	Dianova	-	-	1:200
α-mouse Cy3	goat	Dianova	-	-	1:200
α-rabbit Alexa488	goat	Molecular Probes	-	-	1:200
α-mouse HRP	goat	Amersham	1:10.000	-	-
α-rabbit HRP	goat	Amersham	1:10.000	-	-
α-mouse Alexa546	goat	Molecular Probes			1:200
α-mouse Alexa647	goat	Molecular Probes	-	-	1:200

DSHB = Developmental Studies Hybridoma Bank

4.4 Oligonucleotides

All oligonucleotides, if not otherwise mentioned, were purchased from MWG. Others were purchased from Biospring (BS) or Sigma (S).

Primer pairs for pUASt-*dfer-C:*

Zwim-NotI-01	GACGCGGCCGCTACAGGCAACTCGTTGTCAAGTCCT CGGACG
Zwim-EcoRI-02	GACCAATTCCACCAAGAGACGTCGCATCCATCCCAGC

Primer pairs for pUASt-*dfer-DN:*

Zwim-DN-K570R	GACGACTCCACCAAACTGGATGTGGCTGTCAGGACCTGT CGAATGACCCTGCCCGACGAACAG (BS)
pUASt 3'	TCTCTGTAGGTAGTTTGTCCAATTATGTCACACCAC

Primer pairs for pUASt-*mFer:*

(BglII)-muFer-5'	GAGAGATCTATGGGATTTGGGAGTGACCTG
muFer-(BglII)-3'	GAGAGATCTCTATGTGATCATCTTCTTGATGAC

Primer pairs for *Sym*-pUASt-*dfer-N:*

EcoRI-5'UTR-Z	GAGATTCGAGATACTCGGCGCTG
GST-N-end-401-EcoRI	GAGAATTCTTAGGGCAGCTCCTCGCATCCCAC

Primer pairs for pWIZ-*RNAi-N:*

RNAi-N-5'	GAGTTCTAGACACACAACGAGTACGTGCTGTCCA
RNAi-N-3'	GAGTTCTAGAGGCATAGGTCATCCTTGTTGGA

Primer pairs for pWIZ-*RNAi-SK:*

RNAi-SK-5'	GAGTTCTAGACGCTCTCCACAAATCGTCCGC
RNAi-SK-3'	GAGTTCTAGACTTCTGCACACAAATGCCAATCA

Primer pairs for pWIZ-*RNAi-long:*

RNAi-long-(XhoI)-5'	GACTCTAGACTCGAGCTCCAGTTCCAGTTCAGAGTG
RNAi-long-3'	GACTCTAGACTCTTGGTGCACTGTTTGCACG

Primer pairs for pCRII-*p92dfer-long:*

Start-zwim	ATGGGCTTCTCATCAGCCCTCCAAAGTCG
End-zwim	GTGGCTGTTGTCCAGGCGCAGAATC

Primer pairs for pCRII-*dfer-NT:*

Start-zwim	ATGGGCTTCTCATCAGCCCTCCAAAGTCG
GST-N-end-401-EcoRI	GAGAATTCTTAGGGCAGCTCCTCGCATCCCAC

Primer pairs for pCRII-*p45dfer*$^{140\text{-}481}$*:*

p45-1-(140)	CCATCCGCAATACATTCCGC (S)
p45-2-(481)	GCAATAGCATGATCCTTCATGC (S)

Primer pairs for pCRII-*dfer-C*$^{8\text{-}498}$*:*

testis-Z-up	CAATCACAGTGCCTCACAGTC (S)

testis-Z-low	CAGTGATCCTTCATGCTGAGC (S)

Primer pairs for pCRII-*CG33188:*

CG33188-up	CAACTTGCCACAATGCACCAGG (S)
CG33188-low	GTCTAGCGTGGTCGTGGATTC (S)

Primer pairs for pCRII-*CG18473:*

CG18473-up	CCATTACTCCCAATCTGCTGG (S)
CG18473-low	CATGAATGGGATACACGCTGG (S)

Primer pairs for pCRII-*CG8129:*

CG8129-up	GTGGAGGAAACATAGACACCAC (S)
CG8129-low	GTTTTGCTGCGCTGCTGAAGTG (S)

Primers for recombinant protein expression*:*

GST-N-BamHI-start	GAGGATCCATGGGCTTCTCATCAGCCCTC
GST-N-end-EcoRI	GAGGAATTCCTTAGTGGCTGTTGTCCAGGCG
GST-N-128-EcoRI	GAGAATTCTTAATGATTCAGGCGTGCTGCG
GST-N-BamHI-362-start	GAGGATCCGATGACCTATGCCGCCAGTCG
GST-N-563-end-EcoRI	GAGAATTCTTAGGTGGACTTCAGTTTGGCC

Primers for cell culture expression*:*

(XbaI)-5'UTR-Z	GAGTCTAGAcGAGAGCCGCGACCCAAATAGG (S)
C-term-(XbaI)	GAGTCTAGACTGTGGCTGTTGTCCAGGCGCAG
GST-N-128-EcoRI	GAGAATTCTTAATGATTCAGGCGTGCTGCG
GST-N-BamHI-362-start	GAGGATCCGATGACCTATGCCGCCAGTCG
GST-N-563-end-EcoRI	GAGAATTCTTAGGTGGACTTCAGTTTGGCC

Primer pairs for pCosPer modification and genomic rescue analysis:

COS/Cas-EASFX-1	AATTCAGTCATCCTAGGAGTCTAGCATGCACATGAGGCC GGCCAGACTAT (BS)
COS/Cas-XFSAE-2	CTAGATAGTCTGGCCGGCCTCATGTGCATGCTAGACTCC TAGGATGACTG (BS)
cos/CAS-AS-up	GAGCCTAGGAGTCTAGCATGCGAGTTGCGTGACTACCTA CG (S)
cos/CAS-F-low	GAGGGCCGGCCGCTTCTGCTTCAATCAGCGTG (S)
seqCos-CAS-up	GACATTGACGCTAGGTAACGC (S)
seqCos-CAS-low	GAGTACGCAAAGCTTGGGCTG (S)
genrescue-lowSphI-up	GAGATCTTCACACTGTGCGCC (S)
genrescue-upSphI-low	GGAAGGCTAACACTGGACTC (S)
genrescue-lowFPS-up	CAGGAGTTACTTCGGATGCAG (S)
genrescue-upFPS-low	GCACTTCTCCGACTCCACACC (S)

Primer pairs for Southern Blot analysis:

Kanam-1	GGAACACGTAGAAAGCCAGTC
Kanam-2	GGTAGCCAACGCTATGTCCTG
Probe-upEP-low	CTGGGTCTATTGTGACGCATAG
Probe-upEP-up	GATGCTGATCCTCATAGAGATTC

EcoRI-03	GACGAATTCAGAGCCGCGACCCAAATAGGGAGTAAC
Zwim02	AGCGGTCAGGCTGATGGCGCGTACTCC
Zwim07	ATCGCCCCCTGGGTCTGGTTCAATCG
Zwim08	CTCATCCCCGGCCAAAGTCCTGTCC
Zwim09	AATGGACGCCGAGAATGCCAATC
Zwim10	TATTGCTGCCGTTCGGTTCAATCC
Zwim11	CCTACCCCTCCCCCTACCTCATTCCTCTTC
Zwim12	GGTTATTCGCTGGGCGTTGCTTCTTTATCG
Zwim13	ATGTGCGGCACATTTCGTATCTTTTCAGTC
Zwim14	CATCTCCCCCATCTTCTCATTCCCCTAAC
Zwim-EcoRI-01	GACGAATTCGTTACGCGATTTGCAAGTGAAATCCGACGG
Zwim12	GGTTATTCGCTGGGCGTTGCTTCTTTATCG

Primer pairs for PCR analysis:

Probe-upEP-up	GATGCTGATCCTCATAGAGATTC
Probe-upEP-low	CTGGGTCTATTGTGACGCATAG
EP-200up	ACGACAGAACGCAAAAGTAAGC
EP+200down	CTTCGAGATGCGTGCACTTCAC
EP-800up	ACGAACAAAGGGTAGATCCACG
EP+800down	AGGAAACACAAGCGACAGAAGG
CG8121-up	GACATCTACTGCTATGCTATGG
CG8121-low	GAGTTTGCTGTCGATGCGTGC

Sequencing primers:

In general, standard sequencing primers available at the sequencing companies or specific primers were used. Additional primers are:

pUASt 5’		AAAAGTAACCAGCAACCAAGTAAATCAACTGC
pUASt 3’		TCTCTGTAGGTAGTTTGTCCAATTATGTCACACCAC
EP primer:	Plac1	CACCCAAGGCTCTGCTCCCACAA
	pEP-RV1	AAGCAAAGTGAACACGTCGAGATCTCTGCAG
	pEP-RV2	GCTTGTTTGAATTGAATTGTCGCTCCGTAGACG

4.5 Plasmids, cosmids and BACs

BAC R19J06	Biokat, Open Biosystems, Heidelberg
BAC R32M04	Biokat
pAC-GFP	kindly obtained from G. Merdes, Heidelberg
pBAD/Thio-TOPO	Invitrogen
pBluescript II KS	Stratagene
pBS-*p45*	*p45* cDNA in pBluescript II KS, kindly provided by K. Hill, San Francisco, USA
pCaSpeR-4	kindly obtained from J. Anne, Heidelberg

pCosPer	kindly obtained from V. Pirrotta, Geneva, Swiss
pCRII-TOPO	Invitrogen
pCRT7/CT-TOPO	Invitrogen
pEF4-*hFes*	*hFes* cDNA in modified pECE plasmid, kindly provided by P.Greer, Kingston, Canada
pECE-*mFer*	*mFer* cDNA in modified pECE plasmid, kindly provided by P.Greer, Kingston, Canada
pFLC-*RH-Fps*	Biokat
pGEM-*p92*	*p92* cDNA in modified pGEM-7 plasmid (Promega), kindly obtained from K. Hill, San Francisco, USA
pGEX-4T-2	Promega
pMT-V5/HisB	Invitrogen
pMT-APP695-N-myc	kindly obtained from G. Merdes, Heidelberg
pSYMP-UASt-w^+	kindly obtained from G. Merdes, Heidelberg (Giordano et al. 2002)
pUASt	kindly obtained from G. Merdes, Heidelberg
pUASt-APP695	kindly obtained from G. Merdes, Heidelberg
pUChsΔ2-3	helper plasmid, kindly obtained from G. Merdes, Heidelberg
pWIZ	kindly obtained from G. Merdes, Heidelberg (Lee and Carthew 2003)

4.6 Bacterial cell lines

BL21	*E. coli* B F- *dcm ompT hsdS* (r_B-m_B-) *gal*, Stratagene
BL21(DE3)	*E. coli* B F- *dcm ompT hsdS* (r_B-m_B-) *gal* λ(DE3), Stratagene
DH5α	*E. coli* supE44 ΔlacU169 (80 lacZΔM15) hsdR17 recA1 endA1 gyrA96, thi-1 relA1 (Hanahan et al. 1983)
SURE 2	e14–(McrA–) Δ(*mcrCB-hsdSMR-mrr*)*171 endA1 supE44 thi-1 gyrA96 relA1 lac recB recJ sbcC umuC::*Tn*5* (Kan^r) *uvrC* [F« *proAB lacI*^{q}Z*ΔM15* Tn*10* (Tet^r) Amy Cam^r], Stratagene
TOP10	*E. coli* F- *mcr*A Δ(*mrr-hs*ΔRMS-*mcr*BC) Φ80*lac*ZdM15 Δ*lac*X74 *rec*A1 *arad*139 Δ(*ara-leu*)7697 *gal*U *gal*K *rps*L (Str^R) *end*A1 *nup*G, Invitrogen
XL1-Blue	*E. coli recA -* (*recA1 lac - endA1 gyrA96 thi hsdR17 supE44 relA1* {*F' proAB lacIq lacZDM15Tn10*}), Stratagene
XL1-Blue MR	*E. coli Δ(mcrA)183 Δ(mcrCB-hsdSMR-mrr)173 endA1 supE44 thi-1 recA1 gyrA96 relA1 lac*, Stratagene

4.7 Cell culture lines

S2	Schneider 2 cell line derived from primary culture of late stage *Drosophila melanogaster* embryos (Schneider 1972)
COS-7	African green monkey kidney epithelial cell line (Gluzman 1981)

4.8 Fly lines

The wildtype flies used are from the *Drosophila Oregon R* stock (Lindsley and Grell 1968).

B = *Drosophila* Stock Center Bloomington, Indiana, US
E = Exelexis, Inc.,
Sz = Szeged Drosophila Stock Center, US
L = Laboratory Stock Collection, Paro, Heidelberg
M = G. Merdes Stock Collection, Heidelberg

4.8.1 General fly lines

Genotype	**Donor**
w[1118]	L
y[1] w[1118]; Δ2-3,Sb/TM,Ubx	L
y[1] w[1118]; Δ2-3,Sb/ Δ2-3,Dr	M
w[1118]; BcGla/CyO	B
w[1118]; TM6B,Tb[1]/TM3,Sb[1]	M

4.1.2 GAL4 driver lines and lacZ lines

GAL 4 line	**Genotype**	**Donor**
actin5C	*y[1] w[*]; P{w[+mC]=Act5C-GAL4}17bFO1/TM6B,Tb[1]*	B
apterous	*y[1] w[1118]; P{w$^{+mW.hs}$=GawB}ap^{md544}/CyO*	(Milan et al. 2001)
armadillo	*w[*]; P{w[+mW.hs]=GAL4-arm.S}11*	B
daughterless	*w[*]; P{w[+mW.hs]=GAL4-da.G32}UH1*	B
distalless	*P{w[+mW.hs]=GawB}Dll[md23]/CyO*	B
elav	*P{w[+mW.hs]=GawB}elav[C155]*	B
engrailed	*y[1] w[*]; P{w[+mW.hs]=en2.4-GAL4}e22c/SM5*	B
Gal4^{332}	*w[*]; P{w[+mW.hs]=GawB}332.3*	B
GMR	*w[*]; P{w[+mC]=GAL4-ninaE.GMR}12*	B
MZ1580	*P{w[+mW.hs]=GawB}MZ1580, w[*]*	B
patched	*w[*]; P{w[+mW.hs]=GawB}ptc[559.1]*	B
scabrous	*y[1] w[*]; P{w[+mW.hs]=GawB}sca[109-68]*	B
scalloped	*P{GawB}sd[SG29.1], w[*]*	B
sevenless	*w[1118]; P{w[+mW.hs]=sevEP-GAL4.B}7*	B
twist	*P{GAL4-twi.G}108.4*	B
vestigial	*P{vg-GAL4.B}*	(Huang et al. 2000)
1878	*w[*]; P{w[+mW.hs]=GawB}T80/CyO*	B
69B	*w[*]; P{w[+mW.hs]=GawB}69B*	B
vestigial(In2.1)-lacZ	*P{w+mC EcoI\lacZ[vg.int2.1]=vg(D/V)-lacZ}*	(Ye et al. 1999)

4.1.3 EP lines

Gene	Genotype	Donor
EP cortactin	*w[1118]; Cortactin*[EPg35301]	(Somogyi and Rorth 2004)
EP(3)707	*P{EP}EP707*	Sz

4.1.4 UAS lines

Genotype	Donor
w[1118]; P{UAS-APP N-myc}	M
w[1118]; P{UAS-APPΔCT-GFP N-myc}	P. Soba, Heidelberg
w[1118]; P{UAS-Abl}	(Fogerty et al. 1999)
w[1118]; P{UAS-Abl^{DN}}	(Fogerty et al. 1999)
w[1118]; P{UAS-H}	A. Preiss, University Hohenheim
w[1118]; P{UAS-Su(H)}	A. Preiss
w[*]; P{w[+mC]=UAS-wg.H.T:HA1}3C	B

4.1.5 Mutations

Gene	Genotype	Donor
abl^{3}	*abl[3]/TM3,Sb[1]*	(Fogerty et al. 1999)
ap^{ts78j}wg	*ap[ts78j] wg[1]/SM5*	B
arm^{1}	*y[1] arm[1]/FM7c*	B
CG8129	*w[1118]; PBac{w[+mC]=PB}CG8129[c04459]*	B
CG33188	*w[1118]; PBac{w[+mC]=WH}CG33188[f01391]/TM6B,Tb[1]*	B
cortactin^{M7}	*w[1118]; cortactin[M7]*	P. Rorth, EMBL
dfer^{del1}	*FRT 82B, dfer[st13c]/TM3,Sb[1],Kr-GFP*	A. Brand, Cambridge
EGFR^{f2}	*cn[1] Egfr[f2] bw[1] sp[1]/CyO or BcGla*	B
H^{P8}	*H[P8]/TM3,Sb[1]*	(Nagel et al. 2000)
hep^{1}	*y[1] w[1118] hep[1]/FM7c*	(Glise et al. 1995)
hep^{75}	*w[*] hep[r75]/FM7c*	B
N^{55e11}	*w[a] N[55e11]/FM7, lac-z*	B
sgg^{1}	*sgg[1]/FM7a/Dp(1;2;Y)w[+]*	B
shg^{2}	*cn[1] shg[2] bw[1] sp[1]/CyO*	B
wg^{spd-fg}	*wg[spd-fg]*	B
wg$^{1-17}$	*wg[l-17] b[1] pr[1]/CyO*	B

4.1.6 Deficiency lines

Gene	Genotype	Donor
basket	*w[1118]; Df(2L)Exel7049, P+PBac{XP5.RB3}Exel7049/CyO*	E
β1-integrin	*w[1118]; Df(2L)Exel7080, P+PBac{XP5.RB3}Exel7080/CyO*	E
β1-integrin	*Df(2L)DS6, b[1] pr[1] cn[1]/CyO =or= SM6a*	B
cdc42	*Df(1)Exel6253, w[1118] P{w[+mC]=XP-U}Exel6253/FM7c*	E
CG33188	*w[1118]; Df(3R)Exel9036, PBac{w[+mC]=WHr}Exel9036/TM6B, Tb[1]*	E
cortactin	*w[1118]; Df(3R)Exel6272, P{w[+mC]=XP-U}Exel6272/TM6B,Tb[1]*	E

cortactin	*Df(3R)e-R1, Ki[1]/TM3, Sb[1] Ser[1]*	B
GSK3β	*Df(1)64j4, y[1] w[a] N[spl-1]/Dp(1;2;Y)w[+]/C(1)DX, y[1] f[1]*	B
N-cadherin	*w[1118]; Df(2L)Exel7069, P+PBac{XP5.RB3}Exel7069/CyO*	E
N-cadherin	*Df(2L)M36F-S5/CyO, Dp(2;2)M(2)m[+]*	B
PI3K	*Df(3L)vin3, ru[1] h[1] gl[2] e[4] ca[1]/TM3, ry[*] Sb[1] Ser[1]*	B
p120ctn	*w[1118]; Df(2L)Exel6049, P{w[+mC]=XP-U}Exel6049/CyO*	E
p120ctn	*Df(2R)nap1/Dp(2;2)BG, In(2LR)Gla, wg[Gla-1]*	B
rac1	*Df(3L)Ar14-8, red[1]/TM2,p[p]*	B
ras64B	*w[1118]; Df(3L)GN34/TM3,ry[*]su(Hw)[2]Sb[1]*	B
ras64B	*w[1118]; Df(3L)Exel6100, P{w[+mC]=XP-U}Exel6100/TM6B,Tb[1]*	E
ras82D	*w[1118]; Df(3R)Exel6153, P{w[+mC]=XP-U}Exel6153/TM6B,Tb[1]*	E
stat92E	*w[1118]; Df(3R)Exel6185, P{w[+mC]=XP-U}Exel6185/TM6B,Tb[1]*	E
stat92E	*l(1)10Ae[4]/FM7a*	B
1873	*Df(3R)dsx37/TM2*	B
1891	*Df(3R)Dhod15/TM3,Sb[1]*	B
1893	*Df(3R)by62, red[1]/TM1,p[p]*	B
1931	*Df(3R)by10, red[1] e[1]/TM3,Sb[1]Ser[1]*	B
1932	*Df(3R)by416, red[1] e[1]/TM3, Sb[1]*	B
1937	*Df(3R)GB104, red[1]/TM3, Sb[1] Ser[1]*	B
1962	*Df(3R)p-XT103, ru[1] st[1] e[1] ca[1]/TM3, Sb[1]*	B
1968	*Df(3R)p712, red[1] e[1]/TM3, Sb[1] Ser[1]*	B
3128	*Df(3R)M-Kx1/TM3, Sb[1] Ser[1]*	B

4.1.7 Generated fly lines

In general, transgenic fly lines were produced with insertions in all three chromosomes.

Fly lines	**Chromosome**
w[1118]; P{UAS-dfer}	X., 2., 3.
w[1118]; P{UAS-dfer-A}	X., 2., 3.
w[1118]; P{UAS-dfer-C}	X., 2., 3.
w[1118]; P{UAS-p45dfer}	X., 2., 3.
w[1118]; P{UAS-dfer-DN}	X., 2., 3.
w[1118]; P{UAS-dfer-N}	X., 2., 3.
w[1118]; P{UAS-mFer}	X., 2., 3.
w[1118]; P{UAS-hFes}	X., 2., 3.
w[1118]; P{Sym-UAS-dfer-N}	X., 2., 3.
w[1118]; P{UAS-WIZ-RNAi-dfer-N}	X., 2., 3.
w[1118]; P{UAS-WIZ-RNAi-dfer-SK}	X., 2., 3.
w[1118]; P{UAS-WIZ-RNAi-dfer-A)}	X., 2., 3.
y[1] w[1118]; dfer$^{\Delta 252}$	3.
dfer$^{w39.2}$/TM6,Sb[1]	3.
w[1118]; dfer$^{41.1}$/TM6,Sb[1]	3.
w[1118]; dfer^{49Sb}/TM6,Sb[1]	3.
w[1118]; P{UAS-GR-dfer}	X., 2., 3.
w[1118]; P{UAS-GR-CG}	3.

5 Methods

5.1 Molecular methods

5.1.1 Phenol-chloroform extraction of DNA

An equivalent volume of phenol was added to a DNA solution and thoroughly vortexed for at least 1 min. The emulsion was centrifuged for 5 min with 13.000 rpm at RT (Eppendorf desk centrifuge) and the upper aqueous DNA containing phase was carefully transferred into a new Eppendorf tube. One volume of chloroform was added, vortexed for at least 1 min and centrifuged. The upper aqueous phase was transferred to a new tube and the procedure was repeated once, before the DNA was precipitated with ethanol.

5.1.2 Ethanol precipitation of DNA

TE-buffer pH 8.0: 10 mM Tris-HCl pH 8.0
1 mM EDTA pH 8.0

1/10 volume of 3.5 M sodium acetate pH 5.2 and 2.5 volume 100% ethanol (-20°C) was added to the DNA sample, mixed and incubated for at least 1 h at -20°C. The precipitated DNA was centrifuged for 45 min at 4 °C with 13.000 rpm, washed with 70% ethanol (-20°C) and centrifuged for an additional 10 min at 4 °C with 13.000 rpm. The supernatant was removed and the precipitated DNA was vacuum-dried and diluted in TE-buffer or ddH_2O.

5.1.3 Analysis of DNA fragments by agarose gel electrophoresis

Solutions:		
	1x TAE buffer	40 mM Tris-acetate 1 mM EDTA pH 8.0
	Ethidium bromide stock	10 mg/ml (use 1:20.000)
	6x DNA sample buffer	0.25% (w/v) Bromophenol-blue 60% (w/v) glycerol 0.1 mM EDTA pH 8.0

Depending on the size of the DNA fragments to be separated, 0.7-2% (w/v) agarose gels were used. Ethidium bromide was added to a final concentration of 0.5 µg/ml. Samples supplemented with DNA sample buffer were loaded and electrophoresis was conducted at 100-250 V for 20 min - 2 h at 4°C. After separation, the gels were analyzed using a transilluminator with UV light, photographed and printed with a RAYTEST IDA (Image and Documentation analysis) gel documentation device.
For preparative gels, the fragment of interest was cut out under UV light and the DNA was purified.

5.1.4 Pulsed field gel electrophoresis (PFGE)

0.5x TBE buffer: 45 mM Tris-HCl pH 7.8
45 mM boric acid
1.5 mM EDTA

The electrophoresis exploits the fact that DNA molecules, due to their negative charge, travel in an electrical field towards the anode. The velocity of the DNA is, up to a certain DNA size, reversed proportional to the logarithm of the molecular weight of the DNA and its topology, thus enabling the size of the DNA fragments to be analysed. The conventional electrophoresis allows efficient separation of DNA fragments only up to a size of 15 kb. For larger DNA fragments, pulsed field electrophoresis (PFGE) is recommended. In contrast to the conventional system, which uses static electrical fields, the PFGE electrical fields change between two orientations. Large DNA fragments need time to adjust themselves to the electrical field, again rendering the velocity proportional to the size. In this thesis, the Pulsed Field Electrophoresis System CHEF-DR II from Bio-Rad Laboratories was utilized. Several parameters can be adjusted. For all PFGE performed, the same program was used: the time of electrophoresis (15-16 h), the voltage (200 V), the temperature (4°C) and the changing interval gradient (pulse wave initially 3 sec, increasing with time and ending at 10 sec).
PFGE was carried out with 1% agarose gels and 0.5x TBE buffer. The PFGE low range DNA marker was used. After electrophoresis the gel was stained in an Ethidium bromide solution (1 µg/ml), checked under UV light and documented.
For preparative gels, only cut gel slices containing the edge of the DNA lane and the DNA markers were stained. The DNA fragment of interest was marked under UV light. The marked gel slices were put next to the unstained gel and the DNA fragment was cut out blindly. This gel slice was poured in 3% low melting point (LMP) SeaPlaque GTG Agarose (Cambrex, US), a second PFGE was conducted and the DNA fragment was isolated as just mentioned. The DNA in the LMP agarose slice was extracted either by gelase digestion or using the GeneCAPSULE system.

5.1.5 PCR purification / gel extraction

For the purification of DNA following a PCR reaction or prior to digestion, the QIAquick PCR purification kit (Qiagen) was used according to the manufacturer's protocol. The DNA was eluted in 30 µl ddH_2O. Alternatively, the MinElute PCR purification kit (Qiagen) was used which allows concentration of the DNA in 10 µl ddH_2O.
To purify DNA fragments from agarose, the QIAquick gel extraction kit (Qiagen) was applied as described in the manufacturer's manual. The DNA was eluted in 30 µl ddH_2O.

5.1.6 Extraction of DNA from LMP agarose gels

For the extraction of large DNA fragments from LMP agarose gels, the cut gel slice was incubated after addition of 50x gelase buffer (1 µl/50 mg gel) for 20 min at 70°C to dissolve the agarose and equilibrated for 15 min at 45°C before 10 U gelase were added. In general, gelase digestion was performed for 3 h. Undigested agarose debris was pelleted by centrifugation and the DNA supernatant was transferred into a new tube. To precipitate remaining undigested carbohydrates from the supernatant, 0.1 volume 3 M sodium acetate was added, the solution was incubated on ice for 15 min and then centrifuged for 15 min with 5.000 rpm at 4°C. The supernatant was again transferred into a new tube and ethanol precipitated. Upon addition of 20 µl ddH_2O, the DNA was dissolved through overnight incubation at 4°C and the next day carefully resuspended.

5.1.7 Extraction of DNA by electroelution

To elute large DNA fragments from LMP agarose gels, the GeneCAPSULE™ Electroelution system (Geno Technology, US; KMF) was used. The GeneCAPSULE was prepared as described in the manufacturer's manual. The band of interest was cut out of the gel, the LMP agarose containing the DNA was dissolved and filled into the GenePICK to harden. After assembling the GeneCAPSULE, it was subjected to an overnight electrophoresis at 35 V in TAE buffer with the GeneTRAP side facing the anode. The following day, after electroelution was completed, the current was adjusted to 250 V and its direction reversed for 20 sec. A small hole was punctured in the DNA collection port and the DNA was carefully removed in a 20 µl volume. As the DNA was eluted in TAE buffer, it was dialysed for 30 min in ddH_2O.

5.1.8 Restriction digestion of DNA

For analytical digests, 100-300 ng DNA were used together with 1-10 U of restriction enzyme with its appropriate buffer according to the manufacturer's protocol in a volume of 20 µl. In general, the digests were incubated for 1 h at 37°C.

For preparative digests, 2-4 µg DNA was used with 10-40 U of restriction enzyme. Digests were incubated for 1-4 h up to overnight at 37°C. For some reactions, a heat inactivation step at 65°C for 20 min was necessary to inactivate the restriction enzyme, or a Phospatase treatment to prevent religation. Afterwards, the digested DNA was purified using the QIAquick PCR purification kit or isolated in a preparative agarose gel electrophoresis.

Digestions with two different restriction enzymes were performed either in parallel or sequential with one purification step using the QIAquick PCR purification kit between it.

5.1.9 Phosphatase treatment of DNA

To prevent recircularization of a digested vector DNA in a ligation reaction, the DNA was either treated with Shrimp Alkaline Phosphatase (SAP) or with Calf Intestine Phosphatase

(CIP) to remove the 5'-ends of the DNA. Phophatase treatment was typically performed directly after a restriction digest in the used restriction buffer. For the SAP reaction, 0.5 U/µl DNA was added to the digestion reaction, incubated for an additional hour at 37°C prior to heat inactivation at 65°C for 20 min. For the CIP reaction, 0.5 U/µl DNA was added, subjected to a 1 h incubation at 37°C, and the DNA was either gel purified or spin-column purified using the PCR purification kit.

5.1.10 Nuclease treatment of DNA

As the Mung Bean Nuclease is a very potent enzyme, conditions were adjusted to remove only very short stretches of nucleotides or a restriction site. 3.5 µg PCR purified DNA was incubated with 0.8 U/µl Mung Bean Nuclease in its buffer in a total volume of 36 µl for 30 min at 30°C. The reaction was stopped through addition of SDS to a total concentration of 0.01% SDS and the DNA was then purified using the QIAquick PCR purification kit.

5.1.11 Hybridisation of oligonucleotides

The appropriate oligonucleotides were diluted to a concentration of 1 ng/µl. Annealing was performed by mixing 10 µl of each of the two oligonucleotides, denaturing them at 95°C for 2 min and leaving them on RT to cool down slowly. The hybridized oligonucleotides were ligated into the prepared vector plasmids in a 3:1 molar ratio.

5.1.12 Ligation of DNA fragments

Ligation reactions were prepared with approx. 300 ng vector DNA and a 3 fold molar excess of insert DNA in 10 µl with 1 U T4 DNA Ligase according to the manufacturer's protocol. The reaction was incubated either for 1 h at RT or overnight at 16°C.

5.1.13 TOPO TA cloning

TOPO TA cloning (Invitrogen) allows efficient cloning of Taq-Polymerase-amplified PCR products into various TOPO TA vectors. For PCR amplification, either Taq-Polymerase or the Expand High Fidelity PCR System (Roche) was used. Usually, the ligation reaction was set up with half the volume recommended and was incubated for 15-20 min at RT:

0.5 µl salt solution (TOPO kit)
0.5 µl TOPO TA cloning vector
2 µl PCR product

2 µl of the ligation reaction were used for subsequent transformation into chemo-competent TOP10 cells. This step and all following procedures were conducted according to the manufacturer's protocol.

5.1.14 Ligation of genomic DNA into cosmids

To favor the formation of mixed concatamers between the arms of the cosmid vector and the genomic DNA fragment, the total concentration of DNA in the ligation reaction was greater than 200 ng/µl. The ligation reaction contained a 9:1 molar ratio of vector DNA:genomic DNA fragment in a total volume of 20 µl using 2 U T4 DNA Ligase and was incubated overnight at 16°C. Successful ligation was checked on a 0.4% agarose gel prior to the phage packaging reaction.

5.1.15 Phage packaging of cosmid DNA

SM buffer
5.8 g NaCl
2.0 g $MgSO_4$
50 mM Tris-HCl pH 7.5
5 ml of 2% (w/v) gelatin

Phage packaging

For phage packaging, the Gigapack III Gold Packaging Extract (Stratagene) containing the modified lambda phages was used as described in the manufacturer's protocol. The packaging extract was quickly thawn and 4 µl of the ligated cosmid DNA (0.1-1 µg) was immediately added to the extract. After mixing by careful stirring with a pipette tip, the tube was incubated for 2 h at RT. 500 µl SM buffer was added, followed by 20 µl chloroform and gently mixed. The supernatant was used for the titering reaction.

Titering the cosmid packaging reaction

XL1-Blue MR cells were streaked onto appropriate agar plates and incubated overnight at 37°C. The next day, appropriate LB medium supplemented with 10 mM $MgSO_4$ and 0.2% (w/v) maltose was inoculated with a single colony and grown for 4-6 h shaking at 37°C, not exceeding an OD_{600} ~1.0. Bacteria were pelleted for 10 min at 500 g and gently resuspended in half the original volume with sterile 10 mM $MgSO_4$.

After preparing a 1:10 and 1:50 dilution of the cosmid packaging reaction in SM buffer, 25 µl of each dilution was mixed with 25 µl bacteria and incubated for 30 min at RT. 200 µl LB medium was added and incubated for 1 h at 37°C, shaking the tube gently once every 15 min. The infected bacterial cells were centrifuged for 1 min at 500x g, resuspended in 150 µl LB medium and plated on LB agar plates containing the appropriate antibiotic. The cosmid DNA was isolated either by boiling lysis or Maxi Preparation (Qiagen).

5.1.16 Preparation of bacterial agar plates

LB (Luria-Bertani) medium:
1% (w/v) Bacto-tryptone
0.5% (w/v) yeast extract
1% (w/v) NaCl adjust to pH 7.0

Ampicillin stock (100 mg/ml)
Kanamycin stock (50 mg/ml)
Chloramphenicol stock (34 mg/ml in ethanol)
X-Gal (40 mg/ml in DMSO)

For agar plates, 1.5% Bacto-agar was added to the LB medium. The appropriate antibiotic was supplemented to a final concentration of 100 µg/ml for Ampicillin, 50 µg/ml for Kanamycin and 34 µg/ml for Chloramphenicol, respectively.
X-Gal was used in a final concentration of 100 µg/ml for blue-white screening of *lacZ* positive or negative clones and was added shortly before bacteria were plated.

5.1.17 Freezing of bacteria

Sterile Glycerin (240 µl) was added to 760 µl of an overnight bacterial culture, which was then immediately vortexed, shock-frozen in liquid nitrogen, and stored at -80°C.

5.1.18 Production of electro-competent *E. coli* cells

SOB medium:	2% Bacto-tryptone	
	0.5% yeast extract	
	0.05% NaCl	
	2.5 mM Kcl	
	10 mM $MgCl_2$	
	add 1 l ddH_2O	adjust to pH 7.5
SOC medium:	SOB medium	
	20 mM glucose (sterile)	

This procedure was applied for production of XL1-Blue, XL1-Blue MR, BL21 and BL21(DE3) electro-competent cells. A single colony was inoculated into 10 ml SOC medium and incubated overnight at 37 °C under vigorous shaking. The next day, 4 ml of this culture were inoculated into 1 l prewarmed SOC medium and incubated at 37 °C, until an OD_{600} ~0.6 was reached. The following steps were conducted at 4 °C with precooled material. The culture was centrifuged for 12 min at 5000 rpm/4 °C (JA-10 rotor, Beckman J2-MC centrifuge). The sedimented cells were resuspended in a large volume of ddH_2O and re-centrifuged. This step was repeated twice. Finally, cells were resuspended in 5 ml of freshly prepared 10% glycerin, aliquoted into sterile Eppendorf tubes, and shock frozen in liquid nitrogen. Competent cells were stored at -80 °C.

5.1.19 Transformation of *E. coli* using electroporation

Electro-competent cells were thawed on ice. The DNA (5-100 ng for a retransformation or 2-10 µl of a ligation reaction) was added to a 50 µl cell aliquot and transferred to a precooled cuvette (Equibio). Electroporation was performed at 1250 V with an Eppendorf Electroporator

2510. Afterwards, 1 ml LB medium was added and cells were incubated for 60 min at 37 °C on a roller shaker. Different aliquots of cells (50 µl – 1 ml) were plated on bacterial agar plates supplemented with the appropriate antibiotic and incubated overnight at 37 °C.

5.1.20 Transformation of chemo-competent cells

Chemo-competent DH5α and SURE 2 cells were treated according to (Hanahan 1983). 100 µl cell aliquots were thawed on ice. For SURE 2 cells, ß-mercaptoethanol was added to a final concentration of 25 mM and incubated for 10 min on ice before the transformation reaction. DNA (5-200 ng) was added to the cell aliquots and incubated for 30 min on ice. Cells were heat-pulsed for 30 sec at 42 °C and cooled on ice for 2 min. 1 ml LB medium was added and cells were incubated for 60 min at 37 °C on a roller shaker. Afterwards, different aliquots of cells (50 µl – 1 ml) were plated on bacterial agar plates supplemented with the appropriate antibiotic and incubated overnight at 37 °C.

5.1.21 Plasmid isolation

For DNA isolation in general, alkaline lysis was applied using buffers supplied by Qiagen.

Buffers:	P1	50 mM Tris-HCl pH 8.0
		10 mM EDTA
		100 µg/ml RNase A
	P2	200 mM NaOH
		1% SDS
	P3	3 M potassium acetate pH 5.5

Small scale DNA preparation (Mini Prep)

A single colony was inoculated into 2-3 ml LB medium supplemented with the appropriate antibiotic and incubated overnight at 37 °C under vigorous shaking. 1.5 ml of the overnight culture was transferred into an Eppendorf tube and centrifuged at 5.000 rpm for 3 min. Cells were resuspended in 300 µl P1 buffer and 300 µl P2 buffer was added. After a 5 min lysation step at RT, 300 µl P3 buffer was added for neutralization and the whole mixture was incubated 10 min on ice. The bacterial lysate was centrifuged for 30 min at 4°C/13.000 rpm, 850 µl of the supernatant was transferred to a new tube and the DNA was precipitated by addition of 600 µl isopropanol (RT). The DNA was pelleted in a 45 min centrifugation step and washed once with 70% ethanol (-20°C) as described. The pellet was speed vacuum dried for 2 min and dissolved in 30 µl ddH_20.

Large scale DNA preparation (Midi Prep and Maxi Prep)

The Highspeed Midi kit or the Maxi Prep kit from Qiagen were used to isolate larger quantities of pure DNA according to the manufacturer's protocol. The DNA was eluted/dissolved in 500 µl ddH_20.

5.1.22 Isolation of BACs and cosmids

Small scale DNA preparation (Mini Prep)

A single colony was inoculated into 10 ml LB medium supplemented with the appropriate antibiotic and incubated overnight at 37 °C under vigorous shaking. 6 ml of the overnight culture was pelleted in an Eppendorf tube by repeated centrifugation at 5.000 rpm for 3 min. Cells were resuspended in 300 µl P1 buffer and 300 µl P2 buffer was added. After a 5 min lysation step at RT, 300 µl P3 buffer was added for neutralization and the whole mixture was incubated 10 min on ice. The bacterial lysate was centrifuged for 30 min at 4°C/13.000 rpm, transferred to another Eppendorf tube, and centrifuged for a second time. The supernatant was transferred to a new tube and the DNA was precipitated by addition of 800 µl isopropanol (RT). The DNA was pelleted in a 45 min centrifugation step and washed once with 70% ethanol (-20°C) as described. The pellet was air-dried for 2 min, resuspended in 40 µl TE and kept at 4°C. For restriction digestion, 10 µl were used.

Large scale DNA preparation (Maxi Prep)

The general protocol for the Maxi Prep kit from Qiagen was modified for BAC and cosmid isolation. As these are very low copy plasmids, a higher amount of overnight culture had to be used (500 ml). After sedimentation for 12 min at 5.000 rpm/4°C, cells were resuspended in 30 ml P1 buffer by leaving them 1 h at RT on a shaker. 30 ml P2 buffer was added and left for 5 min at RT for lysis. After addition of 30 ml P3 buffer, the lysed cells were incubated 10 min on ice. Prior to the 30 min centrifugation step at 20.000g/4°C, the solution was cleared from debris using a filter mesh. The supernatant was poured into a preequilibrated Qiagen tip and washed twice with 15 ml QF buffer. The DNA was eluted with 15 ml of QF buffer, prewarmed to 55°C, then precipitated with 10.5 ml isopropanol for 15 min at RT, followed by a 30 min centrifugation at 15.000x g/4°C. The DNA pellet was washed twice for 5 min with 70% ethanol at RT and again centrifuged for 10 min at 15.000g/4°C. The DNA was air-dried for 10 min by leaving the corvex tube inversed on a cellulose paper. 200 µl 1/4x TE-buffer or ddH_2O was added, the tube was closed with parafilm and the DNA was left to dissolved overnight at 4°C. The following day, the DNA was carefully resuspended using a 200 µl pipette tip. For restriction digestion check, 5 µl were used.

5.1.23 Preparation of cosmid DNA from mini lysates

Buffer1	50 mM glucose
	10 mM EDTA
	25 mM Tris pH 8.0
Buffer2	0.2 N NaOH
	1% SDS

A 5 ml culture was inoculated with a single colony and incubated overnight at 37°C for no longer than 12 h. Bacteria were collected by centrifugation for 3 min/5.000rpm. The pellet

was resuspended in 200 µl of ice-cold buffer1 and 400 µl of freshly prepared buffer2 was added, mixed by inversion and incubated on ice for 5 min. Upon addition of 300 µl of ice-cold potassium acetate pH 4.8, the solution was gently inverted twice, incubated on ice for 5 min and centrifuged for 5 min at 5.000 rpm/4°C. 500 µl of the supernatant was transferred to a new tube and a phenol-chloroform extraction was performed once. The pellet was washed with 70% ethanol and resuspended in 50 µl TE. 10 µl were used for restriction digestion.

5.1.24 Preparation of cosmid DNA by boiling lysis

STET buffer	10 mM Tris-HCl pH 8.0
	0.1 M NaCl
	1 mM EDTA pH 8.0
	5% (v/v) Triton X-100
	adjust to pH 8.0

500 ml of an overnight culture were pelleted and frozen at –20°C. The pellet was then resuspended in 10 ml ice-cold STET buffer and transferred into a 50 ml Erlenmeyer flask. 1 ml of freshly prepared 10 mg/ml lysozyme in 10 mM Tris pH 8.0 was added and the solution was heated using a Bunsenburner and shaking the flask constantly until the solution just started to boil. The flask was transferred into boiling water for exactly 40 sec and then cooled for 5 min in ice-cold water. The viscous content was transferred into a tube and centrifuged for 30 min at 20.000 rpm/4°C. The supernatant was transferred to a new tube and 0.6 volume isopropanol was added and left for 10 min at RT. The solution was again centrifuged for 10 min at 20.000 rpm/4°C, the pellet washed with 70% ethanol and air-dried. Upon addition of 200 µl TE, the DNA was left for dissolution overnight at 4°C.

5.1.25 DNA purification by CsCl-ethidium bromide gradient equilibrium centrifugation

CsCl-ethidium bromide gradient equilibrium centrifugation

To obtain very pure DNA for cosmid injection into *Drosophila* embryos, a CsCl-ethidium bromide gradient equilibrium centrifugation step was performed. 4.12 g CsCl was filled into a Beckman Quick Seal polypropylene tube (Nr. 342412) and 2.5 ml DNA-TE solution was added. The solution was warmed to 30°C in a waterbath to facilitate the dissolution of the CsCl salt. Afterwards, 300 µl of 10 mg/ml ethidium bromide was added carefully and the tube was filled up with TE prior to sealing. The solution was ultracentrifuged in a VTi 65.2 rotor (Beckman) for 4.5 h at 60.000x g/20°C. The tube was carefully mounted in a clamp attached to a ring stand and long wave UV light visualized the upper chromosomal DNA band and the lower plasmid DNA band. A needle was used to make a small hole in the top of the tube to allow air to enter. After attaching tape to the outside of the tube, a needle attached to a syringe was inserted into the tube through the tape just below the lower DNA band. The plasmid DNA was then carefully withdrawn.

Removal of ethidium bromide from the DNA solution

An equal volume of water-CsCl-saturated isopropanol was added to the solution and vortexed. After separation of the two phases, the upper organic part containing the ethidium bromide was removed. The extraction was repeated three times until the pink color disappeared.

Removal of CsCl from the DNA solution

Three volumes of ddH_2O were added to the DNA solution and mixed. To precipitate the DNA, two volumes of ethanol were added and incubated on ice for 30 min. After centrifugation at 20.000x g for 15 min/4°C and two wash steps with 70% ethanol, the DNA was dissolved in 100 µl ddH_2O.

5.1.26 Sequencing of plasmids and cosmids

In general, 2-4 µg DNA (PCR kit purified DNA from a Mini prep) was sent together with the appropriate primers in the required concentration to different companies for sequencing (Medigenomix; MWG). For the sequencing of the cosmids, an agar plate with bacterial colonies was sent together with the appropriate primers to MWG.

5.1.27 PCR (Polymerase chain reaction)

The template DNA was amplified by PCR using Taq- (Roche or Quiagen), Pfu- (Roche) or High Fidelity Taq/Pwo-Polymerase (Roche) as appropriate. Specific sense and antisense oligonucleotide primers flanking the desired target sequence were used.

A typical PCR reaction was prepared as follows:

0.1-100 ng	DNA
5 µl	10x appropriate reaction buffer
5 µl	10nM dNTP-mix (dATP, dTTP, dGTP, dCTP; Peqlab)
5 µl	sense primer (0.1 µg/µl)
5 µl	antisense primer (0.1 µg/µl)
1 U	Polymerase
add 50 µl	ddH_2O

For PCR reactions with genomic DNA as a template, 100 ng DNA and the Expand High Fidelity Polymerase System (Roche) were utilized.

The following PCR parameters were adjusted to the appropriate conditions, depending on the primer, the size of the fragment to be amplified and the desired amount of DNA.

5 min	94°C	
30-45 sec	94°C	
30-45 sec	55-62°C	25-35 cycles
30-240 sec	72°C	
7 min	42°C	

5.1.28 Colony PCR

Colony PCR after cloning procedures allows fast and efficient screening of a large number of transformed *E. coli* colonies for positive clones. PCR reactions using primers within the cloned fragment and the appropriate flanking site of the vector were prepared. Single colonies were picked with a sterile toothpick and dipped in the PCR reaction. The toothpick was used to inoculate in parallel small-scale liquid cultures. These cultures were grown overnight in LB-medium containing the appropriate selection antibiotic for isolation of plasmid DNA. The PCR reaction was boiled at 95°C for 5 min prior to the PCR in order to lyse the cells and release plasmid DNA. PCR products were analyzed on an agarose gel, only positive clones show PCR products.

5.1.29 Isolation of genomic DNA (Quick Fly Genomic DNA Prep)

Buffer A: 100 mM Tris-HCl pH 7.5
100 mM EDTA
100 mM NaCl
0.5% SDS

Lithium chloride (LiCl)/potassium acetate (KaAc):
mix 1 part 5 M KAc with 2.5 parts 6 M LiCl just before use

In a standard procedure, 30 flies were anesthetized, collected, and frozen at -80°C. The flies were homogenized with a micropestle (Eppendorf) in 100 µl Buffer A. An additional 100 µl Buffer A was added and grinding continued. After addition of another 200 µl Buffer A, grinding was continued until only cuticles remained. The homogenate was incubated at 65°C for 30 min. 800 µl of freshly prepared LiCl/KAc solution was added, mixed, and left on ice for at least 10 min. After centrifugation at RT/13.000 rpm for 15 min, 1 ml of the supernatant was transferred into a new tube, avoiding floating crud. Following another centrifugation and supernatant transfer step, DNA was precipitated by addition of 600 µl isopropanol, centrifuged at RT/13.000 rpm for 15 min, washed twice with 70% ethanol, and speed vacuum dried for 2-3 min. To prevent any sharing of the DNA, 150 µl ddH_2O was added and the solution was left overnight at 4°C to dissolve. On the following day, the DNA was resuspended by carefully pipetting up and down and incubated at 65°C for 15 min. The DNA was then stored at –20°C.
If more or less flies (min. 5 flies) were used, all volumes were adjusted according to the number of flies.

5.1.30 Plasmid rescue

In order to identify the integration site of an EP-element jumped randomly in the genome of a particular fly line, a “plasmid rescue” had to be performed. This method takes advantage of the fact that the vector backbone of an EP-element contains a Kanamycin resistance gene

and an origin of replication. This allows, after digestion with enzymes cutting within the EP-element and somewhere close in the adjacent genomic region, recircularisation and transformation into bacteria. After isolation of the DNA containing the genomic region, the integration site can then be identified through sequencing using EP-element specific primers. A control digest and ligation reaction have to be included as the procedure is very sensitive to contaminations.

Genomic DNA preparation and digestion

In a first step, genomic DNA had to be isolated according to the Quick Fly Genomic DNA Prep. Genomic DNA corresponding to 5 flies (25 µl) was digested either with 40 U of EcoRI or SacII for 4 h at 37°C as follows:

25 µl	genomic DNA
4 µl	10x restriction buffer
5 µl	RNAse A (100 µg/ml)
1 µl	EcoRI / SacII

To inactivate the enzyme, the reaction was incubated for 15 min at 70°C. In a phenol-chloroform extraction step, 360 µl ddH_2O was added to the digest together with 100 µl TE-saturated phenol, vigorously vortexed for 1 min, and centrifuged for 5 min at RT/13.000 rpm. The upper aqueous DNA containing phase was carefully transferred into a new tube, 200 µl chlorofrom was added, vortexed and centrifuged. The procedure was repeated once, and the DNA was precipitated following addition of 40 µl 3.5 M sodium acetate and 1 ml ethanol (-20°C) and incubation at -20°C for at least 1 h as described. The digested genomic DNA was carefully resuspended in 40 µl ddH_2O and incubated at 65°C for 15 min.

Ligation, transformation, and plasmid preparation

A ligation reaction was set up in a large volume to facilitate the recircularisation:

40 µl	digested genomic DNA
40 µl	10x ligation buffer
add 400 µl	ddH_2O, mix well
add 500 U	T4-DNA-Ligase (400U/µl), mix

The ligation reaction was incubated overnight at RT. The following day, the DNA was precipitated as described and resuspended in 10 µl ddH_2O. After incubation at 65°C for 2 min and a brief spin, 2 µl DNA was transformed into 100 µl electro-competent *E. coli* XL1-Blue as described. The transformed bacteria were plated on LB-Kanamycin plates and incubated overnight at 37°C. From grown colonies, liquid cultures were inoculated and the DNA was isolated performing Mini Prep. After analysis with an EcoRI/XhoI digest, the DNA was sent directly for sequencing.

5.1.31 Single Fly PCR

Gloor and Engels' extraction buffer:	10 mM Tris pH 8.2
	1 mM EDTA
	25 mM NaCl
	200 µg/ml proteinase K (20 mg/ml stock)

Two single male flies per fly line were separately analysed. Single flies were squashed in 50 µl Gloor and Engels' extraction buffer in a 0.5 ml PCR tube using a pipette tip. The homogenate was incubated in a thermocycler at 37°C for 30 min, then at 95°C for 2 min, and stored at 4°C. Typically, 1 µl of the extract was add to a 25 µl PCR reaction using standard conditions for 28-30 cycles, as appropriate for the primers.

5.1.32 Southern Blot

Probe synthesis and test hybridization

For probe production, the PCR DIG probe synthesis kit was used according to the manufacturer's protocol (Roche). The DIG-labeled probe was purified using the PCR purification kit (Qiagen) and eluted in 50 µl ddH_2O. After analysing the efficiency of the PCR by electrophoresis, the DIG incorporation into the probe and its detection efficiency was tested in an direct detection test hybridization. Therefore, 1 µl of different dilutions of the probe, starting from 1:50 up to 1:100.000, were spotted on a positively charged nylon membrane (Roche), UV-crosslinked at 1200 µjoules with the UV Stratalinker (Stratagene) on the upper and lower nylon membrane site, and detection was performed as described in the following.

In general, 25 µl of denatured DIG-labeled probe was added to the hybridization solution. The hybridization solutions can be reused, but have to be incubated for 10 min at 95°C before the next hybridization.

Preparation of DNA, restriction digestion and gel electrophoresis

Genomic DNA was isolated from flies as described. 20 or 30 µl DNA was used which corresponds to 8 and 12 flies, respectively. The DNA was digested with either EcoRI, XhoI, SacI or BamHI for 4 h at 37°C in 50 µl reactions. The DNA was ethanol-precipitated for at least 1 h at -20°C as described, with 1 µl glycogen added to facilitate this process, and dissolved in 20 µl ddH_2O. The DNA samples supplemented with loading buffer were loaded on a 1% agarose gel and run overnight at 30-40 V at 4°C.

Denaturation, neutralization and transfer

Solutions:	Denaturation buffer	0.5 M NaOH
		1.5 M NaCl
	Neutralization buffer	0.5 M Tris-HCl pH 7.5
		3 M NaCl

	20x SSC	3 M NaCl 300 mM sodium citrat pH 7.0

To prepare the separated DNA in the agarose gel for the transfer to a nylon membrane, the gel was submerged in 0.2 M HCl for 10 min at RT on a shaker and rinsed with ddH_2O prior to the incubation for 2x 15 min in denaturation buffer. After a rinse step with ddH_2O, the gel was incubated for 2x 15 min in neutralization buffer, followed by an additional rinse step and a 10 min incubation in 20x SSC buffer. For the capillary transfer to the membrane, the gel was put upside down on Whatman paper hanging in 20x SSC buffer with its left and right end. The positively charged nylon membrane (Roche) was moistened with 20x SSC buffer and put on the upper side of the gel. Three layers of Whatman paper (Schleicher&Schuell) and approx. 10 cm apura paper were put on top of it and fixed with a weighted glass plate. Transfer was done overnight. The following day, the membrane was washed for 5 min in ddH_2O prior to DNA crosslinking with UV light. Crosslinking of the wet membrane was first performed on the upper nylon membrane site, then on the lower one at 1200 µjoules. The blot was either used directly for hybridization or sealed in a hybridization bag and stored at 4°C.

Hybridization

Solutions:	Maleic acid buffer	0.1 M Maleic acid 0.15 M NaCl adjust to pH 7.5 with NaOH platelets
	Wash buffer 1	1x SSC buffer 0.1% SDS
	Wash buffer 2	0.1x SSC buffer 0.1% SDS

The DIG Easy Hybridization solution (Roche) was prepared according to the manufacturer's protocol and prewarmed to 40°C. The nylon membrane was prehybridized by blocking with the solution for 30 min at 40°C. The DNA DIG-labeled probe was denatured by boiling at 95°C for 5 min and immediately put on ice to prevent renaturing. After addition of the probe (in general 25 µl) to 8 ml DIG Easy Hybridization solution, the blot was hybridized overnight at 40°C with gentle agitation. The membrane was first washed twice for 5 min in a large amount of wash buffer 1 at RT and then twice for 15 min in wash buffer 2 at 68°C, both under constant agitation.

Detection

Solutions:	Washing buffer	0.1 M maleic acid 0.15 M NaCl 0.3% (v/v) Tween20 adjust to pH 7.5

Detection buffer	0.1 M Tris-HCl pH 9.5
	0.1 M NaCl
	50 mM magnesium chloride

After transferring the gel into a flat container, it was rinsed for 2-5 min in washing buffer and incubated for 30 min in 100 ml freshly prepared blocking solution according to the manufacturer (Roche). The *anti*-DIG-AP-conjugate was diluted to 75 mU/ml (1:10.000) in 20 ml blocking solution. Antibody incubation was done for 30 min, the membrane was washed twice for 15 min in 100 ml washing buffer and equilibrated with 20 ml detection buffer for 2-5 min. For detection, the membrane was transferred into a hybridization bag, 1 ml CSPD (Roche) was added and left for 5 min. To activate the CSPD, the membrane was incubated after sealing the hybridization bag for 10 min at 37°C. The membrane was then exposed to a film (Roche) for 15 – 30 min.

Stripping and reprobing of Southern Blots

Stripping buffer	0.2 M NaOH
	0.1% SDS

To remove the DIG-labeled probes, the membrane was rinsed briefly in ddH_2O and washed with stripping buffer for 2x 15 min at 37°C. After rinsing thoroughly with 2x SSC buffer, the membrane was prehybridized and then hybridized with a new probe as described.

5.1.33 Isolation of total RNA from fly heads

In order to isolate the total RNA from flies, the S.N.A.P.^{TM} Total RNA Isolation Kit from Invitrogen was applied. Flies were frozen in liquid nitrogen and approx. 40-100 fly heads were collected corresponding to 5-12 mg tissue. The heads were transferred to a sterile tube and homogenized with a micropestle in 600 µl lysis buffer (Invitrogen). All following steps of the total RNA isolation and the DNA removal were performed according to the manufacturer's protocol. The total RNA was eluted in 125 µl RNase-free water.

5.1.34 Reverse Transcription

The cDNA Cycle Kit from Invitrogen was used to generate cDNA from isolated total RNA. Essentially, all steps were performed as described in the manufacturer's manual, using 0.1-1 µg of total RNA and oligo(dT) primers for the reverse transcription reaction. After a subsequent phenol-chloroform extraction, the cDNA was either shock frozen in liquid nitrogen and stored at -80°C or used directly for a PCR reaction.
To amplify the p45 zwim isoform, 50-200 ng cDNA was used in the PCR reaction with the Eco02/Not01 primer pair.

5.1.35 Northern Blot

Preparation of mRNA and gel electrophoresis

Using the mRNAeasy kit from Qiagen, mRNA was isolated out of 150 µg total RNA from all developmental stages of *Drosophila* according to the manufacturer's protocol. The mRNA together with 1 µl glycogen was precipitated with ethanol, washed, and resolved in 5.4 µl ddH_2O. After addition of 5.6 µl freshly deionized glyoxal, 16 µl DMSO, and 3 µl 100 mM sodium phosphate buffer pH 7.0, the mixture was incubated for 1 h at 50°C. The samples supplemented with 4 µl loading buffer were loaded on a 1% agarose gel (1 g agarose in 100 ml 10 mM sodium phosphate buffer) and were run in sodium phosphate buffer for 3.5 h at 95 V at 4°C. During electrophoresis, a pump was used to circulate the buffer from the cathode to the anode.

Northern transfer

Following electrophoresis, the gel was washed 5x 3 min in DEPC-H_2O and incubated for 5 min in 20x SSC. For the capillary transfer of the mRNA to a nylon membrane, the gel was put upside down on Whatman paper hanging in 2x SSC buffer with its left and right end. The positively charged nylon membrane (Hybond NX; Amersham) was moistened with 2x SSC buffer and put on the upper side of the gel. The sides of the transfer apparatus were sealed with parafilm. Three layers of moistened Whatman paper and approx. 10 cm apura paper were put on top of it and fixed with a weighted glass plate. Transfer was done overnight.
The following day, the membrane was washed in 20x SSC buffer and UV-crosslinked (autocross; Stratalinker). The blot was then incubated for 30 min at 80°C.

Hybridization

Solutions:	Prehybridization buffer	5x Denhardt's
		5x SSC buffer
		0.5% SDS
		50% formamide
	Hybridization buffer	5x Denhardt's
		5x SSC buffer
		0.5% SDS
		50% formamide
		0.1 µg/µl hering sperm DNA (Roche)
	Wash buffer 1	2x SSC buffer
		0.1% SDS
	Wash buffer 2	0.1x SSC buffer
		0.1% SDS

The membrane was prehybridized for 2 h at 42°C. The *redi*prime™II kit (Amersham) was

used to mark the probe radioactively with ^{32}P according to the manual, using 25 ng DNA as a template. For the *zwim* probe, the full-length *zwim* / *p92* was labeled using the pGEM-*p92* plasmid. The tubulin probe was kindly obtained from A. Loewer, Heidelberg. Labeled probes were purified with Micro Bio-Spin P-30 Tris Chromatography Columns (BIO-RAD) according to the manufacturer's protocol. The probe was denatured by boiling at 95°C for 5 min and then incubated 5 min on ice, add to the hybridization buffer, and the blot was therein incubated overnight at 42°C with gentle agitation. The following day, the membrane was first washed twice for 10 min with wash buffer 1 at RT and then three times for 10 min each in pre-warmed wash buffer 2 at 65°C. After wrapping the membrane in a nylon, it was exposed to a film for 5-6 h up to overnight at –80°C.

Stripping and reprobing of Northern blots

To remove the radioactive-labeled probes, the membrane was rinsed briefly in ddH_2O and washed with boiling 0.1% SSC buffer for 3x 5 min at 80°C. After rinsing thoroughly with 2x SSC buffer, the membrane was prehybridized and hybridized with a new probe as described.

5.2 Biochemical protein methods

5.2.1 Discontinuous SDS-polyacrylamide gel electrophoresis (SDS-PAGE)

Buffers:	5x Tris glycin SDS buffer	15.1 g Tris-base 72 g glycine 5 g SDS add ddH_2O to 1 l
	2x SDS sample buffer	0.125 M Tris-HCl pH 6.8 20% (w/v) glycerin 4% SDS 10% β-mercaptoethanol 0.01% Bromophenol-blue

Tris-Tricine gels were prepared according to (Laemmli 1970). Generally, 12% gels were used and poured into SDS-PAGE gel chambers from Hoefer. Electrophoresis was started at 150 V until the samples reached the separating gel and continued for 1-2 h at 200-250 V. Protein samples were supplemented with an equal volume of 2x SDS sample buffer and boiled for 5 min at 95°C, followed by a 3 min spin at full speed and loading on the gel.

5.2.2 Bis-Tris-HCl polyacrylamide gel electrophoresis

20x SDS running buffer	1 M Mes (2-(N-morpholino) ethansufonic acid) 1 M Tris-base 0.1% SDS

0.0205 mM EDTA

Separation of proteins by electrophoresis was also carried out using precast 4-12% Bis-Tris gels (Invitrogen) following their protocol.

5.2.3 Coomassie staining of proteins

Coomassie staining solution: 0.1% (w/v) Coomassie Brilliant Blue R-250
45% (v/v) methanol
10% (v/v) acetic acid

Destaining solution: 45% (v/v) methanol
10% (v/v) acetic acid

Following SDS-PAGE, the gel was incubated with Coomassie staining solution on a horizontal shaker for 30-60 min. Afterwards the gel was washed several times with destaining solution, until the nonspecific Coomassie background has been removed. The gel was rehydrated in 4% glycerol for 1-2 h and then dried on Whatman paper in a vacuum gel dryer for 1.5 h at 70 °C.

5.2.4 Western blotting (wet blot)

Transfer

Transfer buffer: 192 mM glycine
25 mM Tris-base
10% methanol (or 20% if two gels were blotted in parallel)

Proteins separated by SDS-PAGE were transferred from the gel to a Hybond nitrocellulose membrane (Amersham) using electrophoresis. After SDS-PAGE, the gel was equilibrated in transfer buffer for 2 min and all other components were soaked in transfer buffer. The gel and the membrane were sandwiched between perforated plastic plates as follows:

Anode (+)
sponge pad
3 Whatman sheets
nitrocellulose membrane
SDS gel
3 Whatman sheets
sponge pad

Cathode (-)

The transfer was performed in a blotting tank (Biorad) for 1.5-2 h at 200 mA at 4°C.

Ponceau S staining

Ponceau S solution: 0.2% (w/v) Ponceau S red

3% (w/v) sulfonic acid
0.1% (v/v) glacial acid

Proteins immobilized on a membrane can be reversibly stained with the Ponceau S dye to evaluate the efficiency of protein transfer after western blotting. The nitrocellulose membrane was stained in Ponceau S solution for less than 1 min. The membrane staining could be completely removed by incubation in PBS.

Detection

10x PBS (Phosphate buffered saline):	10 mM Na_2HPO_4
	2 mM KH_2PO_4
	137 mM NaCl
	2.7 mM KCl
	adjusted to pH 7.4 (hydrochloric acid)
PBST (Phosphate buffered saline Tween20):	PBS
	0.05% Tween20

After western blot transfer of the proteins to the nitrocellulose membrane, the membrane was blocked for 1 h in PBST/5% (w/v) skimmed milk. The primary antibody was diluted in PBST to the appropriate concentration and the blot was incubated either for 2-4 h at RT or overnight at 4 °C. The membrane was then washed three times with PBST for 10 min. Incubation of the blot with the secondary antibody conjugated to horseradish peroxidase (HRP) was carried out for 1-2 h at RT. The membrane was washed again for 3x 10 min with PBST prior to detection. For this purpose, the membrane was incubated with the ECL (Amersham) reagent for 1 min and the chemiluminiscent signal was visualized by exposure of Hyperfilm ECL (Amersham) films. In the case of very weak signals, the blot was washed in PBST and incubated for 1 min with SuperSignal West Femto Maximum Sensitivity Substrate (Pierce) before exposure was repeated.

Reprobing of western blot membranes

Stripping buffer:	62.5 mM Tris-HCl pH 6.7
	100 mM β-mercaptoethanol

Prior to reprobing the membrane with different antibodies, the previous antibodies had to be removed. Therefore, the membrane was incubated in preheated stripping buffer on a horizontal shaker for 30 min at 65°C and extensively washed several times with PBST. The blot was again blocked for 1 h in PBST/5% (w/v) skimmed milk and a new primary antibody could be applied as described.

5.2.5 Coupled in vitro transcription and translation

The T_NT Coupled Reticulocyte Lysate System (Promega) was used for direct *in vitro* translation of proteins. 1 µg of a plasmid encoding the desired protein under control of an

Sp6, T3 or T7 promotor was added to the provided reticulocyte lysate and buffers, which was further supplemented with the appropriate Polymerase according to the manufacturer's protocol. The reaction was incubated for 90 min at 30 °C. The sample was either used immediately for analysis or stored at -80 °C.

5.2.6 Autoradiography of gels with radioactive samples

Fixation solution: 30% (v/v) methanol
60% (v/v) ddH_2O
10% (v/v) acetic acid

After gel electrophoresis, the proteins were immobilized by incubating the gel in fixation buffer on a horizontal shaker for 30 min. Two sheets of Whatman paper were soaked with ddH_2O and the gel was put on top of the Whatman papers and covered with clear film. The gel was dried on a vacuum gel dryer for 1-1.5 h at 70 °C and later exposed to ^{35}S-Methionine sensitive MR-films (Kodak).

5.2.7 Recombinant expression and purification of GST fusion proteins

Elution buffer: 75 mM Hepes pH 7.0
150 mM NaCl
5 mM DTT
20 mM glutathione
adjust to pH 7.8

Expression of GST fusion proteins

For recombinant expression of GST fusion proteins, pGEX-4T-2 vectors and BL21 or BL21 (DE3) bacteria were used. The plasmids with the different GST fusions were transformed into electro-competent BL21 cells. Prior to large-scale protein expression, the different clones were tested in small volumes for expression of proteins and whether the recombinant protein is soluble by applying different conditions (temperature, IPTG concentration, various lysis methods like French press, lysozyme treatment and sonification). For large-scale expression, a single colony was inoculated into 150 ml LB-medium supplemented with Ampicillin and grown at 37 °C overnight with vigorous shaking. The following day, 12.5 ml of the cell culture was added to 1 l LB medium supplemented with Ampicillin and grown at RT for approx. 2-2.5 h under vigorous shaking, until an OD_{600nm} of ~1 was reached. The GST control protein was grown at 37°C for 1 h. Expression of the fusion proteins was then induced by adding 1 M IPTG to a final concentration of 100 µM. After 3-4 h of expression at RT (for the GST control 3 h incubation at 37°C), cells were harvested by centrifugation at 5.500 rpm/4°C for 12 min (JA-10 rotor, Beckman J2-MC centrifuge) and resuspended in 30 ml PBS on ice. Lysozyme was added to a final concentration of 2 mg/ml and incubated for 30 min at 30°C. Triton X-100 was supplemented to a final concentration of 0.5%, cells were incubated for

10 min on ice, and then disrupted by sonification (Branson sonifier tip) with 2-3 x 30 sec bursts at 50% of the maximum output. The cell lysate was centrifuged at 18.000 rpm for 20 min (JA-20 rotor). The supernatant and the pellet of the various bacterial lysates were analysed for their protein content by SDS-PAGE and Coomassie staining.

Purification of GST fusion proteins

For the purification of the GST fusion proteins, each of the recovered supernatants was incubated in a column with 7 ml (50% slurry) of hydrated Glutathione Sepharose™ 4 Fast Flow (Amersham, prepared according to manufacturer's protocol) for 20-30 min at RT. The sepharose with bound GST fusion proteins was sedimented and washed twice with PBS containing 1% Triton X-100 (PBST), followed by two washes with PBS. The GST fusion proteins bound to the sepharose beads were eluted in 2 ml fractions in three elution steps using 4 ml elution buffer (incubation in the first step for 15 min at RT, the next two incubations for 5 min each at RT). To verify the loading of GST fusion protein, 10 µl of the sepharose bead suspension were denatured in SDS sample buffer for 10 min at 95 °C and analysed by SDS-PAGE and Coomassie staining. Additionally, 10 µl of the eluted GST fusion protein fractions were also checked by SDS-PAGE for protein amount and purity. Fractions of interest were pooled, dialysed overnight in PBS at 4°C and lyophilised. Protein aliquots were stored at –20°C. The tubes for dialysis were prepared by boiling them for 10 min in 2% sodium bicarbonate, 2 mM EDTA pH 8.0, rinsing them thoroughly in ddH_2O, and then storing them in 20% ethanol at 4°C.

For reuse, the sepharose beads were washed with PBST and elution buffer, left in a 50% slurry in PBS supplemented with 0.02% NaN_3, and stored at 4 °C.

5.2.8 Immunization of rabbits

Antibodies were produced according to Lane 1982. Prior to antigen injection, 10 ml of pre-immune serum of the two rabbits MX 26 and MX 27 were obtained and stored at –80°C. The two different GST protein fragments of DFer were pooled in 400 µl to a total concentration of 500 µg, supplemented with the same volume of complete Freund's Adjuvant (Sigma) and vortexed vigorously for 5-10 min. The viscous solutions was loaded in a 1 ml syringe (Omnifix-F, Braun) and injected into the rabbits. The rabbits were boosted with the same amount of antigen supplemented with incomplete Freund's Adjuvant every 3 to 4 weeks. Seven days after injection, 5 ml blood was retrieved to test the produced antibodies. The blood was left for 3-4 h at RT, the clotted fraction was detached with a glass needle, and the blood was incubated overnight at 4°C. The following day, the serum was recovered, tested in a western blot or an immunoprecipitation with the pre-immune serum as a control, and stored at –80°C. Ten days after the sixth and last boost, the whole blood was recovered from both rabbits, retrieved, and stored at –80°C.

5.2.9 Antigen-coupling to sepharose

Coupling buffer: 0.1 M $NaHCO_3$
0.5 M NaCl
adjust to pH 8.3

The proteins, which were used as antigens, were dialysed in coupling buffer for 6 h or overnight at 4°C. The antigen was coupled to CnBr-activated Sepharose 4 Fast Flow (Roche). For each protein fragment and each rabbit serum, one antigen column was prepared, leaving a total of six columns (2x GST, 2x zwim-N, 2x zwim-Extra). 500 mg of the sepharose beads was resuspended in 5 ml 1 mM HCl and incubated for 30 min on a rotating shaker to allow swelling. Beads were first washed with 15 gel volumes ice-cold 1 mM HCl, then twice for 15 min with coupling buffer before protein was added to the beads and left coupling overnight at 4°C on a rotating shaker. The following day, the protein solution was recovered; the beads were washed and incubated for 3-4 h at RT with 1 M ethanolamine on a rotating shaker to block reactive sites. Afterwards, beads were first washed with PBS, then three times with 50 mM Tris, 1 M NaCl pH 8.0, followed by one wash with 100 mM glycine pH 2.8, and finally washed several times with PBS. The antigen-coupled beads were stored in 20% ethanol at 4°C. The coupling efficiency was analysed by comparing the amount of protein input to the amount of protein coupled to the sepharose using SDS-PAGE and Coomassie staining.

5.2.10 Purification of polyclonal antibodies by antigen-antibody affinity chromatography

Protein A-agarose chromatography

The serum from each rabbit was first purified separately with Protein A-agarose (Roche). 2 ml gel (50% slurry) were used per column and preequilibrated with 5 volumes of PBS. To prepare the serum for the purification, 10 ml serum was mixed 1:1 with PBS and centrifuged for 10 min at 5.000rpm/4°C. After addition of 1 M Tris pH 8.0 to obtain a neutral pH of 7.5-7.8, the supernatant was subsequently passed over the column and recovered as a flow-through. The agarose beads were washed twice with PBS and the IgGs were eluted with 12-15 ml 100 mM glycine pH 2.8 in 1 ml fractions. All fractions with an OD_{280nm} of ~0.1 were pooled and the pH was neutralised with 1 M Tris pH 8.0. The Protein-A agarose columns were washed several times with 100 mM glycine pH 2.8 and with PBS until a neutral pH was reached. The flow-through was passed on the column and the whole procedure was repeated. When purification was completed, the agarose beads were washed and reequilibrated, left in a 50% slurry in PBS supplemented with 0.02% NaN_3, and stored at 4 °C. The successful purification of IgGs was checked by SDS-PAGE and Coomassie stainings.

Antigen-antibody affinity chromatography

In a second step, an antibody-antigen affinity chromatography was applied with the prepared antigen columns containing GST, DFer-N or DFer-SK as antigens. The purified IgGs of each rabbit were passed over separate columns, starting with the GST antigen column. For each column, the IgGs were passed over twice. After the passage through the GST column, the flow-through was subsequently added to the DFer-N column and recovered, and finally passed over the DFer-Extra column. All columns were washed 2x 3 ml PBS and 3x 10 ml PBS before the antibodies were eluted with 12-15 ml 100 mM glycine pH 2.8 in 1 ml fractions. All fractions with an OD_{280nm} over ~0.02 were pooled and the pH was neutralized with 1 M Tris pH 8.0. Based on the calculation OD_{280nm}=1 equals 0.8 mg/ml, the antibodies were aliquoted in 100 µg fractions, then lyophilized and stored at –20°C. Lyophilized antibodies were redissolved in PBS in a 1 µg/µl concentration supplemented with 0.02% NaN_3 and stored at 4°C for usage. The antigen columns were washed with 100 mM glycine pH 2.8 and reequilibrated in PBS. They were left in a 50% slurry in PBS supplemented with 0.02% NaN_3, and stored at 4 °C.

5.2.11 Immunoprecipitation of *in vitro* translated protein

Washing buffer: PBS
0.5% NP40

Proteins from *in vitro* translation reactions were precipitated with appropriate antibodies and Protein A sepharose (50% slurry; Amersham). Antibodies or 15 µl of serum were preincubated with 30 µl of prepared Protein A sepharose in 50 µl washing buffer on an overhead shaker for 30 min at RT. The sepharose beads were sedimented at 15.000x g for 30 s, and the supernatant was discarded. After washing with washing buffer, 1 ml washing buffer was add together with 20 µl of the *in vitro* translated protein and the samples were incubated on a rotating shaker overnight at 4 °C. The sepharose beads were centrifuged at 15.000x g for 30 s and washed three times with washing buffer. The buffer was completely removed and the sepharose beads were denatured in 2x SDS sample buffer for 7 min at 95 °C for subsequent analyses by SDS-PAGE and Western blotting.

5.2.12 Co- / Immunoprecipitation of cell lysates

Cell lysates were washed with ice-cold PBS and centrifuged at 800x g for 3 min. The cell pellet was lysed by pipetting up and down ten times with 250 µl PBS/1% NP40/Complete Proteinase Inhibitor (Roche) and incubated for 30 min on ice. The aliquots were cleared from cell debris and nuclei by centrifugation at 13.000x g for 15 min. Cell lysates were filled up to a total of 1 ml with PBS/1% NP40/Complete Proteinase Inhibitor and were preincubated for 1 h at 4 °C with 30 µl of prepared Protein A sepharose (50% slurry) to reduce unspecific binding. Antibodies were prebound to 30 µl of prepared Protein A sepharose in 1 ml PBS by incubating on a rotating shaker for 10-20 min at RT. The sepharose beads were sedimented

at 15.000x g for 30 s, and the cell lysate supernatant was transferred to the prebound antibody beads. The samples were incubated overnight at 4 °C on a rotating shaker. The sepharose beads were centrifuged at 15.000x g for 30 s and washed three times with ice-cold PBS/1% NP40. The buffer was completely removed and the sepharose beads were denatured in 80 µl 2x SDS sample buffer for 7 min at 95 °C for subsequent analyses by SDS-PAGE and Western blotting.

5.3 *Drosophila* handling and genetic methods

5.3.1 *Drosophila* handling

Standard fly food:
- 10 l H_2O
- 80 g Agar-agar
- 180 g dry yeast
- 100 g soy-flour
- 220 g beet syrup
- 800 g cornmeal
- 24 g nipagin (methyl-4-hydroxybenzoate, Merck)
- 62.5 ml propionic acid (Sigma)

Fly stocks were raised on standard fly food and crossed at 25°C with 60-70% relative humidity, except when stated otherwise. Fly stocks were maintained at 18°C with 60-70% relative humidity.

5.3.2 P-element mediated germ line transformation

Injection buffer:
- 5 mM KCl
- 0.1 mM NaH_2PO_4, pH 6.8

Bleach solution:
- 4% (v/v) HOCl (Roth) in ddH_2O

Acetic acid agar plates:
- 500 ml ddH_2O
- 12 g Bacto-agar
- 2-3 ml acetic acid

Transgenic flies carrying the gene of interest were generated by P-element mediated germ line transformation (Rubin et al. 1982; Spradling et al. 1982). Adult w^{1118} flies were allowed to lay eggs on acetic acid agar plates for 20-30 min at 25 °C. The embryos were recovered, dechorionized with bleach solution for 2 min and extensively washed with water. About 80-120 embryos were lined on an agar stripe and transferred onto a double-sided sticky tape (3M, Scotch) mounted on a coverslip. The embryos were dehydrated in a closed chamber containing Silica gel for 7 min and covered with Voltalef 10S oil (Lehmann & Voss & Co.). The appropriate pUASt constructs (9 µg) and the helper DNA pUChsΔ2-3 (3 µg) were

ethanol co-precipitated and dissolved in 30 µl injection buffer. Prior to the injection into the treated w^{1118} embryos, the DNA mixture was centrifuged for 5 min at 13.000 rpm/4°C and the supernatant was loaded in a Femtotip needle (Eppendorf). Microinjection was performed at 18°C with the Femtotip needle using an Eppendorf FemtoJet Microinjector at 200-500 hPa injection pressure. In general, about 300-400 embryos were injected per construct and kept in a humid chamber at 18°C until larvae hatched. Larvae were transferred onto standard fly food and kept at 25°C until the founder G_0-Generation hatched.

5.3.3 Injection of cosmids for P-element mediated germ line transformation

To generate the genomic rescue transgenic flies by P-element mediated germ line transformation, large cosmids had to be injected. The cosmid DNA had to be in a concentration of 1 µg/µl and the helper DNA pUChsΔ2-3 of 0.25 µg/µl (Feng et al. 1995). The DNAs were ethanol co-precipitated for 30 min at RT and dissolved carefully in 30 µl injection buffer by a 1 h incubation at 55°C. Prior to the injection into the treated w^{1118} embryos, the DNA mixture was centrifuged for 5 min at 13.000 rpm/4°C and the supernatant was used for injection. As the concentration of the cosmid DNA is quite high and the solution very viscous, and to prevent sharing of the large DNA fragment, a large needle opening was used, increasing the death rate of injected embryos dramatically. Therefore, with an expected rate of approximately 1 transgenic fly out of 1000 injected embryos, 2.500-6.900 embryos per construct had to be injected.

5.3.4 Establishment of transgenic *Drosophila* lines and mapping of the integration site

The hatched founder G_0-Generation flies were crossed to w^{1118}; *BcGla/Cyo* virgins or males and progenies were then screened for the transformation marker *white*, i.e. pigmented eyes. Transformed flies were backcrossed to w^{1118}; *BcGla/Cyo* flies twice and stable homozygous lines were established. The crossings to the to w^{1118}; *BcGla/Cyo* line also allowed the mapping of the chromosomal integration site of the transgene, dependent on the distribution of the transgene and the markers on the progenies. At least 6 independently transformed fly lines per construct (two on each chromosome) were kept as stocks.

5.3.5 Collection of embryos

Acetic acid agar plates:
- 18 g Agar-agar
- 10 g saccharose
- 3.5 ml acidic acid
- add 1 l ddH_2O

To collect embryos, flies were kept in small plastic cages with a mesh on the top and acetic acid agar plates on the bottom at 25°C. Freshly prepared yeast was pasted on the plates to stimulate egg deposition. After the desired time of collection, the plates were replaced with

new ones. The embryos on the agar plate were flooded with water and transferred to sieves using a brush, where washing with water was continued. Embryos were subsequently used for various applications.

5.3.6 Determination of embryonic lethality

Flies with the required mutant genotype where kept in cages and embryos were collected for 6-8 h at 25°C on acidic agar plates. Embryos were left for 2 days at 25°C to allow hatching of the healthy heterozygous larvae. Mutant dead embryos were counted versus the total number of laid embryos.

5.4 *Drosophila* dissections and histological methods

5.4.1 Preparation of fly head extract for western blot analysis

Hatched flies were collected in an Eppendorf tube and frozen in liquid nitrogen. Fly heads were separated from the cell body by flipping the tube several times, and heads were transferred into a new tube. In general, ten fly heads per sample were homogenized in 30 µl 2x SDS sample buffer with a micropestle. 1 µl benzonase (25 U/µl) was added and grinding continued until only cuticles remain. The samples were denatured for 7 min at 95°C.

5.4.2 Alkaline Phophatase treatment of fly head extract

For the Alkaline Phophatase (AP) treatment, the collected fly heads were squashed in 15 µl solution containing 1.5 U AP in AP buffer. The preparation was incubated 1 h at 37°C, 1 µl benzonase and 15 µl 2x SDS sample buffer were added, and the procedure was continued as described.

5.4.3 Preparation of wing imaginal discs for western blot analysis

Crawling third instar larvae were dissected in PBS as described in the following section, and isolated wing discs were kept in PBS on ice. In general, 10 larvae (20 wing discs) per sample were homogenized in 30 µl 2x SDS sample buffer with a micropestle. 1 µl benzonase (25 U/µl) was added and grinding continued. The samples were denatured for 7 min at 95°C.

5.4.4 Cuticle preparation

Crude cuticle preparation

Flies with the required genotype where kept in cages and embryos were collected for 8-12 h at 25°C. In the case of analysing mutant homozygous embryos, these were left for 2 days at 25°C to allow hatching of the healthy heterozygous larvae. Mutant embryos were handpicked, transferred onto a double-sided sticky tape, and dechorionized by slowly rolling them with a needle on the tape. Embryos were put on a drop of Hoyer's medium/lactic acid

(1:1), covered with a cover slip, and devitellinized by slightly applying pressure on the cover slip. The cuticle preparations were left overnight at 65°C for clearing. Cuticles were analysed under a stereo microscope using phase contrast optics.

Cuticle preparation
Embryos were collected for different time points and left for 24-48 h at 25°C. Washed embryos were dechorionized with 3% HOCl for 3 min and fixed by addition of 700 µl 4% PFA/PBS and 700 µl heptan for 10 min on a rotating shaker. Larvae that sedimented to the tip of the tube were removed with a glass pipette. 700 µl PBS was added, tubes were rotated for 2 min and the solution was replaced with 700 µl methanol (-20°C). The preparation was vigorously vortexed for 1 min, thereafter embryos sedimented at the tip. Embryos were washed once with methanol and once with ethanol before they were stored at –20°C. Rehydration was done in a decreasing ethanol series (70%, 50% and 30% ethanol in PBS; 5 min incubation each). Embryos were washed once in PBS, incubated 1 h at 60°C in a glycerin/acetic acid (1:1) solution and then transferred to a drop of Hoyer's medium prior to the overnight incubation at 65°C.

5.4.5 Pharate adult preparation

The pharate adults were collected in their pupal chamber, punctured with forceps in the pupal cuticle, and kept at least 24 h in 70% ethanol/30% glycerol for fixation. Pharate adults were dissected in PBS by peeling off the pupal cuticle that surrounds the animal using forceps and transferred to an Eppendorf tube. 10% KOH was added and the preparation was incubated 5-10 min at 100°C with the lid of the tube open under a glass top. KOH was discarded, ddH_2O added, and the expanded wings were mounted in 80% glycerol/PBS.

5.4.6 In situ hybridization of embryos

Solutions:	Fix solution	10% paraformaldehyde (PFA) (Sigma) in PBS
		50 mM EGTA adjust to pH 7
	HybeB solution	50% formamide
		5x SSC adjust to pH 5
	Hybe solution	50% formamide
		5x SSC
		5 µg/ml heparin (Fluka)
		100 µg/ml hering sperm DNA (Roche)
		0.1% Tween20 adjust to pH 5
	AP buffer	20 mM Tris-HCl, pH 9.5
		100 mM NaCl
		50mM $MgCl_2$

DIG-labeling of RNA probes

The work was done in RNAse-free conditions. The DNA templates were either in a pBS or a pCRII vector; thus *in vitro* transcription was performed using the appropriate T3, SP6 or T7 promoter. DNA was linearized by digestion with an appropriate enzyme and purified with the MiniElute PCR kit from Qiagen. Two labeling reactions were set up (sense and antisense) for each probe:

x µl	1 µg linearized template DNA
2 µl	10x DIG RNA labeling mix (Roche)
2 µl	10x transcription buffer (Roche)
1 µl	20 U RNAsin
1 µl	40 U T7-, T3- or Sp6-RNA-Polymerase
add sterile RNAse-free ddH_2O to a final volume of 20 µl	

In vitro transcription was performed for 4 h at 37°C. The DNA was subsequently digested by addition of 40 U DNAse to the reaction and 20 min incubation at 37°C. The reaction was stopped by addition of 2 µl 0.2 M EDTA pH 8. The labeled RNA was purified using the QIAquick PCR purification kit (Qiagen) and resuspended in 50 µl RNAse-free ddH_2O. The same volume of formamide was added and the RNA was stored at -80°C. Successful transcription was checked on a 1% agarose gel.

Fixation of embryos

Differently staged Oregon R or mutant embryos were collected. The embryos were dechorionized with 3% HOCL for 3 min and extensively washed with water. Embryos were transferred to glass tubes and fixed for 20 min with 1 ml Fix solution and 6 ml heptane on a rotating shaker. The vitelline membrane was removed by adding 10 ml methanol and vortexing for 1 min. The embryos were rinsed three times with methanol and could be stored in methanol at –20°C.

Rehydration, equilibration and in situ hybridization

Embryos were rehydrated by addition of 3:1 methanol/PBS, then 1:3 methanol/PBS, followed by a rinse with PBS containing 0.1% Tween20 (PBT). A second fixation step was performed with Fix solution for 20 min and the embryos were then rinsed three times and washed for 5 min with PBT. At this point, a tube with fixed embryos was removed for the preabsorption of antibodies and was stored at 4°C. Embryos were equilibrated with 500 µl HybeB solution/PBT (1:1), then with 250 µl HybeB solution and finally with 250 µl Hybe solution. Embryos were prehybridized with 250 µl Hybe solution for 1 h at 60°C in a waterbath. 3 µl of the DIG-labeled probe was added to 30 µl of Hybe solution and preheated at 60°C for 10 min. Hybe solution was removed from the tubes, 50 µl portions of embryos were distributed into new tubes, and the preheated solution containing the probe was added. Incubation was performed overnight at 60°C.

The following day, the *anti*-DIG-AP antibody was diluted 1:200 in PBT and incubated for

1-2 h with the prepared embryos for preabsorption. 500 µl of prewarmed Hybe solution was added to the embryos, which were then washed two times with 500 µl of prewarmed HybeB solution for 15 min at 60°C. Then, 500 µl PBT was added, the embryos were rinsed twice with PBT and washed for 5 min, 10 and 20 min in PBT.

Signal detection
Embryos were incubated with preabsorbed *anti*-Dig-AP antibody in a 1:10 PBT dilution for 90 min on a rotating shaker. After rinsing twice and three 15 min washes with PBT, embryos were equilibrated with AP buffer by rinsing once and washing for 5 min. The incubation in staining solution (1:50 dilution of NBT/BCIP (Roche) in AP buffer) was performed in a 24-well plate. The progression of the staining was observed under the microscope and stopped before background appeared. The embryos were then rinsed three times in PBT, washed three times for 5 min, and mounted in 80% glycerol/PBS.

5.4.7 Immunostaining of whole embryos

PFA fixation of embryos and immunostaining
Collected embryos were dechorionized for 3 min in 3% HOCl and washed in PBS. The embryos were transferred to Eppendorf tubes, 600 µl heptan and then 200 µl 4% PFA/PBS were added, and the embryos were incubated for 20 min on a rotating shaker at maximum speed. To devitellinize the embryos, 200 µl methanol were added and the preparation was vigorously vortexed for 1 min. Embryos were rinsed twice with methanol and stored at –20°C.
Embryos were rehydrated in a decreasing methanol series (66%, 33% methanol in PBS containing 0.1% Triton X-100), transferred to a siliconized tube, washed twice in PBS/0.1% Triton X-100, and blocked for 1 h at RT in PBS/0.1% Triton X-100/0.1% bovine serum albumin (BSA, Serva) on a rotating shaker. Incubation with the appropriately diluted primary antibodies was performed in a 100 µl volume of PBS/0.1% Triton X-100/0.1% BSA overnight at 4°C on a rotating shaker. The next day, embryos were rinsed three times and washed twice for 30 min each with PBS/0.1% Triton X-100/0.1% BSA, before they were incubated with the fluorescent secondary antibodies in PBS/0.1% Triton X-100/0.1% BSA/2% goat serum for 2 h at RT on a rotating shaker. Embryos were again rinsed three times and washed twice for 30 min each with PBS/0.1% Triton X-100/0.1% BSA, and mounted in Vectashield (Vector Laboratories, US). Immunostained embryos were analysed by confocal microscopy (Leica) and average projections of z-stacks were used to depict the embryo.

Heat fixation of embryos and immunostaining
Collected embryos were dechorionized for 3 min in 3% HOCl, washed in 150 mM NaCl, and transferred to 15 ml falcon tubes. Fixation was done through adding 5 ml of boiling 150 mM NaCl and immediate shaking for 10 sec, before embryos were cooled on ice and 10 ml ice-cold NaCl solution was added. After 15 min, the NaCl solution was replaced by a 1:1 heptan/methanol solution (-80°C) and embryos were devitellinized by vigorous vortexing for

1 min. Embryos were rinsed and 1 h incubated in methanol on ice. For storage at –20°C, methanol was replaced by ethanol.
Embryos were rehydrated in a decreasing ethanol series (70%, 50% and 30% ethanol in PBS containing 0.5% Triton X-100; 5 min incubation each). Remnants of Triton X-100 were removed by washing twice with PBS/0.1% Tween20. The preparation was blocked for 1 h at RT in PBS/0.1% Tween20/25% goat serum on a rotating shaker. Incubation with the appropriately diluted primary antibodies was performed in a 100 µl volume of blocking solution (PBS/0.1% Tween20/3% BSA/3% goat serum) overnight at 4°C on a rotating shaker. The next day, embryos were rinsed three times and washed three times for 10 min each with blocking solution, before they were incubated with the fluorescent secondary antibodies diluted in blocking solution for 3-4 h at RT on a rotating shaker. Embryos were again rinsed three times and washed three times for 10 min each with blocking solution, then rinsed with ethanol and mounted in Vectashield.

5.4.8 Dissection and immunostaining of imaginal discs and salivary glands

Dissection

Crawling third instar larvae were dissected in PBS. Using two forceps, the larvae were torn in two parts by holding at the mouth hook and pulling out from the middle of the body. For salivary gland preparations, glands were carefully removed leaving them hanging on the mouth hook and collected in PBS in an Eppendorf tube on ice, up to 1 h. For imaginal disc preparations, salivary glands and the fat tissue were carefully removed, and the imaginal discs stuck to the cuticle were collected.

Fixation

The discs and the cuticle were fixed in PBS/3%PFA for 30 min, and then rinsed twice and washed once for 5 min in PBS.

Immunostaining

After blocking three times in PBS/0.3% Triton X-100/5% BSA for 10 min, the preparations were incubated with the primary antibodies at the appropriate concentration in PBS/0.1% Triton X-100/ 1% BSA. Incubation was done in a humid chamber overnight at 4°C on a horizontal shaker. The following day, the discs were rinsed twice in PBS/0.1% Triton X-100 and incubated three times in PBS/0.1% Triton X-100/1% BSA for 15 min each. Afterwards, the preparation was incubated in PBS/0.1% Triton X-100/1% BSA/2% goat serum and the appropriate fluorescent secondary antibodies for 1 hour at RT on a rotating plate. Discs was rinsed once in PBS/0.1% Triton X-100, followed by three washes in PBS/0.1% Triton X-100 for 15 min each, and finally rinsed in PBS.

Final dissection

A drop of PBS was put on a slide, where the preparation was transferred to, and the imaginal

discs were separated from the cuticles and tracheae using needles. Imaginal discs were mounted in Vectashield on a cover slip. Immunostained imaginal wing discs were analysed by confocal microscopy.

5.4.9 Phalloidin staining

For phalloidin staining of tissue, the preparations were incubated after the immunostaining and washing procedure for 30 min in PBS/0.1% Triton X-100/1% BSA/2% goat serum containing appropriately diluted phalloidin. The discs were washed three times for 10 min with PBS prior to the final dissection.

5.4.10 DAPI staining

Following the immunostaining and washing procedure, the tissue was stained with DAPI (50 mg/ml stock in 180 mM Tris-HCl pH 7.5) diluted to 500 ng/µl in PBS for 5 min and then washed twice for 5 min with PBS prior to the dissection.

5.4.11 Histochemical detection of ß-galactosidase activity in imaginal discs

Staining solution: 10 mM sodium phosphate buffer pH 7.2
150 mM NaCl
1 mM $MgCl_2$
6 mM $K_4\{Fe^{II}(CN)_6\}$
6 mM $K_3\{Fe^{III}(CN)_6\}$
0.3% Triton X-100 mix solution, incubate for 5 min at 37°C

0.2% X-gal in DMSO (25 µl from a 8% w/v stock stored at –20°C)
incubate 5 min at 37°C in the dark
centrifuge 5 min at 13.000rpm
take supernatant for staining

Larvae were dissected and the imaginal discs were fixed for 15 min at RT in PBS/1% glutaraldehyde. After fixation, they were washed twice with PBS and the freshly prepared staining solution was added. Staining can be performed from 5 min to overnight at 37°C, dependent on the strength of the staining signal which is monitored under a stereomicroscope. After staining, discs were washed in PBS and mounted in PBS/70% glycerol.

5.5 Cell culture methods

5.5.1 Cultivation of COS-7 cells

Culture medium: Dulbecco's Modified Eagle's Medium (DMEM; Sigma)
1% Penicillin/Streptomycin
(10.000 U Penicillin, 10 mg Streptomycin/ml in 0.9% NaCl)
10% FCS

The cells were cultivated in 10 cm cell culture dishes (Sarstedt) and the cell medium was exchanged every 3-5 days. At 90-100 % confluency, cells were passaged with Trypsin-EDTA (Sigma). Therefore, cells were once washed with sterile 1x PBS and trypsinized with 1.5 ml Trypsin-EDTA for 3-5 min at 37 °C. The detached cells were resuspended in 4.5 ml fresh growth medium until a single cell suspension was present. Dilutions (1:3-1:20) of the resuspended cells were plated in dishes containing 10 ml fresh medium and equally distributed. Cells were cultivated at 37 °C and 5% CO_2.

5.5.2 Cultivation of Schneider 2 (S2) cells

Culture Medium: Schneider´s Medium (Invitrogen)
1% Penicillin/Streptomycin
10% FCS

The cells were cultivated in T-75 cell culture flasks (Costar) with 20 ml growth medium. At 80-90% confluency, the adherent S2 cells detach and proliferate in suspension and have to be passaged. Cells were resuspended until a single cell suspension was present, an aliquot (1:10-1:50) thereof was transferred into a new flask containing 20 ml fresh medium and equally distributed. Cells were cultivated at 25 °C under normal atmosphere.

5.5.3 Freezing of cells for long term storage

Cells at 70-90 % confluency were used for freezing. Cells were either trypsinized or resuspended as described and transferred into 15 ml tubes with 10 ml of fresh medium. The cells were sedimented at 300x g for 5 min and resuspended in 3-4.5 ml 10% (v/v) DMSO in growth medium with 20% FCS. 1.5 ml aliquots were transferred into cryovials (Nunc) and incubated on ice for 1-1.5 h. The vials were stored overnight at -80 °C and then transferred into a liquid nitrogen tank for long term storage.

5.5.4 Thawing of frozen cells

Cells frozen in liquid nitrogen were quickly thawed at 37 °C in a water bath. Cells were transferred into 15 ml tubes with 10 ml of fresh medium and centrifuged at 300x g for 5 min. The cells were resuspended in 5 ml normal growth medium and transferred to 10 cm culture dishes containing 10 ml growth medium.

5.5.5 Transfection of COS-7 cells with Lipofectamine Plus

Cells at 80-90 % confluency were transfected. 2 µg DNA was mixed with 250 µl OptiMEM (Invitrogen) and 15 µl Lipofectamine Plus reagent (Invitrogen) in an Eppendorf tube. After 15 min incubation, 5 µl Lipofectamine in 250 µl OptiMEM was added, inverted several times, and incubated for 15 min.

Cells in a 6 cm culture dish were washed with OptiMEM once and covered with 2 ml OptiMEM. The Lipofectamine/DNA mixture was added dropwise to the cells and incubated for 3-4 h at 37 °C and 5% CO_2. Afterwards, the reagent was removed and fresh normal growth serum was added. After 24 h, the cells were harvested for analysis.

5.5.6 Transient transfection of Schneider cells with Effectene

S2 cells were plated in 6 well dishes at 30-50 % confluency the day before transfection. 2-3 h before transfection, the growth medium was replaced with 1.6 ml fresh medium, and cells were transfected with Effectene (Qiagen) according to the manufacturer's protocol as follows:

1 µg	DNA (or for cotransfection 0.5 µg DNA each)
160 µl	Enhancer buffer
8 µl	Enhancer (Enhancer:DNA = 8:1)

The mixture was vortexed for 1 sec and incubated for 5 min at RT. 25 µl Effectene was added by pipetting up and down five times and incubated for 10 min at RT. 600 µl S2 growth medium was added, the mixture was pipetted up and down twice, directly added dropwise to the cells and incubated for 48 h at 25 °C. Expression was induced by adding $CuSO_4$ (0.5 M stock in ddH_2O) to a final concentration of 500 µM. Cells were generally analysed 48 h later.

5.5.7 Cell lysis

Cells were scraped by pipetting up and down with a 1 ml pipette tip and transferred into an Eppendorf tube. A total volume of 3 ml was centrifuged at 800x g for 3 min and washed once with cold PBS. The PBS was removed and the cells were resuspended in 100 µl of 2x SDS sample buffer. 4 µl bezonase was added, pipetted once up and down, and the samples were heated for 7 min at 95°C prior to SDS-Page analysis.

6 Cloning strategies

All clones were checked following the cloning procedure by digestion with appropriate restriction enzymes for the proper orientation and length of the cloned fragment or by PCR with appropriate primers, and were afterwards sequenced from both ends. Cloning was performed using XL1-Blue *E. coli* host cells if not otherwise mentioned.

6.1 Cloning of pUASt-*dfer*

The published full-length *p92dfer* (=*dfer)* clone was kindly provided in a pGEM-7 vector by K. Hill, San Francisco, and was subcloned into pUASt. Therefore, first the vector backbone had to be split through digestion with XmaI. The desired fragment was cut out of pGEM-*p92dfer* by EcoRI/XbaI or EcoRI digestion and cloned into the appropriately prepared pUASt vector. The obtained plasmids pUASt-*dfer*-EX2 (EcoRI/XbaI digested) and pUASt-*dfer*-E8 (EcoRI digested) were coinjected into embryos to generate transgenic flies.

6.2 Cloning of pUASt-*dfer-D*

The *dfer-D* construct was cloned using a cDNA library, which was generated of fly head tissue with overexpression of the *dfer* transcription unit induced by crossing the EP-line with the *GMR*-GAL4 driver line. *dfer-D* was PCR-amplified from the cDNA library using Eco02/Not01 primer pairs. The product was cloned into the pTOPO vector. Plasmid pTOPO-*dfer-D*-2.3 was EcoRI/NotI digested and cloned into the prepared pUASt vector. For production of the transgenic *dfer-D* flies, the clone pUASt-*dfer-D*-2 (32) was used.

6.3 Cloning of pUASt-*p45dfer*

A pBluescript-vector with the *p45dfer* isoform of *dfer* was also kindly provided by K. Hill, San Francisco, and cloned in addition to the already generated pUASt-*dfer-C* construct. pBS-*p45dfer* was digested with either EcoRI/XbaI or just EcoRI and cloned directly into pUASt. The plasmid pUASt-*p45dfer*-EX12 (EcoRI/XbaI digested) was used for the generation of transgenic flies.

6.4 Cloning of pUASt-*dfer-DN*

The cloning of the dominant-negative (DN) mutant of *dfer* was performed in several steps. The mutation was introduced by PCR using the sense mutagenesis primer Zwim-DN-K570R containing an XcmI restriction site and the 3'pUASt primer on the pUASt-*p92dfer*-EX2 clone as DNA template. The PCR product, consisting of the mutagenized C-terminal part of *dfer*, was subcloned into the pCRII vector. The mutagenized fragment was cut out with XcmI/XbaI. In parallel, *dfer* had to be subcloned from pUASt-*dfer*-EX2 into the pBS vector using EcoRI/XbaI digestion, as the pUASt vector contains XcmI sites. The clone pBS-*dfer*-9 was

XcmI/XbaI digested to remove the wildtype C-terminal *dfer* part. The remaining part of the pBS-*dfer*-9 vector containing the N-terminal part of *dfer* was ligated to the Xcm/XbaI digested mutagenized fragment. The newly obtained pBS-*dfer-DN*-3 was EcoRI/XbaI digested and the *dfer-DN* fragment was cloned into the prepared pUASt vector. The final plasmids pUASt-*dfer-DN*-12 and pUASt-*dfer-DN*–20 were coinjected into embryos for transgenic fly production.

6.5 Cloning of pUASt-*dfer-A*

The *dfer-A* cDNA (= *dfer R-A* transcript) was obtained as clone RH14840 in a pFLC-1 vector from Open Biosystems. The clone was checked by digestion and PCR before it was used for the following cloning steps. After EcoRI/Acc65i digestion, the obtained fragment was cloned into a prepared pUASt vector. The plasmids pUASt-*dfer-A*-93 and pUASt-*dfer-A*-915 were injected into embryos.

6.6 Cloning of pUAS-*dfer-N*

The nucleotides encoding the first 420 aa of DFer were cut out by EcoRI/XhoI digestion from pUASt-*p92dfer*-EX2 and cloned into a prepared pUASt vector. pUASt-*dfer-N*-2 was injected into embryos to generate transgenic flies.

6.7 Cloning of human *fes* into pUASt

pEF4-*hfes* was PvuI digested to destroy the vector backbone. The *hfes* cDNA was cut out by EcoRI digestion and cloned into a prepared pUASt vector. The plasmid pUASt-*hfes*-12 was injected into embryos to generate transgenic flies.

6.8 Cloning of murine *fer* into pCRII and pUASt

The *mfer* cDNA was PCR-amplified from pECE-*mfer* using BglII-mFer-5' and mFer-BglII-3' primers. The PCR fragment was TOPO cloned into pCRII. The clones pCRII-*mfer*-17 and pCRII-*mfer*-24 were used for the following steps. After a BglII digestion, the *mfer* cDNA was cloned into a prepared pUASt vector. The plasmids were retransformed into SURE chemo-competent cells. The clones pUASt-*mfer*-1b2 and pUASt-*mfer*-2b12 were used for transgenic fly production.

6.9 Cloning of *Sym*-pUASt-*dfer-N* and pCRII-*dfer-N* for in *vivo* RNAi

The cloning was performed using chemo-competent SURE cells. The w^+ fragment was cut out of the *Sym*-pUASt-w^+ by EcoRI digestion. The *dfer* 5'UTR-mid region (the first 1413 nt) was PCR-amplified from the pGEM-*p92dfer* template using EcoRI-5'UTR-Z and GST-N-end-401-EcoRI primer. The PCR product was either TOPO cloned into the pCRII vector or directly digested with EcoRI and cloned into the prepared *Sym*-pUASt vector. The obtained plasmids *Sym*-pUASt-*dfer-N*-1 and *Sym*-pUASt-*dfer-N*-5 were coinjected into embryos.

6.10 Cloning of pWIZ-*RNAi-N* for *in vivo* RNAi

The *RNAi-N* fragment (nt 800-1350 of *p92dfer*) was PCR-amplified from the pGEM-*p92dfer* template using RNAi-N-5' and RNAi-N-3' primer and TOPO subcloned into the pCRII vector. The resulting pCRII-*RNAi-N*-1 with T7 sense orientation was digested with XbaI and the *RNAi-N* fragment was cloned into an AvrII digested and SAP treated pWIZ vector. The orientation of the inserted *RNAi-N* was checked by PCR with appropriate primers, being 3'-5' oriented. pWIZ-3'5'N was NheI digested and SAP treated and the XbaI digested *RNAi-N* fragment was cloned in. After ligation, the plasmid was transformed into chemo-competent SURE cells. Clones were screened by PCR for the proper 5'-3' orientation of the second inserted fragment. Plasmid pWIZ-*RNAi-N*-A14 has both the 3'-5' and 5'-3' inserted *RNAi-N* fragments for RNA hairpin production and was injected into embryos for generation of transgenic flies.

6.11 Cloning of pWIZ-*RNAi-SK* for *in vivo* RNAi

The *RNAi-SK* fragment (nt 1520-2070 of *p92dfer*) was PCR-amplified from pGEM-*p92dfer* using RNAi-SK-5'/RNAi-SK-3' primer pairs and TOPO cloned into the pCRII vector. *RNAi-SK* was cut out from pCRII-*SK*-1 (Sp6 sense orientation) with XbaI and cloned into an AvrII digested and SAP treated pWIZ vector. The orientation of the inserted *RNAi-SK* fragment was checked by PCR with appropriate primers. pWIZ-3'5'SK was NheI digested and SAP treated and the XbaI digested *RNAi-SK* fragment was cloned in. The plasmid was transformed into chemo-competent SURE cells. Clones were screened by PCR for the proper 5'-3' orientation of the second inserted fragment. pWIZ-*RNAi-SK*-35 has both the 3'-5' and 5'-3' inserted *RNAi-SK* fragments for RNA hairpin production and was injected into embryos.

6.12 Cloning of pWIZ-*RNAi-long* for *in vivo* RNAi

The *RNAi-long* fragment (nt 2375-2879 from the *dfer R-A* transcript) was PCR-amplified from the pFLC-*dfer-A*-1 plasmid using RNAi-long(XhoI)-5' and RNAi-long-3' primers and TOPO cloned into the pCRII vector. *RNAi-long* was cut out from pCRII-*RNAi-long*-2 (Sp6 sense orientation) by XhoI/XbaI digestion and directionally cloned into an XhoI/AvrII digested and CIP treated pWIZ vector. pWIZ-5'3'long was NheI digested and CIP treated and the XbaI digested *RNAi-long* fragment was cloned in. The plasmid was transformed into chemo-competent SURE cells. The orientation of the second inserted *RNAi-long* fragment was checked for its proper 3'-5' orientation by PCR with appropriate primers. Clone pWIZ-*RNAi-long*-6 has both the 5'-3' and 3'-5' inserted *RNAi-long* fragments for RNA hairpin production and was used for transgenic fly generation.

6.13 Cloning of pCRII-*p92dfer* for *in situ* hybridization

The full-length *dfer* cDNA (*dfer R-B* transcript) was PCR-amplified from pGEM-*p92dfer* using start-zwim/end-zwim primer pairs and the PCR product was TOPO cloned into the pCRII vector. Plasmid pCRII- *p92dfer*-5.1 was T7 sense oriented and used for *in situ* probe production.

6.14 Cloning of pCRII-*dfer-NT* for *in situ* hybridization

The first 1413 nt of *dfer* were PCR-amplified from pGEM-*p92dfer* using start-zwim and GST-N-end-(401)-EcoRI primers. The PCR product was TOPO cloned into the pCRII vector and T7 sense oriented pCRII-*dfer-NT*-4.1 was used for *in situ* probe production.

6.15 Cloning of pCRII-*p45dfer*$^{140\text{-}481}$ for *in situ* hybridization

p45dfer$^{140\text{-}481}$ was PCR-amplified from pBS-*p45dfer* (nt 140-481) using p45-1-(140)/p45-2-(481) primer pairs. The product was TOPO cloned into the pCRII vector. Plasmid pCRII-*p45dfer*$^{140\text{-}481}$-1.3 was Sp6 sense oriented and used for *in situ* probe production.

6.16 Cloning of pCRII-*dfer-D*$^{8\text{-}498}$ for *in situ* hybridization

A 490 bp unique fragment (nt 8-498 of the R-C transcript of *dfer*) was PCR-amplified from wildtype genomic DNA using testis-Z-up/testis-Z-low primers. The PCR product was TOPO cloned into the pCRII vector and SP6 sense oriented pCRII-*dfer-D*$^{8\text{-}498}$ was used for *in situ* probe production.

6.17 Cloning of pCRII-*CG33188* for *in situ* hybridization

A 680 bp fragment of CG33188 (nt 1910-2690) was PCR-amplified from wildtype genomic DNA using CG33188-up/CG33188-low primers. The PCR product was TOPO cloned into the pCRII vector and T7 sense oriented pCRII-*CG33188* was used for *in situ* probe production.

6.18 Cloning of pCRII-*CG18473* for *in situ* hybridization

A 500 bp fragment of CG18473 (nt 144-647) was PCR-amplified from wildtype genomic DNA using CG18473-up/CG18473-low primers. The PCR product was TOPO cloned into the pCRII vector and T7 sense oriented pCRII-*CG18473* was used for *in situ* probe production.

6.19 Cloning of pCRII-*CG8129* for *in situ* hybridization

A 400 bp fragment of CG8129 (nt 1113-1515) was PCR-amplified from wildtype genomic DNA using CG8129-up/CG8129-low primers. The PCR product was TOPO cloned into the pCRII vector and T7 sense oriented pCRII-*CG8129* was used for *in situ* probe production.

6.20 Cloning of GST-DFer/ pGEX-*dfer*

The full-length form of *dfer (p92dfer)* was PCR-amplified using GST-N-BamHI-start and GST-N-end-EcoRI primer from a pUASt-*dfer*-EX2 template. The PCR fragment was BamHI/EcoRI digested and cloned into a prepared pGEX-4T-2 vector. The plasmid was then transformed into BL21 *E. coli* cells for protein expression; clones number 5, 7, 11 and 14 of pGEX-*dfer* were used. Clone pGEX-GST-1 was utilized as a control expressing GST alone.

6.21 Cloning of GST-DFer-N / pGEX-*dfer-N*

The nucleotides encoding the first 128 aa of DFer were PCR-amplified using GST-N-BamHI-start and GST-N-128-end-EcoRI primer from a pGEM-*p92dfer* template. The PCR fragment was BamHI/EcoRI digested and cloned into a prepared pGEX-4T-2 vector. Clone pGEX-*dfer-N*-23 was then transformed into BL21 *E. coli* cells for protein expression.

6.22 Cloning of GST-DFer-SK / pGEX-*dfer-SK*

The nucleotides encoding the aa 362 to 563 of DFer were PCR-amplified using GST-N-BamHI-362-start and GST-N-563-end-EcoRI primer from a pGEM-*p92dfer* template. The PCR fragment was BamHI/EcoRI digested and cloned into a prepared pGEX-4T-2 vector. Clone pGEX-*dfer-DK*-51 was transformed into BL21 *E. coli* cells and used for protein expression.

6.23 Cloning of pMT-*dfer* for cell culture expression

dfer cDNA was cloned into the pMT/V5-HisB vector in frame with the V5 tag. The cDNA was PCR-amplified from pGEM-*p92dfer* using (XbaI)-5'UTR-Z and C-term-(XbaI) primers and the PCR product was TOPO cloned into pCRII. After digestion with XbaI, the *dfer* fragment was cloned into prepared pMT/V5-HisB vector and the direction of insertion was checked by PCR and restriction digestion. pMT-*dfer*-1.1 and pMT-*dfer*-2.5 were used for Schneider cell transfection.

6.24 Cloning of pMT-*dfer-DN* for cell culture expression

The mutated *dfer-DN* cDNA was cloned into the pMT/V5-HisB vector in frame with the V5 tag. *Dfer-DN* was PCR-amplified from pUASt-*dfer-DN*–20 using (XbaI)-N-term and C-term-(XbaI) primers and the PCR product was TOPO cloned into pCRII. The *dfer-DN* fragment was cut out by digestion with XbaI and cloned into prepared pMT/V5-HisB vector. The direction of insertion was checked by PCR and restriction digestion. pMT-*dfer-DN*-4.3 was used for Schneider cell transfection.

6.25 Cloning of pMT-*dfer-A* for cell culture expression

The long isoform *dfer-A* was cloned into the pMT/V5-HisB vector, being not in frame with the V5 tag. The *dfer-A* fragment was cut out of pUASt-*dfer-A*-93 via EcoRI/XbaI digestion and directly cloned into prepared pMT/V5-HisB vector. pMT-*dfer-A*-1.5 and pMT-*dfer-A*-2.14 were used for Schneider cell transfection.

6.26 Modification of pCosPer to pCosPer-ASF

As the exact sequence of the pCosPer is not available, the cosmid had to be first checked by digestion with different restriction enzymes for the absence and presence of specific restriction sites. For the cloning steps of the genomic rescue constructs, SphI and FseI restriction sites were chosen and had to be introduced into the cosmid. The oligonucleotides COS/Cas-EASFX-1 and COS/Cas-XFSAE-2 containing AvrII, SphI and FseI restriction sites with EcoRI and XbaI compatible ends were hybridized and ligated into EcoRI/XbaI digested pCosPer. The resulting pCosPer-ASF-41 and pCosPer-ASF-51 were used for the cloning of the *dfer* genomic rescue construct.

6.27 Modification of pCosPer to pCosPer-45(-S)-L/ASF

As one SphI restriction site, which is required for the genomic rescue of the three adjacent genes to *dfer*, is present in the original pCosPer cosmid, it had to be eliminated by nuclease treatment and religation. The resulting pCosPer-45(-S) cosmid lacks the mentioned SphI restriction site. In a second step, AvrII, SphI and FseI restriction sites were introduced into the plasmid. Therefore, the sites were placed within cos/CAS-AS-up and cos/CAS-F-low primer sequences which were used to PCR amplify a 250 bp lacZ fragment. The PCR fragment was TOPO cloned into pCRII. Via EcoRI digestion, the fragment containing the restriction sites was cloned into prepared pCosPer-45(-S), resulting in pCosPer-45(-S)-1.1-1, pCosPer-45(-S)-1.1-13 and pCosPer-45(-S)-1.2-37.

6.28 Genomic rescue of *dfer* / Cloning of pCosPer-*dfer*

BAC R19J06 contains the *dfer* gene in a DNA fragment of 175.053 bp, which was cloned as NotI fragment into pBACe3.6. The BAC clone was checked through digestion with different restriction enzymes for its proper sequence and by PCR with various specific primers for the presence of the *dfer* genomic region.

The BAC was digested with FseI for 4 h and dephosphorylated by CIP treatment. Two PFGE runs were conducted to isolate the 31 kb DNA band containing the genomic rescue fragment of dfer. The DNA was extracted by gelase digestion.

As the pCosPer-ASF cosmid contains two cos sites, these had to be separated by HpaI restriction digest. Digestion of 10 µg vector was performed and the linearised cosmid was then dephosphorylated by CIP and purified before the second digestion with FseI. The

purified vector was eluted in 10 µl. The FseI genomic DNA fragment was then cloned into the prepared pCosPer-ASF cosmid and packaged into lambda phages. XL1Blue MR cells were used for the phage infection and infected bacteria were screened for positive clones carrying the *dfer* genomic region by PCR and restriction digestion. The orientation and the proper sequence of the genomic DNA ends were checked by PCR using genrescue-lowFPS-up/genrescue-upFPS-low and seqCos-CAS-low/seqCos-CAS-up primers. pCosPer-*dfer*-1, which was additionally purified by CsCl-ethidium bromide gradient equilibrium centrifugation, and pCosPer-*dfer*-2 were used for injection into embryos to generate transgenic flies.

6.29 Genomic rescue of CG 33188, CG 18473, CG 8149 / Cloning of pCosPer-*CG*

BAC R32M04 contains the *dfer* genomic region and the three adjacent genes (CG 33188, CG 18473, CG 8149) in a 148.847 bp DNA fragment, which was cloned as NotI fragment into pBACe3.6. The BAC clone was checked through digestion with different restriction enzymes for its proper sequence and by PCR with various specific primers for the presence of all 4 genes.

The BAC was digested with SphI for 4 h and dephosphorylated by CIP treatment. Two PFGE runs were conducted to isolate the 38 kb DNA band containing the genomic rescue fragment of the three genes. The DNA was extracted using the GeneCAPSULE system.

10 µg of the pCosPer-45(-S)-L/ASF were digested with HpaI and then dephosphorylated by CIP. The purified vector was then digested with SphI and eluted in 10 µl. The SphI genomic DNA fragment was then cloned into the prepared pCosPer-45(-S)-L/ASF cosmid and packaged into lambda phages. XL1Blue MR cells were used for the phage infection and infected bacteria were screened for positive clones by restriction digestion and PCR. The orientation and the proper sequence of the genomic DNA ends were checked by PCR using genrescue-lowSphI-up/genrescue-upSphI-low and seqCos-CAS-low/seqCos-CAS-up primers, and also for the presence of all three genes. pCosPer-CG-1a and pCosPer-CG-5 were injected into embryos for transgenic flies production.

Literature

7 Literature

Adler, P. N., Charlton, J. and Liu, J. (1998). "Mutations in the cadherin superfamily member gene dachsous cause a tissue polarity phenotype by altering frizzled signaling." *Development* **125**(5): 959-68.

Aguzzi, A. and Haass, C. (2003). "Games played by rogue proteins in prion disorders and Alzheimer's disease." *Science* **302**(5646): 814-8.

Ando, K., Iijima, K. I., Elliott, J. I., Kirino, Y. and Suzuki, T. (2001). "Phosphorylation-dependent regulation of the interaction of amyloid precursor protein with Fe65 affects the production of beta-amyloid." *J Biol Chem* **276**(43): 40353-61.

Annaert, W. and De Strooper, B. (2002). "A cell biological perspective on Alzheimer's disease." *Annu Rev Cell Dev Biol* **18**: 25-51.

Arregui, C., Pathre, P., Lilien, J. and Balsamo, J. (2000). "The nonreceptor tyrosine kinase fer mediates cross-talk between N-cadherin and beta1-integrins." *J Cell Biol* **149**(6): 1263-74.

Artavanis-Tsakonas, S., Rand, M. D. and Lake, R. J. (1999). "Notch signaling: cell fate control and signal integration in development." *Science* **284**(5415): 770-6.

Baek, S. H., Ohgi, K. A., Rose, D. W., Koo, E. H., Glass, C. K. and Rosenfeld, M. G. (2002). "Exchange of N-CoR corepressor and Tip60 coactivator complexes links gene expression by NF-kappaB and beta-amyloid precursor protein." *Cell* **110**(1): 55-67.

Baker, N. E. and Zitron, A. E. (1995). "Drosophila eye development: Notch and Delta amplify a neurogenic pattern conferred on the morphogenetic furrow by scabrous." *Mech Dev* **49**(3): 173-89.

Balsamo, J., Arregui, C., Leung, T. and Lilien, J. (1998). "The nonreceptor protein tyrosine phosphatase PTP1B binds to the cytoplasmic domain of N-cadherin and regulates the cadherin-actin linkage." *J Cell Biol* **143**(2): 523-32.

Balsamo, J., Leung, T., Ernst, H., Zanin, M. K., Hoffman, S. and Lilien, J. (1996). "Regulated binding of PTP1B-like phosphatase to N-cadherin: control of cadherin-mediated adhesion by dephosphorylation of beta-catenin." *J Cell Biol* **134**(3): 801-13.

Beck, Y., Pecasse, F. and Richards, G. (2004). "Kruppel-homolog is essential for the coordination of regulatory gene hierarchies in early Drosophila development." *Dev Biol* **268**(1): 64-75.

Beher, D., Hesse, L., Masters, C. L. and Multhaup, G. (1996). "Regulation of amyloid protein precursor (APP) binding to collagen and mapping of the binding sites on APP and collagen type I." *J Biol Chem* **271**(3): 1613-20.

Ben-Dor, I., Bern, O., Tennenbaum, T. and Nir, U. (1999). "Cell cycle-dependent nuclear accumulation of the p94fer tyrosine kinase is regulated by its NH2 terminus and is affected by kinase domain integrity and ATP binding." *Cell Growth Differ* **10**(2): 113-29.

Beumer, K., Matthies, H. J., Bradshaw, A. and Broadie, K. (2002). "Integrins regulate DLG/FAS2 via a CaM kinase II-dependent pathway to mediate synapse elaboration and stabilization during postembryonic development." *Development* **129**(14): 3381-91.

Beumer, K. J., Rohrbough, J., Prokop, A. and Broadie, K. (1999). "A role for PS integrins in morphological growth and synaptic function at the postembryonic neuromuscular junction of Drosophila." *Development* **126**(24): 5833-46.

Billuart, P., Winter, C. G., Maresh, A., Zhao, X. and Luo, L. (2001). "Regulating axon branch stability: the role of p190 RhoGAP in repressing a retraction signaling pathway." *Cell* **107**(2): 195-207.

Bishop, S. A., Klein, T., Martinez Arias, A. and Couso, J. P. (1999). "Composite signaling from Serrate and Delta establishes leg segments in Drosophila through Notch." *Development* **126**(13): 2993-3003.

Blair, S. S., Brower, D. L., Thomas, J. B. and Zavortink, M. (1994). "The role of apterous in the control of dorsoventral compartmentalization and PS integrin gene expression in the developing wing of Drosophila." *Development* **120**(7): 1805-15.

Bokel, C. and Brown, N. H. (2002). "Integrins in development: moving on, responding to, and sticking to the extracellular matrix." *Dev Cell* **3**(3): 311-21.

Bonini, N. M. and Fortini, M. E. (2003). "Human neurodegenerative disease modeling using Drosophila." *Annu Rev Neurosci* **26**: 627-56.

Brand, A. H. and Perrimon, N. (1993). "Targeted gene expression as a means of altering cell fates and generating dominant phenotypes." *Development* **118**(2): 401-15.

Brodsky, M. H. and Steller, H. (1996). "Positional information along the dorsal-ventral axis of the Drosophila eye: graded expression of the four-jointed gene." *Dev Biol* **173**(2): 428-46.

Brody, T., Stivers, C., Nagle, J. and Odenwald, W. F. (2002). "Identification of novel Drosophila neural precursor genes using a differential embryonic head cDNA screen." *Mech Dev* **113**(1): 41-59.

Brower, D. L. (2003). "Platelets with wings: the maturation of Drosophila integrin biology." *Curr Opin Cell Biol* **15**(5): 607-13.

Brown, N. H., Gregory, S. L. and Martin-Bermudo, M. D. (2000). "Integrins as mediators of morphogenesis in Drosophila." *Dev Biol* **223**(1): 1-16.

Brunner, E., Peter, O., Schweizer, L. and Basler, K. (1997). "pangolin encodes a Lef-1 homologue that acts downstream of Armadillo to transduce the Wingless signal in Drosophila." *Nature* **385**(6619): 829-33.

Buckles, G. R., Rauskolb, C., Villano, J. L. and Katz, F. N. (2001). "Four-jointed interacts with dachs, abelson and enabled and feeds back onto the Notch pathway to affect growth and segmentation in the Drosophila leg." *Development* **128**(18): 3533-42.

Campbell, S., Inamdar, M., Rodrigues, V., Raghavan, V., Palazzolo, M. and Chovnick, A. (1992). "The scalloped gene encodes a novel, evolutionarily conserved transcription factor required for sensory organ differentiation in Drosophila." *Genes Dev* **6**(3): 367-79.

Campos-Ortega, J. and Hartenstein, V. (1985). *"The Embryonic Development of Drosophila melanogaster."* Springer-Verlag, Berlin.

Cao, X. and Sudhof, T. C. (2001). "A transcriptionally [correction of transcriptively] active complex of APP with Fe65 and histone acetyltransferase Tip60." *Science* **293**(5527): 115-20.

Cao, X. and Sudhof, T. C. (2004). "Dissection of amyloid-beta precursor protein-dependent transcriptional transactivation." *J Biol Chem* **279**(23): 24601-11.

Care, A., Mattia, G., Montesoro, E., Parolini, I., Russo, G., Colombo, M. P. and Peschle, C. (1994). "c-fes expression in ontogenetic development and hematopoietic differentiation." *Oncogene* **9**(3): 739-47.

Carrell, R. and Corral, J. (2004). "What can Drosophila tell us about serpins, thrombosis and dementia?" *Bioessays* **26**(1): 1-5.

Chan, S. L., Furukawa, K. and Mattson, M. P. (2002). "Presenilins and APP in neuritic and synaptic plasticity: implications for the pathogenesis of Alzheimer's disease." *Neuromolecular Med* **2**(2): 167-96.

Chen, Y. M., Lee, N. P., Mruk, D. D., Lee, W. M. and Cheng, C. Y. (2003). "Fer kinase/FerT and adherens junction dynamics in the testis: an in vitro and in vivo study." *Biol Reprod* **69**(2): 656-72.

Cho, E. and Irvine, K. D. (2004). "Action of fat, four-jointed, dachsous and dachs in distal-to-proximal wing signaling." *Development* **131**(18): 4489-500.

Clark, H. F., Brentrup, D., Schneitz, K., Bieber, A., Goodman, C. and Noll, M. (1995). "Dachsous encodes a member of the cadherin superfamily that controls imaginal disc morphogenesis in Drosophila." *Genes Dev* **9**(12): 1530-42.

Cohen, B., McGuffin, M. E., Pfeifle, C., Segal, D. and Cohen, S. M. (1992). "apterous, a gene required for imaginal disc development in Drosophila encodes a member of the LIM family of developmental regulatory proteins." *Genes Dev* **6**(5): 715-29.

Cohen, B., Simcox, A. A. and Cohen, S. M. (1993). "Allocation of the thoracic imaginal primordia in the Drosophila embryo." *Development* **117**(2): 597-608.

Coulson, E. J., Paliga, K., Beyreuther, K. and Masters, C. L. (2000). "What the evolution of the amyloid protein precursor supergene family tells us about its function."

Neurochem Int **36**(3): 175-84.
Couso, J. P. and Martinez Arias, A. (1994). "Notch is required for wingless signaling in the epidermis of Drosophila." *Cell* **79**(2): 259-72.
Craig, A. W., Zirngibl, R. and Greer, P. (1999). "Disruption of coiled-coil domains in Fer protein-tyrosine kinase abolishes trimerization but not kinase activation." *J Biol Chem* **274**(28): 19934-42.
Craig, A. W., Zirngibl, R., Williams, K., Cole, L. A. and Greer, P. A. (2001). "Mice devoid of fer protein-tyrosine kinase activity are viable and fertile but display reduced cortactin phosphorylation." *Mol Cell Biol* **21**(2): 603-13.
da Cruz e Silva, O. A., Fardilha, M., Henriques, A. G., Rebelo, S., Vieira, S. and da Cruz e Silva, E. F. (2004). "Signal transduction therapeutics: relevance for Alzheimer's disease." *J Mol Neurosci* **23**(1-2): 123-42.
Daubresse, G., Deuring, R., Moore, L., Papoulas, O., Zakrajsek, I., Waldrip, W. R., Scott, M. P., Kennison, J. A. and Tamkun, J. W. (1999). "The Drosophila kismet gene is related to chromatin-remodeling factors and is required for both segmentation and segment identity." *Development* **126**(6): 1175-87.
De Celis, J. F. (2003). "Pattern formation in the Drosophila wing: The development of the veins." *Bioessays* **25**(5): 443-51.
de Celis, J. F. and Bray, S. (1997). "Feed-back mechanisms affecting Notch activation at the dorsoventral boundary in the Drosophila wing." *Development* **124**(17): 3241-51.
de Celis, J. F., Tyler, D. M., de Celis, J. and Bray, S. J. (1998). "Notch signalling mediates segmentation of the Drosophila leg." *Development* **125**(23): 4617-26.
De Strooper, B. and Annaert, W. (2000). "Proteolytic processing and cell biological functions of the amyloid precursor protein." *J Cell Sci* **113 (Pt 11)**: 1857-70.
De Strooper, B. and Woodgett, J. (2003). "Alzheimer's disease: Mental plaque removal." *Nature* **423**(6938): 392-3.
del Alamo Rodriguez, D., Terriente Felix, J. and Diaz-Benjumea, F. J. (2004). "The role of the T-box gene optomotor-blind in patterning the Drosophila wing." *Dev Biol* **268**(2): 481-92.
Diaz-Benjumea, F. J. and Cohen, S. M. (1993). "Interaction between dorsal and ventral cells in the imaginal disc directs wing development in Drosophila." *Cell* **75**(4): 741-52.
Duan, W., Sun, B., Li, T. W., Tan, B. J., Lee, M. K. and Teo, T. S. (2000). "Cloning and characterization of AWP1, a novel protein that associates with serine/threonine kinase PRK1 in vivo." *Gene* **256**(1-2): 113-21.
Duffy, J. B. (2002). "GAL4 system in Drosophila: a fly geneticist's Swiss army knife." *Genesis* **34**(1-2): 1-15.
Eaton, S. (1997). "Planar polarization of Drosophila and vertebrate epithelia." *Curr Opin Cell Biol* **9**(6): 860-6.
Ellis, C., Moran, M., McCormick, F. and Pawson, T. (1990). "Phosphorylation of GAP and GAP-associated proteins by transforming and mitogenic tyrosine kinases." *Nature* **343**(6256): 377-81.
Fan, L., Di Ciano-Oliveira, C., Weed, S. A., Craig, A. W., Greer, P. A., Rotstein, O. D. and Kapus, A. (2004). "Actin depolymerization-induced tyrosine phosphorylation of cortactin: the role of Fer kinase." *Biochem J* **380**(Pt 2): 581-91.
Feng, G., Deak, P., Kasbekar, D. P., Gil, D. W. and Hall, L. M. (1995). "Cytogenetic and molecular localization of tipE: a gene affecting sodium channels in Drosophila melanogaster." *Genetics* **139**(4): 1679-88.
Fischman, K., Edman, J. C., Shackleford, G. M., Turner, J. A., Rutter, W. J. and Nir, U. (1990). "A murine fer testis-specific transcript (ferT) encodes a truncated Fer protein." *Mol Cell Biol* **10**(1): 146-53.
Fogerty, F. J., Juang, J. L., Petersen, J., Clark, M. J., Hoffmann, F. M. and Mosher, D. F. (1999). "Dominant effects of the bcr-abl oncogene on Drosophila morphogenesis." *Oncogene* **18**(1): 219-32.
Fossgreen, A., Bruckner, B., Czech, C., Masters, C. L., Beyreuther, K. and Paro, R. (1998). "Transgenic Drosophila expressing human amyloid precursor protein show gamma-secretase activity and a blistered-wing phenotype." *Proc Natl Acad Sci U S A* **95**(23):

13703-8.
Fristrom, D., Wilcox, M. and Fristrom, J. (1993). "The distribution of PS integrins, laminin A and F-actin during key stages in Drosophila wing development." *Development* **117**(2): 509-23.
Funayama, N., Fagotto, F., McCrea, P. and Gumbiner, B. M. (1995). "Embryonic axis induction by the armadillo repeat domain of beta-catenin: evidence for intracellular signaling." *J Cell Biol* **128**(5): 959-68.
Garcia, R., Yu, C. L., Hudnall, A., Catlett, R., Nelson, K. L., Smithgall, T., Fujita, D. J., Ethier, S. P. and Jove, R. (1997). "Constitutive activation of Stat3 in fibroblasts transformed by diverse oncoproteins and in breast carcinoma cells." *Cell Growth Differ* **8**(12): 1267-76.
Geiger, B., Bershadsky, A., Pankov, R. and Yamada, K. M. (2001). "Transmembrane crosstalk between the extracellular matrix--cytoskeleton crosstalk." *Nat Rev Mol Cell Biol* **2**(11): 793-805.
Gelman, I. H. (2003). "Pyk 2 FAKs, any two FAKs." *Cell Biol Int* **27**(7): 507-10.
Giordano, E., Rendina, R., Peluso, I. and Furia, M. (2002). "RNAi triggered by symmetrically transcribed transgenes in Drosophila melanogaster." *Genetics* **160**(2): 637-48.
Giraldez, A. J. and Cohen, S. M. (2003). "Wingless and Notch signaling provide cell survival cues and control cell proliferation during wing development." *Development* **130**(26): 6533-43.
Glise, B., Bourbon, H. and Noselli, S. (1995). "hemipterous encodes a novel Drosophila MAP kinase kinase, required for epithelial cell sheet movement." *Cell* **83**(3): 451-61.
Gluzman, Y. (1981). "SV40-transformed simian cells support the replication of early SV40 mutants." *Cell* **23**(1): 175-82.
Gottardi, C. J. and Gumbiner, B. M. (2001). "Adhesion signaling: how beta-catenin interacts with its partners." *Curr Biol* **11**(19): R792-4.
Grabbe, C., Zervas, C. G., Hunter, T., Brown, N. H. and Palmer, R. H. (2004). "Focal adhesion kinase is not required for integrin function or viability in Drosophila." *Development* **131**(23): 5795-805.
Greer, P. (2002). "Closing in on the biological functions of Fps/Fes and Fer." *Nat Rev Mol Cell Biol* **3**(4): 278-89.
Greeve, I., Kretzschmar, D., Tschape, J. A., Beyn, A., Brellinger, C., Schweizer, M., Nitsch, R. M. and Reifegerste, R. (2004). "Age-dependent neurodegeneration and Alzheimer-amyloid plaque formation in transgenic Drosophila." *J Neurosci* **24**(16): 3899-906.
Grevengoed, E. E., Fox, D. T., Gates, J. and Peifer, M. (2003). "Balancing different types of actin polymerization at distinct sites: roles for Abelson kinase and Enabled." *J Cell Biol* **163**(6): 1267-79.
Grevengoed, E. E., Loureiro, J. J., Jesse, T. L. and Peifer, M. (2001). "Abelson kinase regulates epithelial morphogenesis in Drosophila." *J Cell Biol* **155**(7): 1185-98.
Groffen, J., Heisterkamp, N., Shibuya, M., Hanafusa, H. and Stephenson, J. R. (1983). "Transforming genes of avian (v-fps) and mammalian (v-fes) retroviruses correspond to a common cellular locus." *Virology* **125**(2): 480-6.
Gunawardena, S. and Goldstein, L. S. (2001). "Disruption of axonal transport and neuronal viability by amyloid precursor protein mutations in Drosophila." *Neuron* **32**(3): 389-401.
Hackenmiller, R., Kim, J., Feldman, R. A. and Simon, M. C. (2000). "Abnormal Stat activation, hematopoietic homeostasis, and innate immunity in c-fes-/- mice." *Immunity* **13**(3): 397-407.
Haigh, J., McVeigh, J. and Greer, P. (1996). "The fps/fes tyrosine kinase is expressed in myeloid, vascular endothelial, epithelial, and neuronal cells and is localized in the trans-golgi network." *Cell Growth Differ* **7**(7): 931-44.
Halder, G. and Carroll, S. B. (2001). "Binding of the Vestigial co-factor switches the DNA-target selectivity of the Scalloped selector protein." *Development* **128**(17): 3295-305.
Halder, G., Polaczyk, P., Kraus, M. E., Hudson, A., Kim, J., Laughon, A. and Carroll, S. (1998). "The Vestigial and Scalloped proteins act together to directly regulate wing-specific gene expression in Drosophila." *Genes Dev* **12**(24): 3900-9.

Hanahan, D. (1983). "Studies on transformation of Escherichia coli with plasmids." *J Mol Biol* **166**(4): 557-80.

Hao, Q. L., Ferris, D. K., White, G., Heisterkamp, N. and Groffen, J. (1991). "Nuclear and cytoplasmic location of the FER tyrosine kinase." *Mol Cell Biol* **11**(2): 1180-3.

Harden, N. (2002). "Signaling pathways directing the movement and fusion of epithelial sheets: lessons from dorsal closure in Drosophila." *Differentiation* **70**(4-5): 181-203.

Harden, N., Lee, J., Loh, H. Y., Ong, Y. M., Tan, I., Leung, T., Manser, E. and Lim, L. (1996). "A Drosophila homolog of the Rac- and Cdc42-activated serine/threonine kinase PAK is a potential focal adhesion and focal complex protein that colocalizes with dynamic actin structures." *Mol Cell Biol* **16**(5): 1896-908.

Heasman, J., Crawford, A., Goldstone, K., Garner-Hamrick, P., Gumbiner, B., McCrea, P., Kintner, C., Noro, C. Y. and Wylie, C. (1994). "Overexpression of cadherins and underexpression of beta-catenin inhibit dorsal mesoderm induction in early Xenopus embryos." *Cell* **79**(5): 791-803.

Heber, S., Herms, J., Gajic, V., Hainfellner, J., Aguzzi, A., Rulicke, T., von Kretzschmar, H., von Koch, C., Sisodia, S., Tremml, P., Lipp, H. P., Wolfer, D. P. and Muller, U. (2000). "Mice with combined gene knock-outs reveal essential and partially redundant functions of amyloid precursor protein family members." *J Neurosci* **20**(21): 7951-63.

Held, L.I., Duarte, C.M. and Derakhshanian, K. (1986). "Extra tarsal joints and abnormal cuticular polarities in various mutants of Drosophila melanogaster." *Roux Arch.* **195**, 145-57.

Herms, J., Anliker, B., Heber, S., Ring, S., Fuhrmann, M., Kretzschmar, H., Sisodia, S. and Muller, U. (2004). "Cortical dysplasia resembling human type 2 lissencephaly in mice lacking all three APP family members." *Embo J* **23**(20): 4106-15.

Hernandez, S. E., Krishnaswami, M., Miller, A. L. and Koleske, A. J. (2004). "How do Abl family kinases regulate cell shape and movement?" *Trends Cell Biol* **14**(1): 36-44.

Hidalgo, A. and Brand, A. H. (1997). "Targeted neuronal ablation: the role of pioneer neurons in guidance and fasciculation in the CNS of Drosophila." *Development* **124**(17): 3253-62.

Hill, K. and Bishop, J.M. (2004). "Dominant Modifiers of Drosophila Fer Over-Expression in the Wing." *45th Annual Drosophila Research Conference*: Poster 420 C.

Hjermstad, S. J., Peters, K. L., Briggs, S. D., Glazer, R. I. and Smithgall, T. E. (1993). "Regulation of the human c-fes protein tyrosine kinase (p93c-fes) by its src homology 2 domain and major autophosphorylation site (Tyr-713)." *Oncogene* **8**(8): 2283-92.

Ho, A. and Sudhof, T. C. (2004). "Binding of F-spondin to amyloid-beta precursor protein: a candidate amyloid-beta precursor protein ligand that modulates amyloid-beta precursor protein cleavage." *Proc Natl Acad Sci U S A* **101**(8): 2548-53.

Hoang, B. and Chiba, A. (1998). "Genetic analysis on the role of integrin during axon guidance in Drosophila." *J Neurosci* **18**(19): 7847-55.

Hoskins, R. A., Nelson, C. R., Berman, B. P., Laverty, T. R., George, R. A., Ciesiolka, L., Naeemuddin, M., Arenson, A. D., Durbin, J., David, R. G., Tabor, P. E., Bailey, M. R., DeShazo, D. R., Catanese, J., Mammoser, A., Osoegawa, K., de Jong, P. J., Celniker, S. E., Gibbs, R. A., Rubin, G. M. and Scherer, S. E. (2000). "A BAC-based physical map of the major autosomes of Drosophila melanogaster." *Science* **287**(5461): 2271-4.

Huang, A. M. and Rubin, G. M. (2000). "A misexpression screen identifies genes that can modulate RAS1 pathway signaling in Drosophila melanogaster." *Genetics* **156**(3): 1219-30.

Huang, C., Ni, Y., Wang, T., Gao, Y., Haudenschild, C. C. and Zhan, X. (1997). "Down-regulation of the filamentous actin cross-linking activity of cortactin by Src-mediated tyrosine phosphorylation." *J Biol Chem* **272**(21): 13911-5.

Hummel, T., Schimmelpfeng, K. and Klambt, C. (1999). "Commissure formation in the embryonic CNS of Drosophila." *Dev Biol* **209**(2): 381-98.

Iijima, K., Ando, K., Takeda, S., Satoh, Y., Seki, T., Itohara, S., Greengard, P., Kirino, Y., Nairn, A. C. and Suzuki, T. (2000). "Neuron-specific phosphorylation of Alzheimer's beta-amyloid precursor protein by cyclin-dependent kinase 5." *J Neurochem* **75**(3):

1085-91.
Iijima, K., Liu, H. P., Chiang, A. S., Hearn, S. A., Konsolaki, M. and Zhong, Y. (2004). "Dissecting the pathological effects of human Abeta40 and Abeta42 in Drosophila: a potential model for Alzheimer's disease." *Proc Natl Acad Sci U S A* **101**(17): 6623-8.
Ilic, D., Furuta, Y., Kanazawa, S., Takeda, N., Sobue, K., Nakatsuji, N., Nomura, S., Fujimoto, J., Okada, M. and Yamamoto, T. (1995). "Reduced cell motility and enhanced focal adhesion contact formation in cells from FAK-deficient mice." *Nature* **377**(6549): 539-44.
Irvine, K. D. (1999). "Fringe, Notch, and making developmental boundaries." *Curr Opin Genet Dev* **9**(4): 434-41.
Irvine, K. D. and Rauskolb, C. (2001). "Boundaries in development: formation and function." *Annu Rev Cell Dev Biol* **17**: 189-214.
Irvine, K. D. and Vogt, T. F. (1997). "Dorsal-ventral signaling in limb development." *Curr Opin Cell Biol* **9**(6): 867-76.
Iwanishi, M., Czech, M. P. and Cherniack, A. D. (2000). "The protein-tyrosine kinase fer associates with signaling complexes containing insulin receptor substrate-1 and phosphatidylinositol 3-kinase." *J Biol Chem* **275**(50): 38995-9000.
Jacinto, A., Wood, W., Balayo, T., Turmaine, M., Martinez-Arias, A. and Martin, P. (2000). "Dynamic actin-based epithelial adhesion and cell matching during Drosophila dorsal closure." *Curr Biol* **10**(22): 1420-6.
Jacinto, A., Woolner, S. and Martin, P. (2002). "Dynamic analysis of dorsal closure in Drosophila: from genetics to cell biology." *Dev Cell* **3**(1): 9-19.
Jiang, H., Foltenyi, K., Kashiwada, M., Donahue, L., Vuong, B., Hehn, B. and Rothman, P. (2001). "Fes mediates the IL-4 activation of insulin receptor substrate-2 and cellular proliferation." *J Immunol* **166**(4): 2627-34.
Kaksonen, M., Peng, H. B. and Rauvala, H. (2000). "Association of cortactin with dynamic actin in lamellipodia and on endosomal vesicles." *J Cell Sci* **113 Pt 24**: 4421-6.
Kaltschmidt, J. A., Lawrence, N., Morel, V., Balayo, T., Fernandez, B. G., Pelissier, A., Jacinto, A. and Martinez Arias, A. (2002). "Planar polarity and actin dynamics in the epidermis of Drosophila." *Nat Cell Biol* **4**(12): 937-44.
Katzen, A. L., Montarras, D., Jackson, J., Paulson, R. F., Kornberg, T. and Bishop, J. M. (1991). "A gene related to the proto-oncogene fps/fes is expressed at diverse times during the life cycle of Drosophila melanogaster." *Mol Cell Biol* **11**(1): 226-39.
Kennerdell, J. R. and Carthew, R. W. (1998). "Use of dsRNA-mediated genetic interference to demonstrate that frizzled and frizzled 2 act in the wingless pathway." *Cell* **95**(7): 1017-26.
Keshet, E., Itin, A., Fischman, K. and Nir, U. (1990). "The testis-specific transcript (ferT) of the tyrosine kinase FER is expressed during spermatogenesis in a stage-specific manner." *Mol Cell Biol* **10**(9): 5021-5.
Kibbey, M. C., Jucker, M., Weeks, B. S., Neve, R. L., Van Nostrand, W. E. and Kleinman, H. K. (1993). "beta-Amyloid precursor protein binds to the neurite-promoting IKVAV site of laminin." *Proc Natl Acad Sci U S A* **90**(21): 10150-3.
Kim, J., Sebring, A., Esch, J. J., Kraus, M. E., Vorwerk, K., Magee, J. and Carroll, S. B. (1996). "Integration of positional signals and regulation of wing formation and identity by Drosophila vestigial gene." *Nature* **382**(6587): 133-8.
Kim, L. and Wong, T. W. (1998). "Growth factor-dependent phosphorylation of the actin-binding protein cortactin is mediated by the cytoplasmic tyrosine kinase FER." *J Biol Chem* **273**(36): 23542-8.
Klambt, C., Schimmelpfeng, K. and Hummel, T. (1997). "Genetic analysis of axon pattern formation in the embryonic CNS of Drosophila." *Invert Neurosci* **3**(2-3): 165-74.
Klein, T. and Arias, A. M. (1998). "Different spatial and temporal interactions between Notch, wingless, and vestigial specify proximal and distal pattern elements of the wing in Drosophila." *Dev Biol* **194**(2): 196-212.
Koo, E. H. (2002). "The beta-amyloid precursor protein (APP) and Alzheimer's disease: does the tail wag the dog?" *Traffic* **3**(11): 763-70.
Kornberg, T., Siden, I., O'Farrell, P. and Simon, M. (1985). "The engrailed locus of

Drosophila: in situ localization of transcripts reveals compartment-specific expression." *Cell* **40**(1): 45-53.
Laemmli, U. K. (1970). "Cleavage of structural proteins during the assembly of the head of bacteriophage T4." *Nature* **227**(5259): 680-5.
Lai, E. C. (2004). "Notch signaling: control of cell communication and cell fate." *Development* **131**(5): 965-73.
Lanier, L. M. and Gertler, F. B. (2000). "From Abl to actin: Abl tyrosine kinase and associated proteins in growth cone motility." *Curr Opin Neurobiol* **10**(1): 80-7.
Lee, M. S., Kao, S. C., Lemere, C. A., Xia, W., Tseng, H. C., Zhou, Y., Neve, R., Ahlijanian, M. K. and Tsai, L. H. (2003). "APP processing is regulated by cytoplasmic phosphorylation." *J Cell Biol* **163**(1): 83-95.
Lee, S. B., Cho, K. S., Kim, E. and Chung, J. (2003). "blistery encodes Drosophila tensin protein and interacts with integrin and the JNK signaling pathway during wing development." *Development* **130**(17): 4001-10.
Lee, Y. S. and Carthew, R. W. (2003). "Making a better RNAi vector for Drosophila: use of intron spacers." *Methods* **30**(4): 322-9.
Letwin, K., Yee, S. P. and Pawson, T. (1988). "Novel protein-tyrosine kinase cDNAs related to fps/fes and eph cloned using anti-phosphotyrosine antibody." *Oncogene* **3**(6): 621-7.
Lewis, J. M., Baskaran, R., Taagepera, S., Schwartz, M. A. and Wang, J. Y. (1996). "Integrin regulation of c-Abl tyrosine kinase activity and cytoplasmic-nuclear transport." *Proc Natl Acad Sci U S A* **93**(26): 15174-9.
Lewis, J. M. and Schwartz, M. A. (1998). "Integrins regulate the association and phosphorylation of paxillin by c-Abl." *J Biol Chem* **273**(23): 14225-30.
Li, H., Leung, T. C., Hoffman, S., Balsamo, J. and Lilien, J. (2000). "Coordinate regulation of cadherin and integrin function by the chondroitin sulfate proteoglycan neurocan." *J Cell Biol* **149**(6): 1275-88.
Li, J. and Smithgall, T. E. (1998). "Fibroblast transformation by Fps/Fes tyrosine kinases requires Ras, Rac, and Cdc42 and induces extracellular signal-regulated and c-Jun N-terminal kinase activation." *J Biol Chem* **273**(22): 13828-34.
Lindsley, D. L. and Grell, E. H. (1969). "Spermiogenesis without chromosomes in Drosophila melanogaster." *Genetics* **61**(1): Suppl:69-78.
Liu, X., Grammont, M. and Irvine, K. D. (2000). "Roles for scalloped and vestigial in regulating cell affinity and interactions between the wing blade and the wing hinge." *Dev Biol* **228**(2): 287-303.
Loewer, A., Soba, P., Beyreuther, K., Paro, R. and Merdes, G. (2004). "Cell-type-specific processing of the amyloid precursor protein by Presenilin during Drosophila development." *EMBO Rep* **5**(4): 405-11.
Luo, L., Tully, T. and White, K. (1992). "Human amyloid precursor protein ameliorates behavioral deficit of flies deleted for Appl gene." *Neuron* **9**(4): 595-605.
MacDonald, I., Levy, J. and Pawson, T. (1985). "Expression of the mammalian c-fes protein in hematopoietic cells and identification of a distinct fes-related protein." *Mol Cell Biol* **5**(10): 2543-51.
Mahoney, P. A., Weber, U., Onofrechuk, P., Biessmann, H., Bryant, P. J. and Goodman, C. S. (1991). "The fat tumor suppressor gene in Drosophila encodes a novel member of the cadherin gene superfamily." *Cell* **67**(5): 853-68.
Martin-Morris, L. E. and White, K. (1990). "The Drosophila transcript encoded by the beta-amyloid protein precursor-like gene is restricted to the nervous system." *Development* **110**(1): 185-95.
Martinez Arias, A. (1993). "Development and patterning of the larval epidermis of Drosophila." In *The Development of Drosophila* (Vol.I) (Bate, M. and Martinez Arias, A., *eds*), pp. 517-608. Cold Spring Harbor Laboratory Press, NY.
Maru, Y., Peters, K. L., Afar, D. E., Shibuya, M., Witte, O. N. and Smithgall, T. E. (1995). "Tyrosine phosphorylation of BCR by FPS/FES protein-tyrosine kinases induces association of BCR with GRB-2/SOS." *Mol Cell Biol* **15**(2): 835-42.
Matakatsu, H. and Blair, S. S. (2004). "Interactions between Fat and Dachsous and the

regulation of planar cell polarity in the Drosophila wing." *Development* **131**(15): 3785-94.

Mattson, M. P. (2002). "Oxidative stress, perturbed calcium homeostasis, and immune dysfunction in Alzheimer's disease." *J Neurovirol* **8**(6): 539-50.

McEwen, D. G., Cox, R. T. and Peifer, M. (2000). "The canonical Wg and JNK signaling cascades collaborate to promote both dorsal closure and ventral patterning." *Development* **127**(16): 3607-17.

McGovern, V. L., Pacak, C. A., Sewell, S. T., Turski, M. L. and Seeger, M. A. (2003). "A targeted gain of function screen in the embryonic CNS of Drosophila." *Mech Dev* **120**(10): 1193-207.

Mello, C. C. and Conte, D., Jr. (2004). "Revealing the world of RNA interference." *Nature* **431**(7006): 338-42.

Merdes, G., Soba, P., Loewer, A., Bilic, M. V., Beyreuther, K. and Paro, R. (2004). "Interference of human and Drosophila APP and APP-like proteins with PNS development in Drosophila." *Embo J* **23**(20): 4082-95.

Micchelli, C. A., Rulifson, E. J. and Blair, S. S. (1997). "The function and regulation of cut expression on the wing margin of Drosophila: Notch, Wingless and a dominant negative role for Delta and Serrate." *Development* **124**(8): 1485-95.

Milan, M. and Cohen, S. M. (2003). "A re-evaluation of the contributions of Apterous and Notch to the dorsoventral lineage restriction boundary in the Drosophila wing." *Development* **130**(3): 553-62.

Milan, M., Weihe, U., Tiong, S., Bender, W. and Cohen, S. M. (2001). "msh specifies dorsal cell fate in the Drosophila wing." *Development* **128**(17): 3263-8.

Mirkovic, I., Charish, K., Gorski, S. M., McKnight, K. and Verheyen, E. M. (2002). "Drosophila nemo is an essential gene involved in the regulation of programmed cell death." *Mech Dev* **119**(1): 9-20.

Misquitta, L. and Paterson, B. M. (1999). "Targeted disruption of gene function in Drosophila by RNA interference (RNA-i): a role for nautilus in embryonic somatic muscle formation." *Proc Natl Acad Sci U S A* **96**(4): 1451-6.

Mlodzik, M. (1999). "Planar polarity in the Drosophila eye: a multifaceted view of signaling specificity and cross-talk." *Embo J* **18**(24): 6873-9.

Mohit, P., Ruchi, B. and Shashidhara, L. S. (2003). "Regulation of Wingless and Vestigial expression in wing and haltere discs of Drosophila." *Development* **130** (8): 1537-47.

Morata, G. and Lawrence, P. A. (1977). "The development of wingless, a homeotic mutation of Drosophila." *Dev Biol* **56**(2): 227-40.

Morel, V. and Arias, A. M. (2004). "Armadillo/beta-catenin-dependent Wnt signalling is required for the polarisation of epidermal cells during dorsal closure in Drosophila." *Development* **131**(14): 3273-83.

Muller, U., Cristina, N., Li, Z. W., Wolfer, D. P., Lipp, H. P., Rulicke, T., Brandner, S., Aguzzi, A. and Weissman, C. (1996). "Mice homozygous for a modified beta-amyloid precursor protein (beta APP) gene show impaired behavior and high incidence of agenesis of the corpus callosum." *Ann N Y Acad Sci* **777**: 65-73.

Muller, U., Cristina, N., Li, Z. W., Wolfer, D. P., Lipp, H. P., Rulicke, T., Brandner, S., Aguzzi, A. and Weissmann, C. (1994). "Behavioral and anatomical deficits in mice homozygous for a modified beta-amyloid precursor protein gene." *Cell* **79**(5): 755-65.

Multhaup, G., Mechler, H. and Masters, C. L. (1995). "Characterization of the high affinity heparin binding site of the Alzheimer's disease beta A4 amyloid precursor protein (APP) and its enhancement by zinc(II)." *J Mol Recognit* **8**(4): 247-57.

Muqit, M. M. and Feany, M. B. (2002). "Modelling neurodegenerative diseases in Drosophila: a fruitful approach?" *Nat Rev Neurosci* **3**(3): 237-43.

Muresan, Z. and Muresan, V. (2004). "A phosphorylated, carboxy-terminal fragment of beta-amyloid precursor protein localizes to the splicing factor compartment." *Hum Mol Genet* **13**(5): 475-88.

Murray, M.J., Hayward, N.M. and Brand, A.H. (2001). "DFer: A cytoplasmic tyrosine kinase involved in neural development and dorsal closure." *Bellen, Taylor*: 230

Myster, S. H., Cavallo, R., Anderson, C. T., Fox, D. T. and Peifer, M. (2003). "Drosophila

p120catenin plays a supporting role in cell adhesion but is not an essential adherens junction component." *J Cell Biol* **160**(3): 433-49.

Nagel, A. C., Maier, D. and Preiss, A. (2000). "Su(H)-independent activity of hairless during mechano-sensory organ formation in Drosophila." *Mech Dev* **94**(1-2): 3-12.

Narindrasorasak, S., Lowery, D., Gonzalez-DeWhitt, P., Poorman, R. A., Greenberg, B. and Kisilevsky, R. (1991). "High affinity interactions between the Alzheimer's beta-amyloid precursor proteins and the basement membrane form of heparan sulfate proteoglycan." *J Biol Chem* **266**(20): 12878-83.

Nelson, W. J. and Nusse, R. (2004). "Convergence of Wnt, beta-catenin, and cadherin pathways." *Science* **303**(5663): 1483-7.

Neumann, C. J. and Cohen, S. M. (1996). "A hierarchy of cross-regulation involving Notch, wingless, vestigial and cut organizes the dorsal/ventral axis of the Drosophila wing." *Development* **122**(11): 3477-85.

Neumann, C. J. and Cohen, S. M. (1997). "Long-range action of Wingless organizes the dorsal-ventral axis of the Drosophila wing." *Development* **124**(4): 871-80.

Ng, M., Diaz-Benjumea, F. J., Vincent, J. P., Wu, J. and Cohen, S. M. (1996). "Specification of the wing by localized expression of wingless protein." *Nature* **381**(6580): 316-8.

Pacquelet, A., Lin, L. and Rorth, P. (2003). "Binding site for p120/delta-catenin is not required for Drosophila E-cadherin function in vivo." *J Cell Biol* **160**(3): 313-9.

Palmer, R. H., Fessler, L. I., Edeen, P. T., Madigan, S. J., McKeown, M. and Hunter, T. (1999). "DFak56 is a novel Drosophila melanogaster focal adhesion kinase." *J Biol Chem* **274**(50): 35621-9.

Papayannopoulos, V., Tomlinson, A., Panin, V. M., Rauskolb, C. and Irvine, K. D. (1998). "Dorsal-ventral signaling in the Drosophila eye." *Science* **281**(5385): 2031-4.

Park, Y., Rangel, C., Reynolds, M. M., Caldwell, M. C., Johns, M., Nayak, M., Welsh, C. J., McDermott, S. and Datta, S. (2003). "Drosophila perlecan modulates FGF and hedgehog signals to activate neural stem cell division." *Dev Biol* **253**(2): 247-57.

Parsons, J. T. (2003). "Focal adhesion kinase: the first ten years." *J Cell Sci* **116**(Pt 8): 1409-16.

Paulson, R., Jackson, J., Immergluck, K. and Bishop, J. M. (1997). "The DFer gene of Drosophila melanogaster encodes two membrane-associated proteins that can both transform vertebrate cells." *Oncogene* **14**(6): 641-52.

Pawson, T., Letwin, K., Lee, T., Hao, Q. L., Heisterkamp, N. and Groffen, J. (1989). "The FER gene is evolutionarily conserved and encodes a widely expressed member of the FPS/FES protein-tyrosine kinase family." *Mol Cell Biol* **9**(12): 5722-5.

Payre, F., Vincent, A. and Carreno, S. (1999). "ovo/svb integrates Wingless and DER pathways to control epidermis differentiation." *Nature* **400**(6741): 271-5.

Pecasse, F., Beck, Y., Ruiz, C. and Richards, G. (2000). "Kruppel-homolog, a stage-specific modulator of the prepupal ecdysone response, is essential for Drosophila metamorphosis." *Dev Biol* **221**(1): 53-67.

Pfeifer, M., Sweeton, D., Casey, M. and Wieschaus, E. (1994). "Wingless signal and zeste-white 3 kinase trigger opposing changes in the intracellular distribution of Arm." *Development* **120**(2): 369-80.

Peifer, M., Rauskolb, C., Williams, M., Riggleman, B. and Wieschaus, E. (1991). "The segment polarity gene armadillo interacts with the wingless signaling pathway in both embryonic and adult pattern formation." *Development* **111**(4): 1029-43.

Peifer, M. and Wieschaus, E. (1990). "The segment polarity gene armadillo encodes a functionally modular protein that is the Drosophila homolog of human plakoglobin." *Cell* **63**(6): 1167-76.

Piedra, J., Miravet, S., Castano, J., Palmer, H. G., Heisterkamp, N., Garcia de Herreros, A. and Dunach, M. (2003). "p120 Catenin-associated Fer and Fyn tyrosine kinases regulate beta-catenin Tyr-142 phosphorylation and beta-catenin-alpha-catenin Interaction." *Mol Cell Biol* **23**(7): 2287-97.

Pirrotta, V. (1988). "Vectors for P-mediated transformation in Drosophila." *Biotechnology* **10**: 437-56.

Podos, S. D. and Ferguson, E. L. (1999). "Morphogen gradients: new insights from DPP."

Trends Genet **15**(10): 396-402.
Preston, C. R. and Engels, W. R. (1996). "P-element-induced male recombination and gene conversion in Drosophila." *Genetics* **144**(4): 1611-22.
Read, R. D., Lionberger, J. M. and Smithgall, T. E. (1997). "Oligomerization of the Fes tyrosine kinase. Evidence for a coiled-coil domain in the unique N-terminal region." *J Biol Chem* **272**(29): 18498-503.
Reichhart, J. M., Ligoxygakis, P., Naitza, S., Woerfel, G., Imler, J. L. and Gubb, D. (2002). "Splice-activated UAS hairpin vector gives complete RNAi knockout of single or double target transcripts in Drosophila melanogaster." *Genesis* **34**(1-2): 160-4.
Reiter, L. T., Potocki, L., Chien, S., Gribskov, M. and Bier, E. (2001). "A systematic analysis of human disease-associated gene sequences in Drosophila melanogaster." *Genome Res* **11**(6): 1114-25.
Rhee, J., Lilien, J. and Balsamo, J. (2001). "Essential tyrosine residues for interaction of the non-receptor protein-tyrosine phosphatase PTP1B with N-cadherin." *J Biol Chem* **276**(9): 6640-4.
Rhee, J., Mahfooz, N. S., Arregui, C., Lilien, J., Balsamo, J. and VanBerkum, M. F. (2002). "Activation of the repulsive receptor Roundabout inhibits N-cadherin-mediated cell adhesion." *Nat Cell Biol* **4**(10): 798-805.
Rodriguez, I. (2004). "The dachsous gene, a member of the cadherin family, is required for Wg-dependent pattern formation in the Drosophila wing disc." *Development* **131**(13): 3195-206.
Rohrbough, J., Grotewiel, M. S., Davis, R. L. and Broadie, K. (2000). "Integrin-mediated regulation of synaptic morphology, transmission, and plasticity." *J Neurosci* **20**(18): 6868-78.
Roman, G. (2004). "The genetics of Drosophila transgenics." *Bioessays* **26**(11): 1243-53.
Rorth, P. (1996). "A modular misexpression screen in Drosophila detecting tissue-specific phenotypes." *Proc Natl Acad Sci U S A* **93**(22): 12418-22.
Rorth, P., Szabo, K., Bailey, A., Laverty, T., Rehm, J., Rubin, G. M., Weigmann, K., Milan, M., Benes, V., Ansorge, W. and Cohen, S. M. (1998). "Systematic gain-of-function genetics in Drosophila." *Development* **125**(6): 1049-57.
Rosato, R., Veltmaat, J. M., Groffen, J. and Heisterkamp, N. (1998). "Involvement of the tyrosine kinase fer in cell adhesion." *Mol Cell Biol* **18**(10): 5762-70.
Rubin, G. M. and Spradling, A. C. (1982). "Genetic transformation of Drosophila with transposable element vectors." *Science* **218**(4570): 348-53.
Ryoo, H. D., Gorenc, T. and Steller, H. (2004). "Apoptotic cells can induce compensatory cell proliferation through the JNK and the Wingless signaling pathways." *Dev Cell* **7**(4): 491-501.
Sabo, S. L., Ikin, A. F., Buxbaum, J. D. and Greengard, P. (2001). "The Alzheimer amyloid precursor protein (APP) and FE65, an APP-binding protein, regulate cell movement." *J Cell Biol* **153**(7): 1403-14.
Salz, H. K., Cline, T. W. and Schedl, P. (1987). "Functional changes associated with structural alterations induced by mobilization of a P element inserted in the Sex-lethal gene of Drosophila." *Genetics* **117**(2): 221-31.
Samarut, J., Mathey-Prevot, B. and Hanafusa, H. (1985). "Preferential expression of the c-fps protein in chicken macrophages and granulocytic cells." *Mol Cell Biol* **5**(5): 1067-72.
Sanson, B., White, P. and Vincent, J. P. (1996). "Uncoupling cadherin-based adhesion from wingless signalling in Drosophila." *Nature* **383**(6601): 627-30.
Scheinfeld, M. H., Matsuda, S. and D'Adamio, L. (2003). "JNK-interacting protein-1 promotes transcription of A beta protein precursor but not A beta precursor-like proteins, mechanistically different than Fe65." *Proc Natl Acad Sci U S A* **100**(4): 1729-34.
Schneider, I. (1972). "Cell lines derived from late embryonic stages of Drosophila melanogaster." *J Embryol Exp Morphol* **27**(2): 353-65.
Schock, F. and Perrimon, N. (2002). "Molecular mechanisms of epithelial morphogenesis." *Annu Rev Cell Dev Biol* **18**: 463-93.
Selkoe, D. and Kopan, R. (2003). "Notch and Presenilin: regulated intramembrane

proteolysis links development and degeneration." *Annu Rev Neurosci* **26**: 565-97.
Senis, Y., Zirngibl, R., McVeigh, J., Haman, A., Hoang, T. and Greer, P. A. (1999). "Targeted disruption of the murine fps/fes proto-oncogene reveals that Fps/Fes kinase activity is dispensable for hematopoiesis." *Mol Cell Biol* **19**(11): 7436-46.
Senis, Y. A., Craig, A. W. and Greer, P. A. (2003). "Fps/Fes and Fer protein-tyrosinekinases play redundant roles in regulating hematopoiesis." *Exp Hematol* **31**(8): 673-81.
Senis, Y. A., Sangrar, W., Zirngibl, R. A., Craig, A. W., Lee, D. H. and Greer, P. A. (2003). "Fps/Fes and Fer non-receptor protein-tyrosine kinases regulate collagen- and ADP-induced platelet aggregation." *J Thromb Haemost* **1**(5): 1062-70.
Sentry, J. W. and Kaiser, K. (1992). "P element transposition and targeted manipulation of the Drosophila genome." *Trends Genet* **8**(10): 329-31.
Seto, E. S. and Bellen, H. J. (2004). "The ins and outs of Wingless signaling." *Trends Cell Biol* **14**(1): 45-53.
Sharma, R. P. and Chopra, V. L. (1976). "Effect of the Wingless (wg1) mutation on wing and haltere development in Drosophila melanogaster." *Dev Biol* **48**(2): 461-5.
Shellenbarger, D. L. and Mohler, J. D. (1978). "Temperature-sensitive periods and autonomy of pleiotropic effects of l(1)Nts1, a conditional notch lethal in Drosophila." *Dev Biol* **62**(2): 432-46.
Simmonds, A. J., Liu, X., Soanes, K. H., Krause, H. M., Irvine, K. D. and Bell, J. B. (1998). "Molecular interactions between Vestigial and Scalloped promote wing formation in Drosophila." *Genes Dev.* **12** (24): 3815-20
Smithgall, T. E., Rogers, J. A., Peters, K. L., Li, J., Briggs, S. D., Lionberger, J. M., Cheng, H., Shibata, A., Scholtz, B., Schreiner, S. and Dunham, N. (1998). "The c-Fes family of protein-tyrosine kinases." *Crit Rev Oncog* **9**(1): 43-62.
Soba, P. (2004). "Studies of the cell biological function of the Amyloid Precursor Protein (APP) family in Drosophila melanogaster and mammals." *PhD thesis*, Heidelberg.
Somogyi, K. and Rorth, P. (2004). "Cortactin modulates cell migration and ring canal morphogenesis during Drosophila oogenesis." *Mech Dev* **121**(1): 57-64.
Spradling, A. C. and Rubin, G. M. (1982). "Transposition of cloned P elements into Drosophila germ line chromosomes." *Science* **218**(4570): 341-7.
Steller, H. and Pirrotta, V. (1985). "Fate of DNA injected into early Drosophila embryos." *Dev Biol* **109**(1): 54-62.
Stevens, A. and Jacobs, J. R. (2002). "Integrins regulate responsiveness to slit repellent signals." *J Neurosci* **22**(11): 4448-55.
Storey, E., Beyreuther, K. and Masters, C. L. (1996). "Alzheimer's disease amyloid precursor protein on the surface of cortical neurons in primary culture co-localizes with adhesion patch components." *Brain Res* **735**(2): 217-31.
Strutt, H., Mundy, J., Hofstra, K. and Strutt, D. (2004). "Cleavage and secretion is not required for Four-jointed function in Drosophila patterning." *Development* **131**(4): 881-90.
Tabata, T. and Takei, Y. (2004). "Morphogens, their identification and regulation." *Development* **131**(4): 703-12.
Takashima, Y., Delfino, F. J., Engen, J. R., Superti-Furga, G. and Smithgall, T. E. (2003). "Regulation of c-Fes tyrosine kinase activity by coiled-coil and SH2 domains: analysis with Saccharomyces cerevisiae." *Biochemistry* **42**(12): 3567-74.
Tapon, N. (2003). "Modeling transformation and metastasis in Drosophila." *Cancer Cell* **4**(5): 333-5.
Telese, F., Bruni, P., Donizetti, A., Gianni, D., D'Ambrosio, C., Scaloni, A., Zambrano, N., Rosenfeld, M. G. and Russo, T. (2005). "Transcription regulation by the adaptor protein Fe65 and the nucleosome assembly factor SET." *EMBO Rep* **6**(1): 77-82.
Tepass, U., Truong, K., Godt, D., Ikura, M. and Peifer, M. (2000). "Cadherins in embryonic and neural morphogenesis." *Nat Rev Mol Cell Biol* **1**(2): 91-100.
Torgler, C. N., Narasimha, M., Knox, A. L., Zervas, C. G., Vernon, M. C. and Brown, N. H. (2004). "Tensin stabilizes integrin adhesive contacts in Drosophila." *Dev Cell* **6**(3): 357-69.
Torroja, L., Chu, H., Kotovsky, I. and White, K. (1999). "Neuronal overexpression of APPL,

the Drosophila homologue of the amyloid precursor protein (APP), disrupts axonal transport." *Curr Biol* **9**(9): 489-92.

Torroja, L., Luo, L. and White, K. (1996). "APPL, the Drosophila member of the APP-family, exhibits differential trafficking and processing in CNS neurons." *J Neurosci* **16**(15): 4638-50.

Torroja, L., Packard, M., Gorczyca, M., White, K. and Budnik, V. (1999). "The Drosophila beta-amyloid precursor protein homolog promotes synapse differentiation at the neuromuscular junction." *J Neurosci* **19**(18): 7793-803.

Tsubota, S. and Schedl, P. (1986). "Hybrid dysgenesis-induced revertants of insertions at the 5' end of the rudimentary gene in Drosophila melanogaster: Transposon-induced control mutations." *Genetics* **114** (1): 165-82.

Turner, P. R., O'Connor, K., Tate, W. P. and Abraham, W. C. (2003). "Roles of amyloid precursor protein and its fragments in regulating neural activity, plasticity and memory." *Prog Neurobiol* **70**(1): 1-32.

Uruno, T., Liu, J., Zhang, P., Fan, Y., Egile, C., Li, R., Mueller, S. C. and Zhan, X. (2001). "Activation of Arp2/3 complex-mediated actin polymerization by cortactin." *Nat Cell Biol* **3**(3): 259-66.

van de Wetering, M., Cavallo, R., Dooijes, D., van Beest, M., van Es, J., Loureiro, J., Ypma, A., Hursh, D., Jones, T., Bejsovec, A., Peifer, M., Mortin, M. and Clevers, H. (1997). "Armadillo coactivates transcription driven by the product of the Drosophila segment polarity gene dTCF." *Cell* **88**(6): 789-99.

Vastrik, I., Eickholt, B. J., Walsh, F. S., Ridley, A. and Doherty, P. (1999). "Sema3A-induced growth-cone collapse is mediated by Rac1 amino acids 17-32." *Curr Biol* **9**(18): 991-8.

Vervoort, M. (2000). "hedgehog and wing development in Drosophila: a morphogen at work?" *Bioessays* **22**(5): 460-8.

Villano, J. L. and Katz, F. N. (1995). "four-jointed is required for intermediate growth in the proximal-distal axis in Drosophila." *Development* **121**(9): 2767-77.

Vleminckx, K. and Kemler, R. (1999). "Cadherins and tissue formation: integrating adhesion and signaling." *Bioessays* **21**(3): 211-20.

Voas, M. G. and Rebay, I. (2004). "Signal integration during development: insights from the Drosophila eye." *Dev Dyn* **229**(1): 162-75.

Voigt, A., Pflanz, R., Schafer, U. and Jackle, H. (2002). "Perlecan participates in proliferation activation of quiescent Drosophila neuroblasts." *Dev Dyn* **224**(4): 403-12.

von Koch, C. S., Zheng, H., Chen, H., Trumbauer, M., Thinakaran, G., van der Ploeg, L. H., Price, D. L. and Sisodia, S. S. (1997). "Generation of APLP2 KO mice and early postnatal lethality in APLP2/APP double KO mice." *Neurobiol Aging* **18**(6): 661-9.

von Rotz, R. C., Kohli, B. M., Bosset, J., Meier, M., Suzuki, T., Nitsch, R. M. and Konietzko, U. (2004). "The APP intracellular domain forms nuclear multiprotein complexes and regulates the transcription of its own precursor." *J Cell Sci* **117**(Pt 19): 4435-48.

Waddington, C. H. (1943). "The development of some 'leg genes' in Drosophila." *J. Genet.* **45**, 29-43.

Wang, Y. and Ha, Y. (2004). "The X-ray structure of an antiparallel dimer of the human amyloid precursor protein E2 domain." *Mol Cell* **15**(3): 343-53.

Wang, Y. J., Chen, G. H., Hu, X. Y., Lu, Y. P., Zhou, J. N. and Liu, R. Y. (2005). "The expression of calcium/calmodulin-dependent protein kinase II-alpha in the hippocampus of patients with Alzheimer's disease and its links with AD-related pathology." *Brain Res* **1031**(1): 101-8.

Watt, F. M. (2002). "Role of integrins in regulating epidermal adhesion, growth and differentiation." *Embo J* **21**(15): 3919-26.

Weaver, A. M., Karginov, A. V., Kinley, A. W., Weed, S. A., Li, Y., Parsons, J. T. and Cooper, J. A. (2001). "Cortactin promotes and stabilizes Arp2/3-induced actin filament network formation." *Curr Biol* **11**(5): 370-4.

Williams, J. A., Bell, J. B. and Carroll, S. B. (1991). "Control of Drosophila wing and haltere development by the nuclear vestigial gene product." *Genes Dev* **5**(12B): 2481-95.

Williams, J. A., Paddock, S. W. and Carroll, S. B. (1993). "Pattern formation in a secondary

field: a hierarchy of regulatory genes subdivides the developing Drosophila wing disc into discrete subregions." *Development* **117**(2): 571-84.

Williams, J. A., Paddock, S. W., Vorwerk, K. and Carroll, S. B. (1994). "Organization of wing formation and induction of a wing-patterning gene at the dorsal/ventral compartment boundary." *Nature* **368**(6469): 299-305.

Williamson, T. G., Nurcombe, V., Beyreuther, K., Masters, C. L. and Small, D. H. (1995). "Affinity purification of proteoglycans that bind to the amyloid protein precursor of Alzheimer's disease." *J Neurochem* **65**(5): 2201-8.

Xu, G., Arregui, C., Lilien, J. and Balsamo, J. (2002). "PTP1B modulates the association of beta-catenin with N-cadherin through binding to an adjacent and partially overlapping target site." *J Biol Chem* **277**(51): 49989-97.

Xu, G., Craig, A. W., Greer, P., Miller, M., Anastasiadis, P. Z., Lilien, J. and Balsamo, J. (2004). "Continuous association of cadherin with beta-catenin requires the non-receptor tyrosine-kinase Fer." *J Cell Sci* **117**(Pt 15): 3207-19.

Yagi, Y., Tomita, S., Nakamura, M. and Suzuki, T. (2000). "Overexpression of human amyloid precursor protein in Drosophila." *Mol Cell Biol Res Commun* **4**(1): 43-9.

Yamazaki, T., Koo, E. H. and Selkoe, D. J. (1997). "Cell surface amyloid beta-protein precursor colocalizes with beta 1 integrins at substrate contact sites in neural cells." *J Neurosci* **17**(3): 1004-10.

Yates, K. E., Lynch, M. R., Wong, S. G., Slamon, D. J. and Gasson, J. C. (1995). "Human c-FES is a nuclear tyrosine kinase." *Oncogene* **10**(6): 1239-42.

Ye, Y., Lukinova, N. and Fortini, M. E. (1999). "Neurogenic phenotypes and altered Notch processing in Drosophila Presenilin mutants." *Nature* **398**(6727): 525-9.

Yee, S. P., Mock, D., Greer, P., Maltby, V., Rossant, J., Bernstein, A. and Pawson, T. (1989). "Lymphoid and mesenchymal tumors in transgenic mice expressing the v-fps protein-tyrosine kinase." *Mol Cell Biol* **9**(12): 5491-9.

Yee, S. P., Mock, D., Maltby, V., Silver, M., Rossant, J., Bernstein, A. and Pawson, T. (1989). "Cardiac and neurological abnormalities in v-fps transgenic mice." *Proc Natl Acad Sci U S A* **86**(15): 5873-7.

Zecca, M., Basler, K. and Struhl, G. (1996). "Direct and long-range action of a wingless morphogen gradient." *Cell* **87**(5): 833-44.

Zeidler, M. P., Perrimon, N. and Strutt, D. I. (1999). "The four-jointed gene is required in the Drosophila eye for ommatidial polarity specification." *Curr Biol* **9**(23): 1363-72.

Zeidler, M. P., Perrimon, N. and Strutt, D. I. (2000). "Multiple roles for four-jointed in planar polarity and limb patterning." *Dev Biol* **228**(2): 181-96.

Zeng, Y. A. and Verheyen, E. M. (2004). "Nemo is an inducible antagonist of Wingless signaling during Drosophila wing development." *Development* **131**(12): 2911-20.

Zirngibl, R., Schulze, D., Mirski, S. E., Cole, S. P. and Greer, P. A. (2001). "Subcellular localization analysis of the closely related Fps/Fes and Fer protein-tyrosine kinases suggests a distinct role for Fps/Fes in vesicular trafficking." *Exp Cell Res* **266**(1): 87-94.

Zirngibl, R. A., Senis, Y. and Greer, P. A. (2002). "Enhanced endotoxin sensitivity in fps/fes-null mice with minimal defects in hematopoietic homeostasis." *Mol Cell Biol* **22**(8): 2472-86.

Appendix

8 Appendix

8.1 Abbreviations

Amino acids:

Alanine	A	Ala
Arginine	R	Arg
Asparagine	N	Asn
Aspartate	D	Asp
Cysteine	C	Cys
Glutamine	Q	Gln
Glutamate	E	Glu
Glycine	G	Gly
Histidine	H	His
Isoleucine	I	Ile
Leucine	L	Leu
Lysine	K	Lys
Methionine	M	Met
Phenylalanine	F	Phe
Proline	P	Pro
Serine	S	Ser
Threonine	T	Thr
Tryptophan	W	Trp
Tyrosine	Y	Tyr
Valine	V	Val

Genes, chromosomal markers, proteins and protein domains:

Aβ	Amyloid-β peptide
abl	*abelson*
ADAM	A Disintegrin and Metalloprotease
A^{ID}	APP intracellular domain
ap	*apterous*
APLP	Amyloid precursor like protein
APP	Amyloid precursor protein
APPL	Amyloid precursor protein like
Arm	Armadillo
BACE	Beta-site APP-cleaving enzyme
Bc	Black cells
BcGla	ln(2LR)*Gla*, Bc^{1} Gla^{1}, 2. chromosome balancer
BCR	Breakpoint cluster region
β-int	*β-integrin*
bsk	*basket*
CaMKII	Calcium/calmodulin-dependent protein kinase II
crt	*cortactin*
ct	*cut*
CTF	C-terminal fragment
Cyo	*Curly of Oster*, 2. chromosome balancer
dfer-A	*dfer* transcript R-A
dfer-B	*dfer* transcript R-B
dfer-C	*dfer* transcript R-C
dfer-D	*dfer* transcript R-D
dfer-DN	*dfer* with dominant-negative mutation
Dpp	Decapentaplegic
EGFR	Epidermal growth factor receptor
en	*engrailed*
ERK	Extracellular singal-regulated kinase

FAK	Focal adhesion kinase
GFP	Green fluorescent protein
Gla	*Glazed*
H	*Hairless*
hep	*hemipterous*
hFes	human Fes
Hh	Hedgehog
JNK	Jun N-terminal kinase
MAPK	Mitogen activated pathway kinase
mFer	murine Fer
N	*Notch*
Ncad	*N-cadherin*
PI3K	*Phoshatidylinositol-3 kinase*
PTP1B	Phosphotyrosine phosphatase 1B
p120ctn	*p120catenin*
sAPP	secreted APP fragment
sd	*scalloped*
sgg	*shaggy*
shg	*shotgun*
St	*Stubble*
STAT	Signal transducer and activator of transcription
Su(H)	*Suppressor of Hairless*
TM	Third Multiple, 3. chromosome balancer
trol	*terribly reduced optic lobes*
Ubx	*Ultrabithorax*
Vg	Vestigial
w	*white*
Wg	Wingless
zwim	*zwirbelmütze*

Other:

aa	Amino acid
AD	Alzheimer's disease
Amp	Ampicillin
AP	Alkaline Phosphatase
A/P	anteroposterior
APS	Ammonium peroxodisulfate
ATP	Adenosine-5'-triphosphate
BAC	Bacterial artificial chromosome
bp	base pair
BSA	Bovine serum albumine
CC	Coiled coil
CG	Computational gene
Ci	Curie
CIP	Calf intestinal phosphatase
CNS	Central nervous system
CT	Cytoplasmic tail
DMSO	Dimethylsulfoxid
DN	dominant-negative
DNA	Desoxyribonucleic acid
dsRNA	double-stranded RNA
DTT	Dithiothreitol
D/V	dorsoventral
E. coli	*Escherichia coli*
ED	Extracellular domain
EDTA	Ethylendiaminotetraacetic acid
EP-element	Enhancer-Promoter element
FCH	Fps/Fes/Fer/CIP4 homology
Fig.	Figures
g	Gravitation

GMR	glass multiple reporter
GR	Genomic rescue
GST	Glutathione-S-Transferase
h	hour
h-	human
Hepes	N-2-Hydroxyethyl)-piperazin-N'-(2-ethansulfonic acid)
HRP	Horseradish peroxidase
ID	Intracellular domain
IPTG	Isopropyl-β-D-Thiogalactoside
kb	Kilobase
kDa	Kilodalton
LB	Luria-Bertani medium
LMP	Low melting point
M	Molar
mA	Milliampere
MCS	Multiple cloning site
MES	2-Morpholinoethane-sulfonic acid
min	Minute
ml	Milliliter
mM	Millimolar
µg	Microgram
µl	Microliter
µM	Micromolar
NBT	Nitro-Blue-Tatrazoliumcholride
NP-40	Nonidet P-40
OD	Optical density
PAGE	Polyacrylamide gel electrophoresis
PBS	Phosphate buffered saline
PBST	Phosphate buffered saline Tween20
PCR	Polymerase chain reaction
pers. comm.	Personal communication
PFA	Paraformaldehyde
PFGE	Pulsed field gel electrophoresis
PMSF	Phenylmethylsulfonylfluoride
RNA	Ribonucleic acid
RNAi	RNA interference
RT	room temperature
RT-PCR	Reverse transcription-polymerase chain reaction
S	second
S2	Schneider cells
SAP	Shrimp alkaline phosphatase
SDS	Sodium dodecylsulfate
SH2	Src-homology-2
SP	Signal peptide
TAE	Tris acetate EDTA buffer
TBE	Tris borate EDTA buffer
TE	Tris-EDTA buffer
TMD	Transmembrane domain
Tris	Tris-(Hydroxymethyl)-aminomethane
Tween 20	Polyoxyethylensorbitan-monolaurate
U	Enzyme units
UAS	upstream activating sequence
3´UTR	3-prime untranslated region
5´ UTR	5-prime untranslated region
rpm	Rotations per minute
UV	Ultraviolet light
V	Volt
v-	viral-
v/v	Volume per volume
Wt	Wildtype
w/v	Weight per volume

8.2 Vector maps

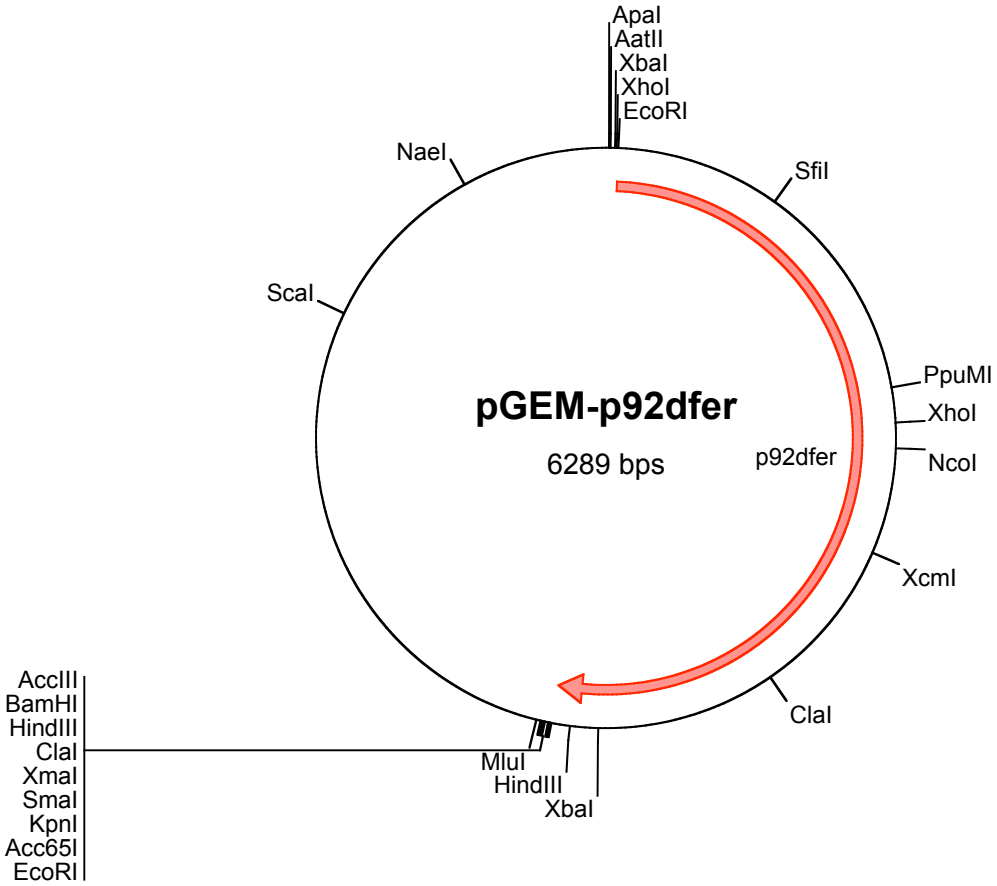

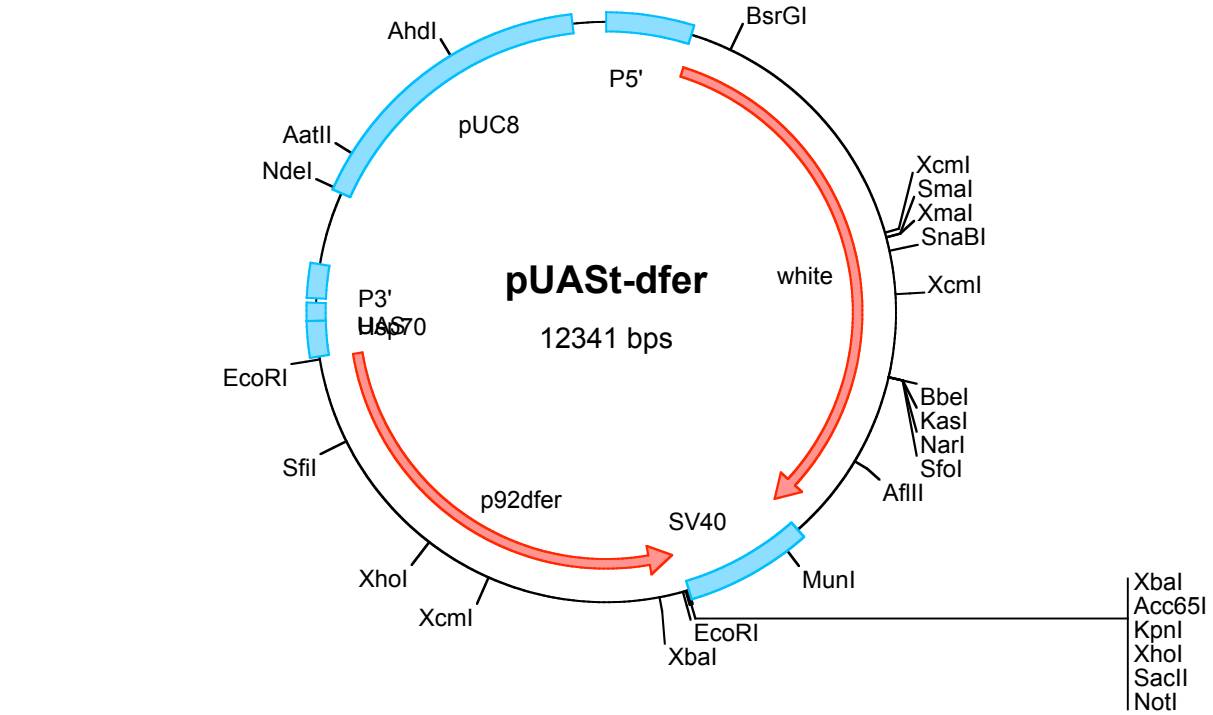

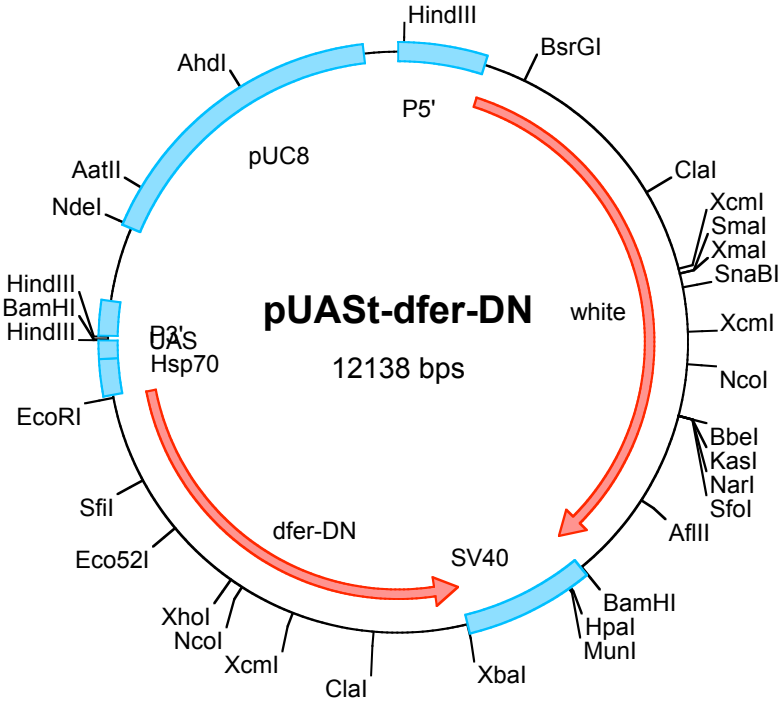
pUASt-dfer-DN
12138 bps
HindIII
BsrGI
AhdI
P5'
pUC8
ClaI
AatII
XcmI
SmaI
NdeI
XmaI
SnaBI
HindIII
BamHI
HindIII
white
XcmI
P3'
UAS
Hsp70
NcoI
EcoRI
BbeI
KasI
NarI
SfoI
SfiI
dfer-DN
AflII
Eco52I
SV40
BamHI
XhoI
HpaI
NcoI
MunI
XcmI
XbaI
ClaI

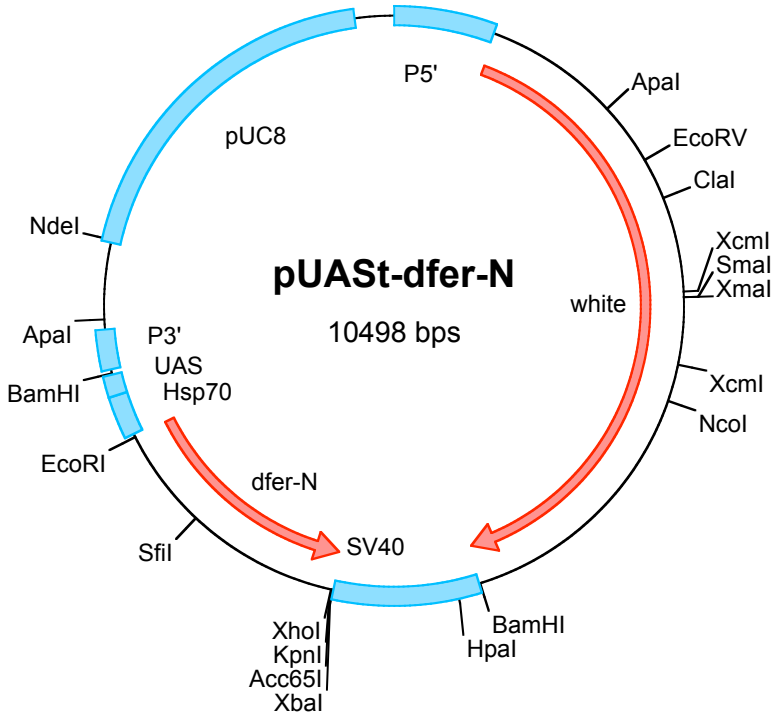
pUASt-dfer-N
10498 bps
P5'
ApaI
pUC8
EcoRV
ClaI
NdeI
XcmI
SmaI
XmaI
white
ApaI
P3'
UAS
XcmI
BamHI
Hsp70
NcoI
EcoRI
dfer-N
SfiI
SV40
XhoI
BamHI
KpnI
HpaI
Acc65I
XbaI

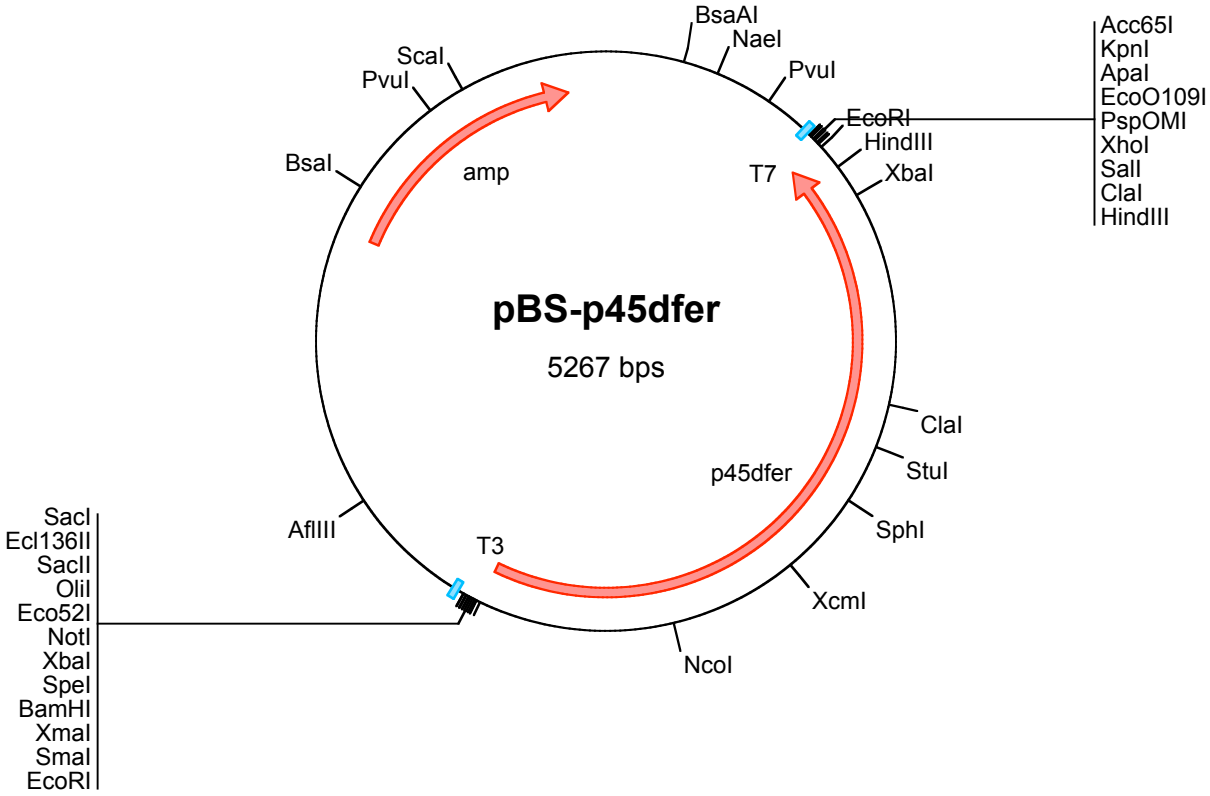
pBS-p45dfer
5267 bps
BsaAI
NaeI
PvuI
EcoRI
HindIII
XbaI
ClaI
StuI
SphI
XcmI
NcoI
AflIII
T3
p45dfer
T7
amp
ScaI
PvuI
BsaI
Acc65I
KpnI
ApaI
EcoO109I
PspOMI
XhoI
SalI
ClaI
HindIII
SacI
Ecl136II
SacII
OliI
Eco52I
NotI
XbaI
SpeI
BamHI
XmaI
SmaI
EcoRI

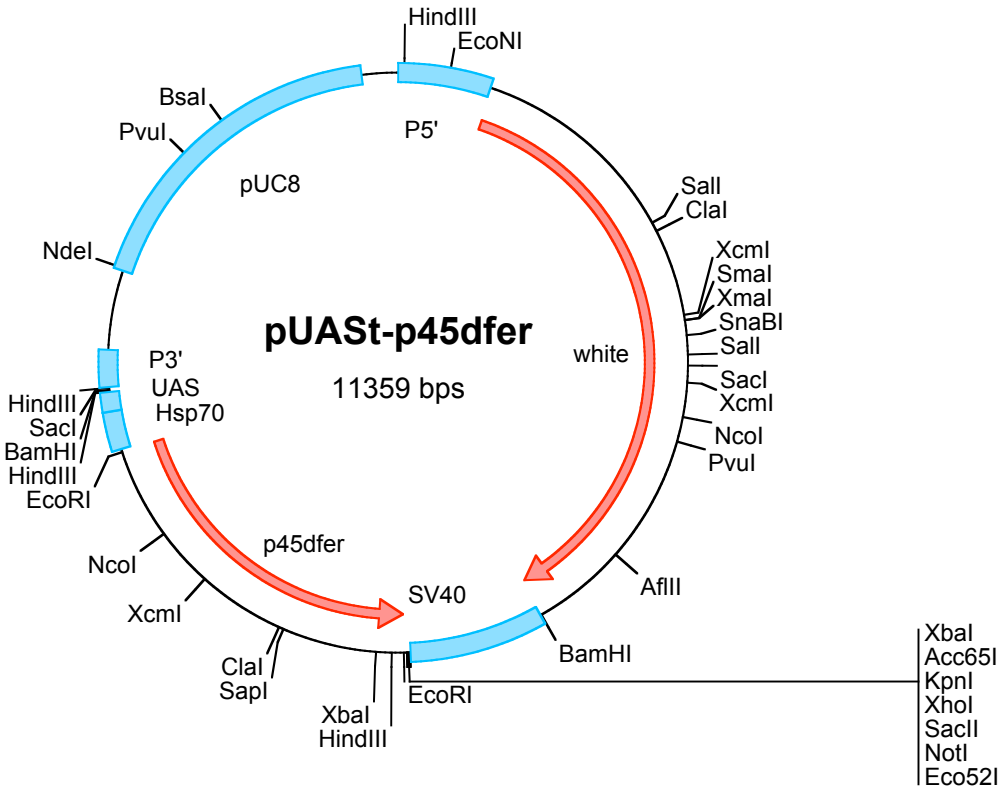
pUASt-p45dfer
11359 bps
HindIII
EcoNI
P5'
white
SalI
ClaI
XcmI
SmaI
XmaI
SnaBI
SalI
SacI
XcmI
NcoI
PvuI
AflII
BamHI
SV40
p45dfer
P3'
UAS
Hsp70
pUC8
BsaI
PvuI
NdeI
HindIII
SacI
BamHI
HindIII
EcoRI
NcoI
XcmI
ClaI
SapI
XbaI
HindIII
EcoRI
XbaI
Acc65I
KpnI
XhoI
SacII
NotI
Eco52I

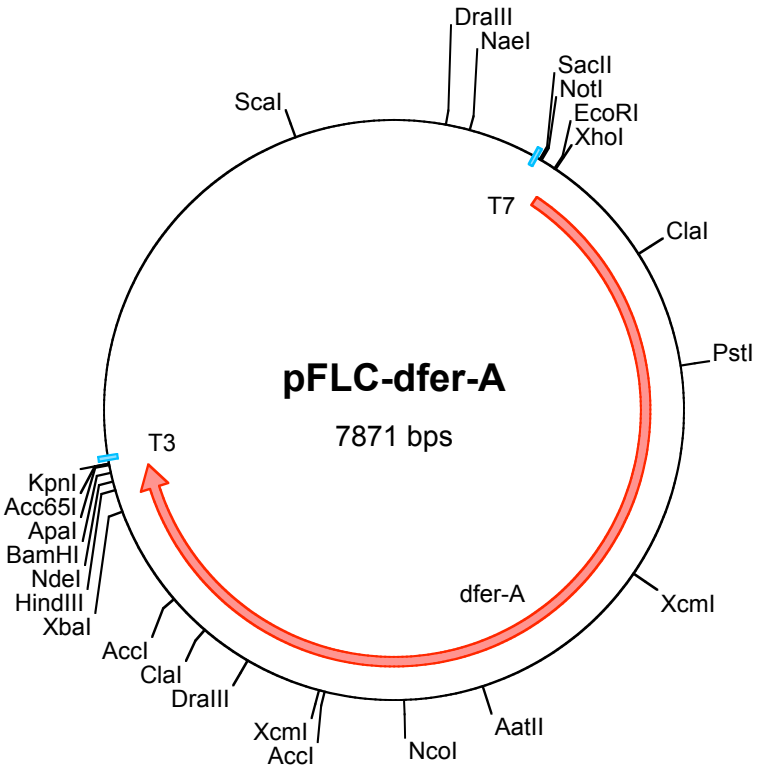
pFLC-dfer-A
7871 bps
DraIII
NaeI
SacII
NotI
EcoRI
XhoI
ScaI
T7
ClaI
PstI
T3
dfer-A
XcmI
AatII
NcoI
XcmI
AccI
DraIII
ClaI
AccI
XbaI
HindIII
NdeI
BamHI
ApaI
Acc65I
KpnI

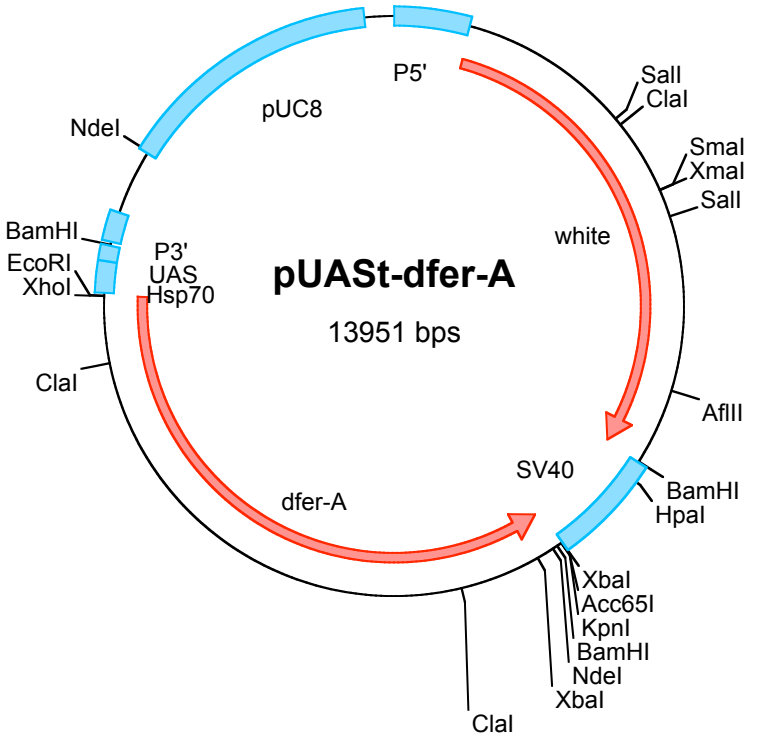
pUASt-dfer-A
13951 bps
P5'
pUC8
SalI
ClaI
SmaI
XmaI
SalI
NdeI
white
BamHI
EcoRI
XhoI
P3'
UAS
Hsp70
ClaI
AflII
SV40
BamHI
HpaI
dfer-A
XbaI
Acc65I
KpnI
BamHI
NdeI
XbaI
ClaI

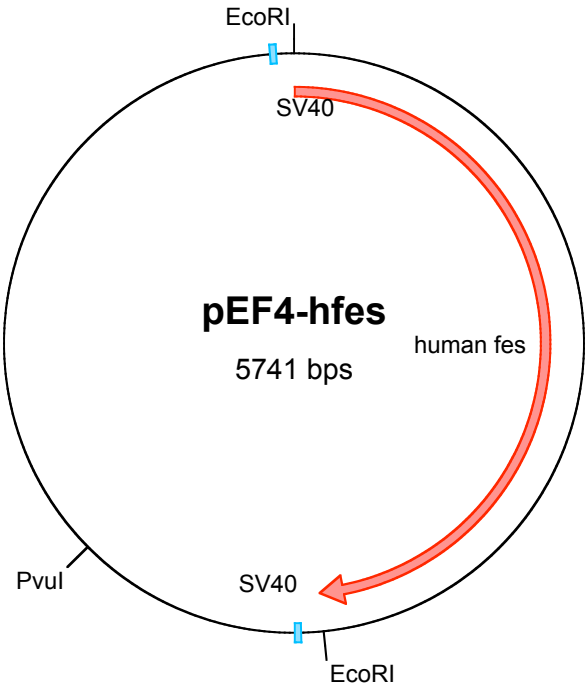
EcoRI
SV40
pEF4-hfes
5741 bps
human fes
PvuI
SV40
EcoRI

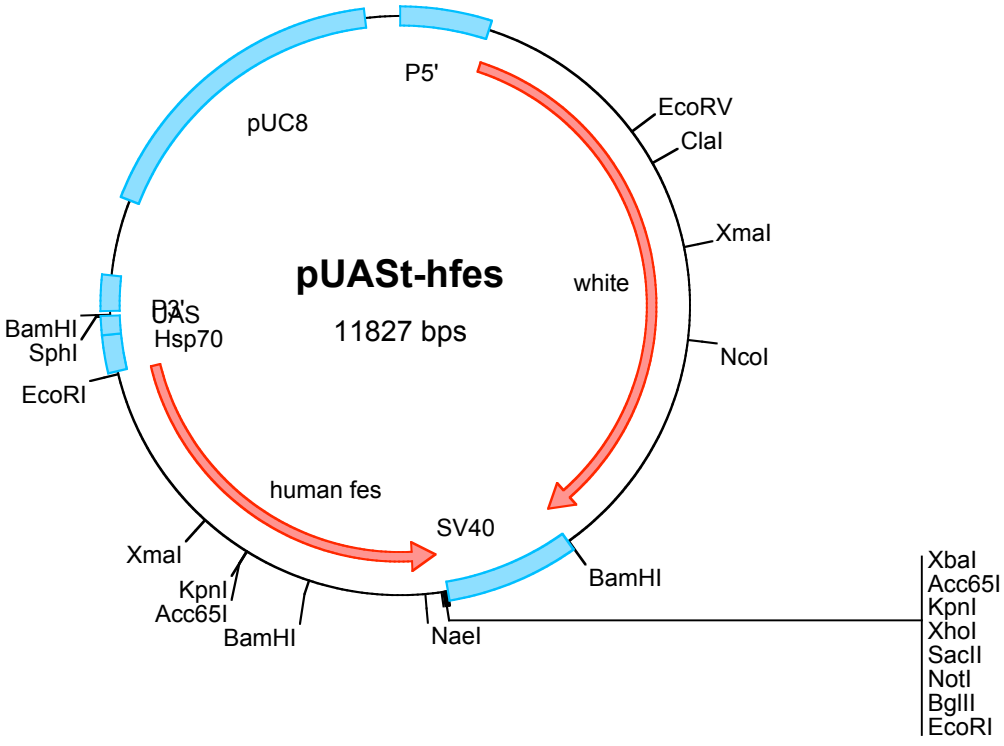
P5'
pUC8
EcoRV
ClaI
XmaI
pUASt-hfes
11827 bps
white
NcoI
BamHI
SphI
EcoRI
UAS
Hsp70
human fes
SV40
XmaI
KpnI
Acc65I
BamHI
BamHI
NaeI
XbaI
Acc65I
KpnI
XhoI
SacII
NotI
BglII
EcoRI

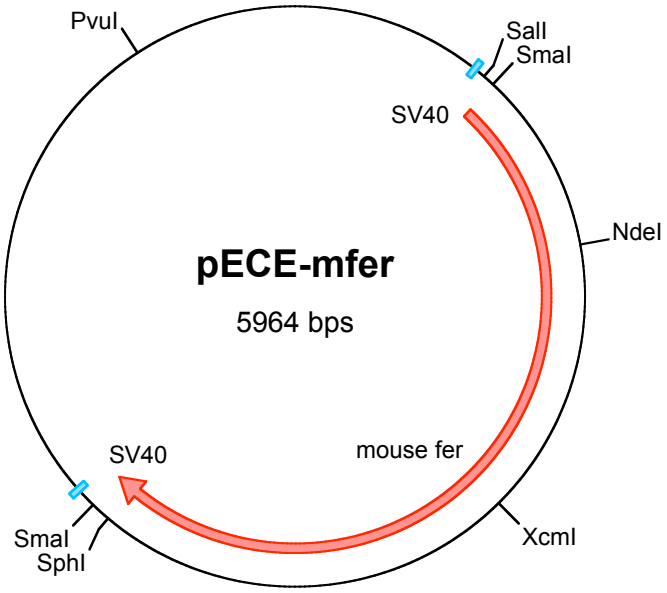
PvuI
SalI
SmaI
SV40
NdeI
pECE-mfer
5964 bps
SV40
mouse fer
SmaI
SphI
XcmI

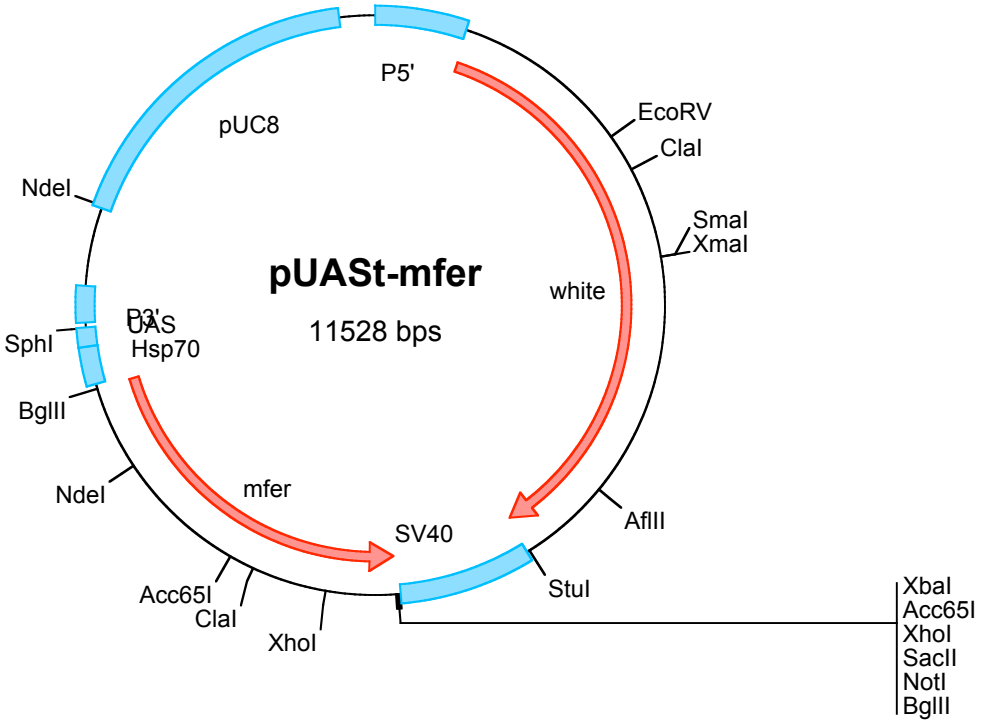
P5'
pUC8
EcoRV
ClaI
NdeI
SmaI
XmaI
pUASt-mfer
11528 bps
white
P3'
UAS
Hsp70
SphI
BglII
NdeI
mfer
SV40
AflII
StuI
Acc65I
ClaI
XhoI
XbaI
Acc65I
XhoI
SacII
NotI
BglII

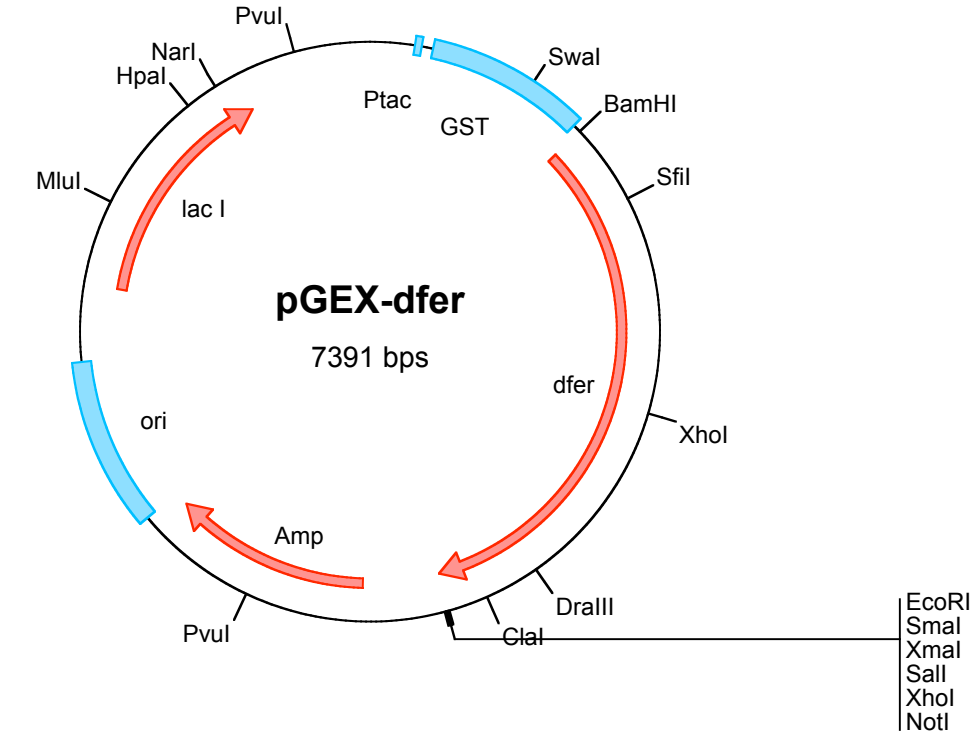
pGEX-dfer
7391 bps
PvuI
NarI
HpaI
MluI
lac I
Ptac
GST
SwaI
BamHI
SfiI
dfer
XhoI
ori
Amp
PvuI
DraIII
ClaI
EcoRI
SmaI
XmaI
SalI
XhoI
NotI

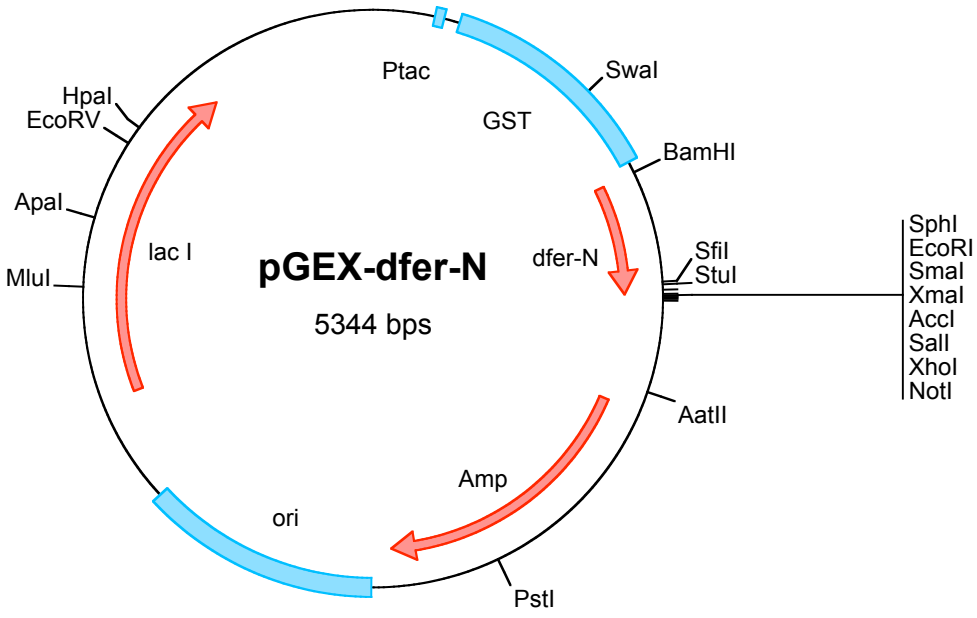
pGEX-dfer-N
5344 bps
Ptac
SwaI
GST
BamHI
HpaI
EcoRV
ApaI
MluI
lac I
dfer-N
SfiI
StuI
AatII
Amp
ori
PstI
SphI
EcoRI
SmaI
XmaI
AccI
SalI
XhoI
NotI

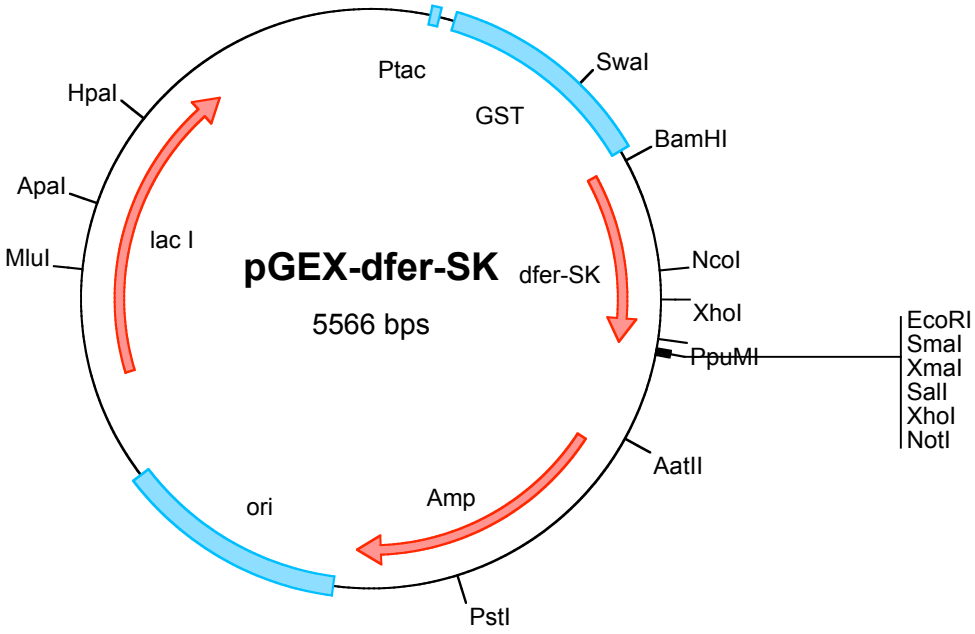
pGEX-dfer-SK
5566 bps
Ptac
GST
SwaI
BamHI
NcoI
XhoI
PpuMI
AatII
Amp
PstI
ori
lac I
MluI
ApaI
HpaI
dfer-SK
EcoRI
SmaI
XmaI
SalI
XhoI
NotI

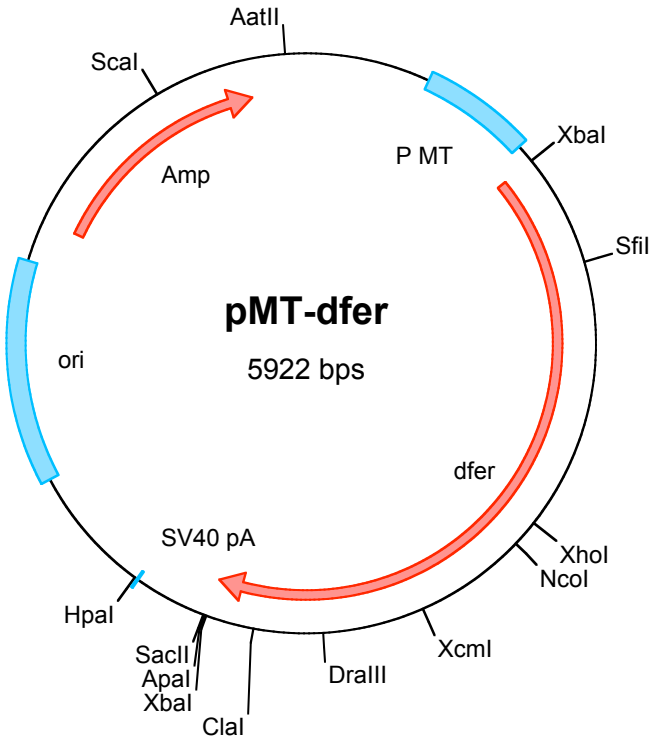
pMT-dfer
5922 bps
AatII
ScaI
XbaI
SfiI
P MT
Amp
ori
dfer
SV40 pA
XhoI
NcoI
HpaI
XcmI
SacII
ApaI
XbaI
DraIII
ClaI

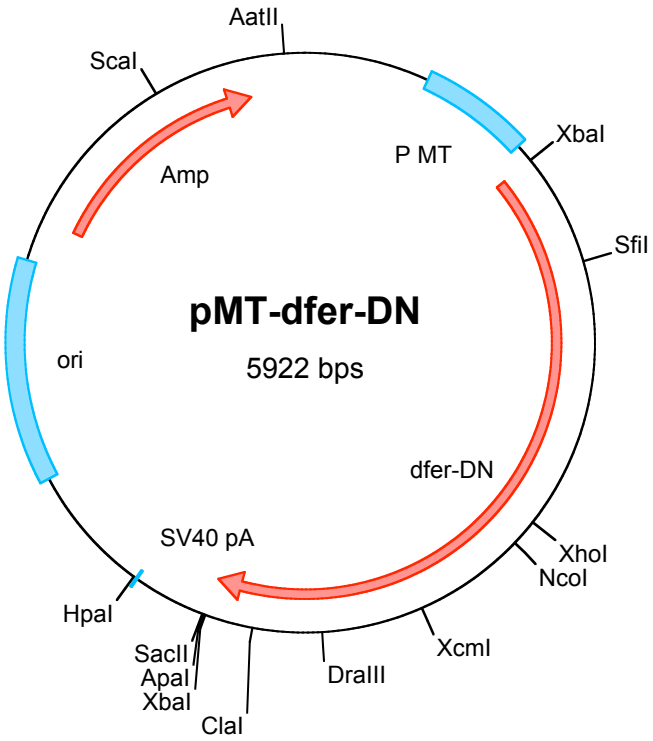
AatII
ScaI
XbaI
P MT
Amp
SfiI
pMT-dfer-DN
5922 bps
ori
dfer-DN
SV40 pA
XhoI
NcoI
HpaI
XcmI
SacII
ApaI
XbaI
DraIII
ClaI

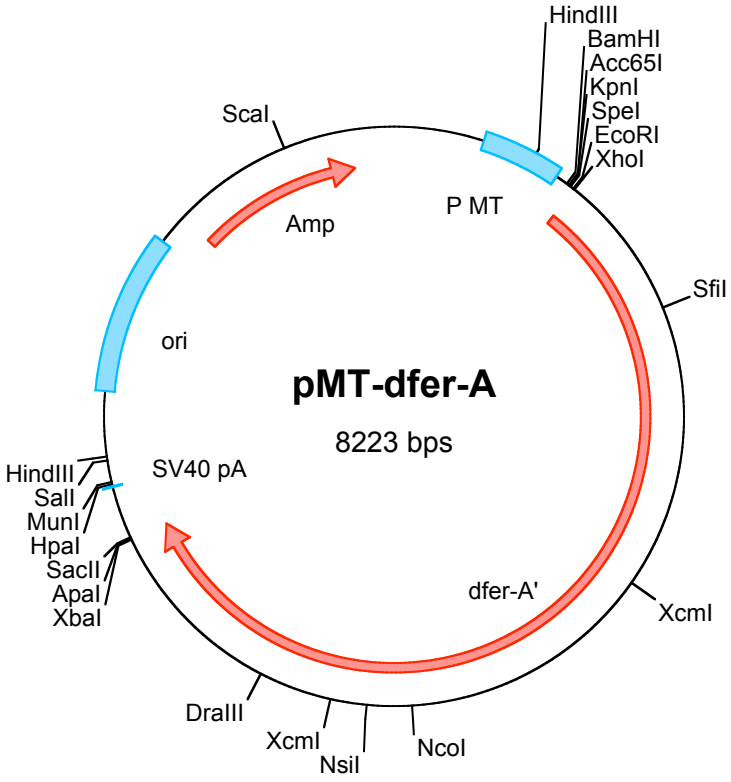
HindIII
BamHI
Acc65I
KpnI
SpeI
EcoRI
XhoI
ScaI
P MT
Amp
SfiI
ori
pMT-dfer-A
8223 bps
SV40 pA
HindIII
SalI
MunI
HpaI
SacII
ApaI
XbaI
dfer-A'
XcmI
DraIII
XcmI
NsiI
NcoI

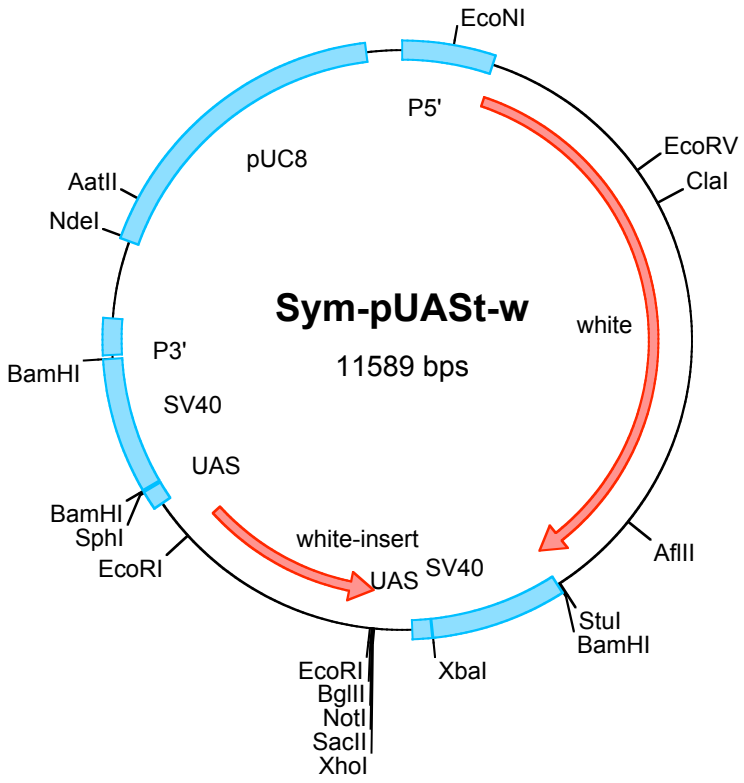
EcoNI
P5'
EcoRV
ClaI
pUC8
AatII
NdeI
Sym-pUASt-w
11589 bps
white
P3'
BamHI
SV40
UAS
BamHI
SphI
EcoRI
white-insert
UAS
SV40
AflII
StuI
BamHI
EcoRI
BglII
NotI
SacII
XhoI
XbaI

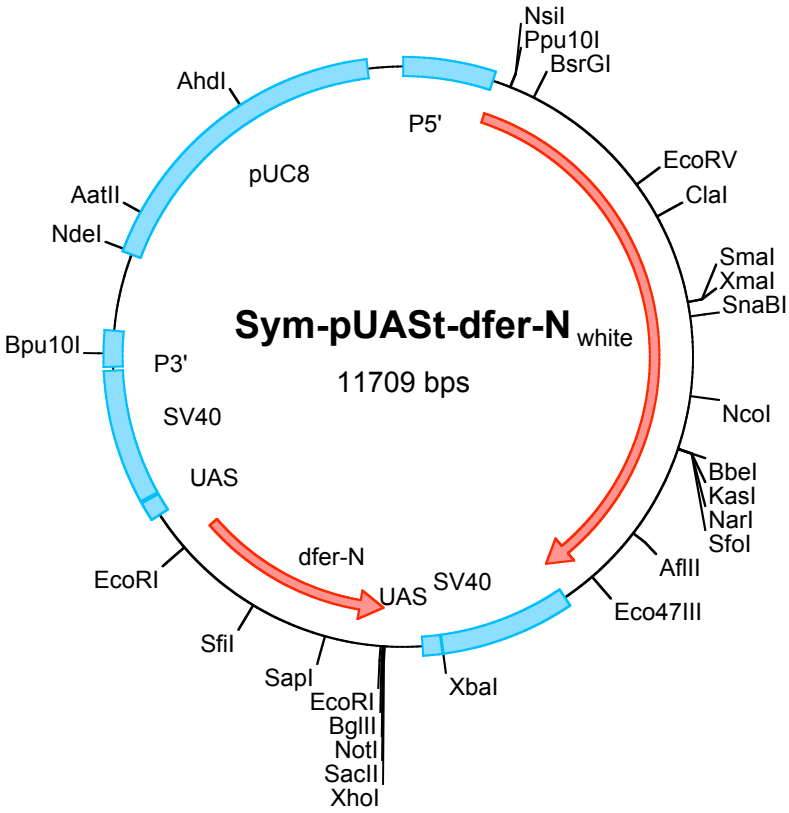
NsiI
Ppu10I
BsrGI
AhdI
P5'
EcoRV
ClaI
pUC8
AatII
NdeI
SmaI
XmaI
SnaBI
Sym-pUASt-dfer-N
11709 bps
white
Bpu10I
P3'
NcoI
SV40
UAS
BbeI
KasI
NarI
SfoI
dfer-N
AflII
EcoRI
UAS
SV40
Eco47III
SfiI
SapI
XbaI
EcoRI
BglII
NotI
SacII
XhoI

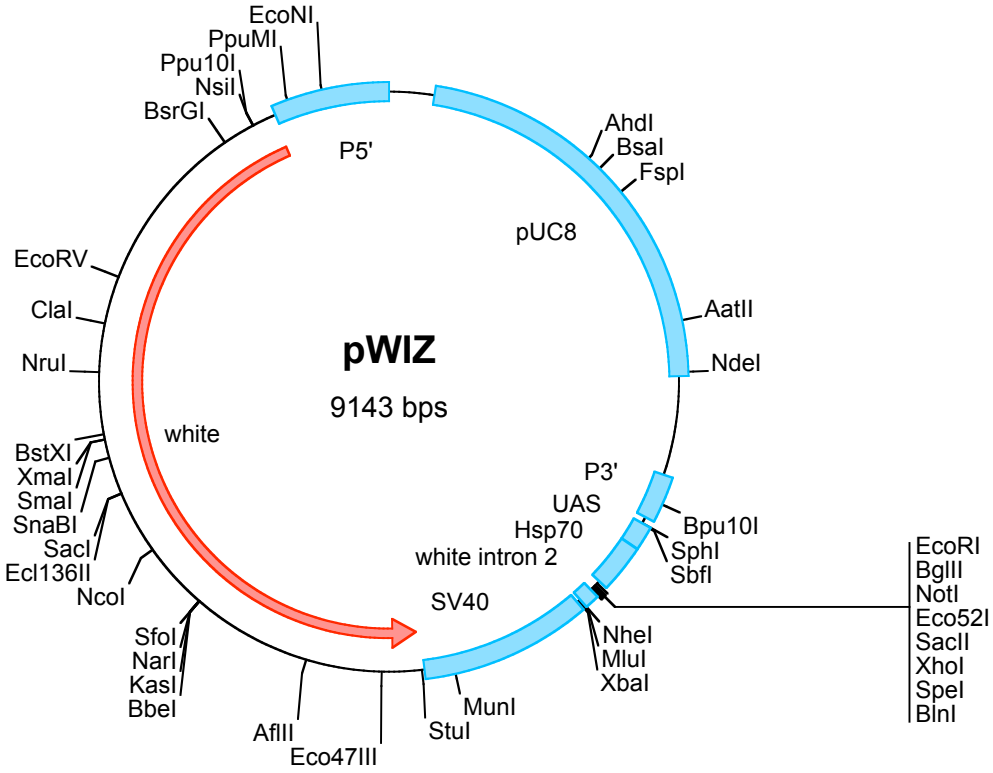
pWIZ
9143 bps
EcoNI
PpuMI
Ppu10I
NsiI
BsrGI
P5'
AhdI
BsaI
FspI
pUC8
AatII
NdeI
P3'
UAS
Hsp70
white intron 2
Bpu10I
SphI
SbfI
EcoRI
BglII
NotI
Eco52I
SacII
XhoI
SpeI
BlnI
NheI
MluI
XbaI
SV40
MunI
StuI
Eco47III
AflII
SfoI
NarI
KasI
BbeI
NcoI
Ecl136II
SacI
SnaBI
SmaI
XmaI
BstXI
white
NruI
ClaI
EcoRV

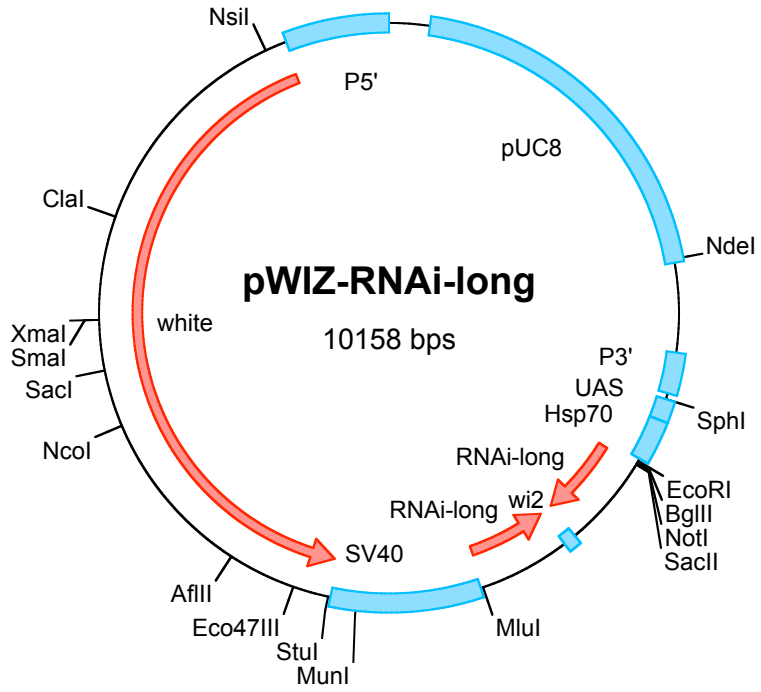
pWIZ-RNAi-long
10158 bps
NsiI
P5'
pUC8
ClaI
NdeI
P3'
UAS
Hsp70
SphI
RNAi-long
wi2
RNAi-long
EcoRI
BglII
NotI
SacII
SV40
MluI
AflII
Eco47III
StuI
MunI
NcoI
SacI
XmaI
SmaI
white

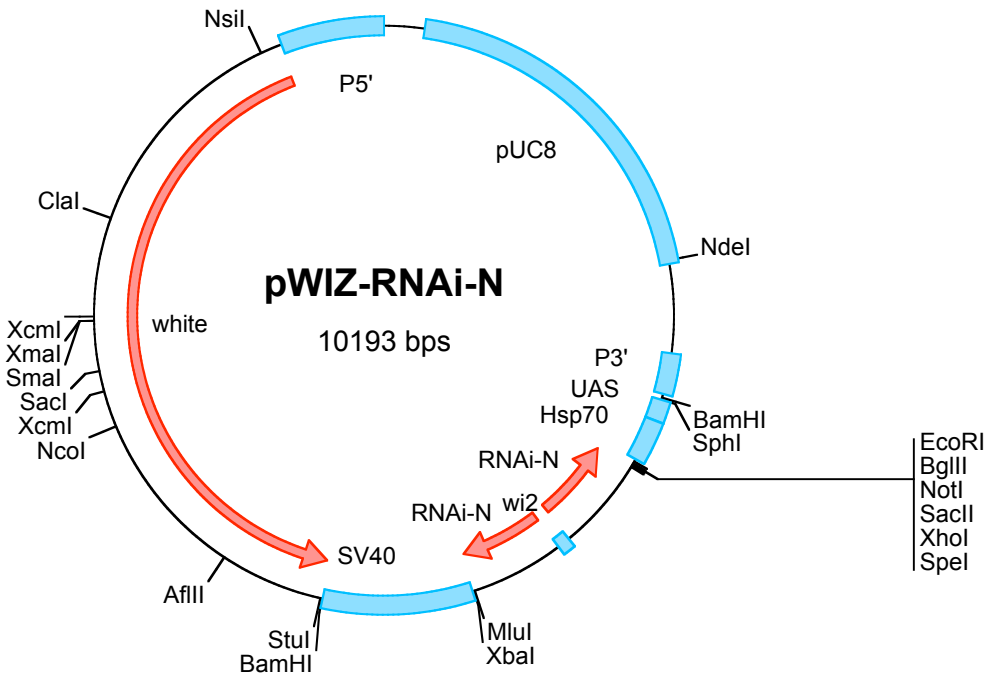
NsiI
P5'
pUC8
ClaI
NdeI
pWIZ-RNAi-N
white
10193 bps
XcmI
XmaI
SmaI
SacI
XcmI
NcoI
P3'
UAS
Hsp70
BamHI
SphI
RNAi-N
EcoRI
BglII
NotI
SacII
XhoI
SpeI
RNAi-N
wi2
SV40
AflII
StuI
BamHI
MluI
XbaI

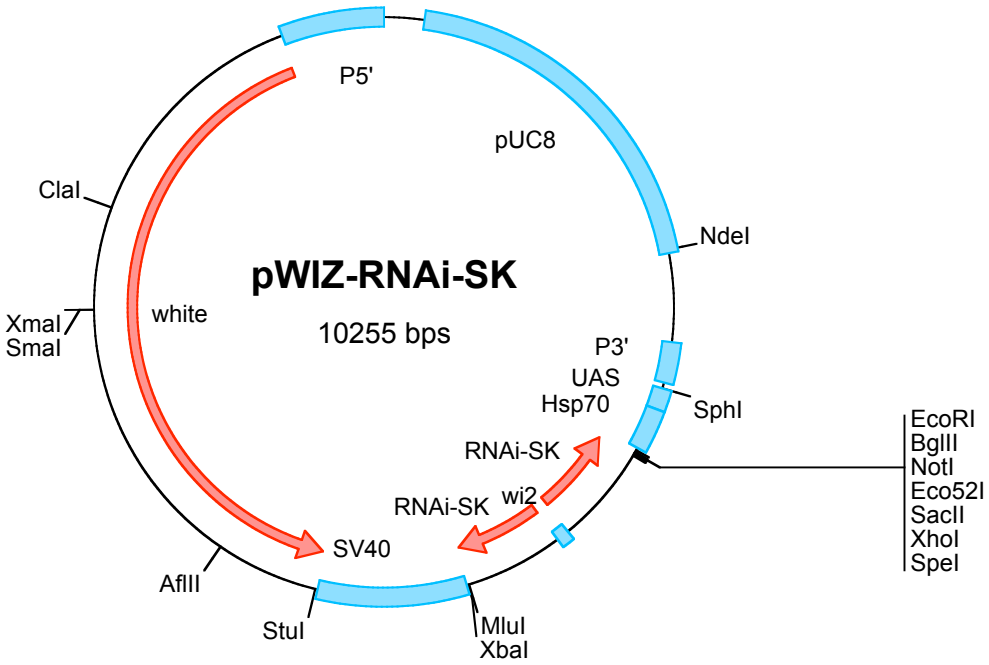
P5'
pUC8
ClaI
NdeI
pWIZ-RNAi-SK
white
10255 bps
XmaI
SmaI
P3'
UAS
Hsp70
SphI
RNAi-SK
EcoRI
BglII
NotI
Eco52I
SacII
XhoI
SpeI
RNAi-SK
wi2
SV40
AflII
StuI
MluI
XbaI

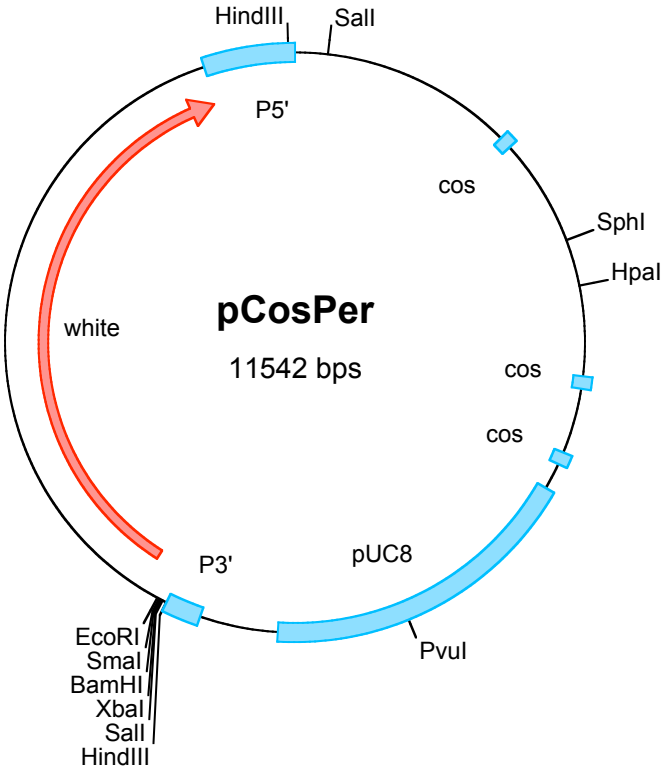
HindIII
SalI
P5'
cos
SphI
HpaI
white
pCosPer
11542 bps
cos
cos
P3'
pUC8
EcoRI
SmaI
BamHI
XbaI
SalI
HindIII
PvuI

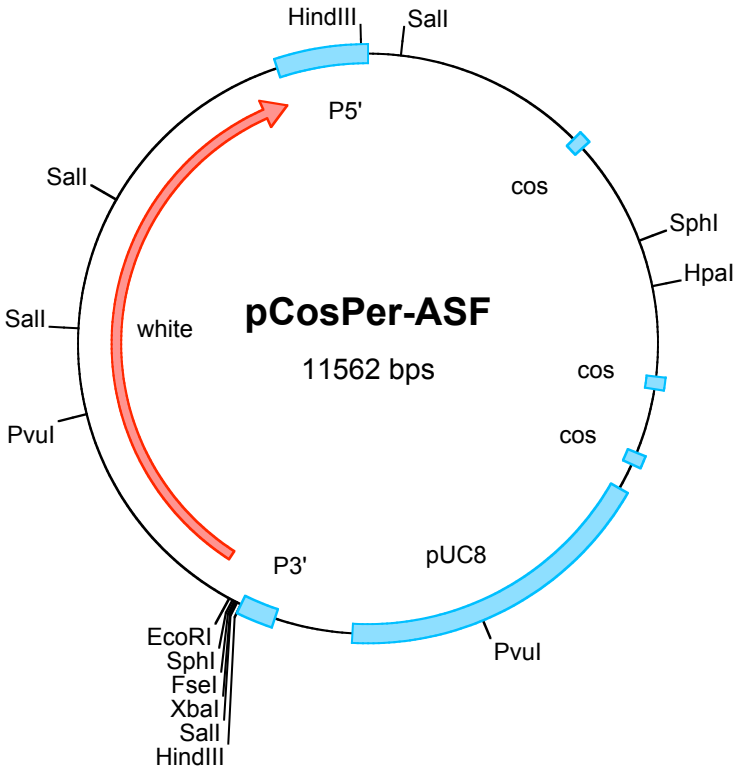
HindIII
SalI
P5'
SalI
cos
SphI
HpaI
SalI
white
pCosPer-ASF
11562 bps
cos
PvuI
cos
P3'
pUC8
EcoRI
SphI
FseI
XbaI
SalI
HindIII
PvuI

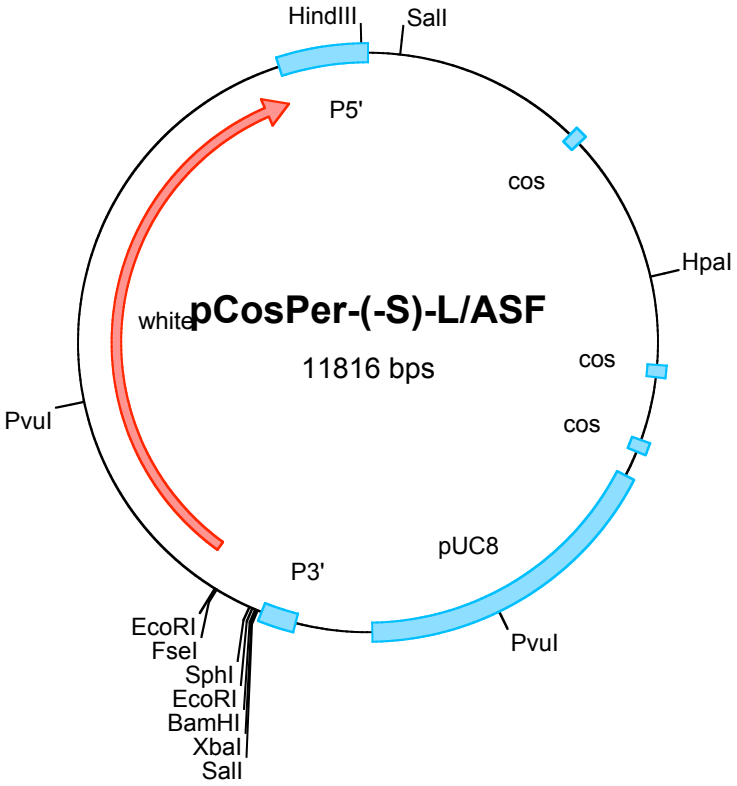
HindIII
SalI
P5'
cos
HpaI
white
pCosPer-(-S)-L/ASF
11816 bps
cos
cos
PvuI
pUC8
P3'
EcoRI
FseI
SphI
EcoRI
BamHI
XbaI
SalI
PvuI

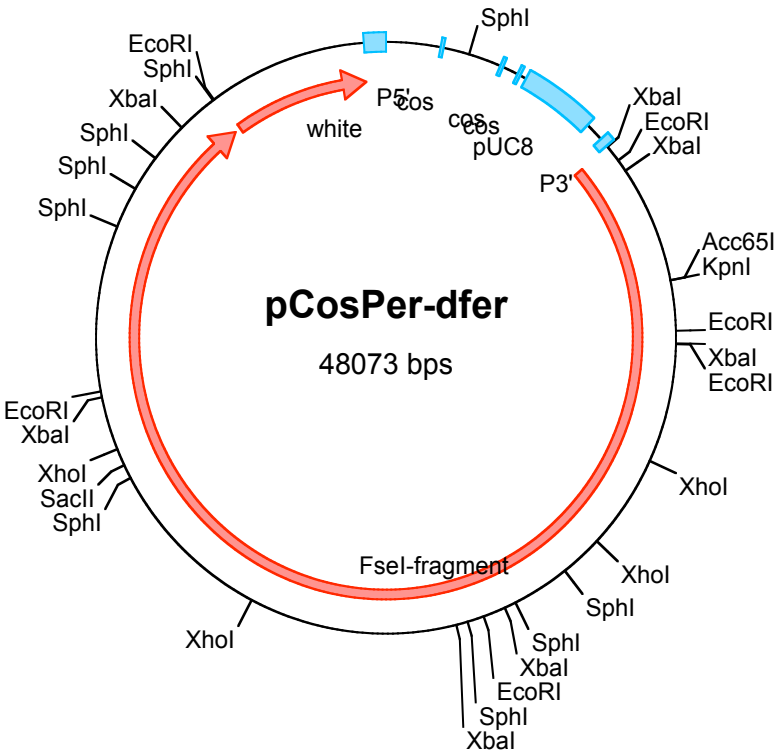
SphI
EcoRI
SphI
XbaI
SphI
SphI
SphI
P5'
cos
cos
cos
white
pUC8
P3'
XbaI
EcoRI
XbaI
Acc65I
KpnI
EcoRI
XbaI
EcoRI
pCosPer-dfer
48073 bps
EcoRI
XbaI
XhoI
SacII
SphI
XhoI
FseI-fragment
XhoI
SphI
SphI
XbaI
EcoRI
SphI
XbaI

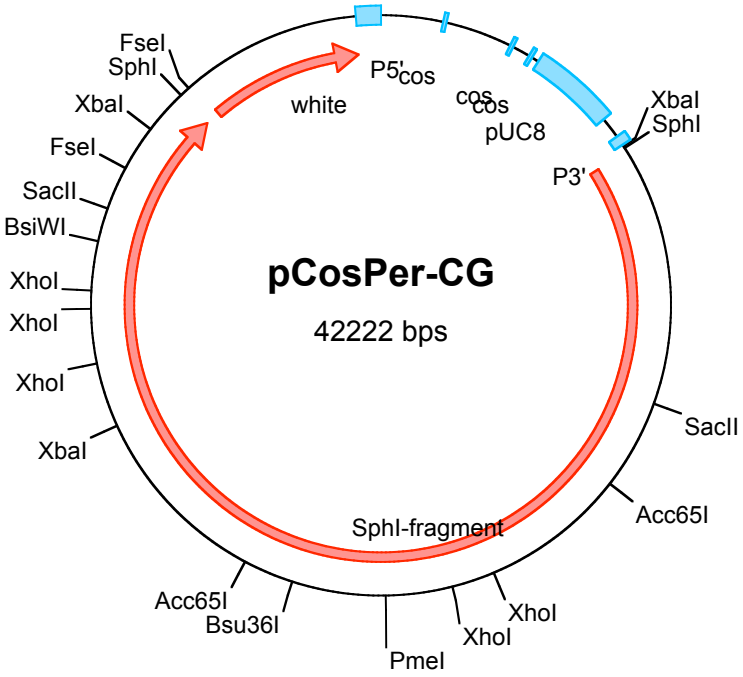
pCosPer-CG
42222 bps
white
P5'
cos
cos
cos
pUC8
P3'
XbaI
SphI
SacII
Acc65I
XhoI
XhoI
PmeI
Bsu36I
Acc65I
XbaI
XhoI
XhoI
BsiWI
SacII
FseI
XbaI
SphI
FseI
SphI-fragment

8.3 Publications

Merdes, G., Soba, P., Loewer, A., Bilic, M. V., Beyreuther, K. and Paro, R. (2004). "Interference of human and Drosophila APP and APP-like proteins with PNS development in Drosophila." *Embo J* **23**(20): 4082-95.

Bilic, M. and Baumbusch, K. (02/09/2004). "Weisen leuchtende Fliegen Forschern den Weg?" *Rhein-Neckar-Zeitung* **203**.

Bilic, M. V., Loewer, A., Paro, R. and Merdes, G. (2004). "Drosophila und humane Krankheitsgene." *BIOforum* **5**

Hiermit erkläre ich an Eides statt, dass ich die vorliegende Dissertation selbstständig und ohne unerlaubte Hilfsmittel durchgeführt habe.

Heidelberg, 17.02.2005

.....

Michaela V. Bilic